Nonalcoholic fatty liver disease: Regulation of glucose and fat metabolism in the liver by Carbohydrate Response Element Binding Protein (ChREBP) and impact of dietary influence

Vorgelegte Dissertation von

Haiam Omar Mohamed Elkatry, M.Sc.

aus Kairo (Ägypten)

von der Fakultät III – Prozesswissenschaften, Institut für Lebensmitteltechnologie und Lebensmittelchemie der Technischen Universität Berlin zur Erlangung der akademischen Grades Doktor der Naturwissenschaften -Dr. rer. nat.- genehmigte Dissertation

Promotionsausschuss:

Vorsitzender: Prof. Dr. Leif-Alexander Garbe

Berichterstatter : Prof. Dr. Dipl.-Ing. Dietrich Knorr

Berichterstatter : Prof. Dr. Andreas Pfeiffer

Tag der wissenschaftlichen Aussprache: 23.09.2011

Berlin 2011

D83

Nonalcoholic fatty liver disease: Regulation of glucose and fat metabolism in the liver by Carbohydrate Response Element Binding Protein (ChREBP) and impact of dietary influence

Submission from

Haiam Omar Mohamed Elkatry, M.Sc.

from Cairo (Egypt)

Faculty III - Process Science, Institute of Food Technology and Food Chemistry,

Technical University of Berlin,

Submitted in Partial Fulfillment of the Requirements for

the Degree Academic of Doctor in Natural Science (Food Science)

-Dr. rer. nat.-

Approved Thesis

This work has been approved by:

Vorsitzender: Prof. Dr. Leif-Alexander Garbe

Berichterstatter : Prof. Dr. Dipl.-Ing. Dietrich Knorr

Berichterstatter : Prof. Dr. Andreas Pfeiffer

Date of Examination: 23.09.2011

Berlin 2011

D83

ZUSAMMENFASSUNG

Deregulationen in der Leberlipidsynthese sind häufig mit Adipositas und Diabetes Typ 2 verbunden und daher ist ein detailliertes Verständnis der beteiligten, regulierenden Stoffwechselwege sehr wichtig, um künftig potentielle therapeutische Targets zu identifizieren. Die Leber ist der wichtigste Ort für den Kohlenhydratstoffwechsel (Glykolyse und Glykogen-Synthese) sowie Triglycerid-Synthese (Lipogenese). Carbohydrate-responsive element-binding protein (ChREBP) wurden in die Regulation durch Glucose der glykolytischen und lipogenen Gene einbezogen, einschließlich der codierten l-Pyruvatkinase (L-PK) und Fettsäuresynthase (FAS). In den letzten zehn Jahren konnte anhand verschiedener Untersuchungen bewiesen werden, dass Nährstoffe, vor allem Glukose und Fettsäuren in der Lage sind, hepatische Genexpressionen in einer Transkriptionsart zu regulieren. Diätetische mehrfach ungesättigte Fettsäuren (PUFAs) sind potente Inhibitoren der hepatischen Lipogenese und Glykolyse. Das Ziel unserer Untersuchungen war es, einen Test zu entwickeln , bei dem die Aktivierung von ChREBP durch die Analyse von cytoplasmatic – nuclear translocation of a green fluorescence– zu ChREBP Hybrid-Protein (ChREBP-GFP) überwacht wird. Der Einfluss verschiedener Zucker und Süßstoffe (Glukose, Fruktose, Saccharin, Aspartam, Cyclamat, Steviosid), einfach ungesättigter Fettsäuren [Oleate (C18: 1)] und mehrfach ungesättigter Fettsäuren [Linoleat (C18: 2) , Eicosapentaensäure (C20: 5), Docosahexaensäure (C22: 6)] und Polyphenole aus Olivenöl (Oleuropein) wurden auf die von geklonten menschlichen ChREBP durch die Analyse der Translokation von ChREBP-GFP aus dem Zytoplasma auf den Nukleus beurteilt und durch ein automatisches Fluoreszenzmikroskop überwacht. Unsere Ergebnisse zeigen, dass hohe Konzentrationen von Glukose, Fruktose, Cyclamat mit Insulin und Saccharin mit bzw. ohne insulinstimulierenden ChREBP Gentranslokation aus dem Zytosol in den Zellkern nachgewiesen wurden und eine erhöhte DNA-Bindung und transkriptioneller Aktivität von ChREBP freisetzen. Andererseits gab es eine suppressive Wirkung von Ölsäure und Eicosapentaensäure auf ChREBP Nukleustranslokation.

Schlüsselwörter: **Alkoholfreie Fettleber, ChREBP translokation, glykolyse, lipogenese, glucose, süßstoffe, olivenöl und mehrfach ungesättigten Fettsäuren**.

ABSTRACT

Deregulations in hepatic lipid synthesis are often associated with obesity and type 2 diabetes, and therefore a perfect understanding of the regulation of this metabolic pathway appears essential to identify potential therapeutic targets. The liver is a major site for carbohydrate metabolism (glycolysis and glycogen synthesis) and triglyceride synthesis (lipogenesis). Carbohydrate-responsive element–binding protein (ChREBP) was implicated in the regulation by glucose of glycolytic and lipogenic genes, including those encoding l-pyruvate kinase (L-PK) and fatty acid synthase (FAS). In the last decade, increasing evidence has emerged to show that nutrients, in particular, glucose and fatty acids, are able to regulate hepatic gene expression in a transcriptional manner. Dietary polyunsaturated fatty acids (PUFAs) are potent inhibitors of hepatic glycolysis and lipogenesis. The aim of my study was to establish an assay to monitor the activation of ChREBP by analyzing cytoplasmatic – nuclear translocation of a green fluorescence – ChREBP hybrid protein (ChREBP-GFP). The influence of different of sugars and sweeteners (glucose, fructose, saccharin, aspartame, cyclamate, stevioside), monounsaturated fatty acids [oleate (C18:1)] and polyunsaturated fatty acids [linoleate (C18:2), eicosapentanoic acid (C20:5), docosahexaenoic acid (C22:6)] and polyphenols from olive oil (oleuropein) on the activity of cloned human ChREBP was assessed by analyzing the translocation of ChREBP-GFP from cytoplasm to nucleus which was monitored by an automatic fluorescence microscope system. My results demonstrate that high concentration of glucose, fructose, cyclamate with insulin and saccharine with or without insulin stimulate ChREBP gene translocation from the cytosol to the nucleus, anabling increased DNA-binding and transcriptional activity of ChREBP. On the other hand, there were a suppressive effect of oleic and eicosapentanoic acids on ChREBP nuclear translocation.

KEY WORDS: Nonalcoholic fatty liver disease, ChREBP translocation, glycolysis, lipogenesis, glucose, sweeteners, olive oil and polyunsaturated fatty acids.

ACKNOWLEDGEMENTS

My study was carried out during the years 2007- 2011 as a scholarship from Nutrition and Food Science Department, Faculty of Home Economics, Helwan University (Egypt) and the financial support from the Egyptian Ministry of High Education are gratefully acknowledged.

I would like to thank my supervisor Prof. Dr. Andreas Pfeiffer that he has given me the opportunity to complete the thesis in the Department of Endocrinology, Diabetes & Nutritional Medicine, Charité, CBF and for the encouragement, exceptional ideas, and tireless optimism that have kept me going.

My sincere gratitude is due to my supervisor, Prof. Dr. Dipl.-Ing. Dietrich Knorr for his helping to register my thesis in Department of Food Biotechnology and Food Process Engineering, Institute of Food Technology and Food Chemistry, Faculty of Process Engineering, Berlin University of Technology, Germany.

I would like to express my deepest and sincere appreciation to Dr. Volker Bähr for the continuous support, scientific advice, providing the necessary laboratory facilities, guiding the experimental work, continuous supervision and every possible help throughout this work.

Special thanks to Dr. Christiane Bumke-Vogt for guiding the experimental work, solving the problems, and supervising this investigation. Her valuable advising and kindly help are greatly appreciated.

I can not forget to extend my thanks to Dr. Martin Osterhoff for supporting the establishment of the sequencing of the ChREBP vector.

To all present and former colleagues at the Department of Endocrinology, Diabetes & Nutritional Medicine, Charité, CBF and Department of Clinical Nutrition, German Institute of Human Nutrition (DIFE), I am thankful for providing a very comfortable atmosphere to complete my work.

I am extremely grateful to the Egyptian Government and Missions Office for the financial support during my studies in Germany, especially, Prof. Dr. Galal Elgemeie and Prof. Dr. El Sayed Tag Eldin.

Gratitude is also extended to all staff members, my colleagues and workers of the Home Economics Department, Faculty of Specific Education, Ain Shams University, Egypt for their continuous encouragements.

Finally, my sincere thanks and gratitude are for my parents, my dear husband Abdelrahman Ahmed, my daughter Toqa and my son Ahmed throughout my studies and during these years abroad. In spite of being away, they were always present for their advices and encouragement during my stay in Germany.

Haiam Omar Mohamed Omar Elkatry

LIST OF CONTENTS

LIST OF FIGURES

LIST OF ABBREVIATIONS

ACBP	Acyl CoA binding protein
ACC	Acetyl-Coenzym A-Carboxylase
Acetyl-CoA	Acetyl-Coenzym A
ADI	Accepted daily intake
AgRP	Agouti related peptide
ALA	Alpha-linolenic acid
AMP	Adenosine monophosphate
AMPK	Adenosine monophosphate-activated protein kinase
APM	Aspartame
ATP	Adenosine triphosphate
ATP-CL	Adenosine triphosphate citrate-lyase
bHLHZip	basic helix-loophelix leucine zipper
BMI	Body mass index
Bp	Base pare
BSA	Bovine serum albumin
BW	Body weight
C	Cells
cAMP	Cyclic adenosine monophosphate
cDNA	complementary DNA
ChIP	Chromatin immuno precipitation
ChoRE	Carbohydrate response element
ChREBP	Carbohydrate Responsive Element Binding Protein
CHS	Cyclo hexyl sulfamic
CMV	Cytomegalovirus
CoA	Coenzyme A
CPT-1	Carnitine parmitoyl transferase 1
CS	Corn syrup
CVD	Cardiovascular disease
DAPI	Diamidino-2-phenylinndol Dihydrochlorid
DHA	Docosahexaenoic acid
DHAP	Dihydroxyacetone 3-phosphate
DMEM	Dulbecco’s modified Medium
DNA	Deoxyribonucleic acid

Elovl	Elongation of very long chain fatty acids protein
EPA	Eicosapentaenoic acid
ER	Endoplasmic reticulum
EtBr	Ethidium bromide
Ex	Exon
FABP	Fatty acid binding protein
FAO	Food and Agriculture Organization
FAS	Fatty acid synthase
FBS	Fetal bovine serum
FCS	Fetal calf serum
FDA	Food and Drug Administration
FFA	Free fatty acids
G3P	Glyceraldehyde 3-phosphate
G6P	Glyceraldehyde 6-phosphate
G6Pase	Glucose 6-phosphatase
G6PDH	Glucose-6-phosphate dehydrogenase
GFP	Green Fluorescent Protein
GK	Glucokinase
GKRP	Glucokinase regulatory protein
GLUT	Glucose transporter
Gp	Glycogen phosphorylase
GPAT	Glycerol-phosphate acyltransferase
GRAS	Generally recognized as safe
HCHO	High carbohydrate
HFCS	High fructose corn syrup
HGP	Hepatic glucose production
HMG	Hydroxy-3-methylglutaryl
HMP	Hexose monophosphate
HNF	Hepatocyte nuclear factor
HSL	Hormone-sensitive lipase
IREs	Insulin response elements
JECFA	Joint FAO/WHO Expert Committee on Food Additive
kDa	Kilo-Dalton
Km	Michaelis constant

KO	Knockout
LA	Linoleic acid
L-PK	Liver pyruvate kinase
LXR	Liver X receptors
MCD	Malonyl-CoA decarboxylase
MEM	Minimal Essential Medium
Mlx	Max-like protein X
mM	MilliMolar
MP	Malatepyruvate
mRNA	Messenger RNA
MS	Metabolic syndrome
NADPH	Nicotinamide adenine dinucleotide phosphate
NAFLD	Non-alcoholic fatty liver disease
NASH	Nonalcoholic steatohepatitis
NEFA	Nonesterified fatty acids
NLS	Nuclear localization signal
OAA	Oxaloacetate
PBS	Phosphate-Buffered Saline
PCR	Polymerase chain reaction
PEP	Phosphoenolpyruvate
PEPCK	Phosphoenolpyruvate carboxykinase
PFK	Pphosphofructo-1-kinase
PG-DH	Phosphogluconate dehydrogenase
PKU	Phenylketonuria
PK	Pyruvate kinase
PKA	Protein kinase A
PP2A	Protein phosphatise 2A
PPAR	Peroxisome proliferator-activated receptor
PUFA	Polyunsaturated fatty acid
RT	Room temperature
RXR	Retinoid X receptor
SCD	Stearoyl- Coenzym A desaturase
SD	Soft drink
shChREBP	Short hairpin RNA against ChREBP

SRE	Sterol regulatory element
SREBP-1c	Sterol Regulatory Element-Binding Protein
TGs	Triglycerides
USF	Upstream stimulatory factor
VLDL	Very-low-density lipoprotein
WBSCR14	Williams-Beuren syndrome critical region 14
X5P	Xylulose 5- phosphate
ZIP-like	Leucine zipper-like

1- INTRODUCTION

The liver is a major site for carbohydrate metabolism (glycolysis and glycogen synthesis) and triglyceride synthesis (lipogenesis). In the last decade, increasing evidence has emerged to show that nutrients - in particular, glucose and fatty acids - are able to regulate hepatic gene expression in a transcriptional manner. Indeed, although insulin was long thought to be the major regulator of hepatic gene expression, it is now clear that glucose metabolism rather that glucose itself also contributes substantially to the coordinated regulation of carbohydrate and lipid homeostasis in liver. (Dentin *et al.* 2006b)

A diet rich in carbohydrates stimulates the glycolytic and lipogenic pathways, whereas starvation or a diet rich in lipids decreases their activity. The genes encoding enzymes involved in these pathways include glucokinase (GK) (Iynedjian *et al.* 1987), L-pyruvate kinase (L-PK) (Vaulont *et al.* 1986) for glycolysis, ATP citrate lyase (Elshourbagy *et al.* 1990), stearoyl- CoA desaturase (SCD-1) (Ntambi 1992), acetyl CoA carboxylase (ACC) (Katsurada *et al.* 1990), and fatty acid synthase (FAS) (Katsurada *et al.* 1989) for lipogenesis. Most of these enzymes are acutely regulated by posttranslational and allosteric mechanisms and are controlled on a long-term basis by a modulation of their transcription rate. Indeed, it is now clear that glycolytic and lipogenic gene transcription requires both insulin and a high glucose concentration to be fully induced (Foufelle & Ferr´e 2002). The absorption of carbohydrate in the diet leads to changes in glucose plasma concentrations but is also concomitant with changes in the concentrations of the pancreatic hormones insulin, and glucagon. (Postic *et al.* 2007)

Recently, carbohydrate-responsive element–binding protein (ChREBP) was shown to play a pivotal role in the induction of glycolytic and lipogenic genes by glucose (Dentin *et al.* 2004; Iizuka *et al.* 2004) by its capacity to bind to the carbohydrate-responsive element (ChoRE) present in promoters of these target genes (Stoeckman *et al.* 2004); (Ishii *et al.* 2004) ChREBP is expressed in liver and is responsive to the nutritional state. The stimulation of ChREBP by glucose occurs at 2 levels. High glucose and insulin concentrations stimulate ChREBP gene expression (Dentin *et al.* 2004) and also stimulate its translocation from the cytosol to the nucleus, thereby increasing the DNA-binding/transcriptional activity of ChREBP (Kawaguchi *et al.* 2001). The fact that the DNA-binding activity of ChREBP in

nuclear extract of livers from rats fed a high-fat diet is decreased compared with that in rats fed a high-carbohydrate (HCHO) diet suggests that ChREBP may be intimately involved in fatty acid inhibition of glycolysis and lipogenesis (Yamashita et al. 2001); (Kawaguchi et al. 2002); (Dentin et al. 2005a).

Nonalcoholic fatty liver disease (NAFLD) is emerging as one of the most common chronic liver disease in the Western countries. NAFLD, which describes a large spectrum of liver histopathological features including simple steatosis, nonalcoholic steatohepatitis, cirrhosis, and hepatocellular carcinoma (Charlton M. 2004), is associated, in the vast majority of the cases, with obesity, insulin resistance, and type 2 diabetes. Therefore, with the epidemic of obesity and type 2 diabetes, NAFLD has become an important public health issue. (Postic *et al.* 2007)

Nonalcoholic fatty liver disease (NAFLD) is a common clinical condition which is associated with metabolic syndrome in 70% of cases. Inappropriate dietary fat intake, excessive intake of soft drinks, insulin resistance and increased oxidative stress result in increased free fatty acid delivery to the liver, and increased hepatic triglyceride accumulation contributes to fatty liver. Most soft drinks have high fructose corn syrup which often contains 55% fructose and 45% glucose. Soft drinks are a leading source of added sugar worldwide, and have been linked to obesity, diabetes, and metabolic syndrome. The consumption of soft drinks can increase the prevalence of NAFLD independently of metabolic syndrome. During regular soft drinks consumption, fat accumulates in the liver by the primary effect of fructose which increases lipogenesis, and in the case of diet soft drinks, by the additional contribution of aspartame sweetener and caramel colorant which are rich in advanced glycation end products that potentially increase insulin resistance and inflammation (Nseir *et al.* 2010).

Polyunsaturated fatty acids (PUFAs) suppress ChREBP activity by increasing its mRNA decay and by altering ChREBP protein translocation from the cytosol to the nucleus both in primary cultures of hepatocytes and in liver in vivo in mice. The PUFA-mediated alteration in ChREBP translocation is the result of a decrease in glucose metabolism (i.e., an inhibition of the activities of GK and G6PDH, the rate-limiting enzyme of the pentose phosphate pathway) (Dentin *et al.* 2005a).

Since ChREBP cellular localization is a key determinant of its functional activity, a better knowledge of the mechanisms involved in regulating its nucleo-cytoplasmic shuttling and/or its post-translation regulation will be crucial in the future

to develop novel therapeutic approaches for the study of diseases characterized by dysregulations of glucose and/or lipid metabolism. Indeed, ChREBP is translocated in the nucleus under high glucose and insulin concentrations in cultured hepatocytes, it is in contrast retained in the cytosol in the presence of PUFAs, well-known inhibitors of lipogenesis (Postic *et al.* 2007).

Therefore, the aim of this study was to establish an assay to monitor the activation of ChREBP by analyzing cytoplasmatic – nuclear translocation of a green fluorescence – ChREBP hybrid protein (ChREBP-GFP). To this end it was attempted to clone the human ChREBP. The influence of different of sugars and seweeteners (glucose, fructose, saccharin, aspartame, cyclamate, stevioside), monounsaturated fatty acids [oleate (C18:1)] and polyunsaturated fatty acids [linoleate (C18:2), eicosapentanoic acid (C20:5), docosahexaenoic acid (C22:6)] and polyphenols from olive oil (oleuropein) on the activity of cloned human ChREBP was assassed by analyzing the translocation of ChREBP-GFP from cytoplasm to nucleus which was monitored by an automatic fluorescence microscope system.

2- REVIEW OF LITERATURE

2-1. The role of liver on glucose and lipid metabolism

Increased consumption of high-carbohydrate and high-fat (so-called cafeteria diet) is one of the most important risk factors in the development of the metabolic syndrome. Excess carbohydrate is mainly converted to triglyceride in the liver, and excess fat accumulation in the body leads to insulin resistance and metabolic syndrome (Browning & Horton 2004); (Iizuka & Horikawa 2008)

In mammals, the liver is crucial for maintaining overall energy homeostasis and for the conversion of carbohydrate into fat (Figure 1). The absorption of a high carbohydrate diet induces several metabolic events aimed at decreasing endogenous glucose production by the liver and increasing glucose uptake and storage in the form of glycogen. When glucose is delivered into the portal vein in large quantities and hepatic glycogen concentrations are restored, glucose is converted in the liver into lipids (through de novo lipogenesis), which are exported as very-low-density lipoprotein (VLDL) and ultimately stored as triglycerides (TGs) in adipose tissue. The activity of the metabolic pathways leading to the synthesis of lipids in liver is strongly dependent upon the nutritional conditions (Postic *et al.* 2007).

Overflow of fat to liver could be due to increased dietary intake. Even after a short term fat feeding, liver fat increases three fold without increase in visceral or skeletal muscle fat (Samuel *et al.* 2004). Indeed the adipose tissue fat is an indicator of liver fat. The intrahepatic lipids increase by 22% for any 1% increase in total adipose tissue, by 21% for any 1% increase in subcutaneous adipose tissue and by 104% for 1% increase in intra-abdominal adipose tissue (Thomas *et al.* 2005). Thus liver bears the brunt as soon as adipose tissue buffering reaches its limit. Zucker rats (fa/fa) have inactivating mutation in the leptin receptor and hence obese and develops fatty liver. Liver specific correction of leptin receptor deficiency results in reduced TG accumulation in the liver but not in other non-adipose tissues. This could be an example of adipokine mediated communication between adipose tissue and liver. Leptin in conditions of ‘calorie excess’ signals liver to increase lipid oxidation and to down regulate lipid synthesis and thus protect it and other organs from steatosis (Lee *et al.* 2001); (Sanal 2008)

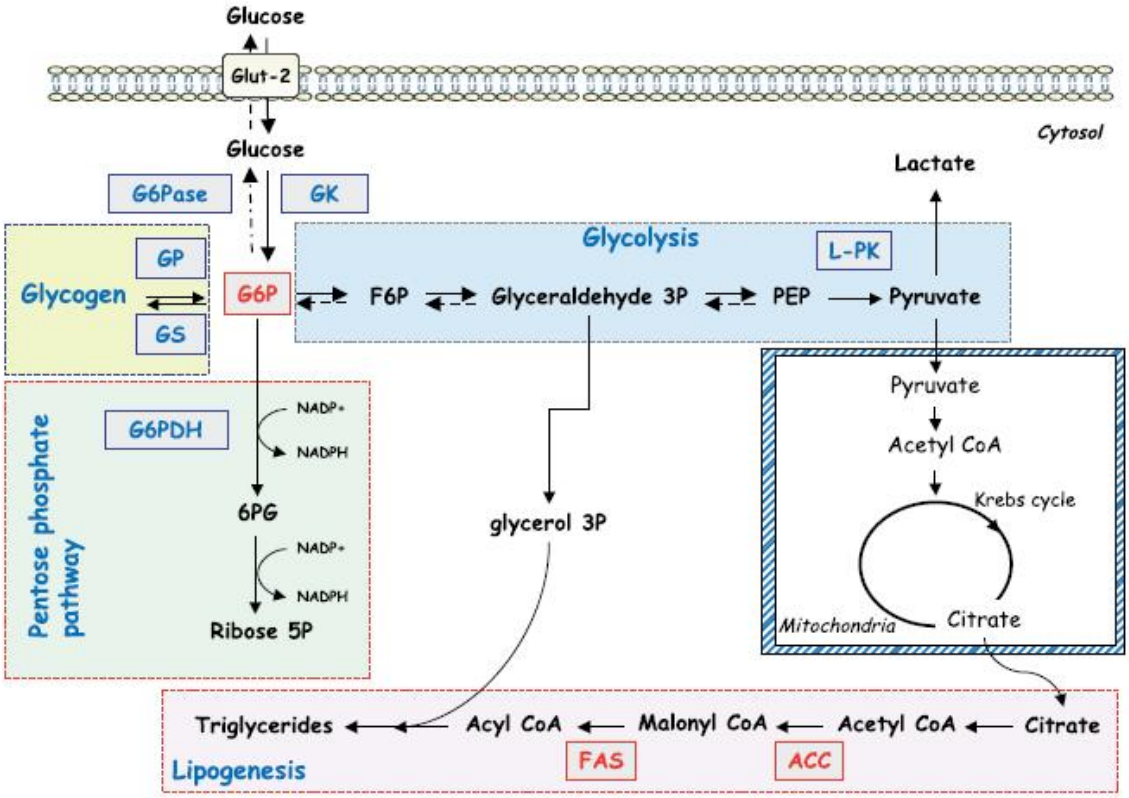

Figure 1. Metabolic pathways leading to the synthesis of triglycerides in liver. (Posticet al. 2007).

2-1-1. Glucose utilization and production in the Liver

Glucose entry into the hepatocyte is mediated by a glucose transporter, GLUT2 (facilitated diffusion), which has a K_m in the 10 mM range and is present constitutively in the plasma membrane (Thorens 1996). Thus, after a meal rich in carbohydrates, the increase in the portal vein glucose concentration (10-15 mM) will result in a proportional increase in glucose influx into hepatocytes. Glucose will then be phosphorylated by glucokinase (GK; hexokinase IV), which, in contrast with other hexokinases, is not inhibited by glucose 6-phosphate, the product of the reaction. Hepatic GK is regulated by a 68 kDa regulatory protein, glucokinase regulatory protein (GKRP) (Vandercammen & Van Schaftingen 1990); (Van Schaftingen *et al.* 1994). GKRP is located mainly in the nucleus of hepatocytes, whereas GK translocates between the nucleus and the cytoplasm. GK binds to GKRP in the nucleus at low glucose concentrations, and is translocated to the cytoplasm at elevated plasma glucose or fructose concentrations (Agius *et al.* 1995).

The K_m for glucose in this system (GK / GKRP) is in the 15-20 mM range. The kinetic characteristics of the glucose transport and phosphorylation steps in hepatocytes imply that the rate of phosphorylation of glucose is proportional to its plasma concentration. Glucose 6-phosphate can then enter several pathways: glycogen synthesis, glycolysis and the pentosephosphate pathway. In the liver, the major function of glycolysis may be to provide pyruvate not for oxidative purposes, but rather for de novo lipogenesis. When glucose is the main substrate used for fatty acid synthesis, the enzymes of the glycolytic pathway can then be considered as an extended part of the lipogenic pathway. The pentose-phosphate pathway is also directly related to lipogenesis, since it can provide the NADPH necessary for the final synthesis of acyl-CoA in the reaction catalysed by fatty acid synthase (FAS). During fasting, or if the carbohydrate content of the diet is low, glucose will be produced by the liver and glucose utilization is then inhibited. Glucose production arises first from the glycogen stores (a maximum of 70-80 g in a human individual) through a pathway called glycogenolysis, which is tightly regulated through successive cascades of enzyme phosphorylation (Bollen *et al.* 1998). Then, when the glycogen stores are depleted, glucose is produced de novo from precursors such as lactate, alanine or glycerol through a pathway called gluconeogenesis, which utilizes some of the reversible enzymatic steps of glycolysis, but also has specific steps catalysed by pyruvate carboxylase, phosphoenolpyruvate carboxykinase (PEPCK), frucose-1,6-bisphosphatase and glucose- 6-phosphatase (Glc-6-Pase) (Hue 2001); (Foufelle & Ferr´e 2002)

Plasma glucose levels stimulate lipogenesis via several mechanisms. First, glucose itself is a substrate for lipogenesis. By being glycolytically converted to acytel-CoA, glucose promotes fatty acid synthesis. Secondly, glucose induces the expression of lipogenic genes. Finally, glucose increase lipogenesis by stimulating the release of insulin and inhibiting the release of glucagon from the pancreas (Kersten 2001).

The conversion of glucose into fatty acids through de novo lipogenesis is nutritionally regulated and both glucose and insulin signaling pathways are elicited in response to dietary carbohydrates to synergistically induce glycolytic and lipogenic gene expression. (Denechaud *et al.* 2008b).

2-1-2. Insulin regulation of hepatic gene expression

Insulin is essential for the maintenance of carbohydrate and lipid homeostasis. Insulin is secreted by pancreatic β cells in response to increased circulating levels of glucose after a meal, a large fraction of glucose absorbed from the small intestine is immediately taken up by hepatocytes, which convert it into glycogen. However, when the liver is saturated with glycogen (roughly 5% of liver mass), any additional glucose taken up by hepatocytes is shunted into pathways leading to synthesis of fatty acids, which will be esterified into TG to be exported to adipose tissue as very low-density lipoproteins (VLDLs). Insulin inhibits lipolysis in adipose tissue by inhibiting hormone-sensitive lipase (HSL), the enzyme regulating FFA release from adipose tissue (Carmen & Victor 2006). Insulin has a "fat-sparing" effect by driving most cells to preferentially oxidize carbohydrates instead of fatty acids for energy. Insulin also regulates glucose homeostasis at many sites, reducing hepatic glucose production (HGP) (via decreased glucose biosynthesis [gluconeogenesis] and glycogen breakdown [glycogenolysis]) and increasing the rate of glucose uptake, primarily into skeletal muscle and adipose tissue.(Postic & Girard 2008)

Insulin is known to modulate the expression of over 100 genes at the transcriptional level in mammals. The transcriptional effects of insulin are widespread and concern multiple biological phenomena. In the liver, the transcription of most of the genes encoding metabolic enzymes is induced by insulin. The genes that are inhibited by insulin are limited, and encode mainly enzymes involved in hepatic glucose production (O'Brien & Granner 1996), (O'Brien *et al.* 2001). In the last few years, important progress has been made in the identification of the partners involved in the events following insulin binding to its receptor. In contrast, the factors involved in the transcriptional effects of insulin were, until recently, largely unknown [although insulin response elements (IREs) have been identified in some genes], despite intensive studies on the two well known insulin-responsive genes, namely those encoding GK and PEPCK (phosphoenolpyruvate carboxykinase). (Foufelle & Ferr´e 2002)

2-1-3. Expression of glycolytic/lipogenic and gluconeogenic genes is regulated by carbohydrate availability in the diet

The expression of several key glycolytic and lipogenic enzymes in the liver is induced by a high-carbohydrate diet (Figure 2): GK (Iynedjian *et al.* 1987), 6-phosphofructo-1-kinase (Rongnoparut *et al.* 1991), 6-phosphofructo-2-kinase} fructose-2,6-bisphosphatase (Colosia *et al.* 1988), aldolase B (Weber *et al.* 1984) and liver pyruvate kinase (L-PK) (Vaulont *et al.* 1986) for glycolysis; ATP citrate-lyase (Elshourbagy *et al.* 1990), acetyl-CoA carboxylase (ACC) (Pape *et al.* 1988), FAS (Katsurada *et al.* 1989) and stearoyl- CoA desaturase (Ntambi 1992) for lipogenesis; and glucose-6-phosphate dehydrogenase (Katsurada *et al.* 1989) and 6-phosphogluconate dehydrogenase (Miksicek & Towle 1983) for the pentose-phosphate pathway. The transcription of the GK gene can be up-regulated in the presence of a high insulin concentration (Iynedjian *et al.* 1989). The genes encoding L-PK, FAS, ACC, S14 and stearoyl-CoA desaturase require both increased insulin and glucose concentrations in order to be induced (O'Callaghan *et al.* 2001). Finally, PEPCK expression can be down-regulated independently by insulin (Sasaki *et al.* 1984) or glucose (Cournarie *et al.* 1999). Interestingly, the transcription of these genes is also modulated by glucagon in the opposite direction compared with insulin (Foufelle & Ferr´e 2002).

Indeed, a diet rich in carbohydrates stimulates the glycolytic and lipogenic pathways, whereas starvation or a diet rich in lipids decreases their activity. The genes encoding enzymes involved in these pathways include glucokinase (GK) (Iynedjian *et al.* 1987), L-pyruvate kinase (L-PK) (Vaulont *et al.* 1986) for glycolysis, ATP citrate lyase (Elshourbagy *et al.* 1990), stearoyl- CoA desaturase (SCD-1) (Ntambi 1992), acetyl CoA carboxylase (ACC) (Katsurada *et al.* 1990), and fatty acid synthase (FAS) (Katsurada *et al.* 1990) for lipogenesis (Figure 1). Most of these enzymes are acutely regulated by posttranslational and allosteric mechanisms but are also controlled on a long-term basis by a modulation of their transcription rate. Indeed, it is now clear that glycolytic and lipogenic gene transcription requires both insulin and a high glucose concentration to be fully induced (Foufelle & Ferr´e 2002). The absorption of carbohydrate in the diet leads to changes in glucose concentrations but is also concomitant with changes in the concentrations of pancreatic hormones, insulin, and glucagon. Fatty acids utilized for the

synthesis of TG in liver are available from the plasma nonesterified fatty acid pool as well as from fatty acids newly synthesized through hepatic de novo lipogenesis. TGs can then be stored as lipid droplets within the hepatocytes or secreted into the blood as VLDLs; they can also be hydrolyzed and the fatty acids channeled toward β oxidation (Marchesini *et al.* 2001); (Postic *et al.* 2007)

Although storage as triglycerides is the principal energy storage fuel in mammals, excessive accumulation of triglycerides in tissues, including liver, is associated with insulin resistance and enhanced cellular apoptosis (i.e., lipotoxicity) (Unger & Orci 2002). The excessive accumulation of cellular lipids is due to an increased expression of enzymes from the glycolytic and lipogenic pathway combined with the impaired entry of fatty acids into the mitochondrial B-oxidation pathway. Therefore, understanding the transcriptional control of glycolytic and lipogenic gene expression not only by fatty acids but also by glucose seems important in both physiology and physiopathology and may yield novel information regarding the treatment and the prevention of the pathogenesis of hepatic insulin resistance and type 2 diabetes (Dentin *et al.* 2006b).

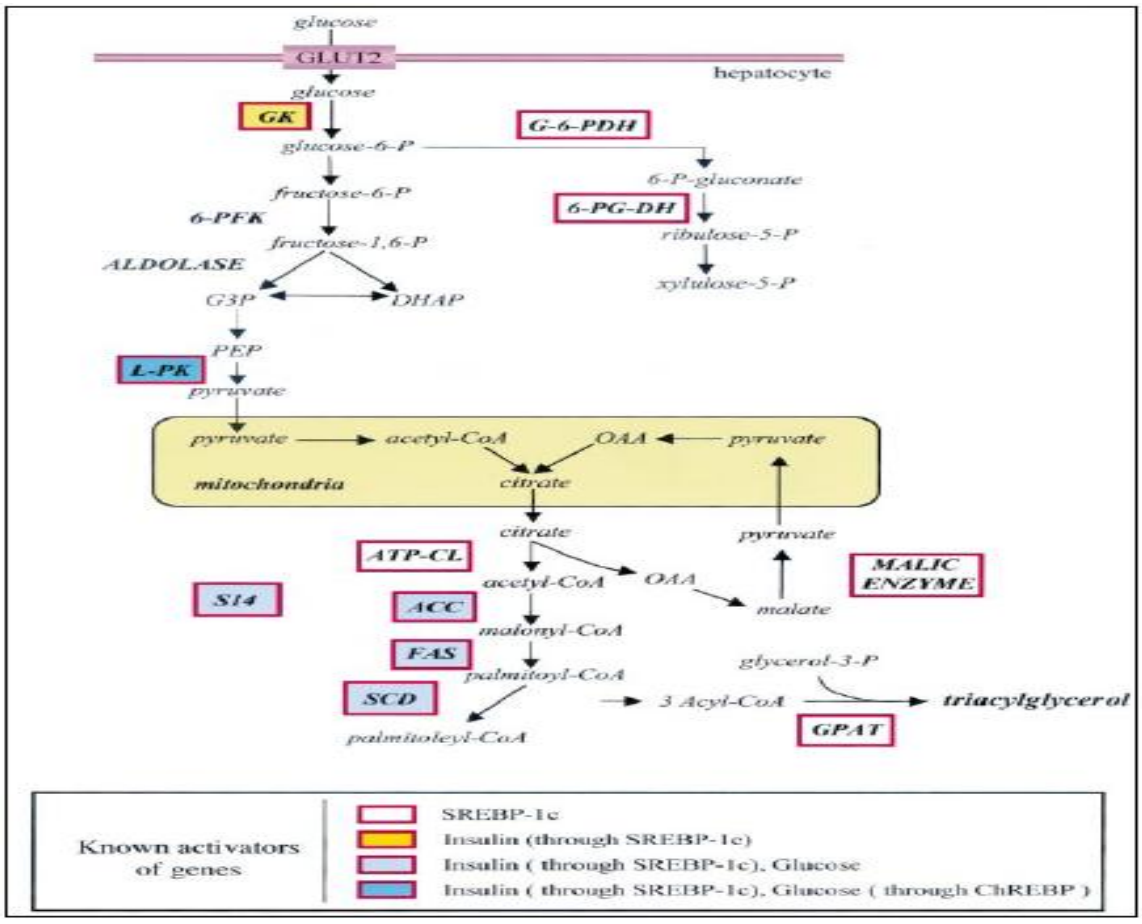

Figure 2. Glycolytic and lipogenic pathways in the liver.

All enzymes indicated in this Scheme are induced at a transcriptional level by a high-carbohydrate diet. Known activators of their transcription are shown at the bottom of the Scheme. Abbreviations used : ATP-CL, ATP citrate-lyase ; DHAP, dihydroxyacetone 3-phosphate ; G-6-PDH, glucose-6-phosphate dehydrogenase ; GPAT, glycerol-phosphate acyltransferase ; G3P, glyceraldehyde 3-phosphate ; OAA, oxaloacetate ; 6-PG-DH, 6-phosphogluconate dehydrogenase ; PEP, phosphoenolpyruvate ; P, phosphate ; 6-PFK, 6-phosphofructo-1-kinase ; SCD, stearoyl-CoA desaturase. (Foufelle & Ferr´e 2002)

2-2. ChREBP (Carbohydrate responsive element –binding protein)

Carbohydrate-responsive element–binding protein (ChREBP) was shown to play a pivotal role in the induction of glycolytic and lipogenic genes by glucose (Dentin *et al.* 2004), (Iizuka *et al.* 2004) by its capacity to bind to the carbohydrate-responsive element (ChoRE) present in promoters of these target genes (Stoeckman *et al.* 2004), (Ishii *et al.* 2004). ChREBP is expressed in many tissues including liver where it is responsive to the nutritional state, (Dentin *et al.* 2005a). ChREBP mediates the transcriptional effect of glucose on both glycolytic (L-PK) and lipogenic (ACC, FAS) gene expression (Dentin *et al.* 2004); (Postic *et al.* 2007)

2-2-1. ChREBP gene

WILLIAMS-BEUREN SYNDROME region 14 (Wbscr 14) was first identified as a gene region for a transcription factor bearing basic helix-loophelix leucine zipper (bHLHZip) structure (Cairo *et al.* 2001). This gene is among at least 14 deleted genes in patients with Williams- Beuren syndrome, which is characterized by various clinical symptoms, including mental retardation, heart abnormalities, unique personality profile, growth retardation, and hypercalcemia (Tassabehji 2003); (He *et al.* 2004).

Uyeda et al. successfully purified a transcription factor that bind to the rat L-PK ChoRE (Yamashita *et al.* 2001). This transcription factor is the same as the Williams-Beuren syndrome critical region 14 (WBSCR14) protein, which is now renamed the carbohydrate response element binding protein (ChREBP) (Cairo *et al.* 2001) with the gene symplol MLXIPL (MLX interacting protein-like). Williams-Beuren syndrome is a

neuro-developmental disorder affecting several systems, and is caused by a heterozygous deletion in chromosomal region 7q11.23 in human. WBSCR14/ChREBP is expressed as a 4.2kb transcript, and the WBSCR14/ChREBP locus encompasses 33kb of genomic DNA with 17 exons (de Luis *et al.* 2000); (Iizuka & Horikawa 2008).

2-2-2. ChREBP protein

ChREBP (864 amino acids and Mr = 94,600) contains several domains, including a nuclear localization signal (NLS) near the N-terminus, polyproline domains, a basic loop-helixleucine- zipper (b/HLH/Zip), and a leucinezipper- like (Zip-like) domain (Figure 3). ChREBP was identified as the long-sought glucose-responsive transcription factor. ChREBP contains several potential phosphorylation sites for cAMP-dependent protein kinase (PKA) and AMP-activated protein kinase (AMPK) (Kawaguchi *et al.* 2001); (Dentin *et al.* 2006b) Mlx (Max-like protein X) that interacts with the bHLH/LZ domain of ChREBP (Figure 3). Mlx is a member of the Myc/Max/Mad family of transcription factors that can serve as a common interaction partner of a transcription factor network (Meroni *et al.* 2000). The evidence that Mlx is the partner of ChREBP was demonstrated using an adenovirus expressing a dominant negative form of Mlx (Ma *et al.* 2005); (Postic *et al.* 2007).

ChREBP requires an interaction partner, Mlx, to efficiently bind to ChoRE sequences and exert its functional activity (Stoeckman *et al.* 2004). Mlx is a basic helix-loop helix/ leucine zipper protein that heterodimerizes with several partners, including ChREBP; MondoA, a paralog of ChREBP expressed predominantly in skeletal muscle, and the repressors Mad1, Mad4, and Mnt (Billin *et al.* 2000), (Meroni *et al.* 2000).

Expressing a dominant negative form of Mlx in hepatocytes completely inhibits the glucose response of a number of lipogenic enzyme genes, including PK, S14, ACC, and FAS (Ma *et al.* 2005). This inhibition is rescued by overexpressing ChREBP but not MondoA. Therefore, Mlx is an obligatory partner of ChREBP in regulating glucose-responsive lipogenic enzyme genes (Ma *et al.* 2006).

The inhibition by a dominant negative form of Mlx directly interferes with the endogenous ChREBP/Mlx complex and abrogates the glucose response of the ACC reporter gene in primary cultures of hepatocytes (Ma *et al.* 2005). This glucose response, however, can be partially restored when ChREBP is overexpressed. The fact that this

rescue only occurs at high concentrations of recombinant ChREBP adenovirus suggests that sufficient ChREBP needs to be provided in the cell in order to titrate out the dominant negative effect of Mlx. (Postic *et al.* 2007).

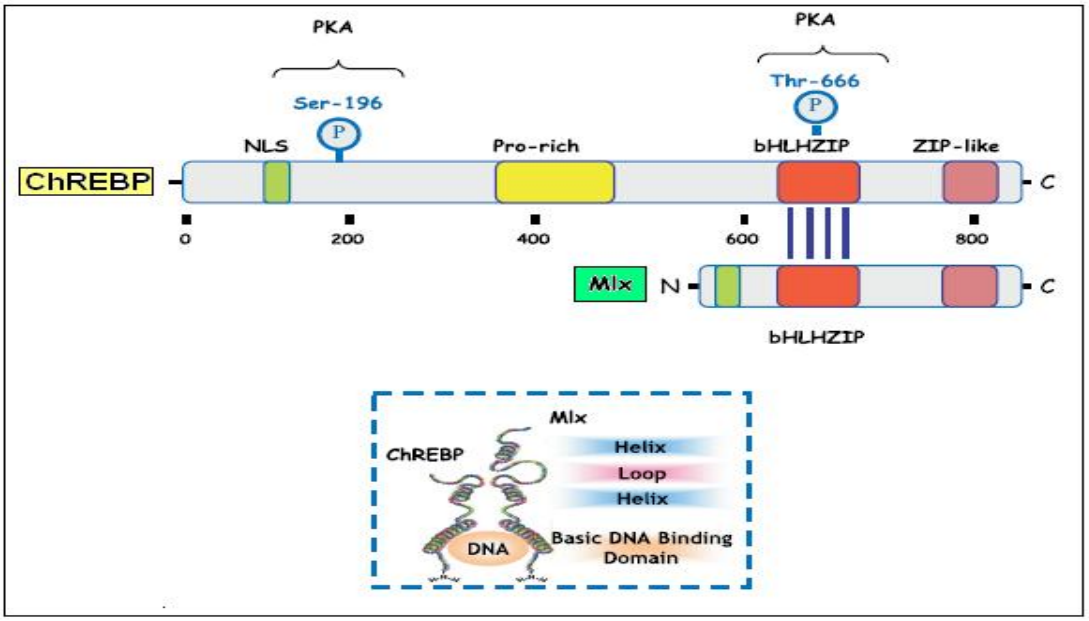

Figure 3. ChREBP and Mlx protein structures. (Postic et al. 2007)

2-2-3. ChREBP function

High carbohydrate intake stimulates the transcription of most genes in the de novo lipogenesis pathway, including enzymes involved in glycolysis [glucokinase and pyruvate kinase (PK)], in fatty acid synthesis [acetyl- CoA carboxylase (ACC) and fatty acid synthase (FAS)] and in NADPH production (malic enzyme) (Vaulont *et al.* 2000). Two signaling pathways control the transcription of lipogenic enzymes: the well known insulin signaling pathway and a less well characterized glucose signaling pathway (Towle 2005). For example, full induction of ACC and FAS mRNA levels requires both glucose metabolism and insulin (Koo *et al.* 2001). A cis-acting sequence that activates the transcription of several lipogenic enzyme genes in response to glucose has been identified. This sequence, designated as the carbohydrate response element (ChoRE), consists of two E box-like motifs related to the consensus sequence CACGTG that are separated by 5 bp (O'Callaghan *et al.* 2001). The two E box sequences are usually not exact fits to the CACGTG consensus, most often matching at four or five positions to the 6 bp consensus. However, the spacing between them within the ChoRE is critical for the

transcriptional response to glucose. All naturally occurring ChoREs analyzed to date have a 5 bp spacing between their two E box motifs. Mutations that change this spacing to 6 bp result in a strongly impaired glucose response, whereas mutations to 4 bp result in a complete loss of the response (Shih *et al.* 1995). This stringent spacing requirement suggests that proteins binding to the two E box motifs might interact sterically (Ma *et al.* 2007). The emergence of ChREBP in the control of lipogenic gene expression in liver prompted us to address its role in the physiopathology of hepatic steatosis. (Marchesini *et al.* 2001). The metabolic and physiological roles of ChREBP may not be limited to the liver. In fact, the function of this transcription may be broader and of particular interest in other sites of expression, including white adipose tissue, brain, and pancreatic β cells (Figure 4) (da Silva Xavier *et al.* 2006).

ChREBP is not only required for the carbohydrate-induced transcriptional activation of enzymes involved in de novo fatty synthesis but also in TG synthesis, since gene expression was significantly decreased after short hairpin RNA against ChREBP treatment in ob/ob mice. Therefore, ChREBP appears to act as a central modulator of fatty acid concentrations in liver by transcriptionally controlling most of the lipogenic program (ACC, FAS, SCD-1), TG synthesis (at the level of glyceraldehydes 3-phosphate acyltransferase), and potentially VLDLexport (R. Dentin&C. Postic, unpublished observations) (Postic *et al.* 2007).

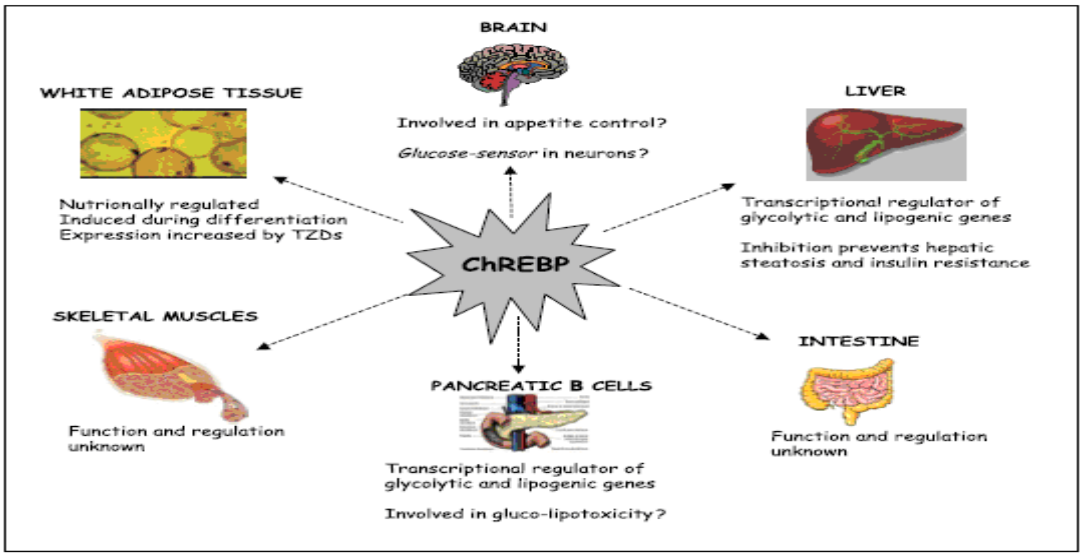

Figure 4. The multiple functions of carbohydrate-responsive element-binding protein (ChREBP). (Postic et al. 2007)

Consequently to adenovirus-mediated inhibition of ChREBP in liver of ob/ob mice, lipogenesis and triglyceride (TG) synthesis are decreased. As a result, the restored inhibition of genes from the gluconeogenic pathway (G6Pase and PEPCK) by insulin leads to the improvement of blood glucose levels. Correction of hepatic steatosis also leads to decreased levels of plasma TG and nonesterified fatty acids (NEFA). As a consequence, insulin sensitivity is restored in skeletal muscles and glycogen synthesis is enhanced, therefore contributing to the decrease in blood glucose concentrations observed. The overall phenotype is a significant improvement in hyperglycemia, hyperinsulinemia and hyperlipidemia. Adapted from Dentin et al. (Dentin et al. 2006a); (Denechaud et al. 2008b).

ChREBP gene expression was reported in the brain, a tissue in which this transcription factor could play a role in the sensing of glucose (Iizuka *et al.* 2004) (Figure 4). Because of leptin deficiency, ob/ob mice are hyperphagic. Interestingly, food consumption was significantly reduced in ob/ob-ChREBP−/− mice and was associated with a 30% decrease in the expression of the appetite-stimulating neuropeptide AgRP. Whether ChREBP directly controls food intake or indirectly controls it through AgRP expression needs to be further addressed (Postic *et al.* 2007).

2-2-3-1. ChREBP and SREBP (Sterol regulatory element binding protein-1c)

The transcription factor SREBP- 1c (sterol regulatory element binding protein-1c) has previously emerged as a major mediator of insulin action on lipogenic genes, such as acetyl CoA carboxylase (ACC) and fatty acid synthase (FAS) (Foufelle & Ferr´e 2002) (Figure 5). However, SREBP-1c activity alone is not sufficient to account for the stimulation of glycolytic and lipogenic gene expression in response to carbohydrate since SREBP-1c gene deletion in mice only results in a 50% reduction in fatty acid synthesis (Liang *et al.* 2002). More importantly, L-pyruvate kinase (L-PK), one of the rate-limiting enzyme of glycolysis is exclusively dependant on glucose (Decaux *et al.* 1989) and is not subjected to SREBP-1c regulation (Stoeckman & Towle 2002). (Denechaud *et al.* 2008b)

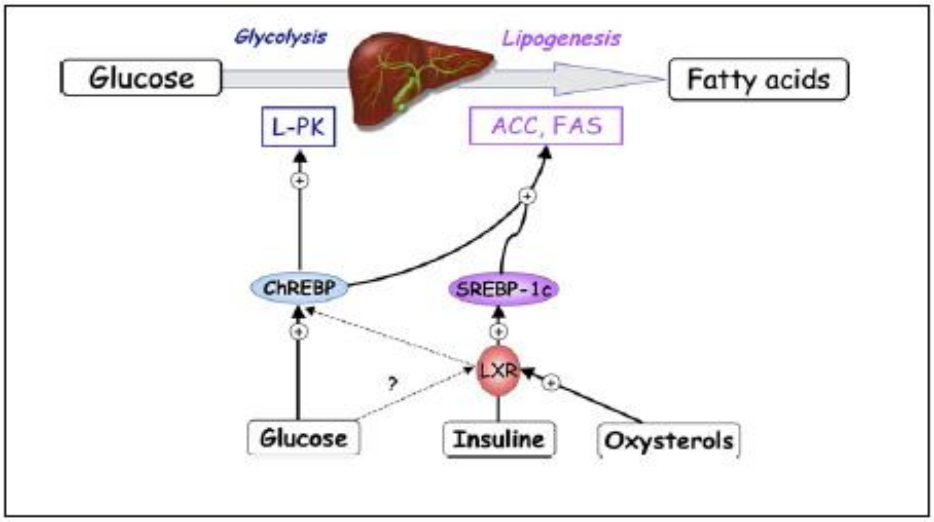

Figure 5. Transcriptional control of glycolysis and lipogenesis.(Denechaud et al. 2008b)

SREBPs are synthesized in a precursor form that is bound to the endoplasmic reticulum (ER) and nuclear membranes. They all have a common tripartite structure: (i) an N-terminal fragment of ≈ 480 amino acids, which is in fact a transcription factor of the basic domain helix-loop-helix leucine zipper ´(bHLH-LZ) family; (ii) a central domain of 80 amino acids containing two transmembrane sequences separated by 31 amino acids that are in the lumen of the ER; and (iii) a regulatory C-terminal domain of ≈ 590 amino acids. The transcriptional part of SREBPs (which allowing dimerization, nuclear import and DNA binding) is composed of a stretch of acidic amino acids comprising the transactivation domain, a domain rich in proline residues, and a bHLH-LZ domain. Unlike other bHLH-LZ transcription factors, which contain a well conserved arginine residue in their basic domain, SREBPs have a tyrosine residue. This amino acid substitution allows SREBPs to bind on both E-boxes (5´- CANNTG-3´, where N represents any base), like all bHLH proteins, and also SRE (sterol regulatory element) sequences (5´- TCACNCCAC-3´). The importance of this tyrosine residue for binding on SRE sequences was demonstrated by Kim et al. (Kim *et al*. 1995), who changed it to an arginine residue, as is present in other bHLH transcription factors. The resulting protein bound only on E-boxes. Conversely, mutation of the arginine residue of upstream stimulatory factor (USF), a classic bHLH-LZ protein, into a tyrosine allows its binding on both E-boxes and SRE sequences (Kim *et al*. 1995). (Foufelle & Ferr´e 2002)

SREBP was first discovered as a transcription factor that controls genes involved in the biosynthesis of cholesterol (Brown & Goldstein 1997), more recently the SREBP-1c isoform has emerged as a major mediator of insulin action on hepatic GK (Foretz *et al.* 1999a) and lipogenic gene expression (Foufelle & Ferr´e 2002). To illustrate this point Kim et al. (Kim *et al.* 2004) have identified two functional sterol regulatory elements (SRE) in the rat GK promoter. The authors demonstrate that SREBP-1c can bind to these SREs and activate the GK promoter. The physiological in vivo interaction between the SREBP-1c protein and SREs of the GK promoter was confirmed by chromatin immuno precipitation (ChIP) assay using primary cultures of hepatocytes, demonstrating the direct involvement of SREBP-1c on GK gene expression. SREBP-1c also inducees other lipogenic genes by its capacity to bind to SREs present in their promoters (Magaå & Osborne 1996) (Figure 6). SREBP-1c itself is rapidly induced by insulin in primary cultures of hepatocytes (Foretz *et al.* 1999b), providing a pathway for insulin mediation of lipogenic gene expression (Horton *et al.* 1998). In addition, transgenic mice that overexpress SREBP-1c in the liver exhibit liver steatosis and increased mRNA of most lipogenic genes (Shimomura *et al.* 1998). Consistent with these observations, SREBP-1c gene knock-out mice have an impaired ability to fully induce lipogenic gene expression after high carbohydrate feeding (Liang *et al.* 2002). The effect of insulin on SREBP-1c was corroborated by in vivo studies showing that SREBP-1c expression were low in livers of diabetic rats, and increased markedly after insulin treatment (Shimomura *et al.* 1999).

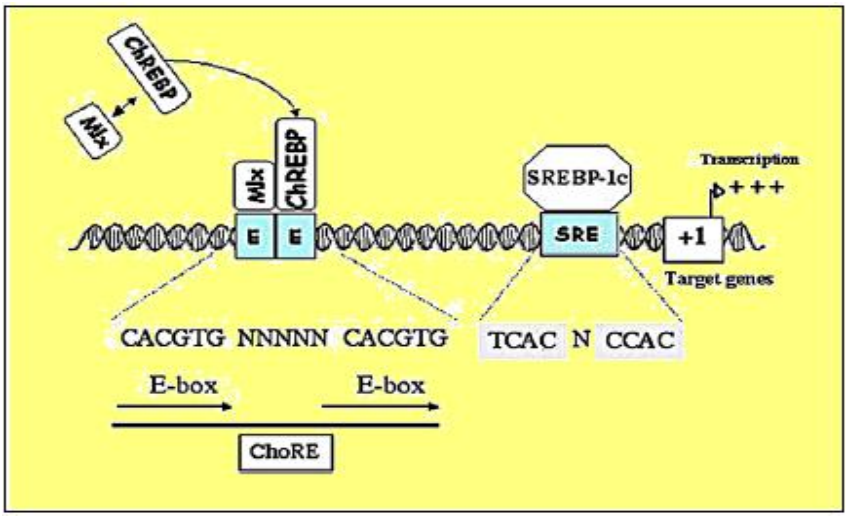

Figure 6. Schematic roles of ChREBP and SREBP-1c in the regulation of glycolytic and lipogenic gene expression in response to insulin and glucose.

Most lipogenic genes (FAS, ACC) have carbohydrate responsive element (ChoRE) for binding the ChREBP–Mlx complex and sterol responsive element (SRE) for binding SREBP-1c, identified through promoter-mapping analysis. The ChREBP–Mlx complex and SREBP-1c act in synergy to induce lipogenic gene in response to high glucose and insulin concentration. (Dentin *et al.* 2005b)

In the fed state, glucose and insulin coordinate hepatic lipogenesis by regulating glycolytic and lipogenic gene expression at the transcriptional level. ChREBP and SREBP 1c share lipogenic genes and genes related to the hexose monophosphate (HMP) shunt (Ma *et al.* 2006). Some groups have reported that hepatic glucokinase is required for the synergistic effects of ChREBP and SREBP 1c on glycolytic and lipogenic gene expression (Figure 7) (Dentin *et al.* 2004). Uyeda et al. Showed that glucose-activated ChREBP directly binds the ChoRE of the L-PK promoter and activates L-PK gene expression (Yamashita *et al.* 2001). However, whether SREBP 1c physiologically mediates the action of insulin on glucokinase remains controversial. The overexpression of dominant active SREBP 1c induce glucokinase gene expression in hepatocytes. However, Liang et al . reported that the response of glucokinase to high-carbohydrate diet refeeding is still conserved in SREBP 1c knockout mice (Liang *et al.* 2002). In addition, Iynedjian et al . reported that SREBP 1c cannot bind to liver-type glucokinase promoter (Hansmannel *et al.* 2006), and Pichard et al .reported that SREBP 1c knockdown by small interfering RNAs results in impaired induction of the FAS gene in response to glucose and insulin but dose not prevent induction of the glucokinase gene (Gregori *et al.* 2006). Glucokinase is a key molecule regulation glycolytic flux, and it is important to identify the various transcription factors that mediate the activation of glucokinase gene expression gene by insulin.

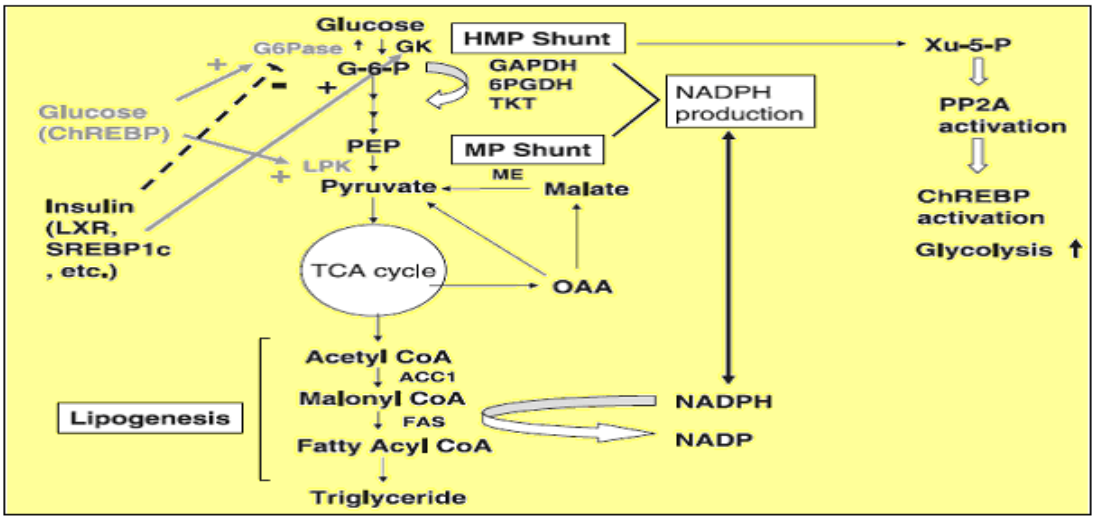

Figure 7. ChREBP and SREBP-1c regulate different steps in glycolysis and gluconeogenesis.

ChREBP and SREBP share the regulation of lipogenesis and the hexose monophosphate (HMP) and malatepyruvate (MP) shunts. Glucose and insulin activate LPK and GK respectively .Glucose also activates G6Pase but insulin inhibits it. (Iizuka & Horikawa 2008)

SREBP-1c plays a major role in the long-term control of glucose and lipid homeostasis by insulin, through the regulation of glycolytic and lipogenic gene expression. Indeed, the induction of glycolytic and lipogenic genes in response to a high carbohydrate diet, although significantly diminished, is not completely suppressed in SREBP-1c knockout mice (Liang *et al.* 2002). Using hepatic GK knockout mice (hGK-KO) (Postic *et al.* 1999), that overexpression of a constitutive active form of SREBP-1c in hGK-KO hepatocytes cultured in the presence of high glucose concentration (25 mM) did not fully induce glycolytic and lipogenic genes compared to what was observed in control hepatocytes (Dentin *et al.* 2004). Therefore, glucose metabolism via GK and SREBP-1c exerts a synergistic effect on the expression of glycolytic and lipogenic genes.

2-2-3-2. ChREBP and LXR (liver X receptors)

ChREBP was also recently identified as a direct target of liver X receptors (LXRs) (Cha & Repa 2007) (Figure5). LXRs are ligand-activated transcription factors that belong to the nuclear hormone receptor superfamily (Mangelsdorf *et al.* 1995). LXRs play a central role in cholesterol and bile acid metabolisms (Zelcer & Tontonoz 2006) but are

also important regulators of the lipogenic pathway (Ulven *et al.* 2005) through the transcriptional control of SREBP-1c (Chen *et al.* 2004), FAS (Joseph *et al.* 2002) ACC (Zhang *et al.* 2003) and stearoyl-CoA desaturase 1 (SCD-1) (Chu *et al.* 2006), the enzyme required for the biosynthesis of monounsaturated fats, palmitoleate and oleate from saturated fatty acids (Flowers *et al.* 2006). In fact, LXRs are central for the insulin-meditated induction of SREBP-1c (Chen *et al.* 2004). Known ligands of LXRs are oxysterols but, interestingly, glucose was also recently shown to activate LXRs and to induce their target genes, including ChREBP (Figure 5) (Mitro *et al.* 2007). This study directly implicated LXRs as master regulators of the glucose-signaling pathway and challenged the role of previously recognized glucose-sensors such as glucokinase (GK), the first enzyme of the glycolytic pathway. Indeed, hepatic GK is acting as a glucose-sensor in liver and is required for the expression of ChREBP as well as the subsequent induction of glycolytic and lipogenic genes. However, as raised by Lazar and Wilson (Lazar & Willson 2007) several concerns aroused from the study of Mitro et al. (Mitro *et al.* 2007) including the fact that both D-glucose and L-glucose (which is inactive in most biological reaction including GK activity) were found to activate LXRs (Matschinsky 1996) and that the experiments were performed in HepG2 cells, an hepatoma cell line that respond poorly to glucose. Clearly, studies performed in a physiological context will be necessary to help understand the physiological relevance of LXRs as glucose-sensors in liver. (Denechaud *et al.* 2008b)

Cholesterol homeostasis genes that require LXR for expression are upregulated in liver and intestine of fasted mice re-fed with a glucose diet, indicating that glucose is an endogenous LXR ligand. LXR-a and LXR-b (also called NR1H3 and NR1H2, respectively) are RXR partners that recognize oxidized cholesterol and control gene expression linked to cholesterol and fatty acid metabolism6–8. Activation of LXRs results in decreased atherosclerosis in rodents. LXR ligands have anti-diabetic effects as well, decreasing liver glucose output and increasing peripheral glucose disposal (Laffitte *et al.* 2003); (Mitro *et al.* 2007)

At the transcriptional level, ChREBP also is regulated loosely in several conditions. The level of ChREBP mRNA in liver in the fed state is the same as or twice as high as the level during fasting (Letexier *et al.* 2005). Repa et al. reported that LXR directly regulates ChREBP gene expression at the transcriptional level (Cha & Repa

2007). The mouse ChREBP gene promoter contents a LXR response element at about 2.4 kbp, and LXR agonists increase hepatic ChREBP mRNA in wild- type mice but not in LXR – α double knockout mice. Moreover, Saez et al. reported that LXR is activated by glucose and that high – glucose treatment increased ChREBP mRNA two – fold in HepG2 cells (Mitro *et al.* 2007). Insulin also regulates the expression and transactivity of the LXR gene (Chen *et al.* 2004). However, despite the hyperinsulinemia and hyperglycemia seen in ob/ob mice, the level of ChREBP mRNA in liver of ob/ob mice is only twice as high as in liver of wild type mice (Iizuka *et al.* 2006); (Iizuka & Horikawa 2008)

Several groups have shown that hepatocyte nuclear factor 4α (HNF4α), plays an important complementary role to ChREBP in the induction of L-PK gene expression (Adamson *et al.* 2006). Both ChREBP (the ChoRE, located from -165 to -145 bp with respect to the transcription start site) and HNF4α binding sites (the L3 element, located from -145 to -127 bp) are required for maximal glucose induced transactivation of the L-PK gene (Diaz Guerra *et al.* 1993). While ChREBP and HNF4α have been implicated as contributing factors in the regulation of the L-PK gene by glucose, the mechanisms underlying both the glucose activation and cAMP-mediated repression of this gene are largely unknown. (Burke *et al.* 2009).

2-2-4. Regulation of ChREBP transcriptional activity

ChREBP is regulated in a reciprocal manner by glucose and cAMP. Studies from the Uyeda's laboratory (Kawaguchi *et al.* 2001) established a model in which ChREBP would be localized in the cytosol under basal conditions, and would then be translocated into the nucleus under high glucose concentrations, thereby allowing its binding to the ChoRE present on glycolytic and lipogenic gene promoters. (Dentin *et al.* 2006b)

Dysregulations in hepatic lipid synthesis are often associated with obesity and type 2 diabetes, and therefore a perfect understanding of the regulation of this metabolic pathway appears essential to identify potential therapeutic targets. The transcription factor ChREBP (carbohydrate-responsive element-binding protein) has emerged as a major mediator of glucose action on lipogenic gene expression and as a key determinant of lipid synthesis in vivo (Postic *et al.* 2007).

2-2-4-1. Activiation of ChREBP by Translocation

The stimulation of ChREBP by glucose occurs at 2 levels. High glucose and insulin concentrations stimulate ChREBP gene expression (Dentin *et al.* 2004) and glucose also stimulates its translocation from the cytosol to the nucleus, thereby increasing the DNA-binding/transcriptional activity of ChREBP (Kawaguchi *et al.* 2001). The fact that the DNA-binding activity of ChREBP in nuclear extract of livers from rats fed a high-fat diet is decreased compared with that in rats fed a high-carbohydrate (HCHO) diet suggests that ChREBP may be intimately involved in fatty acid inhibition of glycolysis and lipogenesis (Kawaguchi *et al.* 2002); (Dentin *et al.* 2005a)

Glucose activates ChREBP by stimulating its gene expression and by regulating its entry from the cytosol into the nucleus thereby promoting its binding to carbohydrate responsive element (ChoRE) present in the promoter regions of its target genes (Uyeda & Repa 2006). ChREBP is required for the induction of L-pyruvate kinase (L-PK), which is exclusively dependant on glucose. Induction of FAS and ACC genes is under the combined action of ChREBP and of SREBP-1c in response to glucose and insulin, respectively. (Denechaud *et al.* 2008b)

ChREBP gene expression is induced by glucose in liver both in vitro (primary cultures of hepatocytes) and in vivo (Dentin *et al.* 2004), but there are post-translational modifications that allow for a rapid activation of ChREBP. By transfecting a ChREBP-GFP fusion protein in primary cultures of hepatocytes, Uyeda and coworkers (Kawaguchi *et al.* 2001) first demonstrated that this transcription factor is rapidly translocated from the cytosol into the nucleus in response to high glucose concentrations (27.5 mM). The endogenous ChREBP protein is indeed addressed into the nucleus in response to high glucose concentrations in primary cultures of mouse hepatocytes and in response to a high-carbohydrate diet in liver of mice (Dentin *et al.* 2005a); (Postic *et al.* 2007)

2-2-4-2. Control of ChREBP activity by phosphorylatio/dephosphorylation

During fasting, protein kinase A and AMP-activated protein kinase phosphorylate ChREBP and inactivate its transactivity. During feeding, xylulose-5-phosphate in the hexose monophosphate pathway activates protein phosphatase 2A, which dephosphorylates ChREBP and activates its transactivity (Figure 8). ChREBP controls 50% of hepatic lipogenesis by regulating glycolytic and lipogenic gene expression. In ChREBP $^{-/-}$ mice, liver triglyceride content is decreased and liver glycogen content is

increased compared to wild – type mice. These results indicate that ChREBP can regulate metabolic gene expression to convert excess carbohydrate into triglyceride rather than glycogen. (Iizuka & Horikawa 2008)

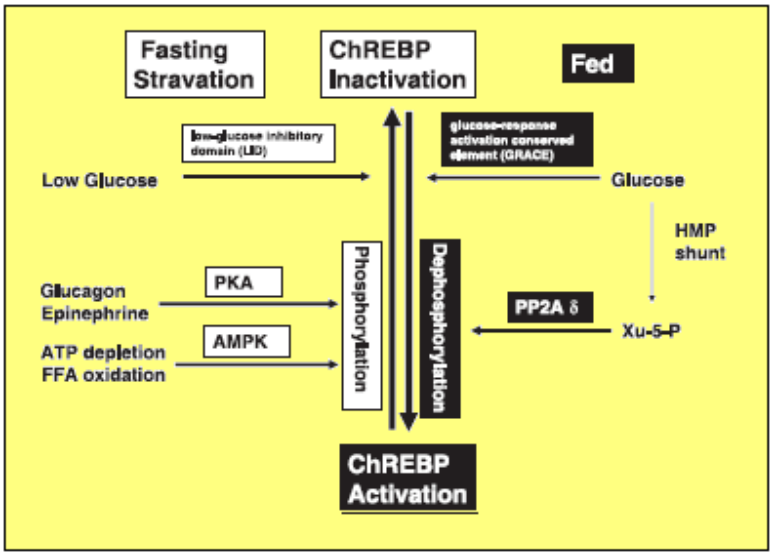

Figure 8. Nutritional conditions determined ChREBP transactivity. (Iizuka & Horikawa 2008)

The nuclear localization signal and basic helix-loop-helixleucine-zipper domains of ChREBP were essential for transcription, and these domains were the targets of regulation by cAMP and glucose. Among three cAMP-dependent protein kinase phosphorylation sites, Ser196 and Thr666 were the target sites. (Kawaguchi *et al*. 2001)

The mechanism responsible for ChREBP nuclear translocation is thought to involve the dephosphorylation of serine residue 196 (Ser-196), target of cAMP dependent protein kinase (PKA) and located near the NLS (Figure 9). ChREBP phosphorylated on Ser-196 is localized in the cytosol. Under high glucose concentrations, protein phosphatase 2A (PP2A) is selectively activated by xylulose 5-phosphate (X5P), an intermediate of the nonoxidative branch of the pentose phosphate pathway, dephosphorylates ChREBP on this particular residue, and allows for its translocation in the nucleus (Kabashima *et al.* 2003). However, because the importance of the PP2A-mediated dephosphorylation of Ser-196 in controlling the translocation process of ChREBP remains to be demonstrated in a physiological context. ChREBP undergoes a second PP2A-mediated dephosphorylation on residue Threonine 666 (Thr-666) that permits its binding to its ChoRE binding site and hence the transcriptional activation of

its target genes (Figure 9). Lange and coworkers (Wu *et al.* 2005) have observed that the phosphorylation status of the endogenous ChREBP protein (using an in-gel phosphoprotein assay) is decreased under conditions of increased glucose flux through hepatic GK. The fact that the overexpression of GK and the lower phosphorylation state of ChREBP were correlated to a 1.5-fold increase in X5P concentrations seems in agreement with the model initially proposed by Uyeda and colleagues (Wu *et al.* 2005). Although there is no doubt that ChREBP is a phosphoprotein, the fact that its activity is activated by dephosphorylation has brought some controversy. Studies from the laboratories of Towle and Chan have strongly challenged these concepts and have suggested that dephosphorylation is not responsible for the activation of ChREBP. The first insight came from the observation that although global phosphorylation of the endogenous ChREBP protein was increased under cAMP conditions, it did not change when hepatocytes were switched from low to high glucose concentrations (Tsatsos & Towle 2006).

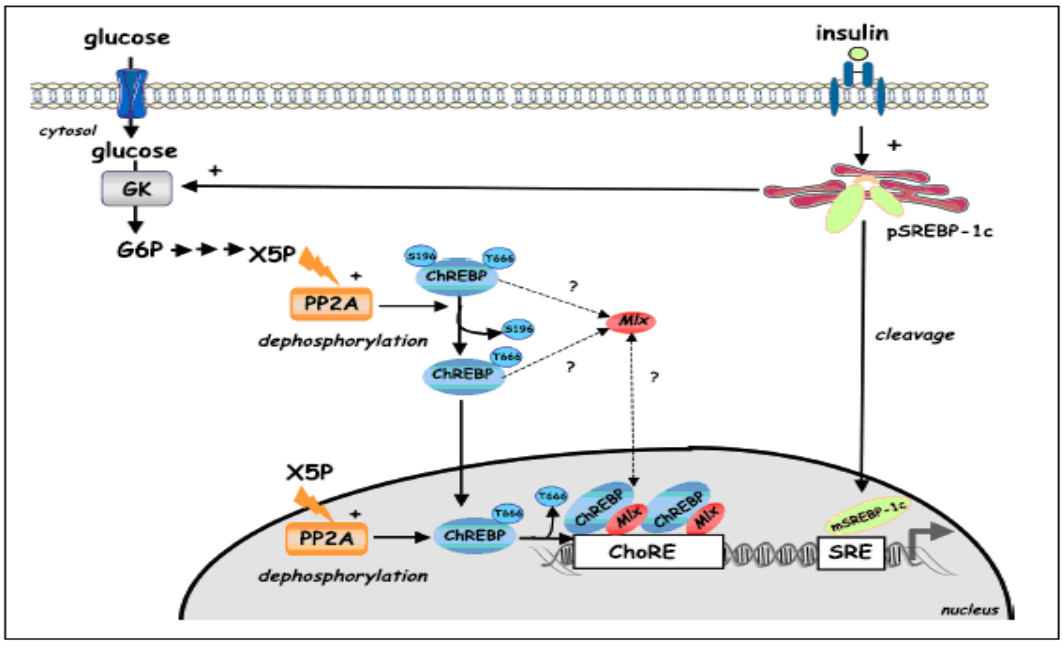

Figure 9. Transcriptional activation of glycolytic and lipogenic genes by ChREBP/Mlx and SREBP-1c in liver. (Postic et al. 2007)

2-2-5. Role of ChREBP in the physiopathology of hepatic steatosis and insulin resistance

2-2-5-1. Obesity

In the past several decade obesity has become extremely common, with prevalence rates skyrocketing among certain groups and communities (Kopelman 2000). In as much as traditional dietary approaches to combat obesity have largely failed, the scientific community has become increasingly interested in the molecular regulation of triglycerides synthesis and in pharmaceutical approaches to reduce fat storage. Accordingly, a heavy research effort is currently directed towards the identification of molecular target for fat storage, and on the development of drugs that specifically reduce adipose tissue mass. (Kersten 2001)

ChREBP deficiency overcomes the fatty liver phenotype, and improves glucose tolerance and insulin resistance in ob/ob mice, suggesting that a reduction of ChREBP activity may have a beneficial effect in the treatment of metabolic diseases associated with hyperglycemia and dyslipidemia. The study by Iizuka and coworkers (Iizuka *et al.* 2006) further underlined the importance of ChREBP in the development of obesity and type 2 diabetes by intercrossing ChREBP knockout mice with ob/ob mice (Iizuka *et al.* 2004; Postic & Girard 2008).

2-2-5-2. Insulin resistance and Diabetes mellitus

ChREBP was associated with a normalization of hepatic insulin signaling in ChREBP knockdown ob/ob mice. Interestingly, insulin sensitivity was restored not only in liver but also in skeletal muscles and adipose tissue, in which a significant improvement in Akt phosphorylation in response to the insulin bolus was observed (Dentin *et al.* 2006a). As a result, glycogen content was restored to control levels in skeletal muscles from shChREBP RNA-treated ob/ob mice. Skeletal muscle is known to play a determinant role in the physiopathology of insulin resistance, and defects in glycogen synthesis have been particularly implicated in its pathogenesis (Petersen & Shulman 2002); (Postic *et al.* 2007)

Hepatic insulin resistance has been associated with steatosis in both rodents (Samuel *et al.* 2004) and humans (Seppala-Lindroos *et al.* 2002). This resistance could result from the contribution of adipose tissue through increased flux of free fatty acids

(FFA) to the liver and by secretion of numerous adipocytokines, which may affect hepatic insulin action. Although the association between hepatic insulin resistance and TG accumulation in liver is clear, the causative role for hepatic insulin resistance in the accumulation of TG has not clearly established. Nevertheless, by markedly preventing TG accumulation in liver of ob/ob mice, ChREBP knockdown significantly restored insulin sensitivity in liver as evidenced by the restoration of protein kinase B (Akt), and Foxo1 phosphorylation by insulin (Dentin *et al.* 2006a). The transcription factor Foxo1 plays a pivotal role in the control of gluconeogenesis by transcriptionnally regulating the expression of PEPCK and G6Pase in liver (Puigserver *et al.* 2002). Insulin-mediated Akt phosphorylation of Foxo1 leads to its nuclear exclusion, ubiquitination and degradation (Matsuzaki *et al.* 2003). The subsequent decrease in nuclear Foxo1 decreases expression levels of PEPCK and G6Pase, thereby decreasing gluconeogenic rates and reducing blood glucose. In agreement with these studies, ChREBP knockdown, by rescuing Foxo1 phosphorylation by insulin, led to an efficient inhibition of PEPCK and G6Pase, associated with a subsequent normalization of blood glucose levels in shChREBP RNA treated-ob/ob mice (Dentin *et al.* 2006a) (Figure10).

Diabetes mellitus (DM) is a chronic metabolic disease with high rates of prevalence and mortality world wide that is caused by an absolute or relative lack of insulin and or reduced insulin activity (Kamtchouing *et al.* 2004). It is characterized by hyperglycemia and long-term complications affecting the eyes, kidneys, nerves, and blood vessels, and is the most common endocrine disorder. Although the leading mechanism of diabetic complications remains unclear, much attention has been paid to the role of oxidative stress. It has been suggested that oxidative stress may contribute to the pathogenesis of different diabetic complications (Ceriello 2000). Furthermore, with diabetes, several features appear including an increase in lipid peroxidation (Gumieniczek 2005), alteration of the glutathione redox state, a decrease in the content of individual natural antioxidants, and finally a reduction in the antioxidant enzyme activities. These changes suggest an oxidative stress caused by hyperglycemia (Chaudhry *et al.* 2007). Many defense mechanisms are involved in alloxan-induced oxidative damage. Among these mechanisms, antioxidants play the role of a free-radical scavenger (Karaoz *et al.* 2002); (JEMAI *et al.* 2009)

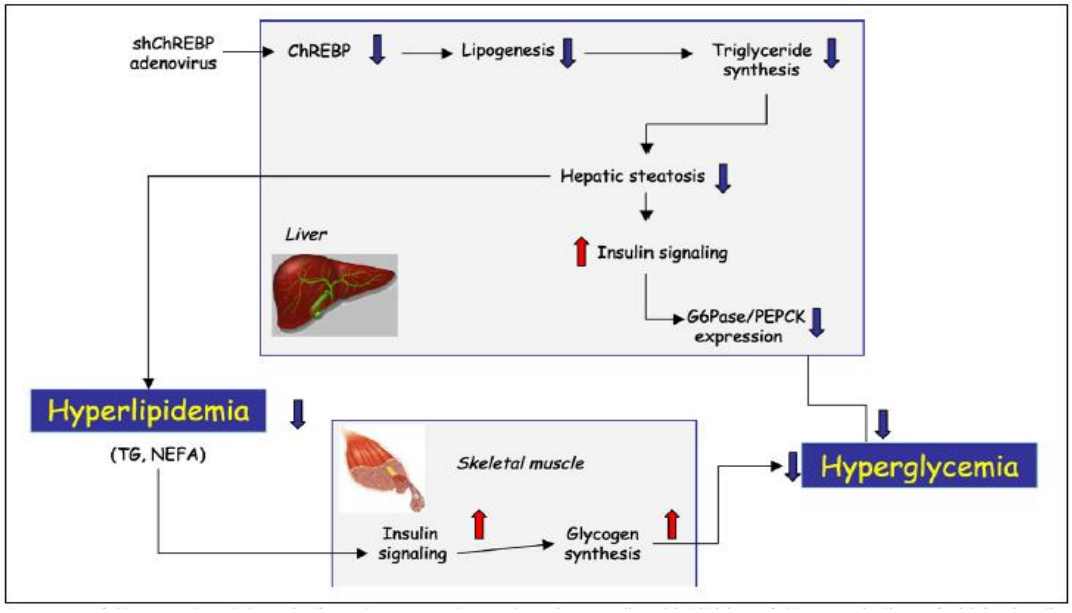

Figure 10. Summary of ChREBP knockdown in liver. (Denechaud et al. 2008b**)**

2-2-5-3. Non-alcoholic fatty liver disease (NAFLD)

Recent studies have reported the association of NAFLD with multiple classical and non-classical risk factors for cardiovascular disease (CVD). Moreover, there is a strong association between the severity of liver histopathology in NAFLD patients and greater carotid artery intima-media thickness and plaque, and lower endothelial flow-mediated vasodilation (as markers of subclinical atherosclerosis) independent of obesity and other metabolic syndrome (MS) components (Mirbagheri *et al.* 2007). Identification of MS is very useful not only as a tool to identify people with cardiovascular and diabetic risk but also NAFLD but much confusion exists in the criteria of MS (Kahn *et al.* 2005b). Criteria for MS should be convenient but flexible to the regional and ethnic differences is important in establishing its association with NAFLD, a disease which progress asymptomatically to cirrhosis (Clark & Diehl 2003). There exists significant genetic environmental and life style diversity in population across different continents and cultures. For example Asian Indians are prone to central obesity and for same degree of weight gain are more insulin resistant (Ferrannini & Balkau 2002); (Sanal 2008)

In recent years, there has been an increasing appreciation for the significance of NAFLD and obesity in Western countries. Estimates of NAFLD in the general population range from 5 to 20%, with up to 75% of patients with obesity and type 2 diabetes (Angulo 2002). Hepatic steatosis is often associated with altered liver function,

hyperlipidemia, and progression to liver cirrhosis (Marchesini *et al.* 1999). Studies have demonstrated an important role for hepatic steatosis in the pathogenesis of insulin resistance, including increased gluconeogenesis and fasting hyperglycemia in patients with type 2 diabetes (Petersen *et al.* 2005); (Dentin *et al.* 2006a)

NAFLD can progress to nonalcoholic steatohepatitis (NASH), a fatty liver with hepatitis. This form of liver injury carries a 20-50% risk for progressive fibrosis, 30% risk for cirrhosis, and 5% risk for hepato- cellular carcinoma (Angulo 2002); (Nseir *et al.* 2010)

NAFLD is the most common cause of liver dysfunction and affects close to 20 million patients in the US (Ahmed & Byrne 2007). The spectrum of NAFLD ranges from simple fatty liver (hepatic steatosis), with benign prognosis, to a potentially progressive form, nonalcoholic steatohepatitis (NASH), which may lead to liver fibrosis and cirrhosis, resulting in increased morbidity and mortality. All features of the metabolic syndrome, including obesity, type 2 diabetes, arterial hypertension, and hyperlipidemia (in the form of elevated triglyceride [TG] levels) are associated with NAFLD/NASH (Abdelmalek & Diehl 2007). NAFLD is generally asymptomatic, although a minority of patients may present with progressive liver injury with complications of cirrhosis, liver failure, and hepatocellular carcinoma. While the clinical diagnosis of NAFLD is usually made based on high transaminase levels, elevated BMI, ultrasound evidence of fat, and features of metabolic syndrome, a liver biopsy is required to determine the presence of NASH and to assess the degree of fibrosis (Adams & Lindor 2007). Despite being potentially severe, little is known about the natural history or prognostic significance of NAFLD. Although diabetes, obesity, and age are recognized risk factors for advanced liver disease, other significant factors leading to progressive liver injury remain to be identified. (Postic & Girard 2008)

Excessive accumulation of triglycerides (TG) is one the main characteristics of non-alcoholic fatty liver disease and fatty acids utilized for the synthesis of TG in liver are available from the plasma non-esterified fatty acid pool but also from fatty acids newly synthesized through hepatic de novo lipogenesis (Figure 11) (Denechaud *et al.* 2008b).

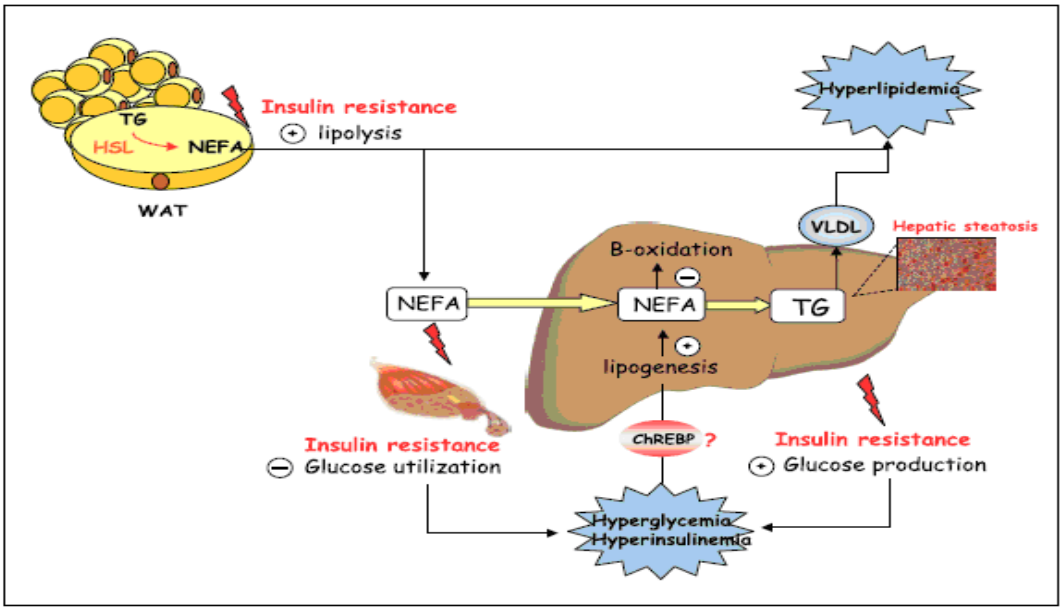

Figure 11. Metabolic defects leading to the development of hepatic steatosis and insulin resistance. (Postic et al. 2007)

NAFLD, which describes a large spectrum of liver histopathological features including simple steatosis, nonalcoholic steatohepatitis, cirrhosis, and hepatocellular carcinoma (Charlton M. 2004), is associated, in the vast majority of the cases, with obesity, insulin resistance, and type 2 diabetes. Therefore, with the epidemics of obesity and type 2 diabetes, NAFLD has become an important public health issue.

Different sources of fatty acids contribute to the development of fatty liver. Under conditions of insulin resistance, insulin does not efficiently suppress lipolysis in the adipose tissue; therefore, peripheral fats stored in adipose tissue flow to the liver by way of plasma nonesterified fatty acids (NEFAs). Because of the circulating NEFAs, skeletal muscles become insulin resistant, and glucose utilization is reduced in this tissue. In addition, the combination of elevated plasma concentrations of glucose and insulin promotes de novo lipid synthesis and impairs β oxidation, thereby participating in the development of hepatic steatosis. The intrahepatic accumulation also has deleterious effects on insulin signaling in liver. Hepatic glucose production is exacerbated, leading to the development of the hyperglycemic phenotype. Recent studies have shown that hepatic lipogenesis contributes significantly to triglyceride (TG) synthesis in humans and that this metabolic pathway is increased in individuals with obesity and insulin resistance (Donnelly *et al.* 2005). Although the molecular mechanisms leading to excess fatty acid

accumulation in insulin-resistant states have not been clearly resolved, recent studies have established that alterations in ChREBP expression can be correlated to the physiopathology of hepatic steatosis in genetically obese ob/ob mice (Iizuka *et al.* 2006); (Postic *et al.* 2007)

2-2-6. Soft drinks consumption and nonalcoholic fatty liver disease

The term soft drinks (SD) more commonly known as soda, soda pop, pop, Coke™, Pepsi™ or tonic, refers to a nonalcoholic beverage that is usually carbonated. Two types of SD are used; regular SD which are sweetened with sugar (fructose) and diet SD which are sweetened with non-caloric sweeteners (aspartame). Up to the 1980s, SD contained most of their food energy in the form of refined cane sugar or corn syrup (CS). Today, high fructose corn syrup HFCS is used almost exclusively as a sweetener in the United States and in other countries because of its lower cost. A global change in dietary habits has occurred over the last few decades resulting from the introduction of sweeteners such as fructose and sucrose by the food industries. For example, regular SD and fruit drinks, major sources of high fructose corn syrup (HFCS) or sugar, have increased from 3.9% of the total energy intake in 1977 to 9.2% of the total energy intake in 2001 (Nielsen & Popkin 2004). Human studies and animal models suggest that dietary factors can affect fatty infiltration and lipid peroxidation in various types of liver disease including NAFLD (Mezey 1998). More recently, increased ingestion of SD was found to be linked to NAFLD (Assy *et al.* 2008) independent of metabolic syndrome, with NAFLD patients consuming 5 times the amount of carbohydrates from SD as compared to healthy persons (Abid *et al.* 2009). Individuals consuming > 1 soft drink daily showed a higher prevalence of metabolic syndrome than that consuming < 1 soft drink per day (Dhingra *et al.* 2007).

2-2-6-1. Fructose

Fructose ($C_6H_{12}O_6$) is a simple sugar with a chemical formula similar to that of glucose. Fructose differs from glucose by the presence of a keto group attached to carbon 2 of the molecule, while glucose has an aldehyde group at carbon 1. In the diet, fructose is consumed in various amounts with fruits, honey, beverages sweetened with HFCS/sucrose and as a constituent of sucrose, the most common sugar (a disaccharide composed of fructose through a 1-4 glycoside bond) (following table). (Nseir *et al.* 2010)

Calories and sugar content in different soft drinks

Soft drinks: calorie content (number of calories)				Soft drinks: sugar content (numbers of teaspoons of sugar)			
	12- oz. Can	20 oz. Bottle	64 oz. Big cup		12- oz. Can	20 oz. Bottle	64 oz. Big cup
Sunkist	190	325	1040	Orange slice	11.9	19.8	63.5
Mountain dew	165	275	880	Mint maid orange soda	11.2	18.7	59.7
Dr. Pepper	160	250	800	Mountain dew	11.0	18.3	58.7
Pepsi	150	250	800	Barq's root beer	10.7	17.8	57.1
Coke classic	140	250	800	Pepsi	9.8	16.3	52.3
Sprite	140	250	800	Squirt	9.5	15.8	50.7
7-Up	140	250	800	Dr. Pepper	9.5	15.8	50.7
				7-Up	9.3	15.5	49.6
				Coke classic	9.3	15.5	49.6
				Sprite	9.0	15.0	48.0

High fructose diets have induced fatty liver in rats and ducks (Davail *et al.* 2005). Such diets have also caused increases in hepatic lipid peroxidation and activation of inflammatory pathways in the liver of rats (Kelley *et al.* 2004). The inborn error of metabolism known as hereditary fructose intolerance, a rare disease which results from a deficiency in the fructose metabolizing enzyme, aldolase B, has demonstrated that fructose consumption can cause progressive liver disease in humans (Havel 2005); (Nseir *et al.* 2010)

A diet high in fructose induces metabolic syndrome including insulin resistance, hypertriglyceridemia and hypertension in animal models (Hwang *et al.* 1987), and shows similar effects in humans (Stanhope *et al.* 2009). Liver is the major site of fructose metabolism (McGuinness & Cherrington 2003). Because fructose enters the glycolytic/gluconeogenic pathway as trioses in liver, metabolizing fructose requires simultaneous activation of part of glycolysis, de novo lipogenesis, part of gluconeogenesis and glycogen synthesis. (Koo *et al.* 2009)

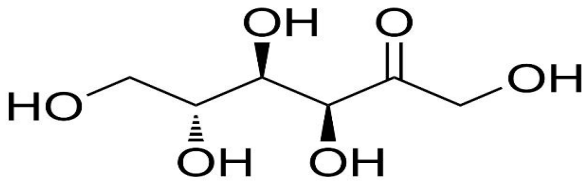

Fructose

2-2-6-2. Aspartame

Aspartame (or APM) $C_{14}H_{18}N_2O_5$ is the name for an artificial, non-saccharide sweetener used as a sugar substitute in many foods and beverages. In the European Union, it is known under the E number (additive code) E951. Aspartame is the methyl ester of a phenylalanine/aspartic acid dipeptide. Aspartame was first synthesized in 1965. Its use in food products was first approved by the United States Food and Drug Administration in 1974. Because its breakdown products include phenylalanine, aspartame is among the many substances that must be avoided by people with the genetic condition phenylketonuria (PKU) (Magnuson *et al.* 2007).

Aspartame is an artificial sweetener. It is 200 times sweeter than sugar in typical concentrations, without the high energy value of sugar. (Prodolliet & Bruelhart 1993) While aspartame, like other peptides, has a caloric value of 4 kilocalories (17 kilojoules) per gram, the quantity of aspartame needed to produce a sweet taste is so small that its caloric contribution is negligible. The taste of aspartame is not identical to that of sugar: the sweetness of aspartame has a slower onset and longer duration than that of sugar. Blends of aspartame with acesulfame potassium—usually listed in ingredients as acesulfame K— are said to taste more like sugar, and to be sweeter than either substitute used alone (Stegink 1987).

Aspartame is also used as sweeteners in the beverage industry mainly in diet SD.. Aspartame is absorbed from the intestine and metabolized by the liver to form phenylalanine, aspartic acid and methanol. Aspartame can contribute to weight gain, obesity, insulin resistance, and type 2 diabetes mellitus (Ferland *et al.* 2007). Recently, Brown et al (Brown *et al.* 2009) showed that artificial sweeteners may trigger the secretion of glucagon like peptide (GLP)-1 by the digestive tract, and thereby curb appetite and calorie intake. (Nseir *et al.* 2010)

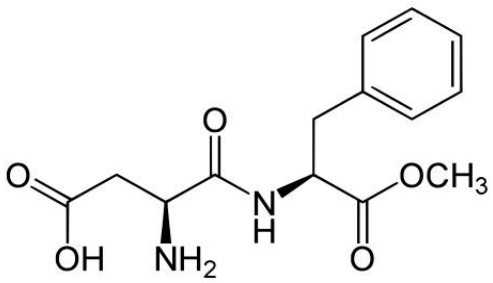

Aspartame

2-2-6-3. Saccharin

Saccharin $C_7H_5NO_3S$ is an artificial sweetener. The basic substance, benzoic sulfimide, has effectively no food energy and is much sweeter than sucrose, but has an unpleasant bitter or metallic aftertaste, especially at high concentrations. It is used to sweeten products such as drinks, candies, biscuits, medicines, and toothpaste. Saccharin is unstable when heated but it does not react chemically with other food ingredients. As such, it stores well. Blends of saccharin with other sweeteners are often used to compensate for each sweetener's weaknesses and faults. A 10:1 cyclamate:saccharin blend is common in countries where both these sweeteners are legal; in this blend, each sweetener masks the other's off-taste. Saccharin is often used together with aspartame in diet soda, so that some sweetness remains should the fountain syrup be stored beyond aspartame's relatively short shelf life. Saccharin is believed to be an important discovery, especially for diabetics, as it goes directly through the human digestive system without being digested. Although saccharin has no food energy, it can trigger the release of insulin in humans and rats, apparently as a result of its taste,(Just *et al.* 2008) as can other sweeteners like aspartame (Ferland *et al.* 2007). In its acid form, saccharin is not water-soluble. The form used as an artificial sweetener is usually its sodium salt. The calcium salt is also sometimes used, especially by people restricting their dietary sodium intake. Both salts are highly water-soluble: 0.67 grams per milliliter water at room temperature. (Fahlberg & Remsen 1879).

Saccharin is one of the oldest known artificial sweeteners currently in use. It was discovered in 1879 by two researchers at Johns Hopkins University.(Fahlberg & Remsen 1879) Though heat-stable and around 300 times sweeter than table sugar, it has a bitter aftertaste that some consumers find unpleasant. Upon initial passage of the Food Additives Amendment of 1958, saccharin was listed as a GRAS substance by the FDA and could thus be freely added to food and beverages. (Burnett 2007)

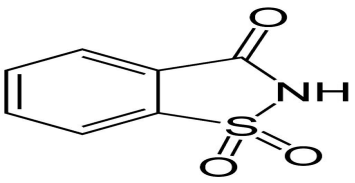

Saccharin

2-2-6-4. Cyclamate

Sodium cyclamate $C_6H_{12}NNaO_3S$ is an artificial sweetener. It is 30–50 times sweeter than sugar (depending on concentration; it is not a linear relationship), making it the least potent of the commercially used artificial sweeteners. Some people find it to have an unpleasant aftertaste, but generally less so than saccharin or acesulfame potassium. It is often used together with other artificial sweeteners, especially saccharin; the mixture of 10 parts cyclamate to 1 part saccharin is common and masks the off-tastes of both sweeteners. It is less expensive than most sweeteners, including sucralose, and is stable under heating.

Cyclamate, derived from the acid N - cyclo – hexyl – sulfamic (CHS), is amply utilized as a non-caloric artificial sweetener in foods and beverages (Suenaga *et al.* 1983); (Yamamura *et al.* 1968) and in the pharmaceutical industry (Barlattani 1970). Cyclamate is odorless and soluble in water, alcohol and glycol propylene (Sain & Berman 1984), and is more stable than aspartame and saccharine, and supports temperature variations (Barlattani). Cyclamate was discovered in 1937, at the University of Illinois, USA (EHHP 2000), by Michael Sveda, who accidentally discovered its sweet taste, 30 times sweeter than that of sucrose but without the bitter flavor of saccharine (Audreith & Sveda 1944), which is 300 times sweeter than sucrose. At the beginning of 1959, the Food and Drug Administration (FDA) added cyclamate to its list of safe substances (Ahmed & Thomas 1992), permitting its use as an artificial sweetener for diabetics. (DE MATOS *et al.* 2006)

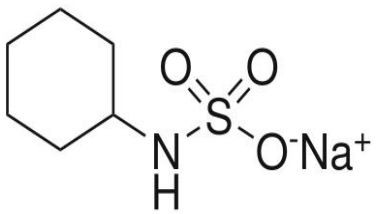

Sodium cyclamate

2-2-6-5. Stevioside

Stevioside is an ent-kaurene type diterpenoid glycoside isolated from leaves of Stevia rebaudiana (Bertoni) Bertoni, a perennial herb of the asteraceae (compositae) family (Geuns 2003). Stevioside and related compounds are responsible for the sweet taste of Stevia leaves (Hutapae *et al.* 1997). Due to the high concentration of such sweet

principles in leaves of Stevia plants, these are known as honey leaf of sweet chrysanthemum or ‘‘sweet herb of Paraguay’’. Extracts are being used commercially in many countries for sweetening a variety of products including pickled vegetables, sea foods, soft drinks, soy sauce, and confectionary products. Stevioside is an intense sweetener and the extract of its source (S. rebaudiana) finds extensive use in countries like Japan, China, Russia, Korea, Paraguay, Argentina, Indonesia, Malaysia, Australia, New Zealand, South America, and others, to sweeten local teas, medicines, food, and beverages (Elkins 1997). In addition, Stevia leaves are also in use for their medicinal benefits in hypertension, obesity, topical dressing for wounds, and other skin disorders; (Brahmachari *et al.* 2010)

Stevioside, an abundant component of Stevia rebaudiana leaf, has become well-known for its intense sweetness (250–300 times sweeter than sucrose) and is used as a non-caloric sweetener in several countries (Chatsudthipong & Muanprasat 2009). Stevioside is considered to be a sugar substitute and commercial sweetener, both in the form of stevioside and stevia extract (Kinghorn & Soejarto 1985). They are used in variety of foods and products, such as pickled vegetables, dried seafood, soy sauce, beverages, candies, chewing gum, yogurt and ice cream, as well as in toothpaste and mouth wash. Stevia extract and stevioside are officially approved as food additives in Brazil, Korea and Japan (Choi *et al.* 2002) and in the United States, they are permitted as a dietary supplement. They have not yet been approved by the European Commission due to safety concern. In 2006, the meeting of the Joint FAO/WHO Expert Committee on Food Additive (JECFA) to evaluate certain food additives and ingredients, flavoring agents, and natural constituent of food announced a temporary accepted daily intake (ADI) of stevioside of up to 5.0 mg/kg body weight (BW) (Chatsudthipong & Muanprasat 2009)

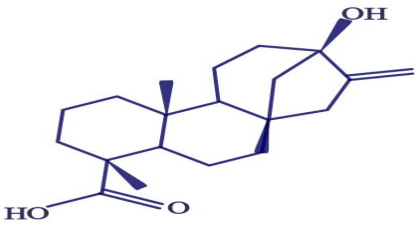

Steviol

2-2-7. Inhibition of ChREBP as a treatment for metabolic syndrome

The importance of ChREBP in the development of obesity and type 2 diabetes was addressed by intercrossing ChREBP-deficient mice with ob/ob mice (ob/ob-ChREBP−/− mice). Fat accumulation was prevented in liver of these mice, and their hyperlipidemic phenotype was significantly improved (Iizuka *et al.* 2006). Liver-specific inhibition of ChREBP improves hepatic steatosis and insulin resistance in obese ob/ob mice. Since ChREBP cellular localization is a determinant of its functional activity, a better knowledge of the mechanisms involved in regulating its nucleo-cytoplasmic shuttling and/or its post-translational activation is crucial in both physiology and physiopathology. (Dentin *et al.* 2006a)

ChREBP knockdown, both under short-term (two days)and long-term (seven days) conditions, significantly improves the fatty liver phenotype of ob/ob mice by decreasing rates of lipogenesis, thereby decreasing hepatic fat accumulation. As expected, the liver-specific inhibition of ChREBP not only markedly affected the expression of ACC and FAS, but also that of SCD-1, the rate-limiting enzyme catalyzing the conversion of saturated long-chain fatty acids into monounsaturated fatty acids, which are the major components of TG (Flowers *et al.* 2006). Interestingly, ChREBP knockdown not only affected the rate of de novo lipogenesis but also had consequences on β oxidation. Lipogenesis and β oxidation are directly correlated because malonyl-CoA, the allosteric inhibitor of CPT-1 (the rate-limiting enzyme of β oxidation) is synthesized by the lipogenic enzyme ACC. The fact that both ACC1 and ACC2 protein content was significantly lower in liver of fasted ChREBP deficient mice probably led to a constitutive activation of L-CPT1 activity in liver. The significant decrease in malonyl-CoA concentrations and the increase in plasma β hydroxybutyrate levels measured in fasted mice support this hypothesis. Therefore, the coordinate modulation in fatty acid synthesis and oxidation in liver led to overall improvement of lipid homeostasis in ChREBP-deficient mice. This study is in agreement with the fact that ACC2 gene knockout is also associated with increased rates of β oxidation in liver, leading to the improvement of overall lipid homeostasis in these mice (Abu-Elheiga *et al.* 2003). The beneficial effect of ChREBP knockdown was apparent on overall glucose tolerance and insulin sensitivity, with a significant improvement in hyperlipidemia, hyperglycemia, and hyperinsulinemia (Postic *et al.* 2007).

2-2-7-1. cAMP

AMP-activated protein kinase (AMPK) is a multisubunit protein kinase, which appears to play a central role in lipid metabolism (Hardie 1992). AMPK was first shown to catalyze phosphorylation and inactivation of 3-hydroxy-3-methylglutaryl-CoA (HMG-CoA) reductase and acetyl-CoA carboxylase, the rate limiting enzymes of cholesterol and fatty acid synthesis, respectively (Hardie & Carling 1997). AMPK is activated by a high AMP/ATP ratio in the cytosol, which occurs under stressed conditions such as heat shock, hypoxia, arsenite treatment, and starvation (Moore *et al.* 1991). The increase in AMP and the concomitant decrease in ATP, activating AMPK, suggests that this protein kinase inhibits activation of biosynthetic enzymes such as acetyl-CoA carboxylase to conserve ATP (Hardie *et al.* 1998); (Kawaguchi *et al*. 2002)

AMPK is a highly conserved serine/threonine kinase that functions as an energy sensor and transducer of cellular metabolism (Hardie 2007). AMPK represents a metabolic checkpoint for the convergence of intracellular signal transduction cascades involved in regulating energy balance by integrating information conveyed by specific nutrient (e.g., glucose and fatty acids) and hormone (e.g., insulin, ghrelin, adiponectin, leptin and glucagon) signals, the levels of which reflect changes in energy status (Kahn *et al*. 2005a). Activation of AMPK requires the phosphorylation of a threonine residue (T172) contained within the alpha catalytic subunit by an upstream kinase such as LKB1 (Stein *et al.* 2000). AMPK has been implicated in the control of hepatic glucose and lipid metabolism, thereby affecting whole body fuel utilization (Viollet *et al*. 2009). In short-term regulation, AMPK phosphorylates and inactivates ACCα, thus inhibiting the production of malonyl-CoA and fatty acid biosynthesis (Viollet *et al*. 2006). In addition, AMPK also phosphorylates and activates malonyl-CoA decarboxylase (MCD) which works to decrease cellular malonyl-CoA. The net effect of these actions is to reduce the level of a potent allosteric inhibitor of carnitine palmitoyl- CoA transferase-1 (CPT-1), a mitochondrial membrane transporter and rate-limiting enzyme controlling fatty acid oxidation (Saggerson 2008). Thus, by modulating malonyl-CoA levels, AMPK acts as a metabolic regulator shifting the balance of hepatic fuel utilization from glucose to fatty acids while inhibiting de novo fatty acid synthesis from glucose. Long-term regulation of glycolytic and lipogenic gene expression in liver results, in part, from decreased DNA binding of SREBP-1c and ChREBP. In addition, it has been also reported that AMPK

directly phosphorylates ChREBP and modulate its DNA binding activity (Kawaguchi *et al*. 2002); (Viollet *et al*. 2009); (Proszkowiec-Weglarz *et al.* 2009).

During starvation for HePG2 cells, concentrations of plasma glucagon and epinephrine are increased. Glucagon and epinephrine increase the intracellular cAMP concentration and activate cAMP-activated protein kinase A (PKA). PKA phosphorylates ChREBP, in activating it (Kawaguchi *et al.* 2001). Phosphorylation of ChREBP at Serine residue 196 (Ser 196) inactivates nuclear import, and phosphorylation at Threonine residue 666 (Thr 666) prevents DNA binding by ChREBP. Similarly, intracellular AMP accumulation inhibits ChREBP trans activity by activating AMP-activated protein kinase (AMPK) and phosphorylating ChREBP . (Kawaguchi *et al*. 2002)

2-2-7-2. Polyunsaturated fatty acids

Dietary fat is an important macronutrient for growth and development of all animals. Excessive levels of dietary fat or an imbalance of saturated fat versus unsaturated fat or n-6 versus n-3 polyunsaturated fat (PUFA) have been implicated in the onset and progression of several chronic diseases, including coronary artery disease and atherosclerosis (Harris 2003), diabetes and obesity (Kelley *et al.* 2002), cancer (Cho *et al.* 2003), Parkinson's disease, major depressive disorders and schizophrenia (Julien *et al.* 2006). As such, considerable clinical and basic science research has been directed at understanding the biochemical and molecular basis of fatty acid effects on complex physiological systems impacting human health. The understanding of the role dietary fat plays in these chronic diseases is complicated by the fact that fat has many physiological roles. Dietary fat is a substrate for energy metabolism, membrane formation and signaling molecules; dietary fat also regulates gene expression (Jump *et al.* 2008).

Since the original description of dietary fat as a regulator of gene expression over a decade ago, many transcription factors have been identified as prospective targets for fatty acid regulation, including several nuclear receptors like the peroxisome proliferator activated receptor family (PPAR) (α, β, γ1 and γ2), retinoid X receptor α (RXR α), liver X receptor α (LXR α) and hepatic nuclear factor α and γ (HNF4 α and γ) as well as several basic helix-loop-helix leucine-zipper transcription factors (bHLH-LZ) like sterol regulatory element binding protein-1 (SREBP-1), carbohydrate regulatory element binding protein (ChREBP) and max-like factor X (MLX) (Botolin *et al*. 2006); (Dentin *et al*. 2005a); (Xu *et al.* 2003); (Jump *et al*. 2008)

Glucose metabolism in liver is inhibited by administration of fatty acids, the so-called "glucose sparing" effect (Williamson & Krebs 1961). Fatty acids inhibit genes of key enzymes of glycolysis and lipogenesis such as L-pyruvate kinase (L-PK), 1 acetyl-CoA carboxylase, and fatty acid synthetase. L-PK, regulating the flux of metabolites through the pyruvate-phosphoenolpyruvate cycle (Liimatta *et al.* 1994), is known to play an important role in hepatic glucose and lipid metabolism. The activity of L-PK is subject to acute control by covalent modification and allosteric effectors. On the other hand, long term control of L-PK is achieved by regulating L-PK gene transcription (Foufelle *et al.* 1996). Fatty acids inhibit transcription of L-PK and other enzymes in glycolysis and lipogenesis pathways, whereas excess glucose induces expression of these genes (Duplus *et al.* 2000); (Kawaguchi *et al.* 2002)

A diet that provides 2–5% of energy from (n-3) and (n-6) PUFA leads to a coordinate suppression of glycolytic and lipogenic genes and to an induction of genes involved in fatty acid oxidation (Clarke 2004). This metabolic balance in liver leads to a ''partitioning'' of fatty acids away from triglyceride synthesis toward fatty acid oxidation. The positive effects of PUFA may in fact delay the onset of insulin resistance and lipotoxicity and in turn improve the metabolic phenotype of type 2 diabetes. (Dentin *et al.* 2006b)

Two general mechanisms characterize fatty acid control of these transcription factors. Fatty acids bind directly to the transcription factor and control transcription factor activity. In this fashion, fatty acids act like hydrophobic hormones regulating the function of nuclear receptors and their impact on transcriptional processes. Non-esterified fatty acids bind PPAR (α, β, γ1 and γ2) (Xu *et al.* 1999a); (Xu *et al.* 1999b), HNF-4 (α and γ) (Dhe-Paganon *et al.* 2002), RXR α (Mata de Urquiza *et al.* 2000) and LXR α (Ou *et al.* 2001). All of these proteins are members of the nuclear receptor super family of ligand-regulated transcription factors. Amongst these nuclear receptors, however, PPAR subtypes are the most widely accepted fatty acid-regulated transcription factors. In the second mechanism, fatty acids control the nuclear abundance of key transcription factors, such as SREBP-1, NFκB, ChREBP and MLX (Xu *et al.* 2003); (Jump *et al.* 2008). The mechanisms controlling the nuclear abundance of these transcription factors is less clear, but likely does not involve direct binding of the fatty acid to the transcription factor. While 22:6,n-3 acts like many PUFA to control gene expression by regulating

transcription factor function, 22:6,n- 3 also has unique regulatory effects on gene transcription. As such, these effects are not shared by other fatty acids. (DiRusso *et al.* 2005)

Fatty acid effects on hepatic gene expression require their entry into cells. Non-esterified fatty acids (NEFA) enter cells through fatty acid transport protein (FATP) or fatty acid transporter (FAT, CD36) or diffusion (Figure 12). NEFA are rapidly converted to FA-CoA by FATP (Coleman *et al.* 2002) or fatty acyl-CoA synthetases (Hertzel & Bernlohr 2000). When fatty acids enter hepatocytes as complex lipids, like chylomicron remnants, the complex lipids are hydrolyzed by lipases to form NEFA. In either case, intracellular NEFA is maintained at a very low level by quickly converting the NEFA to fatty acyl CoA. Fatty acyl-CoAs are also kept at low intracellular levels. Both NEFA and FA-CoA are bound to fatty acid binding protein (FABP) and fatty acyl CoA binding protein (ACBP), proteins that transport fatty acids to intracellular compartments for metabolism (Wolfrum *et al.* 2001) or to the nucleus to interact with transcription factors (Patton *et al.* 1994). The bulk of FA-CoA is rapidly assimilated into complex lipids. Hepatocytes challenged with exogenous fatty acids rapidly assimilate the fatty acids into neutral and polar lipids, while a minor fraction will be β-oxidized. These metabolic pathways keep intracellular NEFA and FA-CoA very low. Intracellular NEFA, however, are not solely dependent on exogenous fatty acids; intracellular NEFA can also arise from the hydrolysis of complex lipids by lipases acting on phospholipids or triglycerides (Hunt & Alexson 2002) or by the hydrolysis of FA-CoA by thioesterases (Jump *et al.* 2008). As such, these pathways may contribute to the pool of NEFA in cells. The intracellular NEFA fraction of cells plays an important role in lipid-mediated regulation of transcription factor function.

Polyunsaturated fatty acids (PUFA) play a key role in membrane composition and function, metabolism and the control of gene expression. Certain PUFA, like the n-3 PUFA, enhance hepatic fatty acid oxidation and inhibit fatty acid synthesis and VLDL secretion, in part, by regulating gene expression. (Dentin *et al.* 2005a)

.

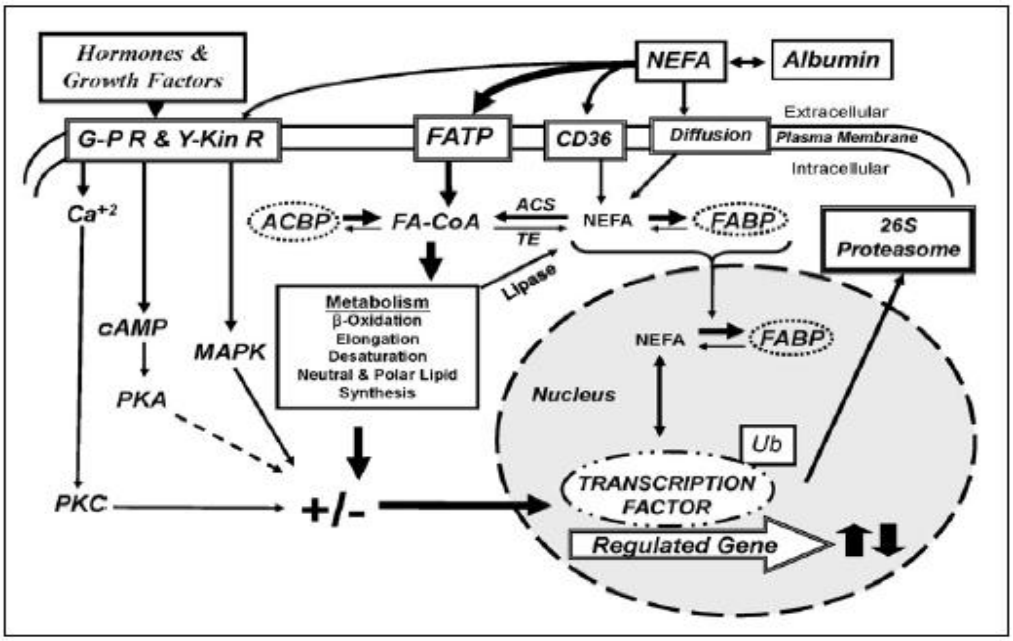

Figure 12. Summary of PUFA control of hepatic PPARα, SREBP-1 and MLX nuclear abundance (Jump et al. 2008).

Studies with PPARα null mice and over expression of native and mutant forms of SREBP-1c, LXRα, ChREBP or MLX in primary hepatocytes have revealed several major metabolic pathways that are targeted by PUFA. Each pathway involves changes in gene expression. First, n-3 PUFA induction of mono- (microsomal) and β-oxidation (mitochondrial and peroxisomal) requires PPARα. Second, PUFA suppression of de novo lipogenesis (fatty acid synthase, FAS), fatty acid elongation (Elovl-6) and monounsaturated fatty acid synthesis (Δ^9desaturase [Δ^9D], also known as stearoyl CoA desaturase, SCD1) involves three transcription factors, SREBP-1, ChREBP and MLX (Xu *et al.* 2003); (Wang *et al.* 2005). Third, PUFA suppression of the glycolytic enzyme, l-pyruvate kinase, does not involve PPARα, SREBP-1 or LXRα (Xu *et al.* 2003), but involves ChREBP and MLX heterodimer (Wang *et al.* 2006). Fourth, PUFA suppression of PUFA synthesis lowers levels of fatty acid elongase-5 (Elovl-5), Δ^5desaturase (Δ^5D) and Δ^6desaturase (Δ^6D). PUFA control of SREBP-1 nuclear abundance explains part of this mechanism (Jump *et al.* 2008).

PUFA, and in particular n-3 PUFA, function as feed-forward activators of fatty acid oxidation at the level of gene expression to control mitochondrial, peroxisomal and microsomal lipid metabolism. N-3 PUFA also function as feedback inhibitors of

glycolysis, de novo lipogenesis, mono- and polyunsaturated fatty acid synthesis to control the production and cellular content of saturate, mono- and polyunsaturated fatty acids. These regulatory schemes not only reduce overall hepatic lipid content and VLDL secretion, but also eliminate excessive very long chain PUFA that may promote oxidant stress or impair membrane integrity. (Xu *et al.* 2003). Feeding rats a diet containing n-3 PUFA or WY14643 (a peroxisome proliferator activated receptor α (PPARα) agonist) suppressed hepatic mRNA of L-PK but did not suppress hepatic ChREBP or HNF-4α nuclear abundance. Hepatic MLX nuclear abundance, however, was suppressed by n-3 PUFA but not WY14643. (Xu *et al.* 2003); (Jump *et al.* 2005)

Polyunsaturated fatty acids (PUFA) are potent inhibitors of hepatic glycolysis and de novo lipogenesis, through the inhibition of genes involved in glucose utilization and lipid synthesis, including L-PK, FAS, and ACC. With the identification of the transcription factor SREBP-1c, the molecular mechanism responsible for the PUFA inhibition of lipogenic genes has made important progress. Indeed, PUFA inhibit SREBP-1 gene transcription, enhance SREBP-1c mRNA turnover and interfere with the proteolytic processing of SREBP-1c protein (Stoeckman & Towle 2002). However, the PUFA-mediated suppression of L-PK gene expression cannot be directly attributed to SREBP-1c since L-PK expression is not subjected to SREBP-1c regulation (Moriizumi *et al.* 1998) and its promoter does not contain a sterol regulatory element-binding site (SRE) (Dentin *et al.* 2005a). PUFA suppress ChREBP activity by increasing ChREBP mRNA decay and by altering ChREBP protein translocation from the cytosol to the nucleus, independently of an activation of the AMP-activated protein kinase (AMPK), previously shown to regulate ChREBP activity (Postic *et al.* 2007). In the presence of PUFA, ChREBP is retained in the cytosol through the specific inhibition of GK and G6PDH activities, two key enzymes of glycolysis and of the pentose phosphate pathway, respectively. Figure 13 (Dentin *et al.* 2005a)

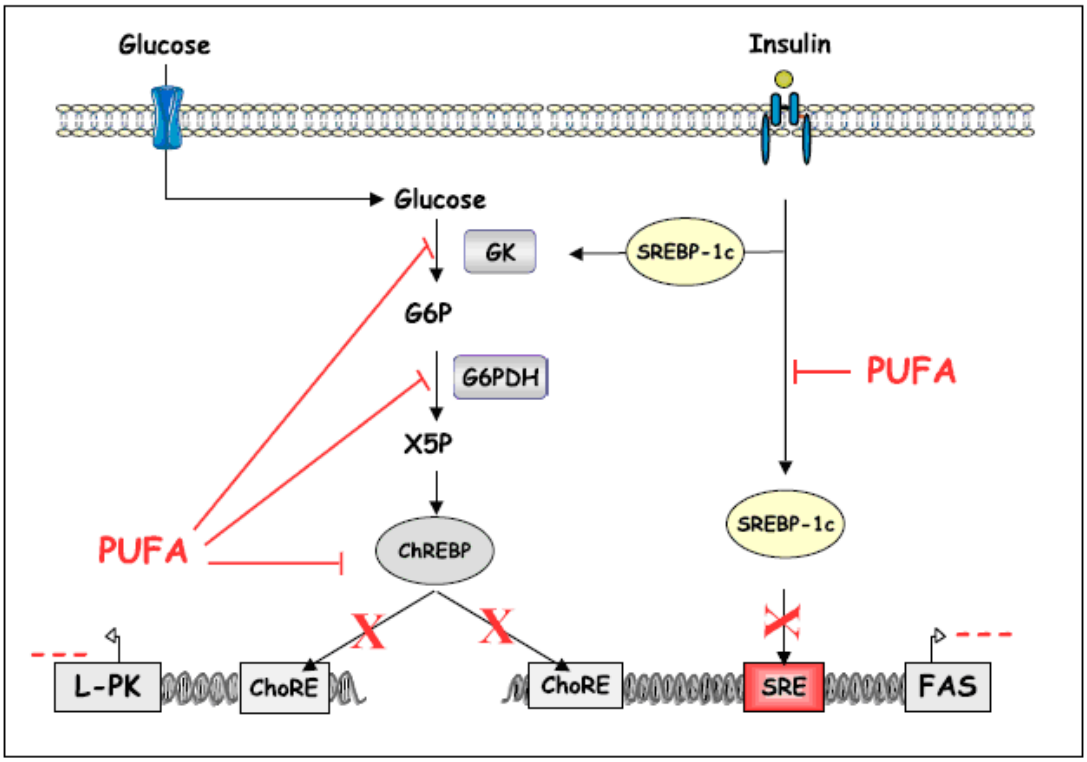

Figure 13. Inhibitory effect of PUFA on ChREBP and SREBP-1c expression and activation. (Postic et al. 2007

ChREBP is central for the coordinated inhibition of glycolytic and lipogenic genes by PUFA. PUFA [linoleate (C18:2), eicosapentaenoic acid (C20:5), and docosahexaenoic acid (C22:6)] suppresses ChREBP activity by increasing its mRNA decay and by altering ChREBP protein translocation from the cytosol to the nucleus both in primary cultures of hepatocytes and in liver in vivo. The PUFA-mediated alteration in ChREBP translocation is the result of a decrease in glucose metabolism (i.e., an inhibition of the activities of GK and G6PDH, the rate-limiting enzyme of the pentose phosphate pathway) (Pawar *et al.* 2002) (Figures 1 and 13). It remains to be determined whether PUFAs also exert a transcriptional effect on ChREBP gene expression. In the case of SREBP-1c, one of the mechanisms by which PUFAs suppress its gene transcription is through liver X receptor (LXR). PUFAs, by displacing oxysterol from LXR, antagonize the transactivation of LXR, at least in HEK293 cells (Cha & Repa 2007). The recent observation that LXR transcriptionally regulates ChREBP gene expression (Postic *et al.* 2007) in liver may suggest that the inhibitory effect of PUFA on ChREBP occurs in an LXR-dependent manner. (Decaux *et al.* 1989)

Insulin and glucose both augment L-PK gene expression, but it was demonstrated that the role of insulin in this process is to increase glucokinase (GK) levels to stimulate glucose metabolism (Doiron *et al.* 1996). While increased glucose metabolism, possibly through the pentose phosphate pathway (Jump & Clarke 1999), is important for the induction of hepatic L-PK, PUFAs inhibit its transcription (Dentin *et al.* 2005a); (Burr *et al.* 1930)

2-2-7-2-1. Linoleic acid

Linoleic acid (LA) is an unsaturated omega-6 fatty acid. It is a colorless liquid at room temperature. In physiological literature, it is called 18:2 (n-6). Chemically, linoleic acid is a carboxylic acid with an 18-carbon chain and two cis double bonds (cis-Δ^9, cis-Δ^{12} octadecadienoic acid).; the first double bond is located at the sixth carbon from the omega end. Linoleic acid is one of two essential fatty acids that humans and other animals must ingest for good health because the body requires them for various biological processes, but can not synthesize them from other food components. (Nutter *et al.* 1943)

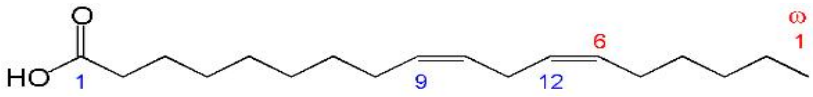

Linoleic Acid

Dietary sources: Safflower 78% Grape seed oil 73% Poppyseed oil 70% Sunflower oil 68% Hemp oil 60% Corn oil 59% Wheat germ oil 55% Cottonseed oil 54% Soybean oil 51% Walnut oil 51% Sesame oil 45% Rice bran oil 39% Pistachio oil 32.7% Peanut oil 32% Canola oil 21% Chicken fat 18-23% Egg yolk 16% Linseed oil 15% Lard 10% Olive oil 10% Palm oil 10% Cocoa butter 3% Macadamia oil 2% Butter 2% Coconut oil 2%. (Simopoulos 1999)

2-2-7-2-2. Docosahexaenoic acid

Docosahexaenoic acid (DHA) is an important omega-3 polyunsaturated fatty acid (n-3 PUFA) (all-cis-docosa-4,7,10,13,16,19-hexa-enoic acid or 22:6(n-3)) that has been shown to have beneficial effects on preventing human cardiovascular diseases, cancer, schizophrenia, and Alzheimer's disease (Innis 2007). DHA also plays an important role in infant brain and retinal development (Barclay *et al.* 1994).

In the aquaculture industry, n-3 PUFAs are essential nutrients for cultured marine fish. The major commercial source of n-3 PUFAs is fish oil, which faces challenges such as odor/taste problems, heavy metal contamination, and limited supply (New & Wijkstroem 2002). Currently, the aquaculture industry is experiencing rapid increases in fish oil price due to flat supply and increased global demand for this commodity. In fact, the Food and Agriculture Organization (FAO) of the United Nations predicts that fish oil demand in 2015 will be 145% of historical global production capacity (Pyle *et al.* 2008). The inability to expand fish oil production makes development of fish oil alternatives imperative. (Simopoulos 2002)

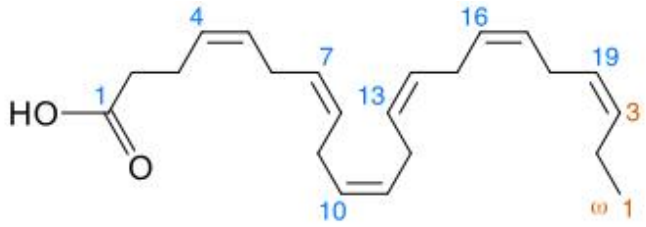

Docosahexaenoic acid

2-2-7-2-3. Eicosapentaenoic acid

Eicosapentaenoic acid (EPA or also icosapentaenoic acid) is an omega-3 fatty acid (cis-5,8,11,14,17-Eicosapentaenoic acid or 20:5 (n-3)). It also has the trivial name timnodonic acid. In chemical structure, EPA is a carboxylic acid with a 20-carbon chain and five cis double bonds; the first double bond is located at the third carbon from the omega end. EPA and its metabolites act in the body largely by their interactions with the metabolites of arachidonic acid; EPA is a polyunsaturated fatty acid that acts as a precursor for prostaglandin-3 (which inhibits platelet aggregation), thromboxane-3, and leukotriene-5 groups (all eicosanoids).

It is obtained in the human diet by eating oily fish or fish oil—cod liver, herring, mackerel, salmon, menhaden and sardine. It is also found in human breast milk. However, fish do not naturally produce EPA, but obtain it from the algae they consume. It is available to humans from some non-animal sources (eg, commercially, from spirulina and microalgae). Microalgae are being developed as a commercial source. EPA is not usually found in higher plants, but it has been reported in trace amounts in purslane. Microalgae, and supplements derived from it, are excellent alternative sources

of EPA and other fatty acids, since fish often contain toxins due to pollution. The human body can (and in case of a purely vegetarian diet often must, unless the aforementioned algae or supplements derived from them are consumed) also convert alpha-linolenic acid (ALA) to EPA, but this is much less efficient than the resorption of EPA from food containing it, and ALA is itself an essential fatty acid, an appropriate supply of which must be ensured. Because EPA is also a precursor to docosahexaenoic acid (DHA), ensuring a sufficient level of EPA on a diet containing neither EPA nor DHA is harder both because of the extra metabolic work required to synthesize EPA and because of the use of EPA to metabolize DHA. Medical conditions like diabetes or certain allergies may significantly limit the human body's capacity for metabolization of EPA from ALA. (Villarreal *et al.* 2007)

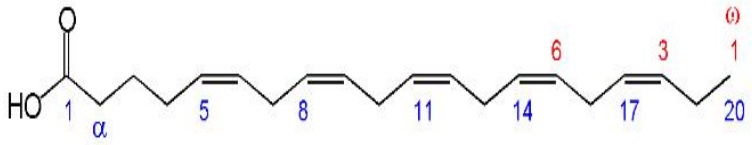

Eicosapentaenoic acid

2-2-7-2-4. Oleic Acid

Oleic acid is a mono-unsaturated omega-9 fatty acid found in various animal and vegetable sources. It has the formula CH_3 $(CH_2)_7CH=CH(CH_2)_7COOH$. Triglyceride esters of oleic acid comprise the majority of olive oil, though there may be less than 2.0% as actual free acid in the virgin olive oil, while higher concentrations make the olive oil inedible. It also makes up 36-67% of peanut oil, (Moore & Knauft 1989) 15-20% of grape seed oil, sea buckthorn oil, and sesame oil, (Untoro *et al.* 2006) and 14% of poppyseed oil.(Nutter *et al.* 1943) It is also abundantly present in many animal fats, comprising between 37-56% of chicken and turkey fat (Kokatnur *et al.* 1979), 44-47% of lard, etc. Oleic acid is the most abundant fatty acid in human adipose tissue(Edgecombe *et al.* 2000a).

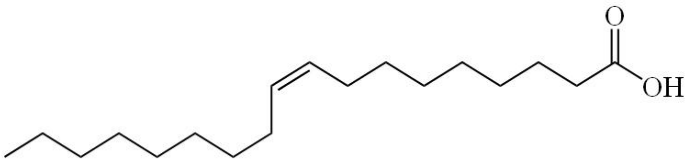

Oleic Acid

2-2-7-3. Oleuropein, an Antioxidant Polyphenol from Olive Oil.

Epidemiological studies have shown that the incidence of heart disease and certain cancers is lower in the Mediterranean region. This has been attributed to the high consumption of olive oil in the Mediterranean diet, which contains polyphenolic compounds with antioxidant activity. Although many in vitro studies have been performed to elucidate mechanisms by which these compounds may act, there are only few data relating to their fate after ingestion (Edgecombe *et al.* 2000b); (Sudjana *et al.* 2009). Therefore, we decided to investigate one of the major olive oil polyphenolics, oleuropein.

Oleuropein is a compound ($C_{25}H_{32}O_{13}$) found in olive leaf from the olive tree (and leaves of privet) together with other closely related compounds such as 10-hydroxyoleuropein, ligstroside, and 10-hydroxyligstroside. All these compounds are tyrosol esters of elenolic acid that are further hydroxylated and glycosylated. Oleuropein and its metabolite hydroxytyrosol have powerful antioxidant activity both in vivo and in vitro and give extra-virgin olive oil its bitter, pungent taste. Oleuropein preparations have been claimed (Oi-Kano *et al.* 2008) to strengthen the immune system. A study in rats suggests oleuropein enhances thermogenesis by increasing the thermogenin content in brown adipose tissue and the secretion of noradrenaline and adrenaline .

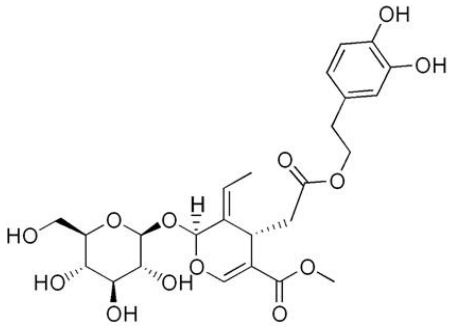

Oleuropein

3- MATERIALS AND METHODS

3.1. Materials

3.1.1 Chemicals and Biochemicals:

Name	Company	Country
Agarose Electrophoresis Grade	Invitrogen	Karlsruhe, G
Ammonium Acetate 7.5 M and Loading solution for Mega Bace	GE Health care	München, G
Antarctic Phosphates	New England Biolabs	USA
Aspartam 99%	Sigma Aldrich	Steinheim, G
Bovines Serum-Albumin (BSA)	Sigma Aldrich	Steinheim, G
Cyclamat 99%	Sigma Aldrich	Steinheim, G
D-(-)-Fructose D-Levulose Fruit sugar 99%	Sigma Aldrich	Steinheim, G
DAPI	Sigma Aldrich	Steinheim, G
Dimethylsulfoxid	Carl Roth GmbH	Karlsruhe, G
DNA Marker 1 kb and 100bp	Fermentas	St.Leon/Rot, G
Docosahexaenoic acid 99%	Sigma Aldrich	Steinheim, G
Dulbecco's modified Medium (DMEM)	Biochrom	AG Berlin, G
Eicosapentaenoic acid 99%	Sigma Aldrich	Steinheim, G
Ethanol 99%	Carl Roth GmbH	Karlsruhe, G
Ethidium Bromid (10 mg/ml)	Invitrogen	Karlsruhe, G
Fetal Calf Serum (FCS)	Biochrom AG	Berlin, Germany
Formaldehyd (37%)	Sigma Aldrich	Steinheim, G
Go Taq Green Master Mix	Promega	Mannhein, G
Humanes Insulin	Sigma Aldrich	Steinheim, G
Human Liver cDNA	Applied Biosystems Ambion	Foster city, USA
LB-Agar	Carl Roth GmbH	Karlsruhe, G
LB-Medium (Lennox)	Carl Roth GmbH	Karlsruhe, G
Ligation Kit	Stratagene	California, USA

Linoleic acid 99%	Sigma Aldrich	Steinheim, G
Lipofectamin 2000 (1 mg/ml)	Invitrogen	Karlsruhe, G
Loading buffer	Fermentas	St.Leon/Rot, G
Master Mix (Dyenamic TM sequencing)	GE Health care	München, G
Minimal Essential Medium (MEM)	Biochrom AG	Berlin, G
Oleic acid 99%	Sigma Aldrich	Steinheim, G
Oleuropein 99%	Sigma Aldrich	Steinheim, G
Optimem l Gibco	Invitrogen	Karlsruhe, G
PBS Gibco	Invitrogen	Berlin, G
Poly-D-Lysin hydrobromid	Sigma Aldrich	Steinheim, G
S.O.C. Medium	Invitrogen	Karlsruhe, G
Saccharin 99%	Sigma Aldrich	Steinheim, G
Stevioside 99%	Sigma Aldrich	Steinheim, G
Triton X 100 Gibco	Invitrogen	Karlsruhe, G
Trypsin LE	Invitrogen	Karlsruhe, G
X-Gal	Carl Roth GmbH	Karlsruhe, G

3.1.2 Restriction EnzymesAll restriction enzymes were purchased from

1- New England Biolabs GmbH, Frankfurt

Enzymes 20,000 units/ml	**Recognition Site**	**Buffer**	**Heat Inactivation**
BamH1	**5'-G^G A T C C-3'** **3'-C C T A G^G-5'**	Buffer 4+ BSA	No
EcoR1	**5'-G^A A T T C-3'** **3'-C T T A A^G-5'**	Buffer 1+ BSA	65°C for 20 minutes
EcoRv	**5'-G A T^A T C-3'** **3'-C T A^T A G-5'**	Buffer 3+ BSA	80°C for 20 minutes
Hind111	**5'-A^A G C T T-3'** **3'-T T C G A^A-5'**	Buffer 2+ BSA	65°C for 20 minutes
Mfe1	**5'-C^A A T T G-3'** **3'-G T T A A^C-5'**	Buffer 4+ BSA	65°C for 20 minutes

Mlul	**5'…A^CGCG T…3'** **3'…T GCGC^A…5'**	Buffer 3+ BSA	65°C for 20 minutes
Sgf1	**5'…CGC AT^CGC…3'** **3'…CGC^TA GCG…5'**	Buffer 3+ BSA	65°C for 20 minutes
Sma1	**5'-C C C^G G G-3'** **3'-G G G^C C C-5'**	Buffer 4+ BSA	65°C for 20 minutes

2- Fermentas GmbH, Sankt Leon-Rot Germany (Fast digest buffer).

Enzymes 20,000 units/ml	**Recognition Site**	**Heat Inactivation**
Ava1	**5'-C^Py C G Pu G-3'** **3'-G Pu G C Py^C-5'**	80°C for 20 minutes
Bglll	**5'-A^G A T C T-3'** **3'-T C T A G^A-5'**	No
Nco1	**5'-C^C A T G G-3'** **3'-G G T A C^C-5'**	65°C for 20 minutes
PshA1	**5'-G A C N N^N N G T C-3'** **3'-C T G N N^N N C A G-5'**	65°C for 20 minutes
Pst1	**5'-C T G C A^G-3'** **3'-G^A C G T C-5'**	80°C for 20 minutes
Sac1	**5'-G A G C T^C-3'** **3'-C^T C G A G-5'**	65°C for 20 minutes
Xho1	**5'-C^T C G A G-3'** **3'-G A G C T^C-5'**	65°C for 20 minutes

3.1.3 Extraction kits:

Gel Extraction kit	Qiagen	Duesseldorf, G
NucleoSpin Plasmid for high copy Plasmide	Macherey-Nagel	Düren, G
GeneElute High Performance Plasmid Maxiprep Kit	Sigma-Aldrich	Steinheim, G

3.1.4 PCR Primers for human ChREBP mRNA NM 032951

All Primers were purchased from (MoLbiol, Germany).

Nr.	Name	Sequence	5'	'3	Ampl.
1	Up ChREBP mRNA	actcggactcggacacagac	113	132	2976
2	Low ChREBP mRNA	aggagcagagagagggaacc	3069	3088	
3	Up ChREBP Gen	actcgaagaggcgtgtgagt	45	65	1192
4	Low ChREBP Gen	gcattaccttgggcttacca	1217	1236	
5	Up ChREBP Gen	actcgaagaggcgtgtgagt	303	322	
6	Up ChREBP mRNA	actcggactcggacacagac	113	132	1585
7	Low Ex10 ChREBP	agggtgctggatacaagtgg	1678	1697	
8	Up Ex9 ChREBP	gcctctcttctctcccaggt	1332	1351	1662
9	Low Ex17 ChREBP	acagcatcctcctctttcca	2974	2993	
10	Up Ex9 ChREBP	gcctctcttctctcccaggt	1332	1351	1654
11	Low 1Ex17 ChREBP	(ctcctctttccaccgttgag)	2966	2985	
12	Up ChREBP mRNA	actcggactcggacacagac	113	132	723
13	Low Ex6 ChREBP	cggactgagtcatggtgaag	816	835	
14	Up Ex4 ChREBP	taccacaagtggcgcatcta	589	608	1113
15	Low 1Ex10 ChREBP	gaggagggtgctggatacaa	1682	1701	
16	Up 1Ex1 ChREBP	agactcggactcggacacag	111	130	725
17	Low Ex6 ChREBP	cggactgagtcatggtgaag	816	835	
18	Up 1Ex4 ChREBP	ggaggggaactactggaagc	543	562	1476
19	Low Ex13 ChREBP	gcggagatgtgtgtgatacg	1999	2018	
20	Up Ex2 ChREBP	agagacaagatccgcctgaa	397	416	1301
21	Low Ex10 ChREBP	agggtgctggatacaagtgg	1678	1697	
22	Up 1Ex4 ChREBP	ggaggggaactactggaagc	543	562	1749
23	Low Ex15 ChREBP	tcaaaacgctggtgtgtgat	2272	2291	
24	Low Ex15 ChREBP	acttccagttgtgcagcgtac	2330	2350	
25	Up Ex1a ChREBP	actcacacgcctcttcgagt	303	322	2206
26	Low Ex17a ChREBP	gcgtagggagttcaggacag	2489	2508	
27	Up Ex2 ChREBP	agagacaagatccgcctgaa	397	416	2472
28	Low Ex17b ChREBP	aaacacagcggtccaaagac	2849	2868	

29	Up Ex4 ChREBP	ggaggggaactactggaagc	543	562	1966
30	Low Ex17a ChREBP	gcgtagggagttcaggacag	2489	2508	
31	Up Ex2 ChREBP	agagacaagatccgcctgaa	397	416	1895
32	Low Ex15 ChREBP	tcaaaacgctggtgtgtgat	2272	2291	
33	upEx1aChREBP	actcacacgcctcttcgagt	303	322	1989
34	LowEx15ChREBP	tcaaaacgctggtgtgtgat	2272	2291	
35	Up Ex4 ChREBP	taccacaagtggcgcatcta	589	608	2500
36	Low ChREBP mRNA	aggagcagagagagggaacc	3069	3088	
37	Up Ex4 ChREBP	taccacaagtggcgcatcta	589	608	2499
38	Low 1 ChREBP mRNA	ggagcagagagagggaacct	3068	3087	
39	up 2Ex4 ChREBP	gatgcgggaataccacaagt	579	598	2499
40	Low ChREBP 2 mRNA	gagggaacctccttttctgc	3058	3077	
41	up 1Ex6 ChREBP	tcctggacctcaattgcttt	773	792	2316
42	Low ChREBP mRNA	aggagcagagagagggaacc	3069	3088	
43	up 1Ex6ChREBP	tcctggacctcaattgcttt	773	792	2315
44	Low 1ChREBP mRNA	ggagcagagagagggaacct	3068	3087	

3.1.5 Sequencing Primers:

Reverse Primer		**Forward primer**	
M13	caggaaacagctatgac	M13	ctggccgtcgttttac
Low2346	atgctgaacacccagaacttc	UP1155	cgccttcctgagttctgattt
Low2349	aggatgctgaacacccagaac	Up1157	ccttcctgagttctgatttcc
Low XL39	attaggacaaggctggtggg	Up VP1.5	ggactttccaaaatgtcg

Primer	**Sequence**	**Number**	**Primer length**	**N moles**
1	tac tac aag aag cgg ctc cgt aa	D9817C02	23-mer	32,5
2	ttt acc aac tcc cgc ctc cca ca	D9817C03	23-mer	92,9
3	cgc ctt cct gag ttc tga ttt cc	D9817C04	23-mer	16,3
4	tca gtg ccc agc cca gcc tca ag	D9817C05	23-mer	16,0
5	ggc agt gaa cgg cgg ctg tca gg	D9817C06	23-mer	16,0

6	gct ggc gta ggg agt tca gga ca	D9817C07	23-mer	16,4
7	acc ttg agg ctg ggc tgg gca ct	D9817C08	23-mer	20,1
8	ggc tgt ggg agg cgg gag ttg gt	D9817C09	23-mer	21,7
9	ccg gag gag ggt gct gga tac aa	D9817C10	23-mer	13,8
10	ccc tga cag ccg ccg ttc act gc	D9817C11	23-mer	16,9

3.1.6 Vectors

3.1.6.1 TOPO TA Cloning, PCR 2.1

TOPO TA Cloning, TOP 10 kit, PCR 2, 1 TOPO vector was purchased from (Invitrogen, Germany).

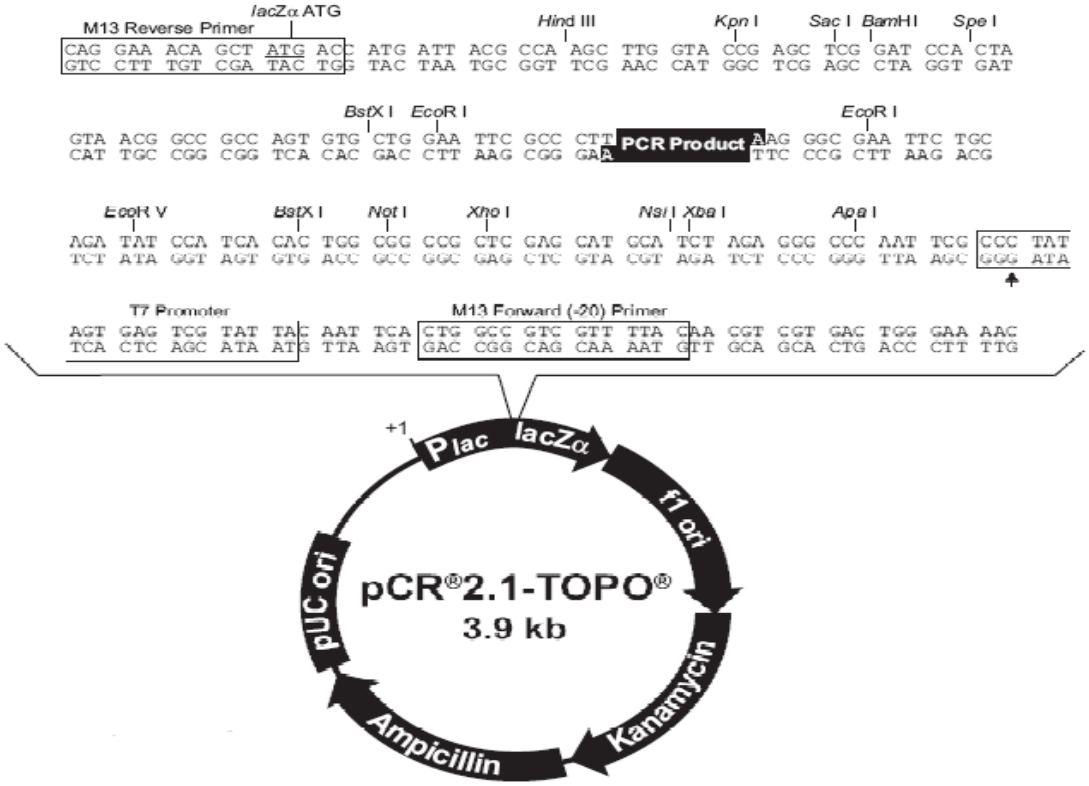

3.1.6.2 GFP-mouse ChREBP vector

The vector encoding for GFP-mouse ChREBP vector was kindly provided by Ms. Catherine Postic, Insitut Cochin, Département d'Endocrinologie, Métabolisme et Cancer, Université Paris Descartes, Paris, France. The murine full-length wild-type ChREBP-ζ isoform (GenBank accession no: AF245475) has been cloned into pEGFP- C1 from Clontech (Dentin et al., 2005a) and sent to us as a drop on filter paper.

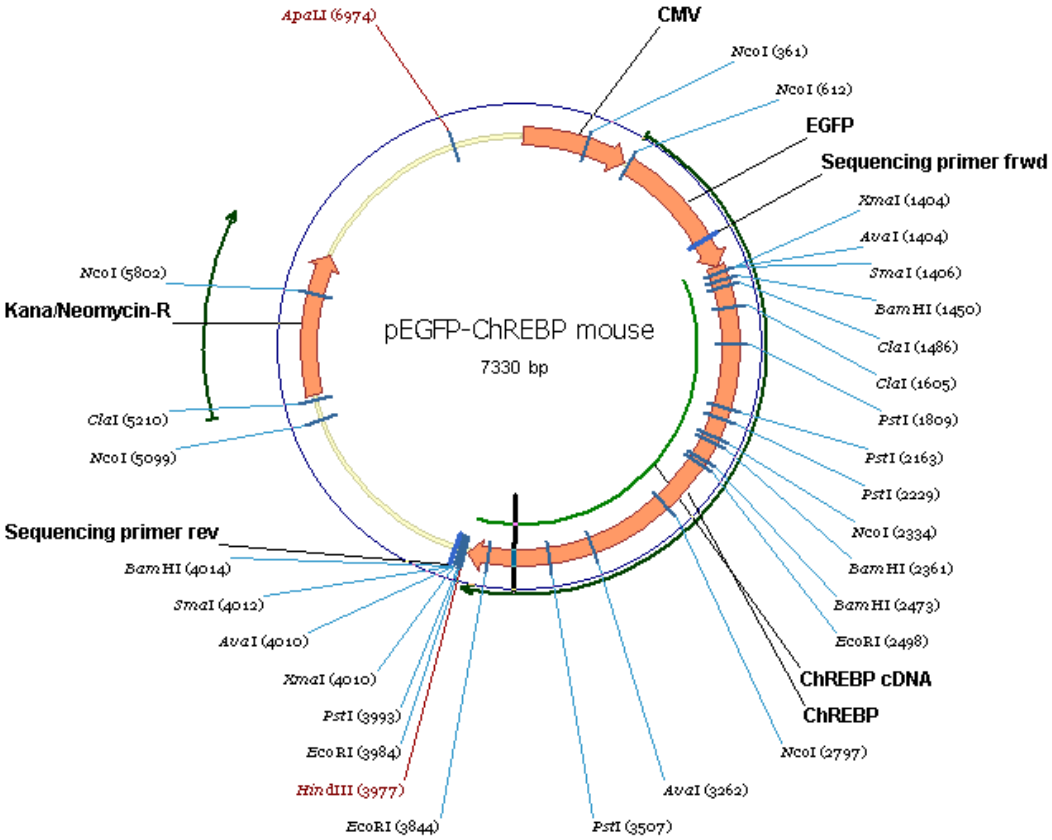

3.1.6.3 TrueORF cDNA Clones and PrecisionShuttle Vector System

TrueORF Vectors: PCMV6-Entry, PCMV6-AC-GFP and PCMV6-AN-GFP were purchased from (Origene, USA).

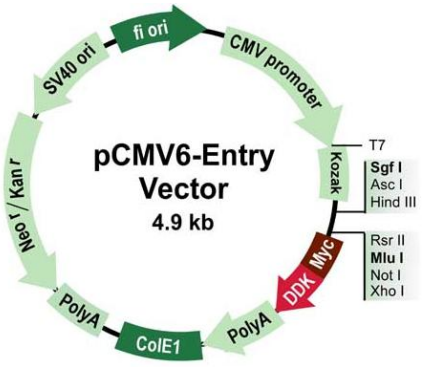

PCMV6-Entry (human ChREBP)

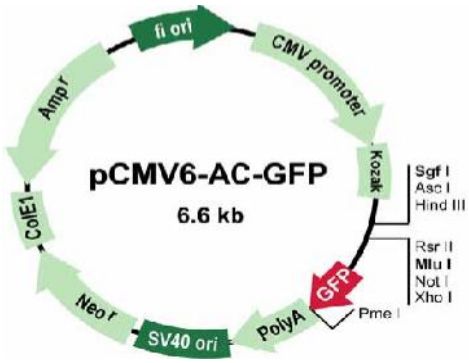

PCMV6-AC-GFP

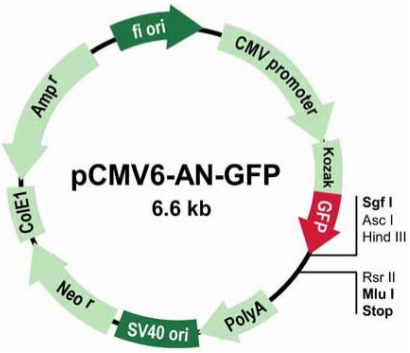

PCMV6-AN-GFP

3.1.7 Culture Medium

Dulbecco´s MEM (DMEM)	Dulbecco´s modified Eagle´s medium, with 3,7 g/l NaHCO3, 1 or 4,5 g/l D-Glucose (25 mM), W stable glutamin and Na-Pyruvat; Biochrom AG (Berlin, D)
MEM-EARLE (EMEM)	MEM (Minimal essential medium) with W 2,2 g/l NaHCO3, W stable glutamin, and LE (low Endotoxin); Biochrom AG (Berlin, D)
PBS-Dulbecco	PBS-Dulbecco, with Ca^{2+} , Mg^{2+}, and LE (low Endotoxin); Biochrom AG (Berlin, D)

3.1.8 Antibiotics:

Ampicillin 50-100 µg/ml	US Biological	Swampscott, USA
Kanamycin 30 mg/ml	US Biological	Swampscott, USA
Geneticin (G418) 40 mg/ml	Calbiochem	Darmstadt, D

3.1.9 Consumable materials:

Biocoat Poly-D-Lysin 96 well Microplates	BD Biosciences Europe	Erembodegem, Belgien
T75 and T25 culture flasks (75 and25 cm^2)	Nunc	Dreieich, G
6 , 12 , 24 well Plates	Nunc	Dreieich, G

96 well PCR Plates	Applied Biosciences	Darmstadt, G
Petri dishes (100 mm)	Nunc	Dreieich, G

3.1.10 Instruments and machines

Microwave	Bosch GmbH	Stuttgart , G
Vortex Shaker	VWR international GmbH	Darmstadt , G
Deep freezing storage device (with liquid nitrogen)	Taylor – Wharton	Theodore, Alabama USA
Gel Electrophoresis Appratus Live Technologies Horizon 58	Gibco BRL	Gaithersburg , USA
Water Bath FS2 Haake	Thermo Haake GmbH	Karlsruhe, G
Mixing Block MB-102	Biozym scientific GmbH	Oldendorf, Germany Water Bath FS2 Haake
Shaker Incubator CH-4103	Infors AG	Bottmingen,G
T Gradient Thermo cycler	Biometra	Goettingen, G
Master Cycler 5330	Eppendorf	Hamburg, G
Micro Centrifuge 5415 C	Eppendorf	Hamburg, G
Reprostar ll UV light	CAMAG	Berlin, G
BD Pathway 435 System	BD Biosciences	Erembodegem, Bel
Horizontal Gelelektrophoresekammer (Modell 200)	Gibco, Invitrogen	Karlsruhe, G
Inkubator Heraeus 6000	Heraeus Instruments	Hanau, G
Kryobehälter (air liquid)	Tec Lab	Königsstein, G
Light microscope	Olympus	Hamburg, G
Steril bank HF48	Gelaire	Burladingen, G
Steril bank Lamin Air 2448	Heraeus Instruments	Hanau, G
Thermomixer 5436	Eppendorf	Hamburg, G
Universal 320 centrifuge	Hettich	Thüringen, G

centrifuge Multifuge 3 C-R	Heraeus Instruments	Hanau, G
Trans illuminator Rainbow CCTV RMB92	Peq Lab Biotechnologie GmbH	EEC - China
MITHRAS LB490 Spektrophotometer	Berthold Technologies	Wildbad, G

3.1.11 Software

Attovision 1.6	BD Biosciences	Erembodegem, Bel
BD Image Data Explorer	BD Biosciences	Erembodegem, Bel
Vector NTI 9.0	Informax AG	Oxford, UK
Primer 3 Oligo	Centerline Capital Group	United States
Excel 2007	Microsoft GmbH	(Unterschleißheim, G)
Windows Xp professional	Microsoft GmbH	(Unterschleißheim, G)
NCBI Entrez Gene	National Center for Biotechnology Information	(Bethesda, MD, US)

3.2. Methods:

3.2.1 Polymerase chain reaction (PCR)

The polymerase chain reaction (PCR) is a technique to amplify a single or few copies of a piece of DNA across several orders of magnitude, generating thousands to millions of copies of a particular DNA sequence. The method relies on thermal cycling, consisting of cycles of repeated heating and cooling of the reaction for DNA melting and enzymatic replication of the DNA.

PCR in Eppendorf Master Cycler 5330

Go-TAG green Master mix 2x	12.5 µl
Primer up 10 µM	1.0 µl
Primer low 10 µM	1.0 µl
Aqua ad inj.	9.5 µl
Human Liver cDNA 0.5 ng/µl	1.0 µl

2-34 cycles

1	95° C	2 min
2	95° C	45 Sec
3	53° C	1 min
4	72° C	2 min
5	72° C	10 min
6	4° C	Pause

PCR 3h 37m in Master Cycler 5330

PCR in T gradient

1	2 min	95° C	denaturation
2	45 sec	95° C	denaturation
3	1 min	60° C	annealing
	Gradient Gradient	Column Nr Temperature	1 55.0
4	1 min 30 sec	72° C ->2 35	elongation
5	10 min	72° C	fill up
6	pause	15° C	Stop and cool

Annealing Gradient, in the middle 60 °C with a rang of 10 °C

2	3	4	5	6	7	8	9	10	11	12
55.2	55.9	57.0	58.2	59.4	60.6	61.8	63.0	64.1	64.8	65.0

Step 2, 35 cycles

PCR 3h 37m in T gradient

T gradient

T Gradient

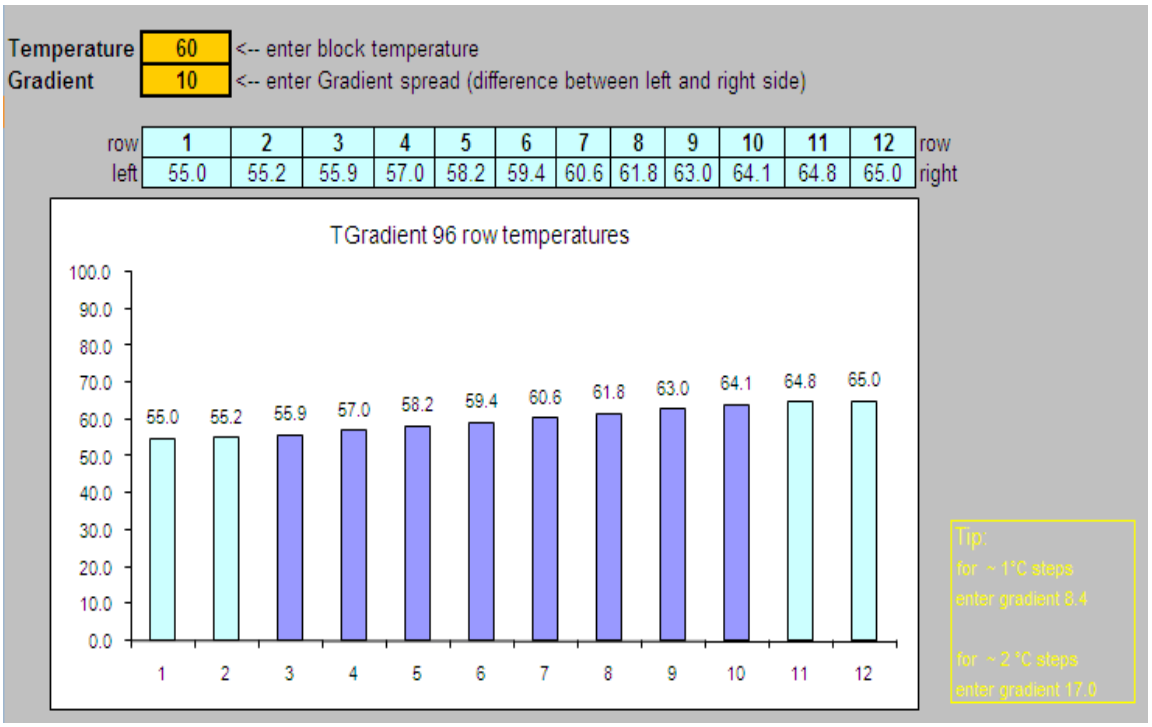

3.2.2 Agarose gel electrophoresis

Agarose gel electrophoresis is a method used to separate DNA molecules by size. This is achieved by moving negatively charged nucleic acid molecules through an agarose matrix with an electric field (electrophoresis). Shorter molecules move faster and migrate farther than longer ones. The most common dye used to make DNA or RNA bands visible for agarose gel electrophoresis is ethidium bromide (EtBr). It fluoresces under UV light when intercalated into DNA. By running DNA through an EtBr-treated gel and visualizing it with UV light, any band containing more than ~20 ng DNA becomes distinctly visible. DNA fragments were separated in 1 % agarose gels via agarose gel electrophoresis. To this end, 20 ml TAE buffer were supplied with 0.2 g agarose and heated until agarose was melted in a microwave (180W for 1min 30sec). Gels were supplemented with 0.5 µg/ml EtBr. 5 µl of the samples were mixed with 1 µl loading buffer and separated at 75 V. 3 µl 1kb ladder (Fermentas) were used to identify the sizes of the separated DNA bands that were visualised with UV light.

10xTAE buffer:

· 48.4 g Tris base
· 14.8 g EDTA_H2O
· 32.8 g sodium acetate, anhydrous
· 34 g glacial acetic acid
· added to 1 l with H2O
· pH = 7.8

Loading buffer:

· 0.25 % bromophenol blue
· 0.25 % xylencyanol
· 30 % glycerol

Ethidium bromide:

· 10 mg/ml in H_2O

3.2.3 DNA Extraction

Fragment was excised from the agarose gel with a clean, sharp scalpel, the gel slice was weighted in a colorless tube, then buffer QG was added to gel at ratio 3:1, sample was incubated at 50°C for 10 min, the tube was mixed by vortex every 2-3 min during the incubation. After the gel slice had dissolved completely, isopropanol was added to the sample with same volume of gel (1:1) and mixed, a QIA quick spin column was placed in a provided 2 ml collection tube, the sample was applied to the QIA quick column, and centrifuged for 1 min. The flow-through was discarded and QIA quick column was placed in the same collection tube, 0.5 ml of buffer QG was added to QIA quick column and centrifuged for 1 min, then 0, 75 ml of buffer PE was added to QIA quick column and centrifuged for 1 min. The flow- through discarded and the QIA quick column was centrifuged for an additional 1 min, QIA quick column was placed into a clean 1.5 ml micro centrifuge tube. DNA was eluted by 50µl of EB buffer; finally the DNA was stored at -20°C until used.

3.2.4 DNA Transformation

The transformation is the process of the admission of DNA Plasmid in bacteria. This method is used to multiply small quantities of DNA Plasmid, transformation can occur chemically through heat shock.

3.2.5 Heat shock transformation with E.coli

TOPO TA cloning used by adding 4µl fresh PCR product, 1 µl salt solution (1.2 M NaCl, 0.06 M MgCl2) and 1 µl TOPO vector in 1.5 ml micro centrifuge tube, the reaction was mixed gently and incubated for 30 minutes at room temperature (22-23°C) then the tube was placed in ice. One shot competent E. coli, continued (top 10) was used by adding 2 µl TOPO cloning reaction into a vial of one shot chemically competent *E. coli* with a sterile pipette tip and mixed gently. The cells/plasmid mix was incubated in ice for 5 minutes. The sample was heated for 30 seconds at 42°C without shaking. Immediately, the tubes were transferred to ice, 250 µl of S.O.C. medium was added, the tube was caped tightly and shacked horizontally at 200 rpm at a 37°C in shaking incubator for 1 hour. 35µl of X-Gal was added in every plate to indicate whether a cell expresses the β-galactosidase enzyme, which is encoded by the lacZ gene, in a technique called blue/white screening and incubated at 37°C for 10 min. 10 or 50 µl from the transformation reaction was spread on a pre-warmed selective agar plate with ampicillin or Kanamycin to ensure even spreading of small volumes, 20 µl of S.O.C. medium was added to the transformation mixture. The plates were incubated overnight at 37°C. Colonies from each plate were picked and cultured overnight in LB medium containing 1 µg/ml ampicillin or 30 mg/ml Kanamycin at 37°C in shaking incubator.

S.O.C. – Medium:

2.0	%	Trypton
0.5	%	yeast extract
10	mM	NaCl
2, 5	mM	KCl
10	mM	MgCl2
10	mM	MgSO4
20	mM	Glucose

LB Agar:

10 g/l Trypton
5 g/l Hefeeextrakt
5 g/l Natriumchlorid
15 g/l Agar
PH = 7

LB-Medium (Lennox):

10 g/l Trypton
5 g/l yeast extract
5 g/l Natriumchlorid
PH = 7

3.2.6 Isolation of DNA Plasmid

3.2.6.1 DNA Mini preparation

1.5 ml of *E. coli* LB culture was centrifuged for 1 min at 11,000 x g, the supernatant was discarded and removed as much of the supernatant as possible. 250 µl buffer A1 was added and re-suspend the cell pellet by Vigorous vortexing. Then, 250 µl buffer A2 was added and the samples were mixed gently by inverting the tube 6 times and incubated at room temperature for a maximum of 5 min, 300 µl buffer A3 was added and mixed gently by inverting the tube 6 times without vortex. The tubes were centrifuged for 5 min at 11,000 x g at room temperature. The supernatant was placed in a 2 ml NucleoSpin column collecting tube and centrifuged for 1 min at 11,000 x g., then the flow through was discarded. Washing with 500 µl pre-warmed AW buffer (50°C) and a centrifugation (1 min; 11,000 x g) before proceeding with washing buffer A4. The NucleoSpin plasmid column was placed back into the 2 ml collecting tube and 600 µl A4 buffer was added and centrifuged for 1 min at 11,000 x g., the flow-through was discarded, then centrifugation for 2 min at 11,000 x g. The NucleoSpin plasmid column was placed in a 1.5 ml micro-centrifuge tube and 50 µl buffer AE was added and incubated 1 min at room temperature then centrifugation for 1 min at 11,000 x g, finally the plasmid stored at -20°C until used.

3.2.6.2 DNA Maxi preparation

For preparation of high amounts of plasmid DNA, 150 ml LB medium supplemented with ampicillin or Kanamycin were inoculated with 150 µl liquid culture of an *E. coli* JM109 clone that was checked for the correct vector by restriction analysis. Cultures were incubated in shaking incubator at 37 °C over night. Plasmid was extracted via the Kit GenElute High Performance Plasmid Maxi prep Kit (Sigma) .150 ml of an overnight culture was pelleted at 5,000 X g, 10 min. supernatant was discarded. Cells

were resuspended in 12ml of resuspention solution and vortexed. 12 ml of Lysis solution was added and inverted 6-8 times to mix without vortex and allowed 3-5 min to clear. The plunger from a filter syringe was removed and the barrel was placed in upright position 12 ml of neutralization solution was added to the lysed cells and inverted 6-8 times to mix. 9 ml of binding solution was added and inverted 1-2 times to mix. The mix was added in barrel of the filter syring and let sit for 5 min. The binding column was placed into a collection tube provided. 12 ml of column preparation solution was added to the column and spined in a swinging bucket roter at 3,000 X g, 2min.The flow-through was discard. The filter syring was hold over the column and the plunger was inserted to expel half of the cleared lysate and spined at 3,000 X g, 2min. The remainder of the cleared lysate was added to the column, the spin was repeated and the flow through was discard. 12 ml of wash solution 1 was added and spined at 3,000 X g, 2min and the flow through was discarded. 12 ml of wash solution 2 was added and spined at 3,000 X g, 2min and the flow through was discarded. The column was transferred to a new collection tube and 3ml of elution solution was spined at 3,000 X g, 5 min.

3.2.7 Digestion with restriction enzymes

The amount of plasmid DNA was calculated as follows: µl of DNA plasmid for digestion = 200 ng / Concentration.

3.2.7.1 Digestion with enzymes from New England Biolabs

Puffer	2,5 µl
BSA	0,25 µl
Restriction enzyme	0,8 µl enzyme
DNA	200 ng ChREBP Plasmid DNA
Water	To reach the total volume to 25 µl

Incubation at 37 ºC for 1hr, then samples are picked in pockets of the gel (Elektrophorese, 75V, 30-45-min).

3.2.7.2 Digestion with enzymes from Fermentas

10x Fast Digest Puffer	2,5 µl

Restriction enzyme	1 µl enzyme
DNA	200 ng ChREBP Plasmid DNA
Water	To reach the total volume to 25 µl

Incubation at 37 ºC for 1hr, then samples are picked in pockets of the gel (Elektrophorese, 75V, 30-45-min).

3.2.8 DNA Sequencing

Proposed DNA-quantity for sequencing in each direction is 500-1000ng for plasmid, preparation of 2 tubes per sample for forward and reverse sequencing Primers. Addition of 1µl (= 5pmol) Primer to diluted DNA-samples (11µl containing 800ng DNA), the sample became 12µl, 8µl Master mix for sequencing added (in DIfE) with Dye Terminator-Mix, Program MODY sequencing was used as 96°C hold, 96°C 2´, 96°C 45´´, 50°C 1´, 60°C 4´, repeat 35x go to 3 , 4°C hold, ramp rate 1°C/sec. Precipitation of amplified DNA: Addition of 2µl CH3COONH4 7,5M to 20µl reaction and vortex, addition of 59µl Ethanol 96% to the reaction mixture (22µl) and vortex then centrifugation 13000 rpm /15 minute at room temperature, and the supernatant was discarded. Addition of 100µl Ethanol 70% for washing of sediment, centrifugation 13000 rpm /10 minute at room temperature, and the supernatant discarded. Sediments re-suspended in 10µl Loading buffer, vortex 5 seconds, and the sample was transferred into 96 well plate to measure by the sequencer.

3.2.9 DNA Ligation

Molar ration of vector to insert should be in the range of 1:2 to 1:10, and the following formula used to calculate DNA amount for ligation:

$$\text{…..ng of Insert} = \frac{\text{10 ng of Vector} * \text{(n bp) of Insert} * (1{:}2\text{-}1{:}10)}{\text{(n bp) of Vector}}$$

X µg of vector DNA , Xµg of insert DNA, 1µl of 10X ligase buffer ,1µl of 10 mM rATP(pH 7.5) and 0.5µl of T4 DNA ligase (4U/µl) were added in microcentrifuge tube

and the volume was completed to 10µl by sterile water. The sample of ligation reaction was incubated at 4°C overnight and then transformation.

3.2.10 Vector Encoding for GFP- Labelled Mouse ChREBP

In order to visualise nucleo-cytoplasmatic translocation of the transcription factors ChREBP the cDNA sequences of the murine full-length wild-type ChREBP-ζ isoform (GenBank accession no: AF245475) was cloned into pEGFP-C1 vectors, thus coupling ChREBP to the C-terminus of EGFP (a variant of green fluorescent protein).
The vector encoding for GFP-ChREBP was kindly provided by Ms. Catherine Postic Insitut Cochin, Département d'Endocrinologie, Métabolisme et Cancer, Université Paris Descartes, Paris, France. The vector was sent to us as a drop on filter paper. The piece of paper containing plasmid DNA was cut out and supplied with 100 µl BE-Buffer to extract DNA. Plasmid DNA was stored at 4 °C until transformation of competent *E. coli* JM109 cells in order to multiply the plasmid DNA.

3.2.11 Transformation of Competent E.coli JM 109 with Mouse ChREBP

For transformation, *E. coli* JM109 cells made competent with CaCl2, KCl, and MnCl2 were used. 100 µl of competent *E. coli* JM109 were supplied with 1 µl ChREBP plasmid DNA (41 ng) .Cells was incubated on ice for 30 min. A heat shock was performed at 42 °C for 30 s to allow DNA uptake into cells. After incubating cells on ice for 2 minutes, 400 µl SOC medium were added to each transformation reaction and incubated shaking for 1 h at 37 °C. 100 µl of the transformation reactions were plated on agar plates supplemented with kanamycin (final concentration: 30µg/ml). Thus, clones were selected for the presence of ChREBP vector, as they contain a kanamycin resistance gene. Plates were incubated over night at 37 °C.

After transformation of *E. coli* JM109, 4 – 8 colonies were checked for the content of the desired plasmid. To this end, the chosen colonies were grown over night in 15 ml LB medium (Lennox) supplemented with kanamycin (30µg/ml) at 37 °C and 180 rpm. Plasmids were extracted with Mini preparation NucleoSpin Plasmid kit (Macherey-Nagel) according to the manufacturer's instructions for high-copy plasmids.
Success of plasmid preparations was proven by measuring DNA concentration spectrophotometrically. The identities of the isolated plasmid were checked again via

restriction digest. ChREBP is analyzed with EcoR1 and BamH1, then maxipreparation for mouse ChREBP were done.

3.2.12 Cell Culture

3.2.12.1 Cell lines and their cultural terms

For cell culture U2OS (humane Osteosarcoma cells, ATCC Nr.: HTB-96, P29), HUH7 (human Hepatoma cells from Dr. Billicke, Charite, Campus Virchow medical center) and HepG2 cells (human Hepatoma cells, No. ATCC: HB-8065) were used, The HUH7,U2OS were cultured in T75 culture flasks with 25 ml Dulbecco's Modified Eagle Medium (DMEM) ; 25 mM glucose supplemented with 10 % Fetal Calf Serum (FCS). The HepG2 cells were cultured in T75 cultural flasks with 20 ml essential medium (MEM; 5 mms of glucose, 10% FCS). Cells were incubated at 37 °C, 5% CO2 and> 95% of air humidity.

3.2.12.2 Cells passaging and freezing

For cell passage or long-term storage, cells were grown in T75 cultural flasks with 20 ml essential medium (MEM; 5 mms of glucose, 10% FCS) to a density of 80 % confluence. Culture medium was aspirated completely and cells were incubated with 3 ml Trypsin LE at 37 °C for 5 minutes to promote detachment of cells from the flask bottom. Cells were taken up in 9 ml culture medium with 10% FCS to deactivate trypsin and pelleted at 450 x g for 5 minutes. Supernatant was aspirated and cells were resuspended in 2 ml new culture medium for passage or 1 ml freezing medium (DMEM with 20 % FCS and 10 % DMSO) and slowly cooled to -80 °C to avoid cell damage. Afterwards their storage occurred with -196 °C in liquid nitrogen. For cell passage 0.5* 10^6 cells were seeded into new culture flasks with 25 ml DMEM and medium was changed after 2 h to remove DMSO. Culture medium was changed every 3 day. For cell freezing, cells diluted in freezing medium were stored in cryotubes and transferred into a freezing container, which contains isopropanol, thus allowing a slow cooling down (approx. 1 °C per minute) to -80 °C

3.2.12.3 Cells Counting

Thoma-counting chamber was used for counting of the cells. After addition of 10 µl of the suitable cell suspendion on the placees intended on the counting chamber cells were examined under the microscope light in tenfold enlargement. Cells were counted in

four group squares (depicted in yellow and grey). Each group square covers an area of 0.04 mm^2 and has a height of 0.1 mm, leading to a volume of 0.004 mm^3 = 4 nl. Cells counted in four group squares were averaged and cell concentration was calculated. Example to the calculation of the cell number: 20 cells/4 nl. 4* 250,000 = 5 Mil. cells / ml

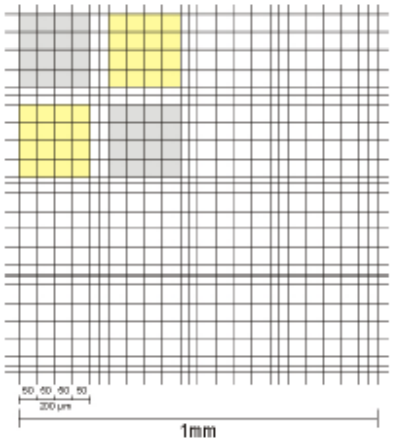

Scheme of the centre square of a Thoma counting chamber. Cells were counted in four group squares (depicted in yellow and grey). Each group square covers an area of 0.04 mm^2 and has a height of 0.1 mm, leading to a volume of 0.004 mm^3 = 4 nl. Cells counted in four group squares were averaged and cell concentration was calculated.

3.2.12.4 Coating of 96 well microtiter plates with Poly-D-Lysine.

100 ml of sterile tissue culture grade H_2O are added to 5mg Poly-D-Lysine (Sigma P6407) Final concentration of Poly-D-Lysine is 50µl/ml. Mixed by pipeting several times and Stored at 2-8°C or -20°C. 80 µl of Poly-D-Lysine solution (50 µg/ml, Sigma) were added to each well of black-walled clear bottomed 96 well micro titer plates (BD Biosciences). After incubating plates for 2 h at room temperature (RT), Poly-D-Lysine solution was aspirated and plates were washed with sterile H_2O. Plate was dried and stored at 4 °C.

3.2.12.5 Transient Transfection

Transfection is the delivery of DNA, RNA, proteins, and macromolecules into eukaryotic cells. Goals for transfection include the study of gene regulation as well as protein expression and function. The success of transfection depends on transfection efficiency, low cytotoxicity, and reproducibility. There are different methods of

transfection : Calcium Phosphate, DEAE-Dextran, Electroporation and Lipofectin. In this study lipofectamin 2000 was used.

3.2.12.6 Test of the best condition of DNA/lipofectamin ratio and cells count for HUH7, HepG2 and U2OS

100 µl cell suspension (in DMEM + 10 % FCS) per well containing different cell numbers (30000-20000-10000-5000) were seeded into a Poly-DLysine coated 96 well plate and incubated at 37 °C, 5 % CO_2, and 100 % humidity until 80 % confluence was reached to determine the best cell numbers for each type of cells as will coming in results section. For transfection , lipofectamine 2000 was diluted (as the following table) in Opti-MEM, mixed, and incubated for 5 minutes at RT. Plasmid DNA was diluted in Opti-MEM to 8 ng/µl. Equal volumes of plasmid DNA dilutions and lipofectamine dilutions were mixed by different concentrations (1:0.5 - 1:1.5 - 1:2.5 - 1:3.5) and incubated 20 minutes at RT. 50 µl of the transfection mix were added to each well containing 100 µl culture medium, thus adding 200 ng plasmid DNA to each well. After 5 h, Opti-MEM was replaced by high glucose medium (DMEM + 4.5 g/l glucose + 10 % FCS) Plates were incubated for 24 hours before fixation. DNA/Lipofectamin-ratio of 1:3.5 and a cell number of 20,000 U2OS cells per Well. While, in HUH7, the ratio of 1:3.5 and 30,000 cells per Well. Considering of HEPG2, 50,000 cells per Well and a DNA/Lipofectamin-ratio of 1:3.5. To transfect cells in different tissue culture formats, vary the amounts of lipofectmine 2000 CD, DNA, cells, and medium used in proportion to the relative surface area.

Culture vessel	**Surf. area per well (cm2)**	**Vol. of Plating medium**	**Volumes Opti-MEM**	**DNA**	**Lipofecta min**
96 Well	0,3 cm^2	100 µl	2 x 25 µl	0,2 µg	0,5 µl
24 Well	2 cm^2	500 µl	2 x 50 µl	0,8 µg	2,0 µl
12 Well	4 C	1 ml	2 x 100 µl	1,6 µg	4,0 µl
6 Well	10 cm^2	2 ml	2 x 250 µl	4,0 µg	10 µl
60 mm	20 cm^2	5 ml	2 x 0,5 ml	8,0 µg	20 µl
10 cm	60 cm^2	15 ml	2 x 1,5 ml	24 µg	60 µl

Up and down scale for transfection

3.2.12.7 Fixation and staining of cells with 4'-6-diamidino-2-phenylindole (DAPI).

To be able to analyze the cells for some days following the experiment, cells were fixated and nuclei were stained with DAPI, a fluorescent dye, which binds to the minor groove of DNA. DAPI has an absorption maximum at 358 nm and an emission maximum at 461 nm. Medium was removed and cells were supplied with 100 µl 4 % paraformaldehyd (in PBS). After 30 minutes of incubation in the dark at RT, paraformaldehyd was removed and plates were washed with PBS. 50 µl per well DAPI staining solution were added and incubated at RT in the dark for 30 min. Plates were washed twice with PBS and 100 µl PBS were added to each well before plate was sealed.

DAPI staining solution: 1 µl 1:10 prediluted DAPI stock solution (10.9 mM)
15 µl Triton X-100
5 ml PBS

3.2.12.8 Analysis of transfected cells by fluorescence microscope.

After fixation, cells were analyzed by fluorescence microscope, using the BD Pathway 435 bioimager and the program BD Attovision, which allow for automated, and high-content cellular image analysis. To this end, the bioimager was programmed to focus the centre of each well of a 96 well microtiter plate and excite the fixated cells with the appropriate wavelengths for DAPI and GFP, the following table show the wavelengths in which DAPI and GFP absorbs light and emits.

Fluorescent dye	Absorption maximum	Emission maximum
DAPI	358 nm	461 nm
GFP	395 nm	509 nm

Emission light was directed through a dichroic mirror and a filter wheel before being captured via a CCD camera with a shutter speed of 1 s. Thus, for each well, 2 TIFF images were taken with one image showing DAPI staining and the other image depicting GFP fluorescence. Qualitative as well as quantitative analyses of transcription factor translocation were based on these 12-bit images, which provide a dynamic intensity range from 0 (lowest possible intensity) to 4095 (highest possible intensity). Qualitative assessment of transcription factor translocation was performed by merging images showing DAPI staining, thus cell nuclei, with the same image showing GFP fluorescence.

DAPI was chosen to be displayed in red, whereas GFP was chosen to be depicted in green. Thus, overlay of the two dyes resulted in yellow and was therefore distinguishable from unblended GFP and DAPI. Quantitative assessment of transcription factor content in nucleus and cytoplasm was approached with a segmentation algorithm, which enables the bioimager to distinguish between nucleus and cytoplasm and finally allows using the GFP fluorescence intensity to assess relative transcription factor content in both compartments. To this end, the bioimager was programmed such that nuclei were recognised by DAPI staining. Since recognition of cell borders is difficult due to overlaps, cytoplasm was framed as a defined, nucleus-shaped ring (width: 20 pixels) around the nucleus. Nuclear and cytoplasmatic GFP fluorescence intensities were assessed for every cell by determining the intensity value between 0 – 4095 of each pixel in the nucleus and in the cytoplasm respectively and calculating the average intensity per pixel for the according compartment. Nuclear and cytoplasmatic GFP-contents were set in relation by forming the GFP intensity ratio nucleus/cytoplasm. Eventually, ratios calculated for each cell per well were averaged. Cells with an overall GFP-fluorescence intensity (cytoplasm + nucleus) below 1000 were declared untransfected and were consequently excluded from the analysis. Significance analysis was performed by T-test.

Total amount of cells per well was assessed by DAPI staining. Thus, transfection efficiency was calculated as follows:

$$\text{Transfection Efficiency} = \frac{\text{Total cells - Untransfected cells}}{\text{Total cells}}$$

The fluorescence microscope

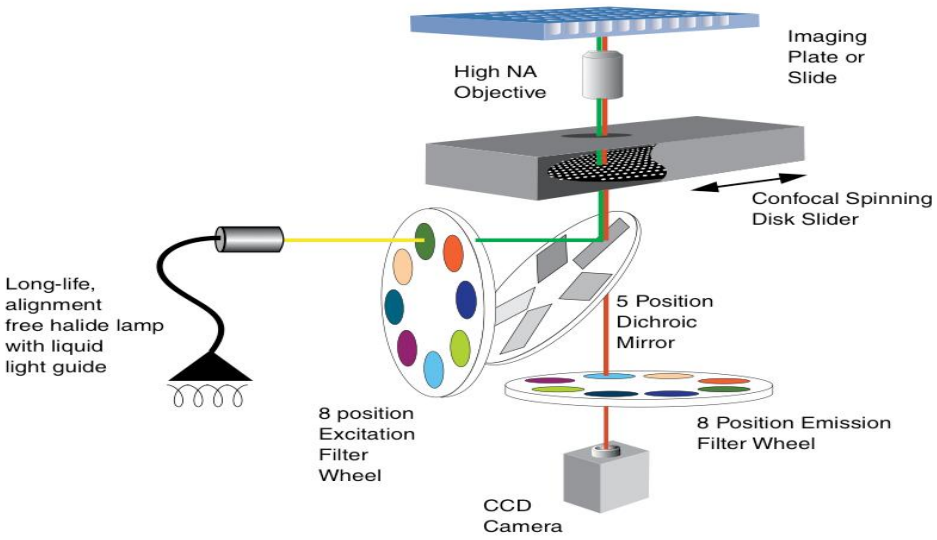

Schematic representation of the BD Pathway light path.

3.2.12.9 Picture analysis by the fluorescence microscope

Pathway 435 system allowed with the help of the software Attovision 1.6 the admission of 2 TIFF pictures. One showed DAPI-and one the GFP fluorescence. The pictures were used for qualitative as well as quantitative statements to the translocation of the transcription factors. The qualitative assessment was carried out by coalescence respective DAPI-and GFP picture. DAPI staining corresponded to the nucleus and is shown in red. GFP was shown green and showed the localization of the GFP marked transcription factor. If DAPI-and GFP pictures were merged, one could recognize by the yellow compound color if the GFP signal existed in the nucleus.

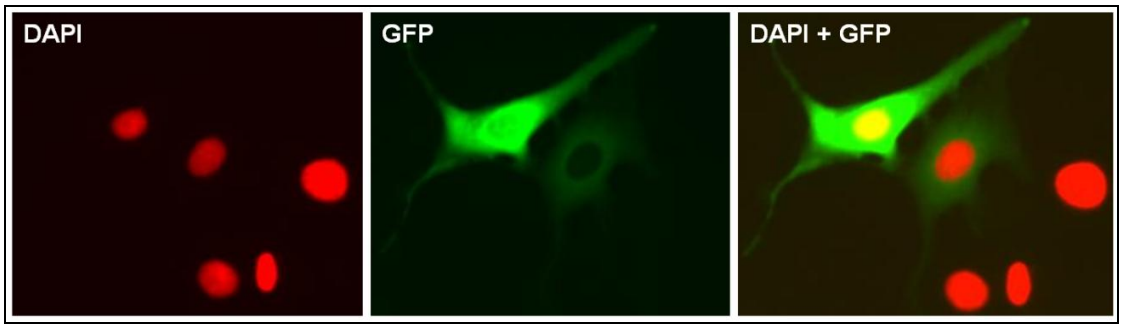

Exemplary representation from DAPI-, GFP-, and two merged pictures. red: With DAPI colored nucleuses; green: GFP marked transcription factors ChREBP; yellow: Coalescence from DAPI-and GFP signal.

The quantitative assessment of the translocation of the transcription factor was carried out by a segmentation program. After the testing of the possible variations an algorithm which delivered the most realistic data was used. With the help of the segmentation, the definition of nuclus and cytoplasm became possible what made the relative localization of the GFP marked transcription factors in every cell measurable.

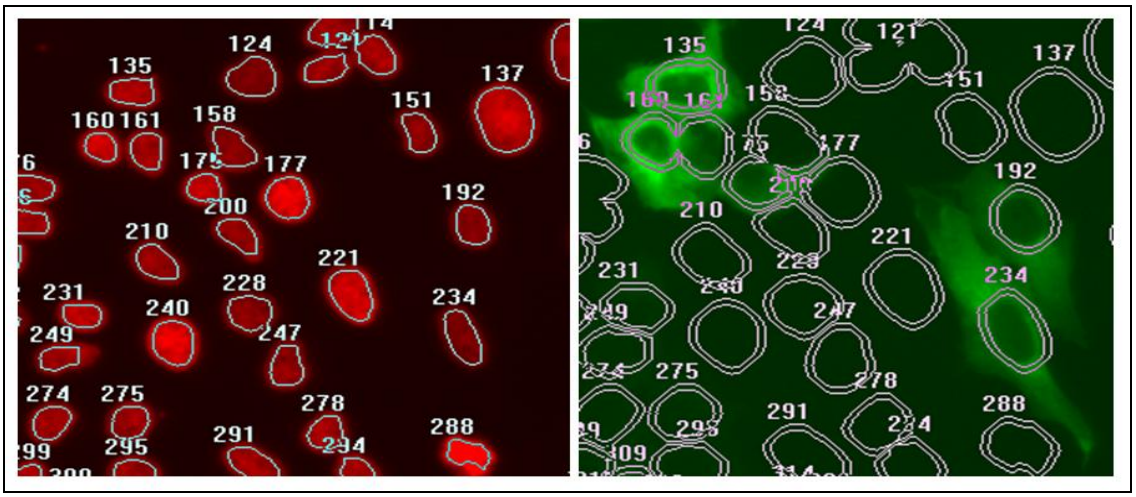

DAPI-Segmentation (on the left); GFP-Segmentation (on the right).

DAPI signal was used to define the borders of the nucleus. To discriminate the GFP signal from the cytoplasm from GFP signal in the nucleus, an adequate segmentation program had to be found. The segmentation program was used as Cyt Nuc ring tape ". Here a movement of the border of the nucleus was carried out about 3 pixels inwards and the measurement of the cytoplasmas took place within 5 pixels of wide ring. Therefore, the fluorescence intensity GFP could be measured in the nucleus and in a defined part of the cytoplasma of every cell. The relation of the dimensions of the agreed surfaces played no role, because the average GFP intensity per pixel was determined. The GFP intensities in the nucleus and in the cytoplasma were put in the relation (Ratio) to each other.

Ratio = GFP intensity in the nucleus / GFP intensity in the Cytoplasm**.**

A relatively smaller ratio allowed to conclude that there is more ChREBP in the cytoplasma, as well as a relatively bigger ratio that there is more ChREBP in the nucleus. For the evaluation of the data we used the progam BD Image data explorer employing microsoft excel in 2007 including microsoft access in 2007. At least 100 cells per well

were evaluated and the average of the ratios was determined. If the sum of the GFP intensities was in the nucleus and cytoplasma smaller than 1000 these cells were not evaluated as transfected and were excluded from the calculation.

3.2.12.10 Glucose and insulin stimulation

Around the effect of high glucose and insulin on the translocation of the transcription factor (ChREBP). After 5 h of the transfection DNA / lipofectamin (1: 2.5) in HUH7, HepG2 and U2OS the Medium was changed to DMEM containing 5 mM Glucose and 2% FCS. Next morning cells were on starvation with 5mM Glucose and 0% FCS for 1 h and then stimulated with 25mM Glucose and 100 nM Insulin for 2 hours. Finally, cells were fixed and analyzed fluorescence microscope.

3.2.12.11 The effect of sweeteners on the translocation of h.ChREBP

Fructose, aspartame, natrium cyclamate, saccharin and stevioside were used at different concentrations with or without insulin as following:

Fructose	5mM	25mM
Aspartame, Cyclamate, Saccharin	0.1mM	1mM
Stevioside	10µM	100µM

3.2.12.12 The effect of PUFAs on the translocation of h.ChREBP

Docosahexaenoic, Eicosapentaenoic, Linoleic, Oleic acid and Oleuropein were purchased from Sigma Aldrich at 99% concentration. We prepared 52.8 mM PUFAs by dissolving in NaOH 50 mM. BSA was arrived as 30% solution (4.5mM), we prepared 1.1 and 0.825 mM BSA by dissolving in water.

1 part PUFAs (52.8mM) + 3 parts BSA (1.1mM) = Ratio PUFAs / BSA =16 **First stock**

1 part first stock + 3 parts BSA (0.825mM) =Ratio PUFAs / BSA = 4 **Second stock**

we used 0.825 mM BSA to prepare the second stock because the final concentration of BSA after adding the PUFAs in first stock became 0.825mM.

For experiments using PUFAs, the cells were transfected for 5 h then the Medium was changed to DMEM containing 5 mM Glucose and 2% FCS overnight. Cells were starvated with 5mM Glucose and 0% FCS for 1 h then the medium was changed to a serum-free medium containing 25 mM glucose, 100 nM insulin, and different concentration of albumin-bound oleate [C18:1 (n-9)], linoleate [C18:2 (n-6)], EPA

[C20:5 (n-3)], DHA [C22:6 (n-3)] or oleuropein at a fatty acid/albumin ratio of 4:1 for 2 hour. For all studies fatty acid–free BSA was used.

	mM Fa	**mM BSA**	**ratio FA/BSA**	**mM NaOH**
1 part FA (52.8mM) + 3 part BSA (1.1 mM)	13.2	0.825	16	12.5
1 part FA BSA mixture + 0,2 parts BSA (0,825 mM)	11	0.825	13.33333	10.41667
add 10µl to 100µl cells, in 10 µl it must be 1*11	11	0.825	13.33333	10.41667
resulting incubate	1	0.075	13.33333	0.94697
1 part 11mM FA + 9 parts BSA (0,825 mM)	1.1	0.825	1.333333	1.041667
1 part 1,1mM FA + 9 parts BSA (0,825 mM)	0.11	0.825	0.133333	0.104167
3 parts 11mM FA + 7 parts BSA (0,825 mM)	3.3	0.825	4	3.125
3 parts 1,1mM FA + 7 parts BSA(0,825 mM)	0.33	0.825	0.4	0.3125

FA Concentrations added (10µl too 100µl cells)	**FA Concentrations in incubate**	**BSA**	**ratio FA/BSA**	**nM NaOH**
11 mM	1 mM	0.075 mM	13.33	946.9697
3.3 mM	0.3 mM	0.075 mM	4.00	284.0909
1.1 mM	0.1 mM	0.075 mM	1.33	94.69697
0.33 mM	0.03 mM	0.075 mM	0.40	28.40909
0.11 mM	0.01 mM	0.075 mM	0.13	9.469697

3.2.13 Stable transfection

1 million of U2OS cells were seeded in 6ml DMEM with 4.5g glucose/l and 10% FCS in 25 cm^2 flask for 24h. 25µl lipofectamin 2000 was added to 600 µl Optimem and incubated 5 min at RT, after that, 22.7 µl of h.ChREBP (10µg) was added to 602 µl Optimem, both were combined, mixed gently, and incubated 20 min at RT. 1.25 ml of transfection mix was added to the cell in 25 cm^2 flask and incubated at 37°C for 5 h.
Medium was exchanged to DMEM 4,5g glucose/L and 10% FCS for 2 days incubation. G418-stock was prepared freshly 400mg/10ml sterile water, filtrated and divided to 10 tubes and stored at -20°C. 500µl of G418 were add to 50ml DMEM 4,5g glucose/L +

FCS10% . The medium exchanged to DMEM+10%FCS+400µg/ml G418 for 3 days two times. After 7 days, splitting and dilution of by G418 selected cells was done by trypsination Cells were seeded in 100µl DMEM+10% FCS+400µg/ml G418 per well in a 96 well plate. The medium was exchanged to DMEM+10%FCS+400µg/ml G418 every 3 days. Some wells in the 96-well plate appeared about 80% confluent. Those cells were trypsinized with each 20µl Tryp-LE for 5min at 37°C, stopped by adding of 150µl DMEM+10%FCS+G418 400µg/ml, and transfered into 12 well plates with 1ml DMEM+10%FCS+G418. The cells were passaged from 12 wells to 6 wells by adding 250µl Tryp-LE in every well for 5min at 37°C. Then 1 ml medium and centrifugation at 490g for 5 min, resuspension of sedimented cells in each 1ml medium and seeded in 6 well plate which has 1ml of DMEM+10%FCS+G418 400µg/ml. Exchange of medium with DMEM+10%FCS+400µg/ml G418 every 3 days . 6-well plates were trypsinized with 500µl Try-LE in every well for 5min at 37°C, 2ml DMEM+FSC 10% add, then centrifugation at 490g for 5 min, resuspension of sedimented cells in each 5ml DMEM+10%FCS+G418 400µg/ml for T25-flasks, 100µl transferred in 96-well (coated plate) for control of GFP after fixation and DAPI-staining.. Cells were fixed, stained with DAPI and measured with fluorescence microscope. Imaging for Dapi and GFP and make merge between them had done to select some wells more than 80% density and transferred these wells from 25 cm^2 flasks to 75 cm^2 flasks till 80% density. Cells from 75 cm^2 Flasks were freezed in Kryo-vials DMEM (4,5g Glucose/L) +20% FCS+10% DMSO+G418 400µg/ml.

3.2.14 Statistical analysis

The significance of the results was determined in Excel 2007 by means of the student´s t tests (Paired). The errors bars correspond to the standard error of mean (SEM). Differences were considered statistically significant at $P< 0.05$. The statistical significance between the measurement results of the effect of sweeteners and PUFAs, were tested by the program PASW statistics 18, general liner model (repeated measure). Differences were considered statistically significant at $P< 0.05$.

4- RESULTS AND DISCUSSION

Carbohydrate-responsive element–binding protein (ChREBP) was shown to play a pivotal role in the induction of glycolytic and lipogenic genes by glucose (Dentin *et al.* 2004), (Iizuka *et al.* 2004) by its capacity to bind to the ChoRE present in promoters of these target genes (Stoeckman *et al.* 2004), (Ishii *et al.* 2004). ChREBP is expressed in liver and is responsive to the nutritional state (Dentin *et al.* 2005a). Liver-specific inhibition of ChREBP improves hepatic steatosis and insulin resistance in obese ob/ob mice. Since ChREBP cellular localization is a determinant of its functional activity, a better knowledge of the mechanisms involved in regulating its nucleo-cytoplasmic shuttling and/or its post-translational activation is crucial in both physiology and physiopathology (Postic *et al.* 2007).

First I tried to clone the human ChREBP (NCBI Reference Sequences NM_032951 and NT_007758.11) in a GFP expression vector by multiple PCRs using human liver cDNA as template and a set of primer pairs. With this human ChREBP-GFP vector I wanted to test the influence of the different dietary elements on the activation and translocation of human ChREBP from cytoplasm to the nucleus.

Second, I tried to test the influence of the different dietary elements on the translocation of mouse GFP-ChREBP. The vector encoding for GFP-ChREBP was kindly provided by Ms. Catherine Postic, Insitut Cochin, Département d' Endocrinologie, Métabolisme et Cancer, Université Paris Descartes, Paris, France. The murine full-length wild-type ChREBP-ζ isoform (GenBank accession no: AF245475) has been cloned into pEGFP-C1 from Clontech (Dentin *et al.* 2005a) and sent to us as a drop on filter paper.

Third, I used human ChREBP, TrueORF cDNA Clones and Precision Shuttle Vector. AC, AN GFP vectors and human ChREBP were purchased from Origene company to construct a human ChREBP-GFP vector. With this construct I tested the influence of different fatty acids on this regulation which appears to be scarcely investigated. This signal transduction is of utmost importance for concepts of nutrition. If hepatic lipogenesis is inhabitable by n3 and n6 fatty acids, their intake should influence the development of fatty liver. This would be of relevance especially for diabetics with impaired glucose tolerance. Comparing monounsaturated fatty acids with polyunsaturated fatty acids, the polyunsaturated fatty acids may be more important. The action of

ChREBP and its translocation from cytoplasm to the nucleus was monitored by fluorescence microscope. The influence of different fatty acids (MUFA and PUFA n3/n6) on the translocation of the human ChREBP was tested. In addition the impact of polyphenols from olive oil and different kind of sweeteners on this translocation was investigated.

4-1. Cloning of human ChREBP NM-032951 in vitro

I attempted to clone human ChREBP by using human liver cDNA as template by multiple overlapping PCRs. Human ChREBP (864 amino acids and Mr = 94,600) has 17 Exons, that contains several domains, including a nuclear localization signal (NLS) near the N-terminus, polyproline domains, a basic loop-helixleucine- zipper (b/HLH/Zip), and a leucinezipper- like (Zip-like) domain. ChREBP has an additional PKA phosphorylation sites at Ser 196 and Thr 666 (Figure 14 A, B).

A

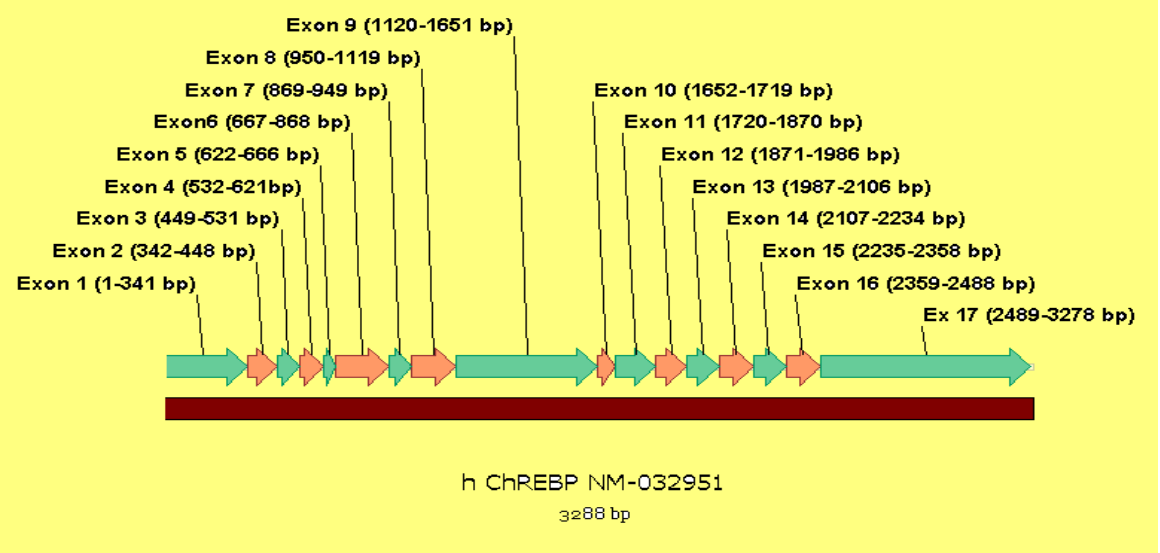

B

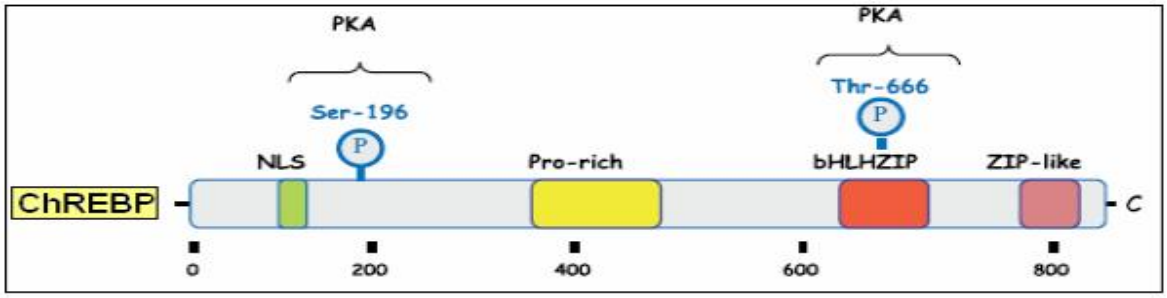

Figure 14. (A) Human ChREBP-cDNA with sequences deriving from 17 exons according to gene bank. (B) Human ChREBP structure. (Postic et al. 2007)

4-1-1. ChREBP amplification: upstream-exon 1 DNA plasmid with 5`-UTR + promoter sequences

The upper part of human ChREBP was generated by PCR using the upper PCR primer ChREBP gen 5` actcgaagaggcgtgtgagt 3` and lower PCR primer ChREBP gen 5` gcattaccttgggcttacca 3` (number 3,4 according to the mRNA list in materials) and using human liver cDNA as template. The PCR product was 1192 bp. according to the gen bank (Figure 15).

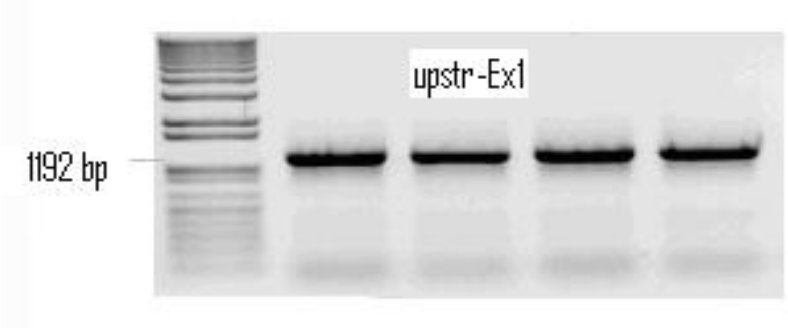

Figure 15. Upstream-exon 1 DNA.
Upstream-exon 1 DNA after PCR and agarose gel analysed.DNA bands are in accord with the fragment sizes calculated on the basis of the vector maps.

Cloning of upstream-exon 1 DNA in TOPO PCR 2,1 vector

The DNA was extracted and cloned in TOPO TA PCR vector, the size of TOPO PCR 2,1 vector is 3931 bp, and the size of DNA upstr-Ex1 is 1192 bp, so, after cloning the size of upstream-exon 1 DNA plasmid vector became 5123 bp. (Figure 16)

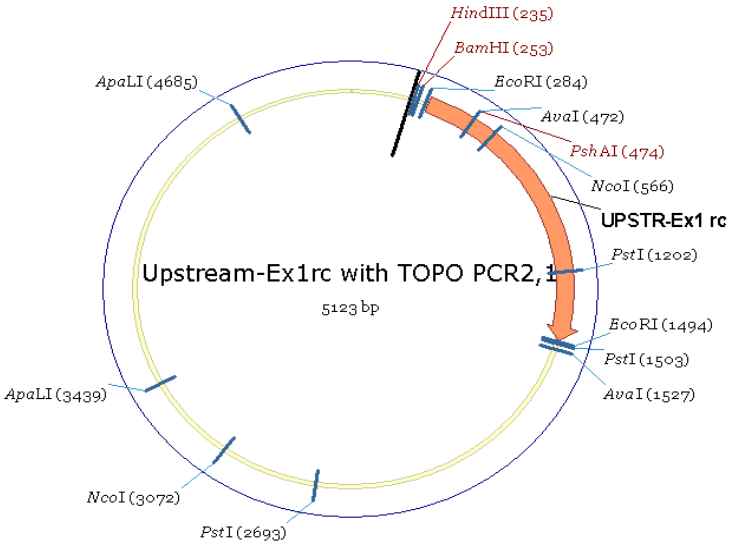

Figure 16. Upstream-exon 1 DNA plasmid in TOPO TA vector.

Digestion of upstream-exon 1 DNA plasmid

After transformation and extraction of upstream-Exon 1 DNA plasmid with mini preparation the ratio, absorbance and the concentration (µg/ml) were measured. There were 1, 99 - 0,46 and 231 respectively. The restriction enzymes PshA1 and Pst1 were used to test the plasmid and the result was according to the expected. The recognition sites of PshA1 and Pst1 in upstream-exon 1 DNA plasmid were predicted with the program vector NTl by Invitrogene (see Figure 17). Agarose gel electrophoresis with the isolated, digested plasmid revealed one band of 1192 bp for PshA1 and three bands of 3632, 1190 and 301bp for Pst1.

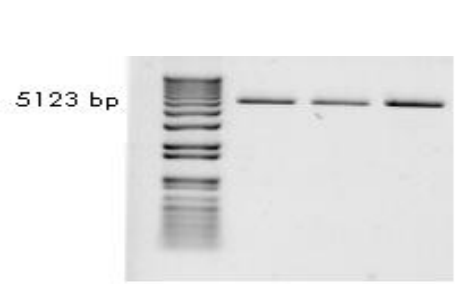

A: Digestion with pshA1

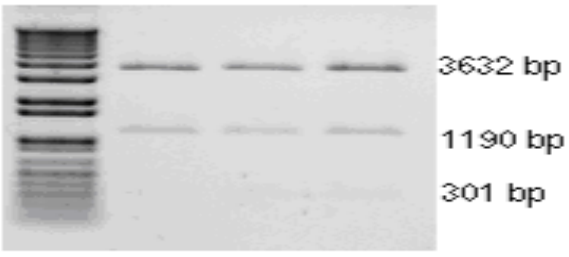

B: Digestion with pst1

Figure 17. Digestion of Upstream-exon 1 DNA plasmid with PshA1 and Pst1.

Plasmid DNA was digested with pshA1 and pst1 respectively and analysed in 1% agarose gel. Each lane contains 20 ng digested plasmid DNA. DNA bands are in accord with the fragment sizes calculated on the basis of the vector maps.

Sequencing of upstream-exon 1 DNA plasmid by M13 sequencing primer

The sequence of the amplification was determined using the forward and reverse sequencing Primer M13 for each sample. There were some samples congruent and others were different. Sequencing of the major part of the insert was successful (shown a M13 labeled blue line, the upstream-exon 1 insert is shown in orange and part of exon 1 of ChREBP in green in Figure (18A). Figure (18B) showed the sequencing of the part of vector before the exon 1 of ChREBP is shown in (black), sequencing Primer M13 (red), upstream-exon 1 (violet) and the part of upstream-exon 1 which covered with Primer M13 (yellow).

A

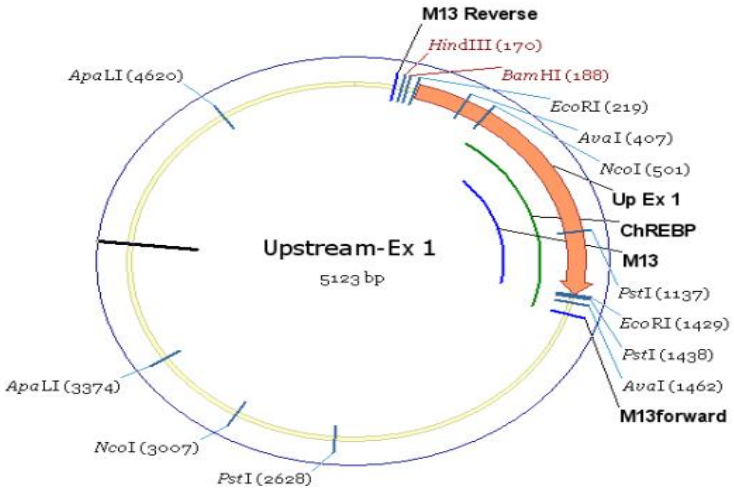

B

Figure 18. The covering of sequencing primer M13 to upstream-exon 1 DNA plasmid (A,B).

4-1-2. ChREBP amplification: exon 1 to exon 6 DNA

The second part of human ChREBP was generated by PCR using the upper PCR primer ChREBP gen 5` agactcggactcggacacag 3` and lower PCR primer ChREBP gen 5` cggactgagtcatggtgaag 3` (number 16,17 according to the mRNA list in materials) and using human liver cDNA as template. The PCR product was 725 bp. according to the gen bank. (Figure 19)

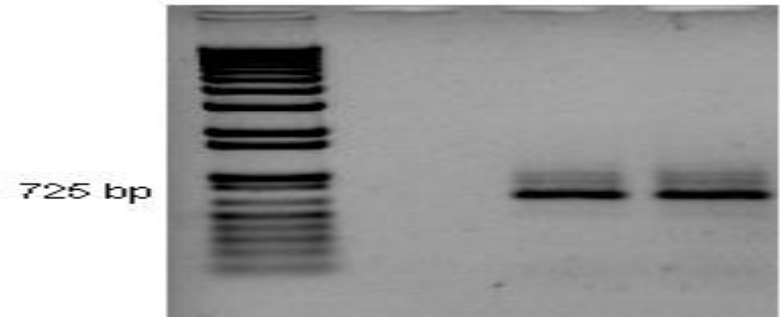

Figure 19. Exon 1 to Exon 6 DNA

Exon 1 to Exon 6 DNA after PCR and agarose gel analysed. DNA bands are in accord with the fragment sizes calculated on the basis of the vector maps.

Cloning of exon 1 to exon 6 DNA in TOPO PCR 2,1 vector

The DNA was extracted and cloned in TOPO TA PCR vector, the size of TOPO PCR 2,1 vector is 3931 bp, and the size of DNA exon 1 to exon 6 is 725 bp, so, after cloning the size of exon 1 to exon 6 vector became 4656 bp. (Figure 20)

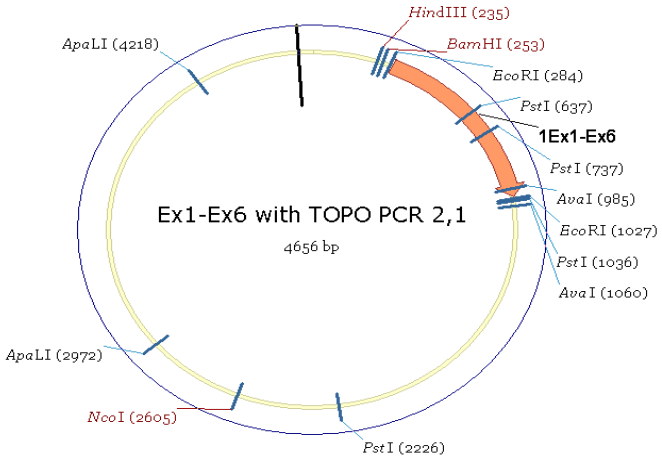

Figure 20. Exon 1 to exon 6 DNA plasmid in TOPO TA vector.

Digestion of exon 1 to exon 6 DNA plasmid

After transformation and extraction of exon 1 to exon 6 DNA plasmid with mini preparation the ratio, absorbance and the concentration (µg/ml) were measured. There were 1.82 – 1.05 and 525 respectively. The restriction enzyme EcoR 1 was used to test the plasmid and the result was according to expected (see Figure 21). The restriction digest of exon 1 to exon 6 DNA plasmid with EcoR 1 delivered two fragments of 3913 and 743 bp. This result was predicted with the program vector NTl by Invitrogene.

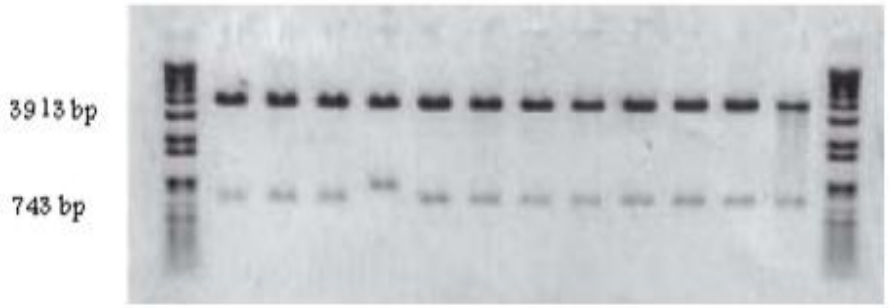

Figure 21. Digestion of exon 1 to exon 6 DNA plasmid with EcoR 1.

DNA plasmid was digested with EcoR 1 and analysed in 1% agarose gel. Each lane contains 20 ng digested plasmid DNA. DNA bands are in with the fragment sizes calculated on the basis of the vector maps.

Sequencing of exon 1 to exon 6 DNA plasmid by M13 sequencing primer

The sequence of the amplification was determined using the forward and reverse sequencing Primer M13 for each sample. There were some samples congruent and others were different. Sequencing of the major part of the insert was successful (shown a M13 labeled blue line, the exon 1 to exon 6 insert is shown in orange in Figure 22A). Figure 22B showed the sequencing Primer M13 (red) and the part of exon 1 to exon 6 which covered with Primer M13 (yellow).

A

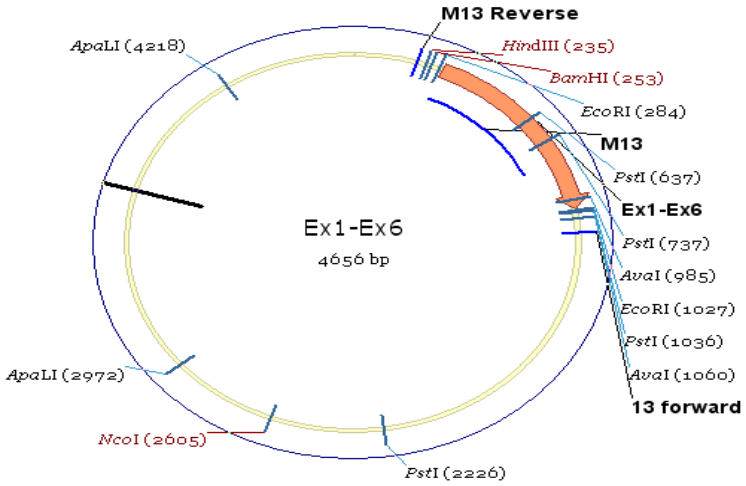

B

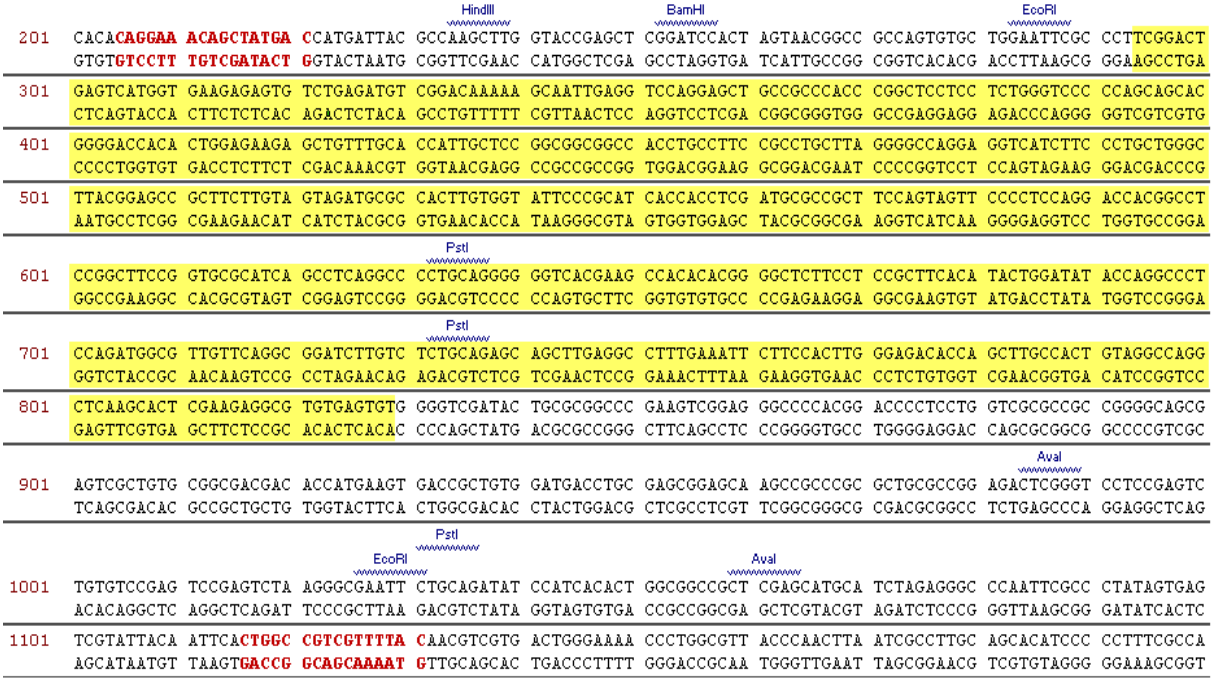

Figure 22. The covering of sequencing primer M13 to exon 1 to exon 6 DNA plasmid (A,B).

4-1-3. Ligation between upstream-Ex1 and Ex1-Ex6 DNA plasmid vectors

Double cuts for the upstream-Ex1 and Ex1-Ex6 DNA plasmid vectors with BamH1 and PshA1 were made. The fragments (a) 5 µg of Topo PCR 2,1 upstream-Ex1 (big fragment) after PshA1 and BamH1 (4902 bp) as a vector and (b) 1.5 µg of Topo PCR 2,1 Ex1-Ex6 (small fragment) after PshA1 and BamH1 (734 bp) as an insert (Figures 23, 24) were isolated. After ligation between (a) upstream-Ex1 and (b) Ex1-Ex6, a new vector (up Ex6) was created with the size of 5686 bp (Figure 25).

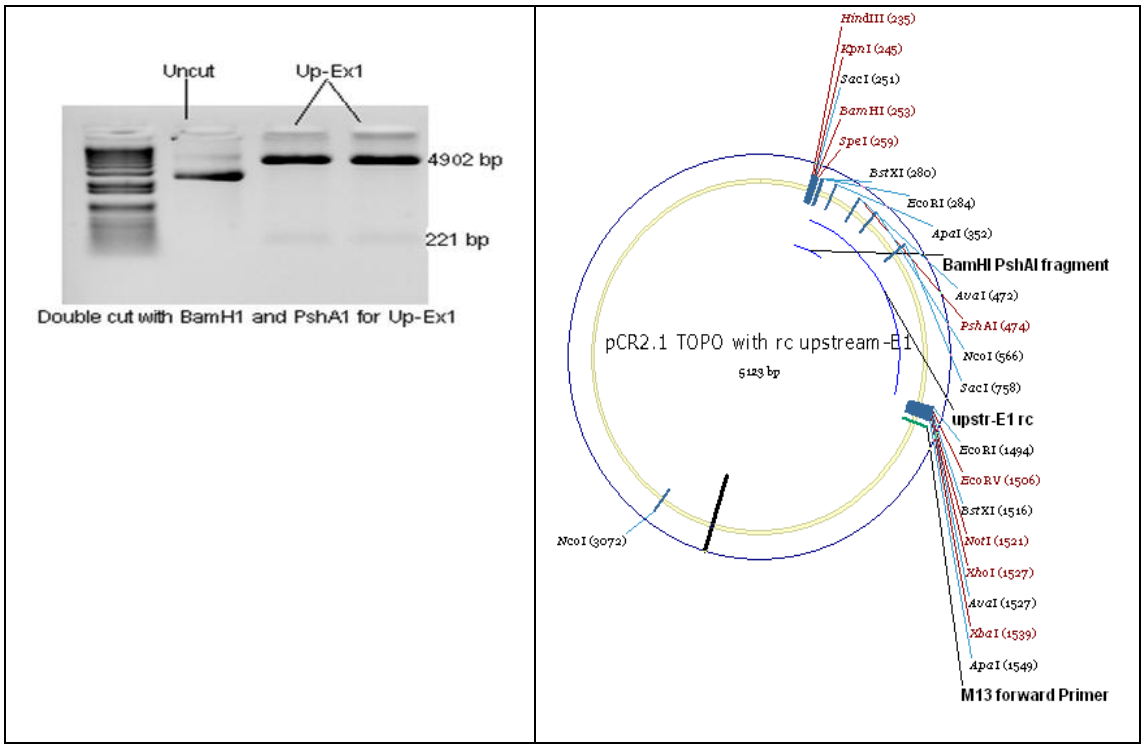

Figure 23. Double cut for Upstream-Ex1 DNA plasmid vectors with BamH1 and PshA1.

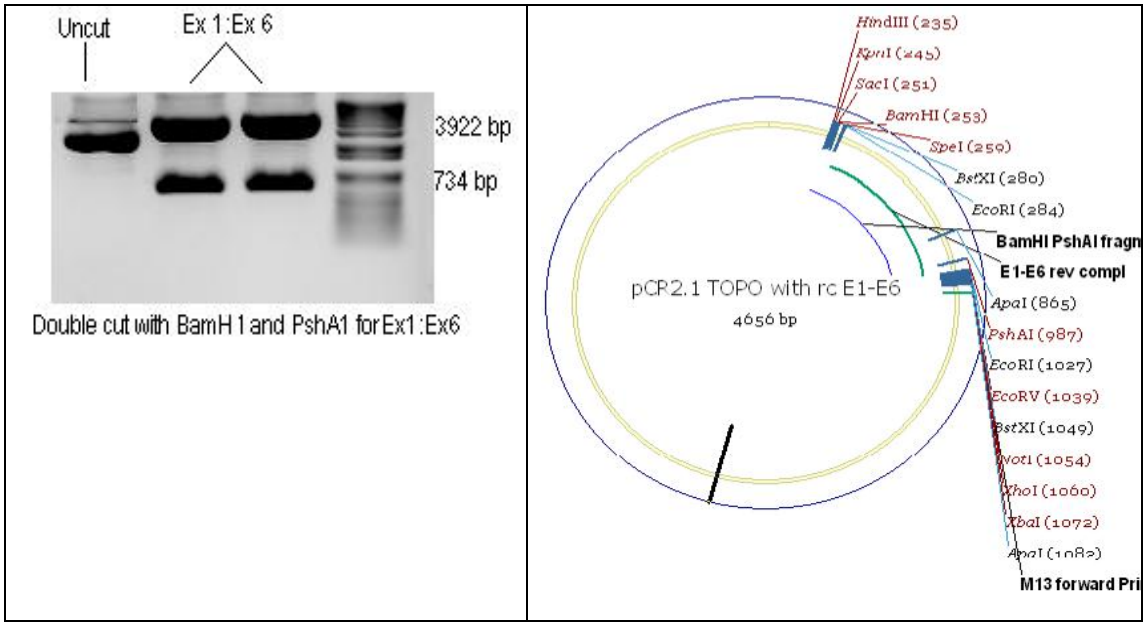

Figure 24. Double cut for Ex1-Ex6 DNA plasmid vectors with BamH1 and PshA1.

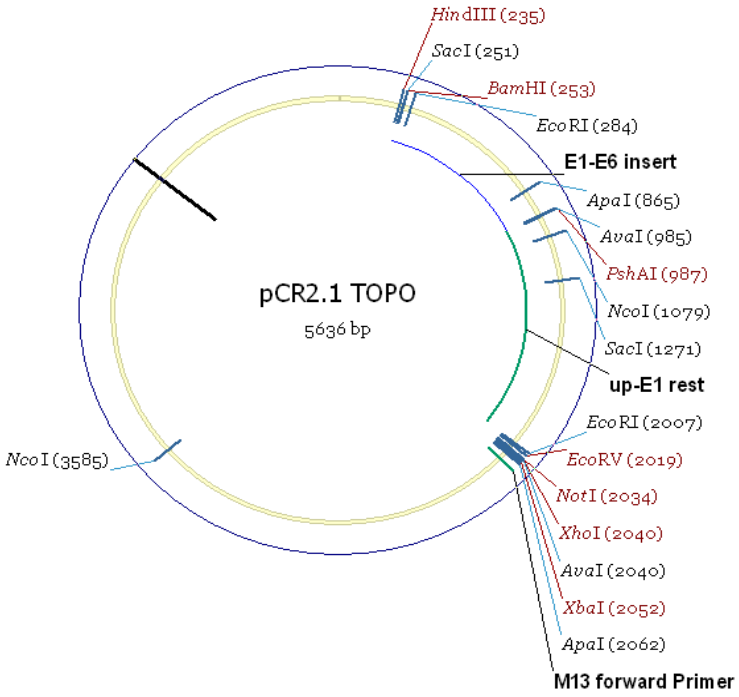

Figure 25. Up Ex6 after ligation between upstream-Ex1 and Ex1-Ex6 DNA plasmid

Digestion of up exon 6 DNA plasmid

After transformation and extraction of up exon 6 DNA plasmid with mini preparation the ratio, absorbance and the concentration (µg/ml) were measured. There were 1.789 – 1.279 and 639.5 respectively. The restriction enzymes Ava1, Nco1 and double cut with BamH1, Nco1 were used to test the plasmid and the result were according to expected (see Figure 26). The restriction digests of up exon 6 DNA plasmid with Ava1delivered two fragments of 4581 and 1055 bp. and with Nco1 revealed two bands at 3130 and 2506 bp. The double cut with BamH1and Nco1 was expected to result in three fragments 2506, 2304 and 826 bp (see Figure 27). This result was predicted with the program vector NTl by Invetrogene.

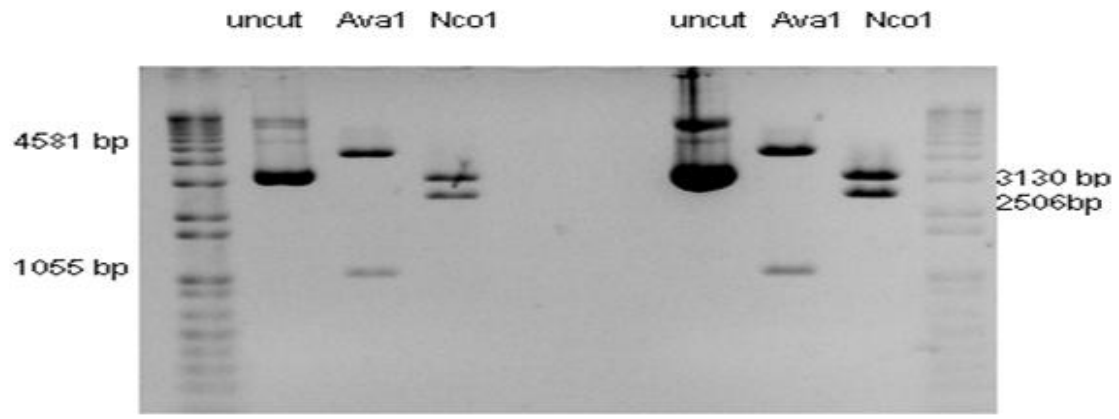

Figure 26. Digestion of up exon 6 DNA Plasmid with Ava1 and Nco1

DNA was digested with Ava1 and Nco1 and analysed in 1% agarose gel. Each lane contains 20 ng digested plasmid DNA. DNA bands are in accord with the fragment sizes calculated on the basis of the vector maps.

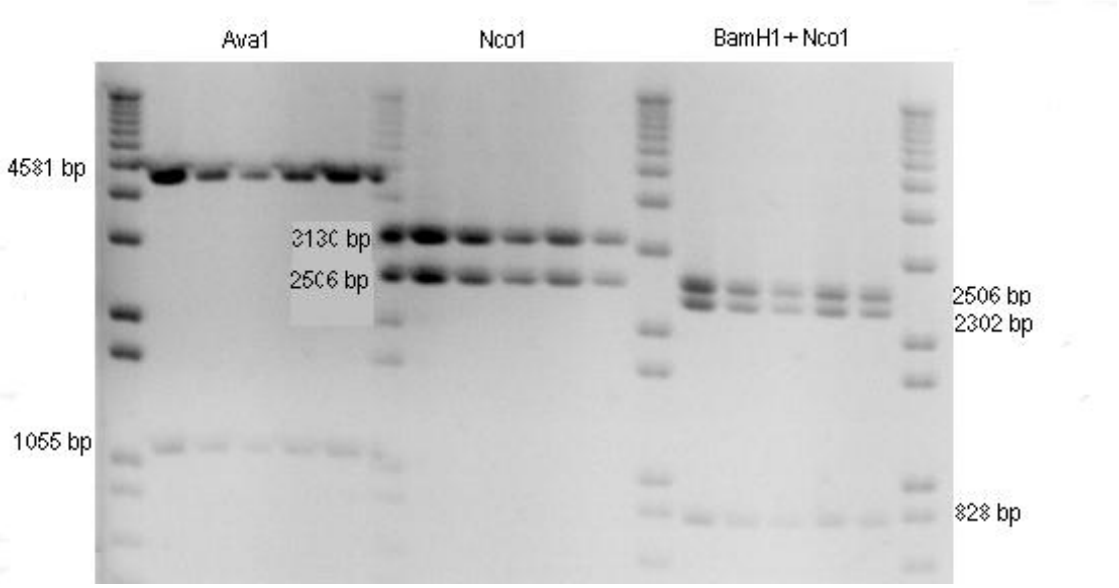

Figure 27. Digestion of up exon 6 DNA with Avo1, Nco1and BamH1+Nco1

DNA plasmid was digested with Avo1, Nco1and BamH1+Nco1 and analysed in 1% agarose gel. Each lane contains 20 ng digested plasmid DNA. DNA bands are in accord with the fragment sizes calculated on the basis of the vector maps.

Sequencing of up exon 6 DNA plasmid by M13 Sequencing primer

The sequence of the amplification was determined using the forward and reverse sequencing Primer M13 for each sample. There were some samples congruent and others

were different. Sequencing of the major part of the insert was successful (shown a M13 labeled green line, the up Exon 6 insert is shown in orange in Figure (28A). Figure 28B showed the sequencing Primer M13 (red) and the part of up Exon 6 which covered with Primer M13 (yellow).

A

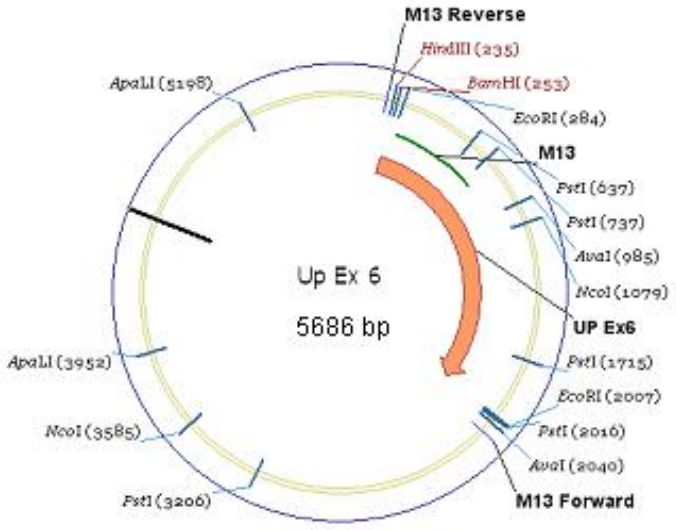

B

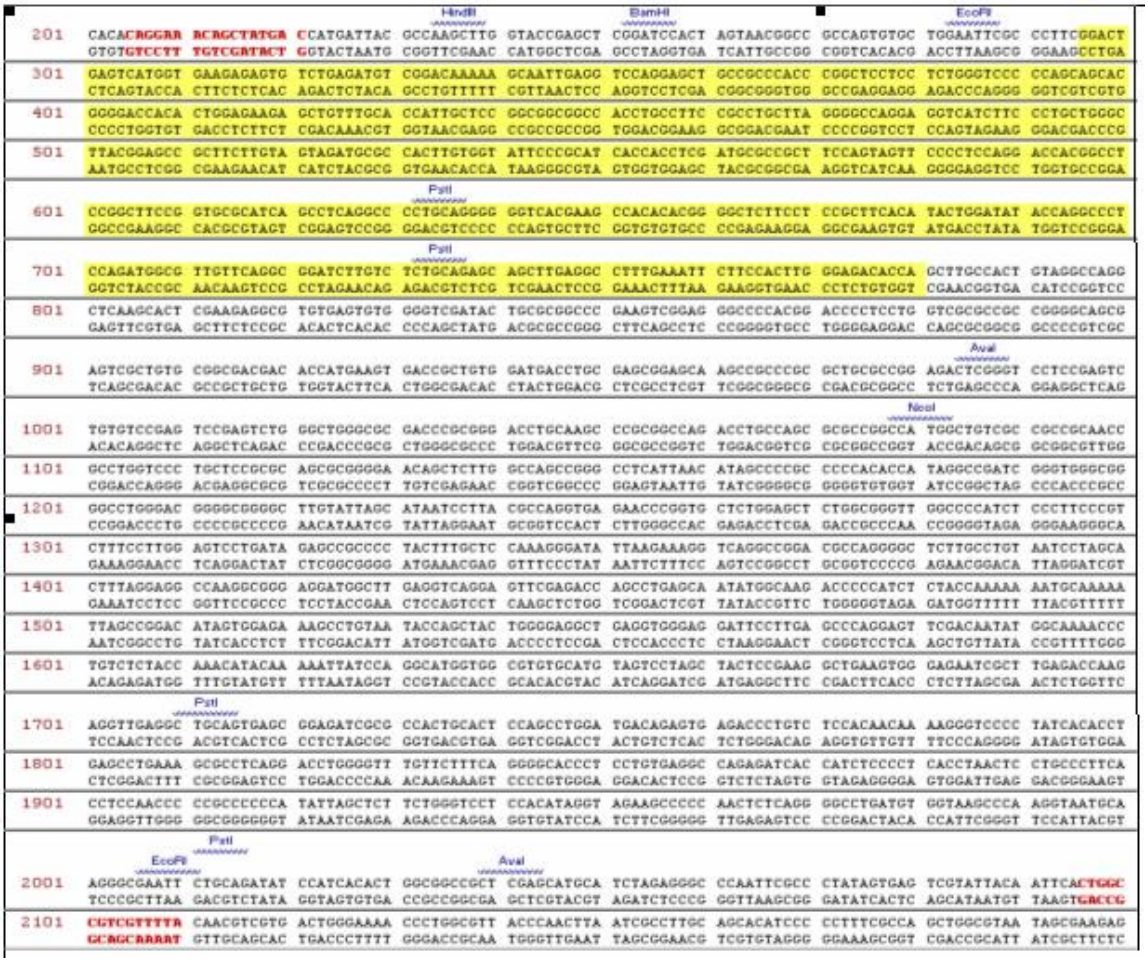

Figure 28. The covering of sequencing primer M13 to up exon 6 DNA plasmid (A,B)

4-1-4. ChREBP amplification: exon 9 to exon 17

The third part of human ChREBP was generated by PCR using the degenerate oligonucleotide primers, upper PCR primer ChREBP gen 5` gcctctcttctctcccaggt 3` and lower PCR primer ChREBP gen 5` acagcatcctcctctttcca 3` (number 8,9 according to the mRNA list in materials) and the sequence of human liver cDNA. The PCR product was 1662 bp according to the gene bank data (Figure 29).

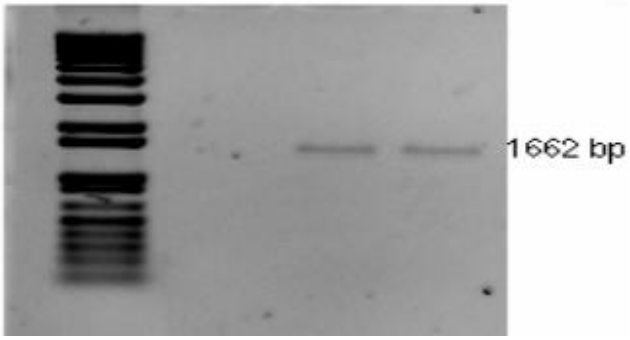

Figure 29. Exon 9 to exon 17 DNA.
after PCR and agarose gel analysed**.** DNA bands are in accord with the fragment sizes calculated on the basis of gene bank data.

Cloning of exon 9 to exon 17 DNA in TOPO PCR 2,1 vector

The DNA was extracted and cloned in TOPO TA PCR vector, the size of TOPO PCR 2,1 vector is 3931 bp. and the size of DNA exon 9 to exon 17 is 1662 bp, so, after cloning the size of exon 9 to exon 17 DNA plasmid vector became 5593 bp. (Figure 30)

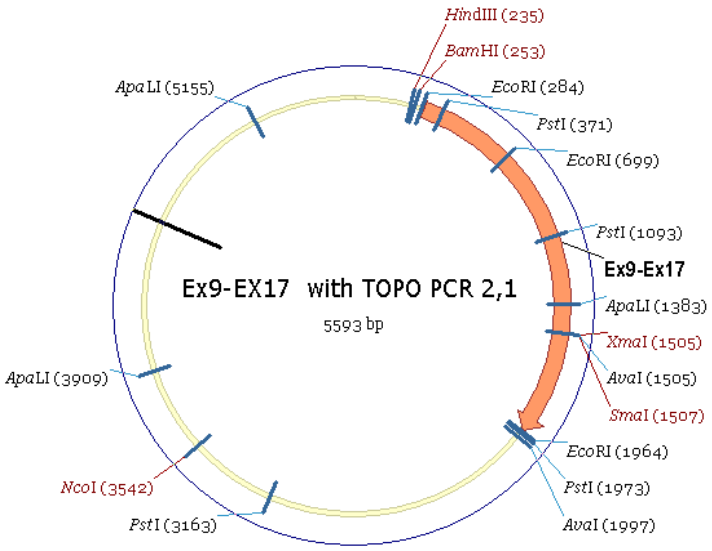

Figure 30. Exon 9 to exon 17 DNA plasmid in TOPO TA vector.

Digestion of exon 9 to exon 17 DNA plasmid

After transformation of E.coli with this vector and extraction of exon 9 to exon 17 DNA plasmid with mini preparation the ratio, absorbance were measured and the concentration was calculated (µg/ml). These were 1, 82 - 0,49 and 244.5 respectively. The restriction sites of EcoR 1 in exon 9 to exon 17 DNA plasmid were predicted with

the programme vector NTI by Invitrogene (see Figure 31). Agarose gel electrophoresis with the isolated, digested plasmids revealed of three bands of 3913, 1265 and 415 bp.

Digestion with EcoR 1

Figure 31. Digestion of exon 9 to exon 17 DNA plasmid with EcoR 1.

DNA plasmid was digested with EcoR 1 and analysed in 1% agarose gel. Each lane contains 20 ng digested plasmid DNA. DNA bands are in accord with the fragment sizes calculated on the basis of the vector map.

Sequencing of exon 9 to exon 17 DNA plasmid by M13 Sequencing primer

The sequence of the amplification was determined using the forward and reverse sequencing Primer M13 for each sample. There were some samples congruent and others were different. Sequencing of the major part of the insert was successful (shown a M13 labeled blue line, the exon 9 to exon 17 insert is shown in orange in Figure (32A). Figure 32B showed the sequencing Primer M13 (red) and the part of exon 9 to exon 17 which covered with Primer M13 (yellow).

A

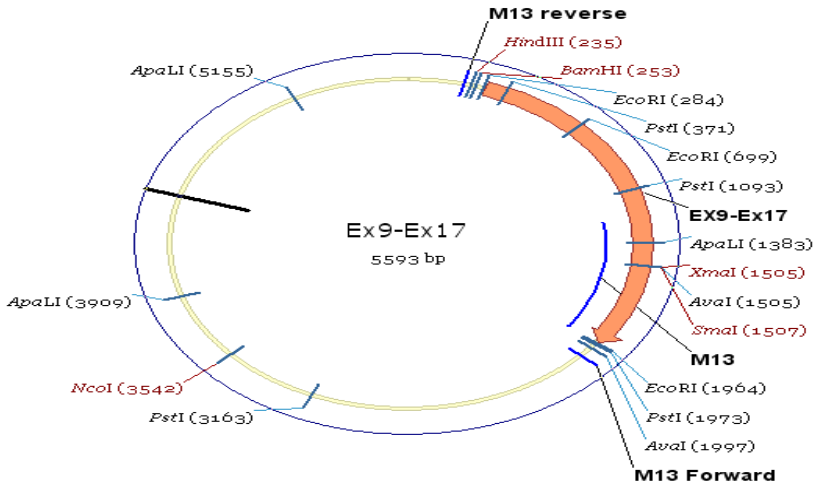

B

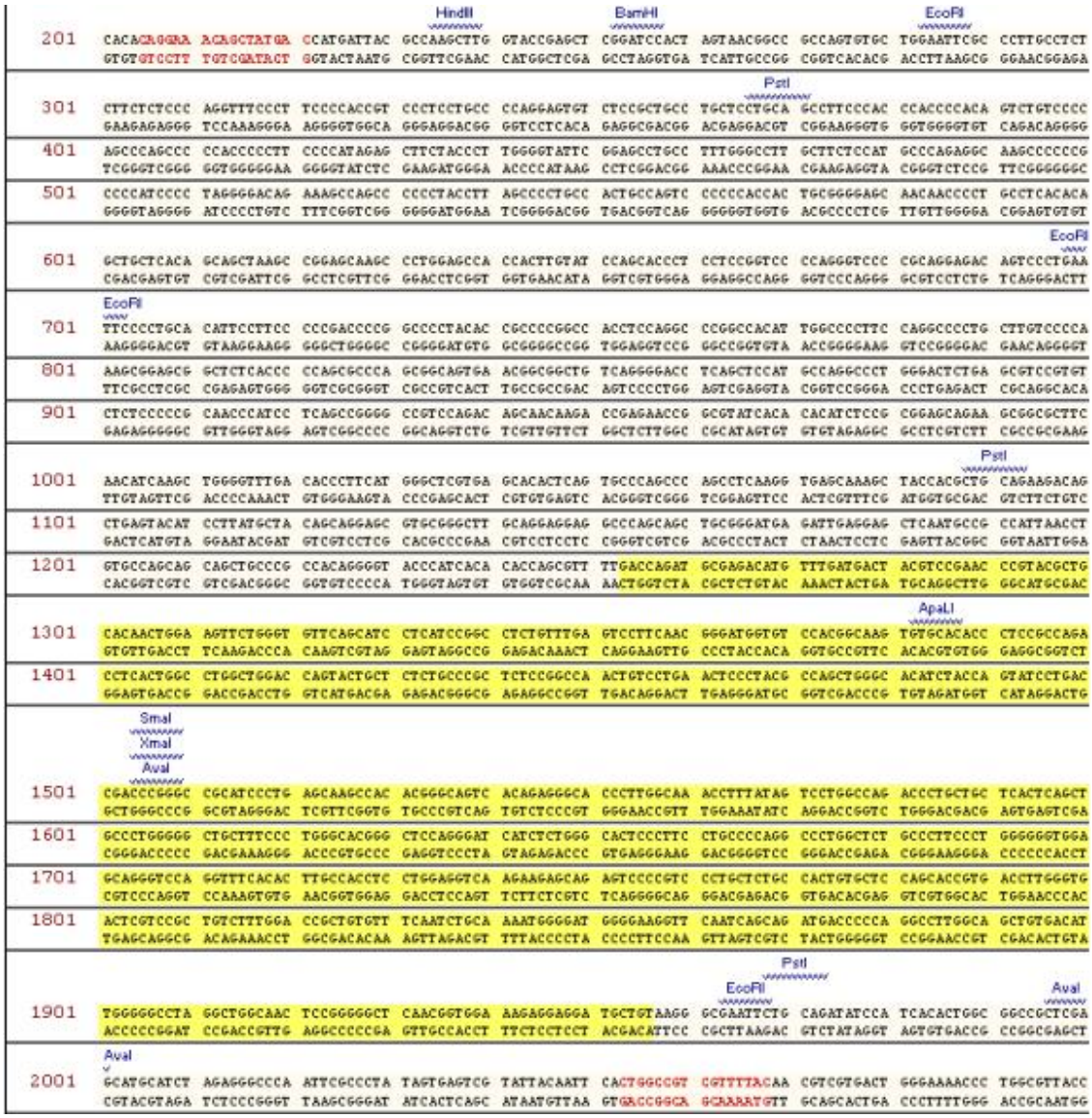

Figure 32. The covering of sequencing primer M13 to exon 9 to exon 17 DNA plasmid

4-1-5. ChREBP amplification: 1 exon 6 to exon 17 (low 1 ChREBP) DNA

The last part of human ChREBP was generated by PCR using upper PCR primer ChREBP gen 5` tcctggacctcaattgcttt 3` and lower PCR primer ChREBP gen 5` ggagcagagagagggaacct 3` (number 43,44 according to the mRNA list in materials) and the sequence of human liver cDNA. The PCR product was 2315 bp. according to the gene bank (Figure 33).

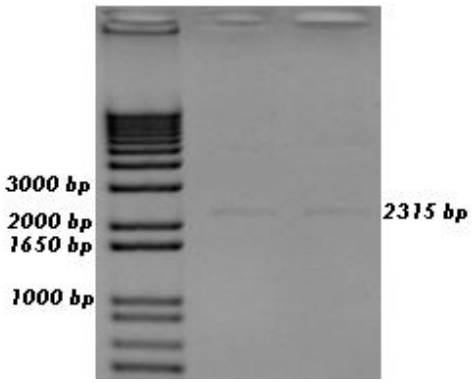

Figure 33. 1 Exon 6 to Exon 17 (low 1 ChREBP) DNA.

DNA after PCR and agarose gel analysed**.** DNA bands are in accord with the fragment sizes calculated on the basis of the vector maps.

Cloning of 1 exon 6 to exon 17 (low 1 ChREBP) DNA in TOPO PCR 2,1 vector

The DNA was extracted and cloned in TOPO TA PCR vector, the size of TOPO PCR 2,1 vector is 3931 bp, and the size of DNA 1 exon 6 to exon 17 (low 1 ChREBP) is 2315 bp, so, after cloning the size of upstream-exon 1 DNA plasmid vector became 6246 bp. (Figure 34)

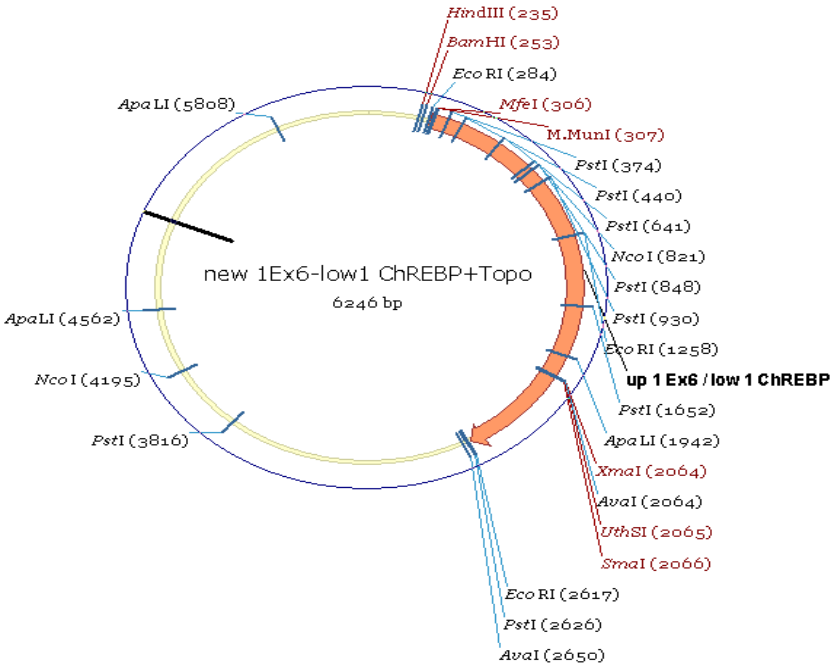

Figure 34. 1 Exon 6 to exon 17 (low 1 ChREBP) DNA plasmid in TOPO TA vector.

Digestion of 1 exon 6 to exon 17 (low 1 ChREBP) DNA plasmid

After transformation and extraction of 1 exon 6 to exon 17 (low 1 ChREBP) DNA plasmid with mini preparation the ratio, absorbance and the concentration (µg/ml) were measured, there were 1, 815 - 0,706 and 353 respectively. The recognition sites of EcoR 1 in 1 Exon 6 to Ex 17 (low 1 ChREBP) DNA plasmid, were predicted with the programme vector NTI by Invitrogene (see Figure 35A). Agarose gel electrophoresis with the isolated, digested plasmids revealed of three bands of 3913, 1359 and 974 bp. Sma 1 and BamH1digest was expected to deliver one band at 6246 bp. This was clear shown only with the sample number 2 as Figure 35B.

A **Digestion with EcoR 1**

B

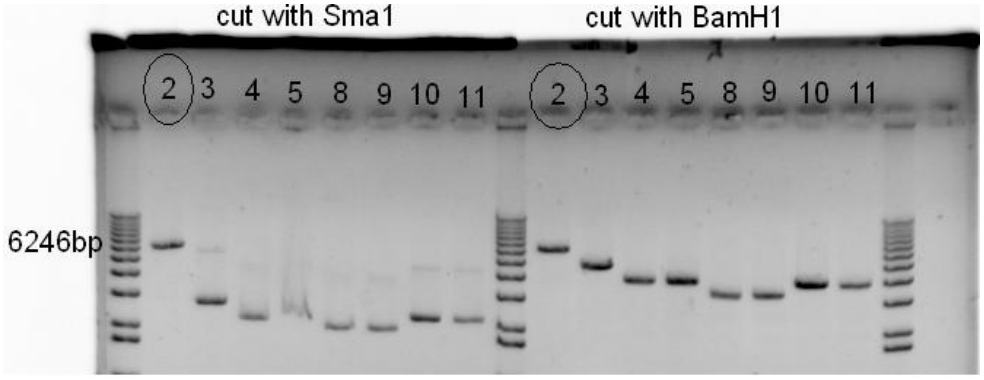

Figure 35. Digestion of 1 exon 6 to exon 17 (low 1 ChREBP) DNA plasmid with EcoR 1 (A), Sma 1 and BamH1 (B).

DNA plasmid was digested with EcoR 1, Sma 1 and BamH1 and analysed in 1% agarose gel. Each lane contains 20 ng digested plasmid DNA. DNA bands of sample 2 are in accord with the fragment sizes calculated on the basis of the vector maps.

Sequencing of 1 exon 6 to exon 17 (low 1 ChREBP) DNA plasmid by M13 sequencing primer

The sequence of the amplification was determined using the forward and reverse sequencing Primer M13 for each sample. There were some samples congruent and others were different. Sequencing of the major part of the insert was successful (shown a M13 labeled green line, 1 exon 6 to exon 17 insert is shown in orange in Figure (36A). Figure 36B showed the sequencing Primer M13 (red) and the part of exon 1 exon 6 to exon 17 which covered with Primer M13 (yellow).

A

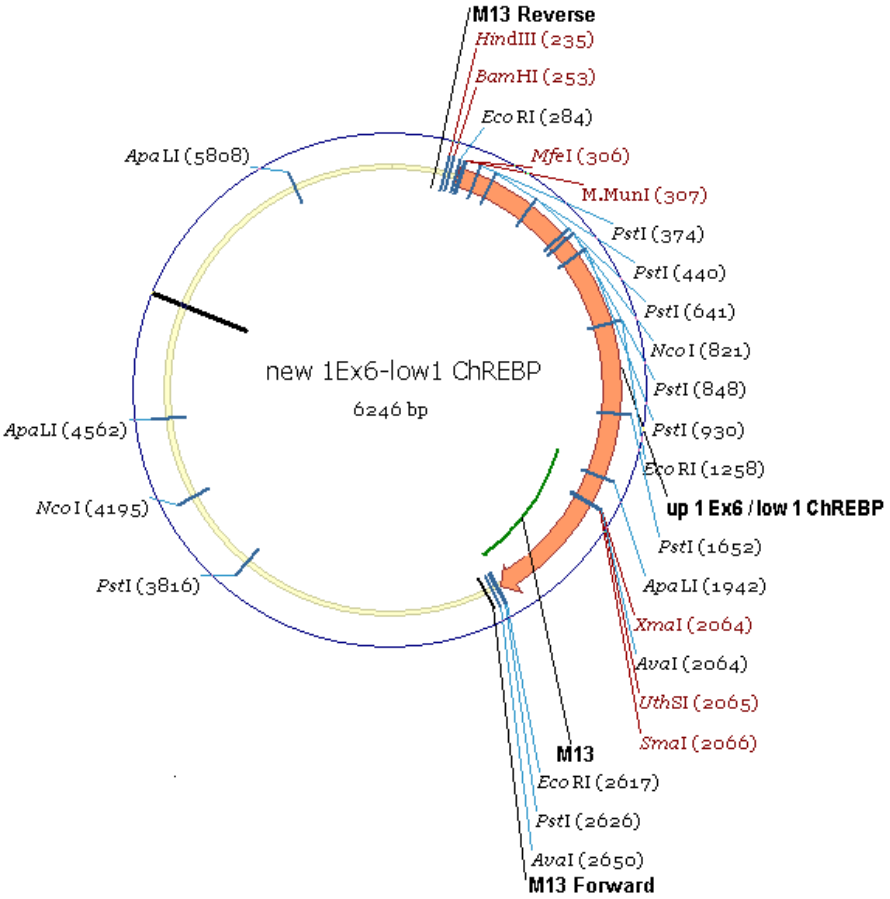

B

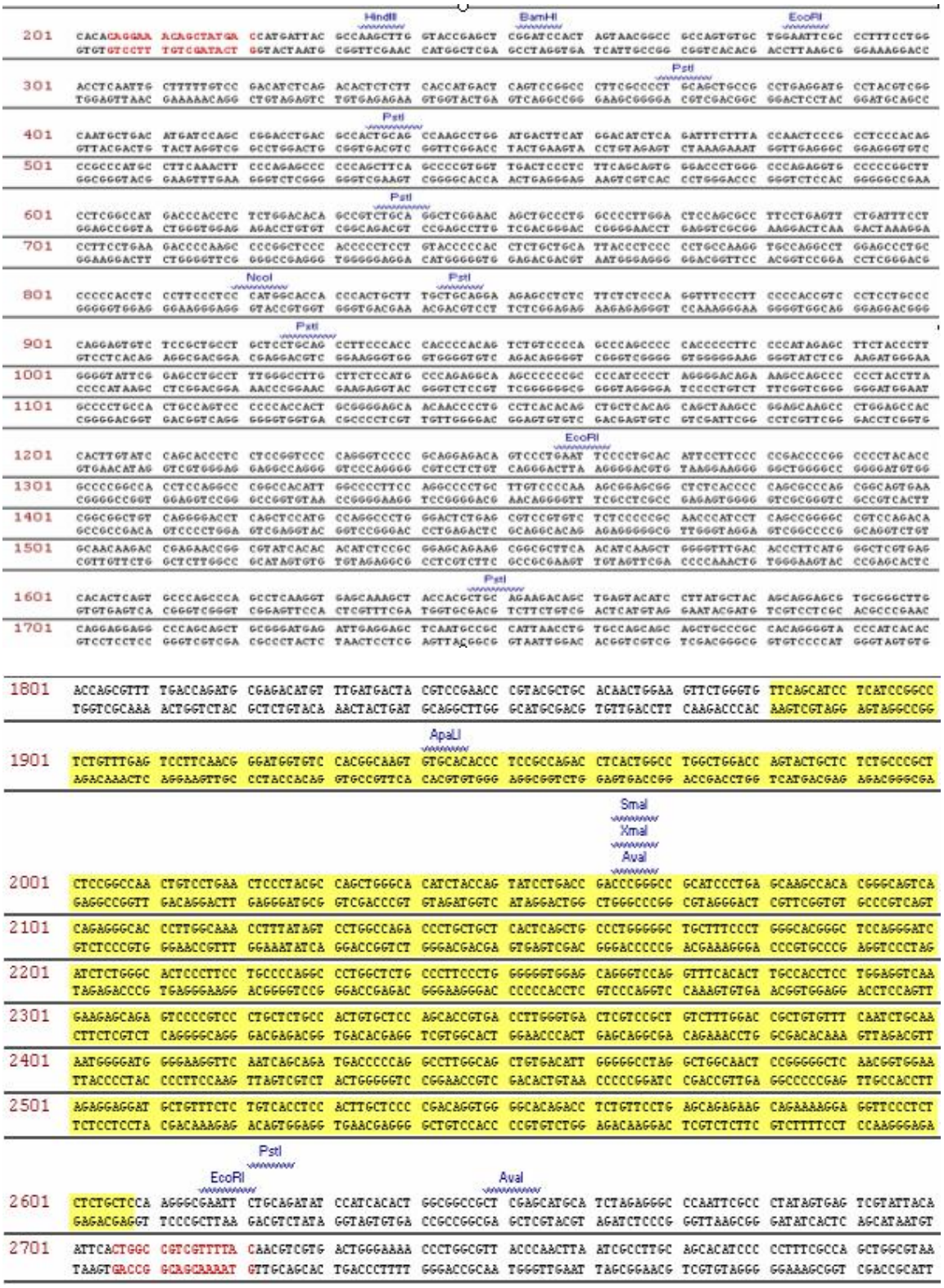

Figure 36. The covering of sequencing primer M13 to 1 exon 6 to exon 17 DNA plasmid

4-1-6. Ligation between up exon 6 and 1 exon 6 to exon 17 (low 1 ChREBP) DNA plasmid vectors

Analysis of two possible orientations for up exon 6 by TOPO Cloning

To ligate up exon 6 with 1 exon 6 to exon 17 (low 1 ChREBP) DNA plasmid vector, up exon 6 has two possibility of orientation. In order to digest with double cut by Mfe1 and BamH1, samples were checked which one was at the suitable orientation (Figure 37B), all up Ex 6 samples were analysed by restriction enzyme Ava1. I found that samples number 1 and 7 were in the suitable orientation. (Figure 37A)

A

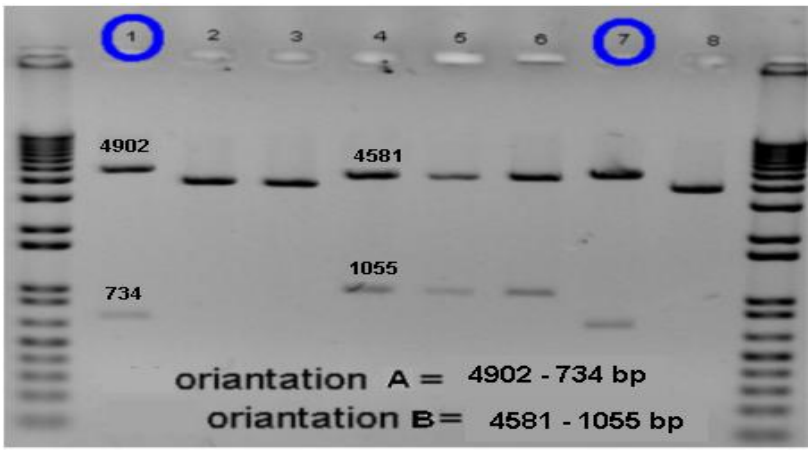

B

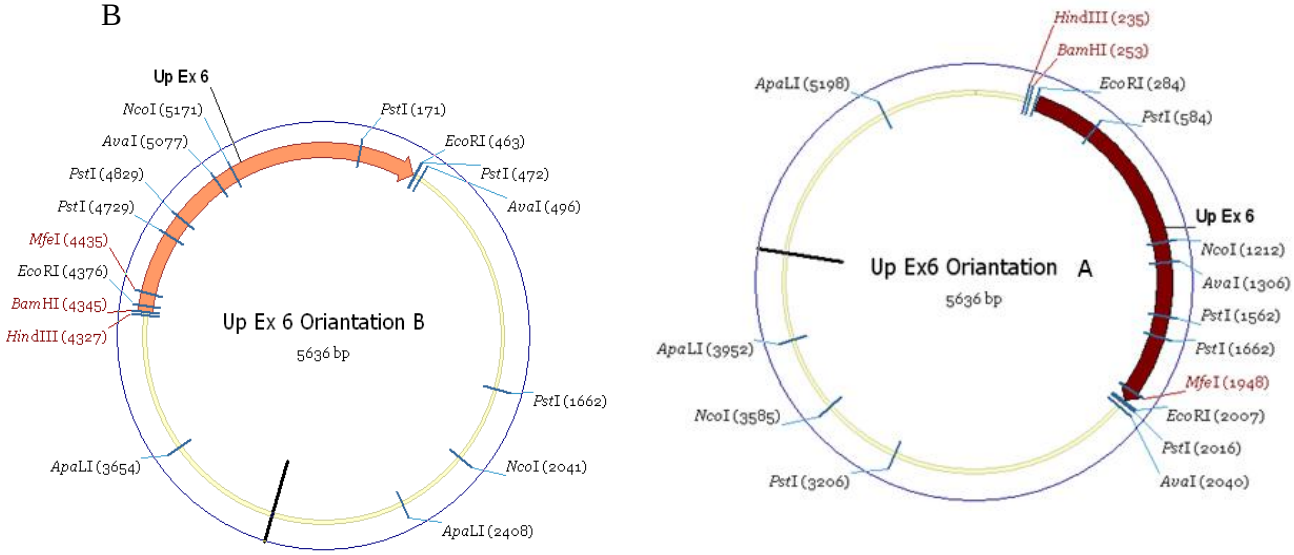

Figure 37. Digestion and two possible orientation of up exon 6 DNA.

DNA plasmid was digested with Ava1 and analysed in 1% agarose gel. Each lane contains 20 ng digested plasmid DNA. DNA bands number 1 and 7 were in the suitable orientation (A).Analysis of two possible orientation for up exon 6 by TOPO cloning (B).

Double cut for up exon 6 and 1 exon 6 to exon 17 (low 1 ChREBP) DNA plasmid vectors with BamH1 and Mfe1 was done. 2 µg of Topo PCR 2,1 1 exon 6 to exon 17 (low 1 ChREBP) (big fragment) after Mfe1 and BamH1 (6193 bp) as a vector (Figure 38 B) and 1.5 µg of Topo PCR 2,1 up exon 6 (small fragment) after Mfe1 and BamH1 (1695 bp) as an insert (Figure 38A) .

A **B**

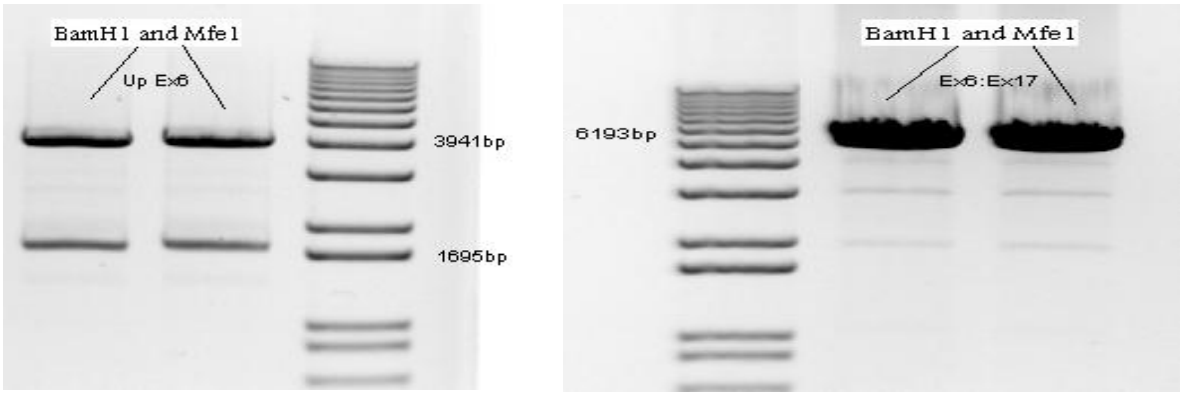

Figure 38. Double cut of up exon 6 and 1 exon 6 to exon 17 (low 1 ChREBP).

DNA plasmid vectors with BamH1 and Mfe1. Double cut for up exon 6 was expected to result in two fragments 3941 and 1695 bp and the small fragment was used for ligation (**A).** The fragments resulting of double cut for 1 exon 6 to exon 17 (low 1 ChREBP) were 6193 and 53 bp. The small fragment was not expected to visible in the agarose gel due to its small size and the big was used for the ligation **(B).**

After ligation between up exon 6 and 1 exon 6 to exon 17 (low 1 ChREBP) DNA plasmid vectors, the size of the new vector (Topo human ChREBP) became 7888 bp (Figure 39) as the calculation of the vector map.

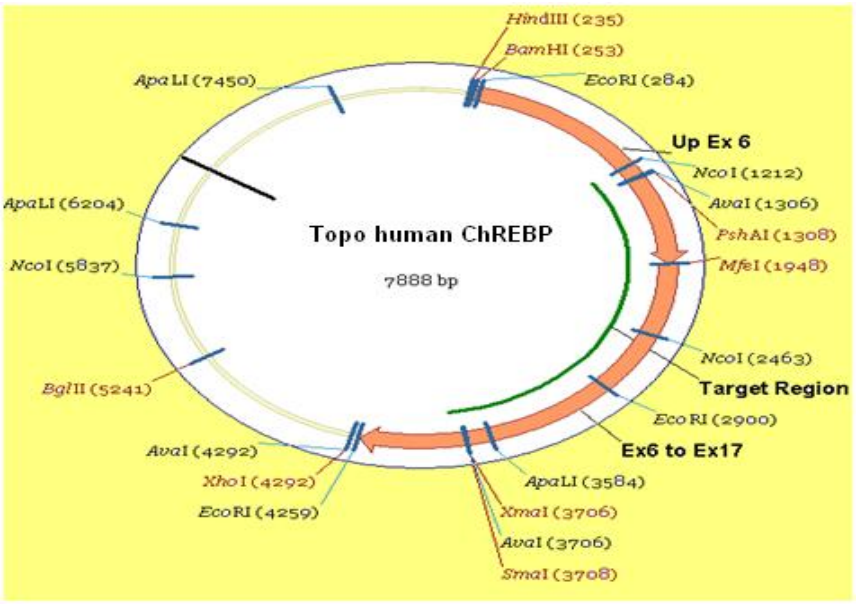

Figure 39. Topo human ChREBP.

Digestion of Topo human ChREBP DNA plasmid

After transformation and extraction of Topo human ChREBP DNA plasmid with mini preparation the ratio, absorbance and the concentration (µg/ml) were measured, there were 1.835 – 0.589 and 294.5 respectively. The restriction enzyme EcoR 1 was used to test the plasmid and the result was according to the expected (see Figure 40).The restriction digest of Topo human ChREBP DNA plasmid with EcoR 1 delivered three fragments of 3913, 2616 and 1359 bp for sample number 5 only. This result was predicted with the program vector NTl by Invetrogene.

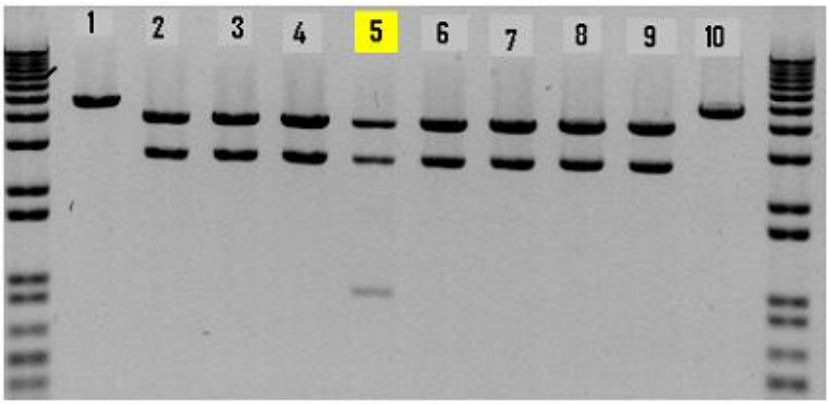

Figure 40. Digestion of Topo human ChREBP DNA plasmid with EcoR 1.

Plasmid DNA was digested with EcoR 1 and analysed in 1% agarose gel. Each lane contains 20 ng digested plasmid DNA. DNA bands are in accord with the fragment sizes calculated on the basis of the vector maps.

4-1-7. Ligation between Topo human ChREBP and pEGFP-N1

To ligate Topo human ChREBP with pEGFP-N1, the restriction enzymes BamH1 and Xho1 were shown to cut only once (Figure 41 A) and tested (Figure 41 B)

A

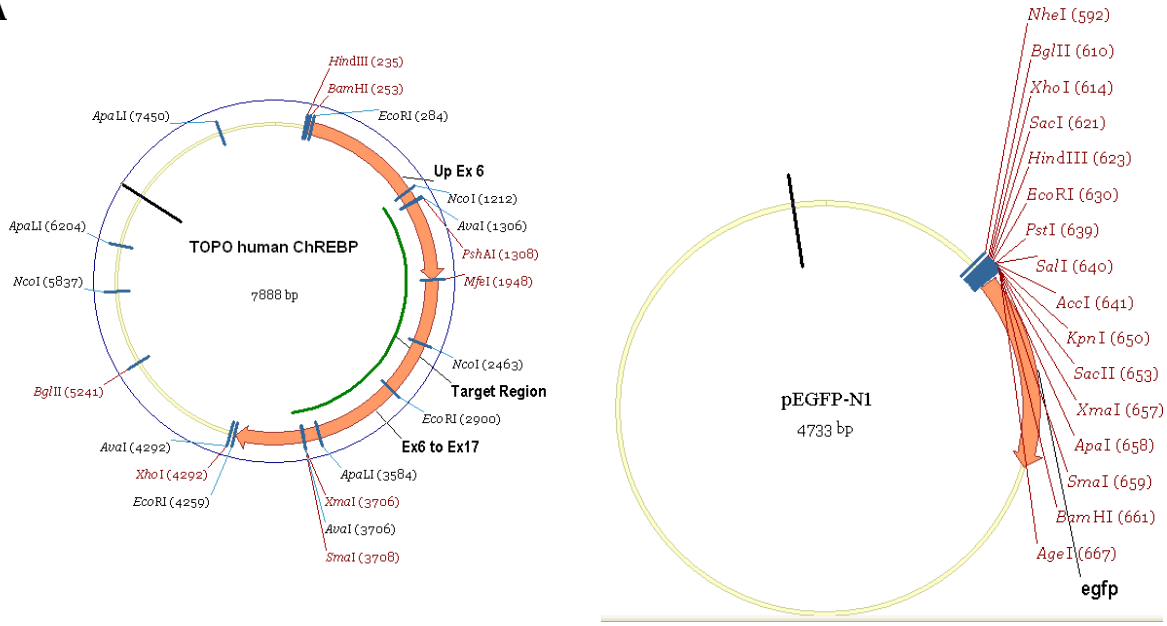

B

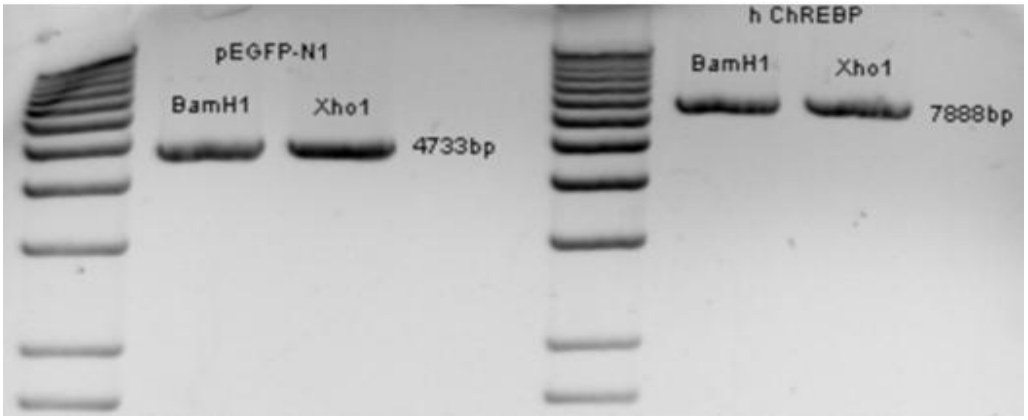

Figure 41. Digestion of Topo human ChREBP and pEGFP-N1 with BamH1 and Xho1 (A,B).

DNA Plasmid was digested with BamH1 and Xho1which expected to deliver one fragment: 4733 bp for pEGFP-N1 and 7888 bp for Topo human ChREBP **.**

Double cut with 1- (BamH1 - Xho1), 2-(BamH1 - Bgl ll), 3- (BamH1 - Sma 1), 4- (Hindlll – Xho1), 5- (Hindlll - Bgl ll) and 6- (Hindlll- Sma 1) for Topo human ChREBP

Restriction site analysis with the program vector NTI by Invitrogene showed that double cuts with BamH1 and Xho1 should generate fragments of 4039 and 3849 bp, incubation with BamH1 and Bg III should result in fragments of 4988 and 2900bp, with BamH1 and Sma 1 should result in fragments of 3455 and 4433 bp, with Hind III and Xho1 in fragments of 4057 and 3831, Hind III and Bg III should produce fragments 5066 and 2882 bp, Hind III and Sma 1 should produce of 3473 and 4415 bp. The restriction enzymes produced not the expected fragments. (Figure 42).

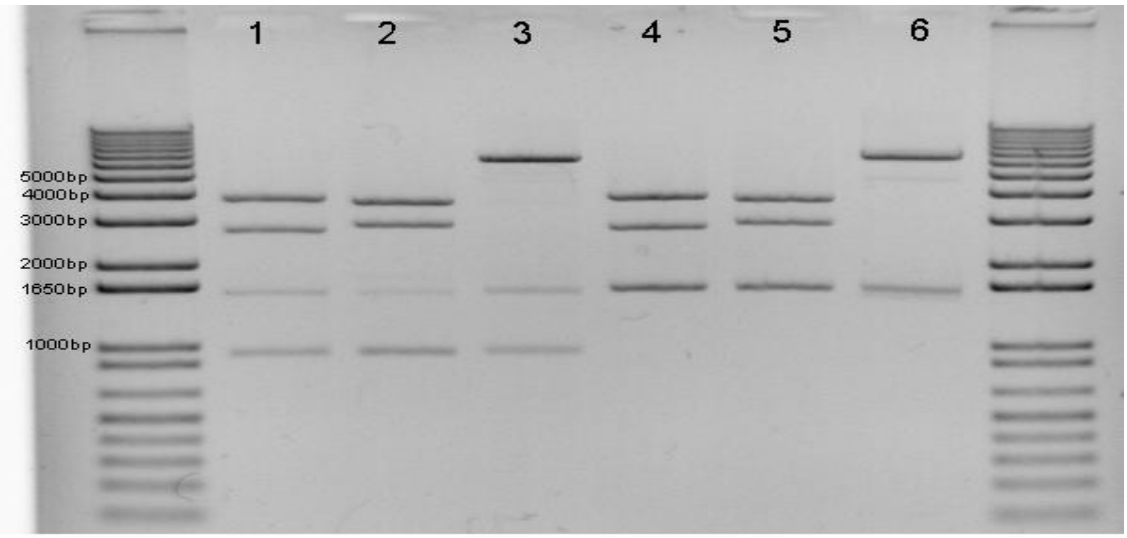

Figure 42. Double cut for Topo human ChREBP with different restriction enzymes.

Sequencing of Topo human ChREBP DNA plasmid

The sequence of the amplification was determined using ten different sequencing primers (Figure 43). The primers were designed to test Topo human ChREBP DNA plasmid and cover all the regions of ChREBP (shown in orange) but they did not succeed. Only two of them covered small part of ChREBP (shown in blue) and the others didn't work.

Sequencing primers
tac tac aag aag cgg ctc cgt aa
ttt acc aac tcc cgc ctc cca ca
cgc ctt cct gag ttc tga ttt cc
tca gtg ccc agc cca gcc tca ag
ggc agt gaa cgg cgg ctg tca gg
gct ggc gta ggg agt tca gga ca
acc ttg agg ctg ggc tgg gca ct
ggc tgt ggg agg cgg gag ttg gt
ccg gag gag ggt gct gga tac aa
ccc tga cag ccg ccg ttc act gc

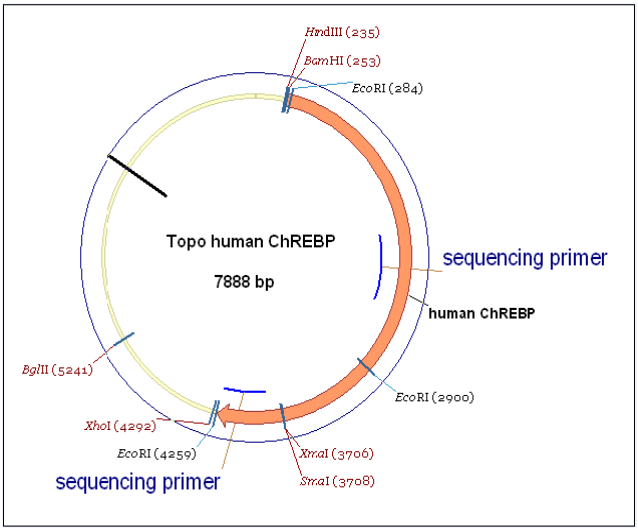

Figure 43. Sequencing of Topo human ChREBP DNA plasmid

The previous result shows us that it is impossible to cut and ligate the Topo human ChREBP inside pEGFP-N1 vector. No other laboratory up to then succeeded to clone human ChREBP. The reason for this obstacle is still not clear. Therefore, I followed two strategies: On the one hand I used GFP linked to mouse ChREBP kindly provided by Ms. Catherine Postic (Institut Cochin, Université Paris Descartes, Paris), on the other hand at that time a company offered to clone human ChREBP by an other method and a vector encoding human ChREBP was ordered, sequenced and employed.

4-2. GFP-mouse ChREBP vector

The vector encoding mouse GFP-ChREBP was kindly provided by Ms. Catherine Postic, Insitut Cochin, Département d'Endocrinologie, Métabolisme et Cancer, Université Paris Descartes, Paris, France. The murine full-length wild-type ChREBP-ζ isoform (GenBank accession no: AF245475) has been cloned into pEGFP- C1 from Clontech (Dentin *et al.* 2005a) and sent to us as a drop on filter paper. The piece of paper containing plasmid DNA was cut out and supplied with 100 µl BE-Buffer to extract DNA. Plasmid DNA was stored at 4°C until transformation of competent E. coli JM109 cells in order to multiply the plasmid DNA. (Figure 44)

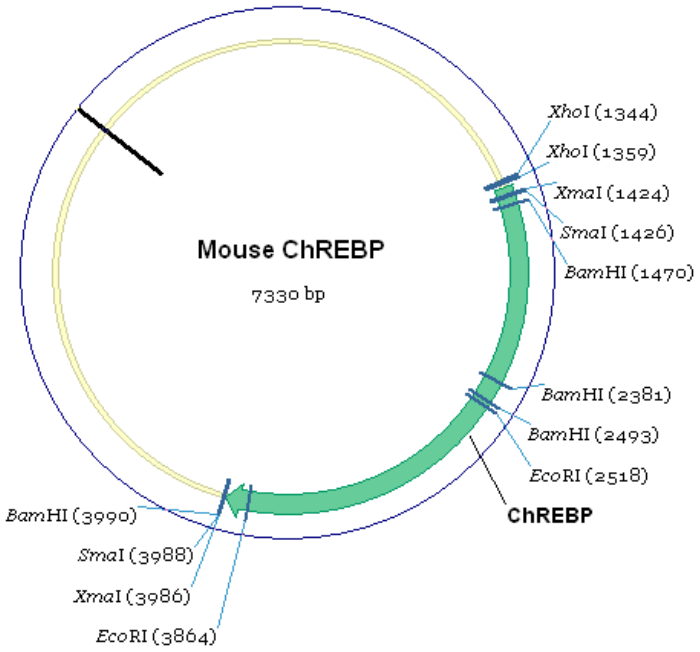

Figure 44. pEGFP mouse ChREBP vector.

4-2-1. Digestion of GFP-mouse ChREBP vector

To examine the mouse ChREBP vector, the GFP- ChREBP vector was introduced by the heat shock transformation in competent E.coli JM109 and was increased, then the GFP- ChREBP vector extracted by minipreparation, after that measurement of ChREBP concentration, finally restriction enzyme digestion for the ChREBP and agarose gel electrophoresis.

Restriction analysis of GFP-mouse ChREBP vector with EcoRI and BamHI

The recognition sites of EcoRI in mouse ChREBP were predicted with the program vector NTI from Invitrogen (see Figure 45). Agarose gel electrophoresis with the isolated, digested plasmids of 8 clones with EcoRI revealed two bands corresponding to the calculated 1346 bp and 5984 bp fragments for every clone (A). BamH1 digest was expected to create four fragments of the size of 112, 911, 1497, and 4810 bp. The bands shown correspond to these sizes, the fragment with the size of 112 bp was not visible in the agarose gel due to its small size (B).

A: EcoR 1 **B: BamH1**

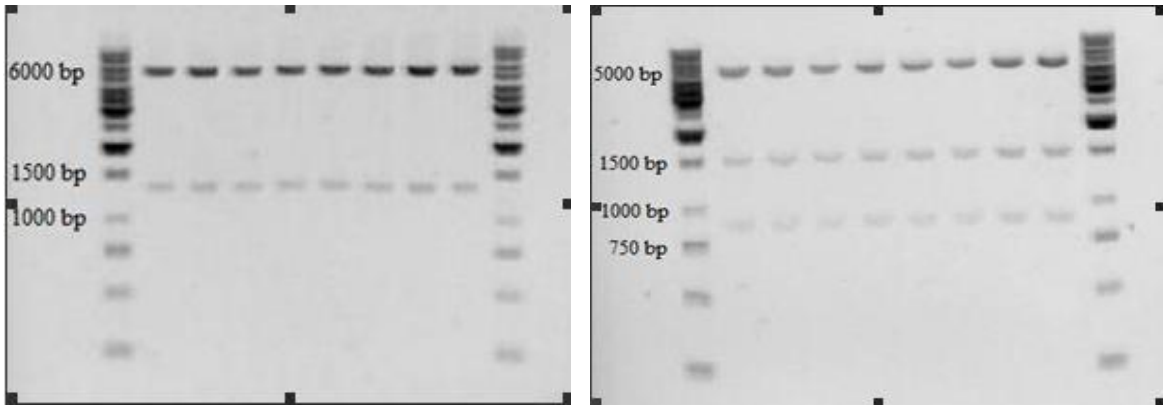

Figure 45. Digestion of GFP-mouse ChREBP vector with EcoRI (A) and BamH1 (B). Plasmid DNA of 8 transformants was digested with EcoR 1 and BamH1 respectively and analysed in 1% agarose gel. Each lane contains 20 ng digested plasmid DNA. DNA bands are in accord with the fragment sizes calculated on the basis of the vector maps.

4-2-2. The best condition of cell line (HUH7, U2OS and HepG2) for transfection

To optimize transfection, the influence of different DNA/lipofectamin ratios and different cell numbers were examined. It could be assessed that the best condition of transfection depends strongly on the DNA/lipofectamin ratio and the cell number. Also the kind of cells played a strong role. U2OS are more affectively transfected by lipofectamin than HUH7 and HepG2. The results of ChREBP transfection in U2OS , HUH7 and HebG2 respectively were presented in Figure 46 A,B,C.

A

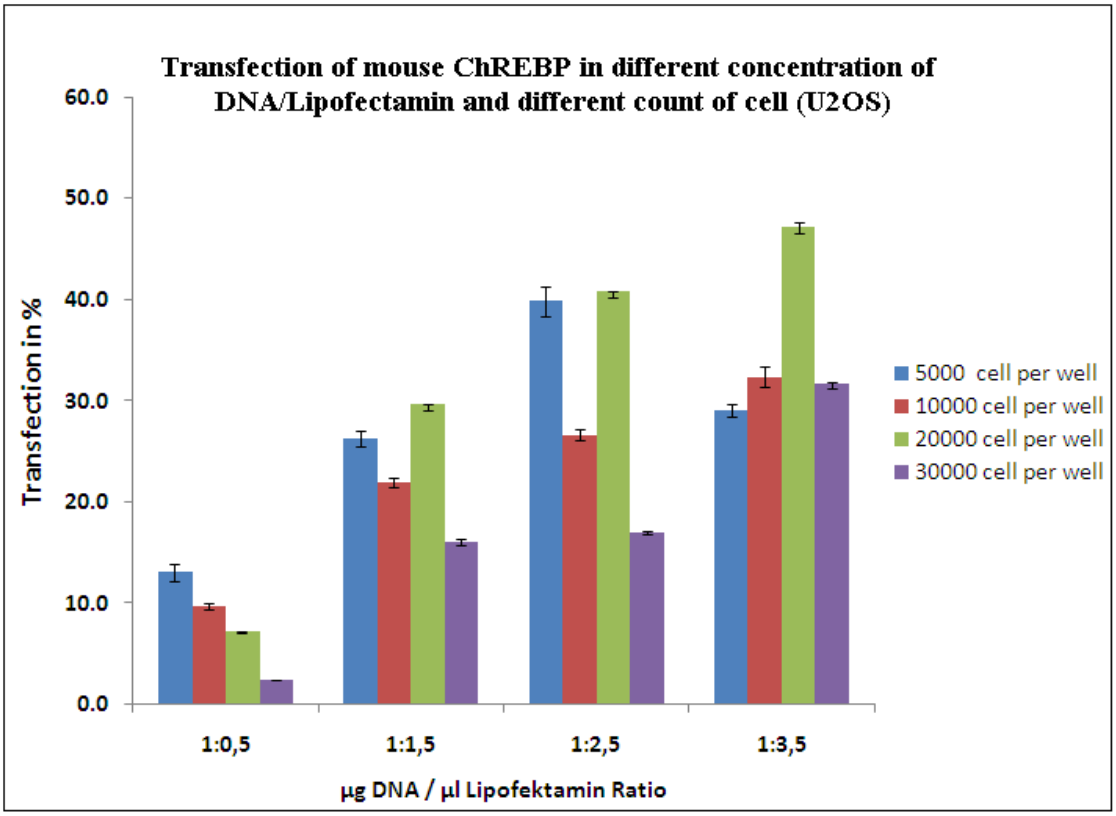
Transfection of mouse ChREBP in different concentration of DNA/Lipofectamin and different count of cell (U2OS)
Transfection in %
60.0
50.0
40.0
30.0
20.0
10.0
0.0
1:0,5
1:1,5
1:2,5
1:3,5
µg DNA / µl Lipofektamin Ratio
5000 cell per well
10000 cell per well
20000 cell per well
30000 cell per well

B

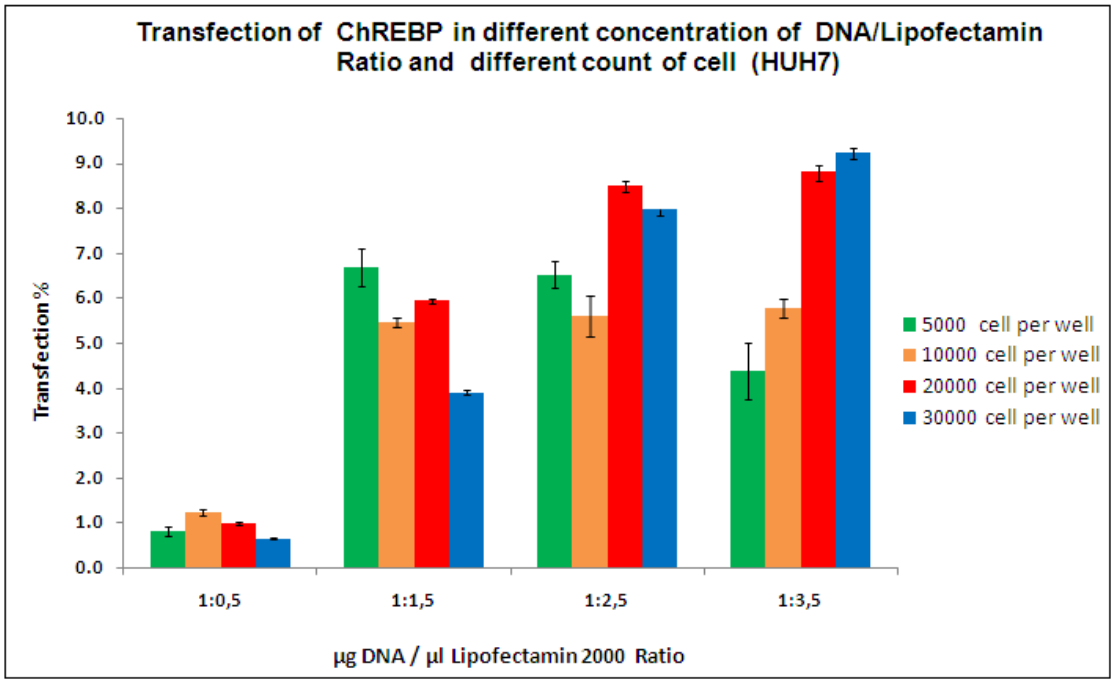
Transfection of ChREBP in different concentration of DNA/Lipofectamin Ratio and different count of cell (HUH7)
Transfection %
10.0
9.0
8.0
7.0
6.0
5.0
4.0
3.0
2.0
1.0
0.0
1:0,5
1:1,5
1:2,5
1:3,5
µg DNA / µl Lipofectamin 2000 Ratio
5000 cell per well
10000 cell per well
20000 cell per well
30000 cell per well

C

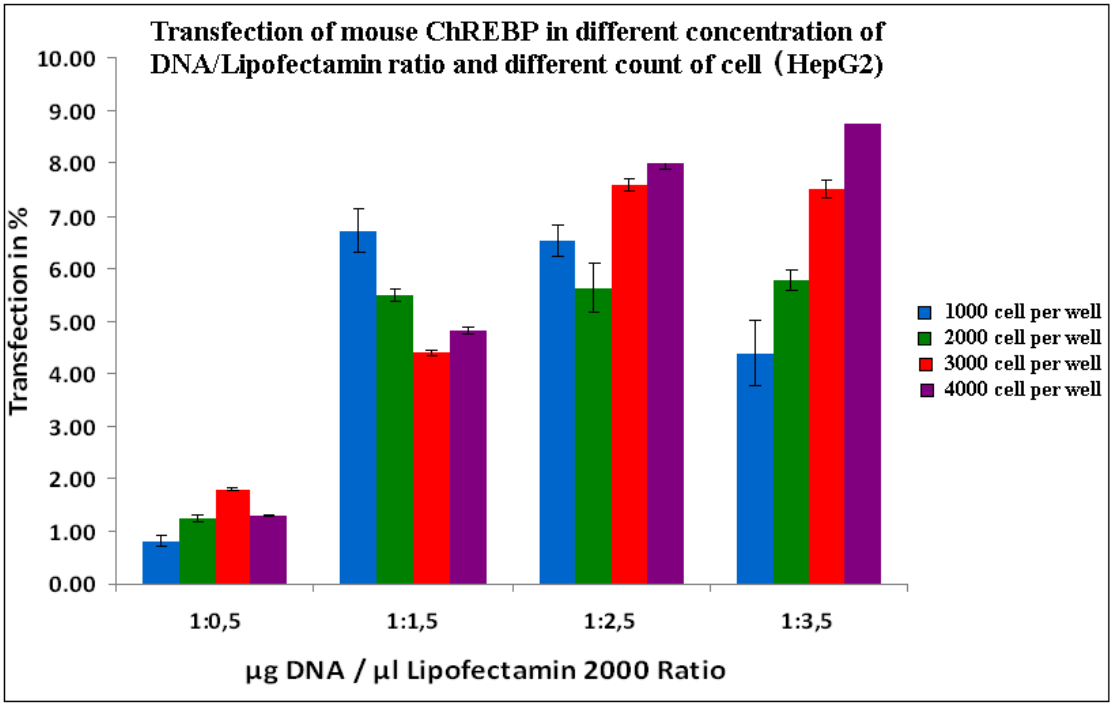

Figure 46. Transfection efficiency dependent on DNA/lipofectamin ratio and cell number for ChREBP in U2OS (A), HUH7 (B) and HepG2 (C) cells.

It is evident from the data that the transfection was higher in U2OS in all cell numbers tested than that in HUH7 and in HEPG2. In the following investigations, a DNA/lipofectamin-ratio of 1:3.5 and a cell number of 20,000 cells per well was used for ChREBP transfection in U2OS. In HUH7, the best ratio of DNA/lipofectamin was 1:3.5 and 30,000 cells per well and in HEPG2, 50,000 cells per well and a DNA/lipofectamin-ratio of 1:3.5 were the best conditions of ChREBP transfection.

4-2-3. The effect of glucose with or without insulin on the translocation of mouse ChREBP in U2OS, HUH7 and HePG2

The effect of glucose and insulin on the translocation of ChREBP in U2OS, HUH7 and HepG2 cells was studied (Figure 47 A, B, C). The cells were transfected with 8 ng/µl of pEGFP mouse ChREBP vector, after 24h of transfection, the cells were starvated (5 mM of glucose, and 0% FCS) for 24h. After that the cells were stimulated for 1 h with 5 mM glucose without insulin or 25 mM of glucose with or without 100 nM insulin.

A

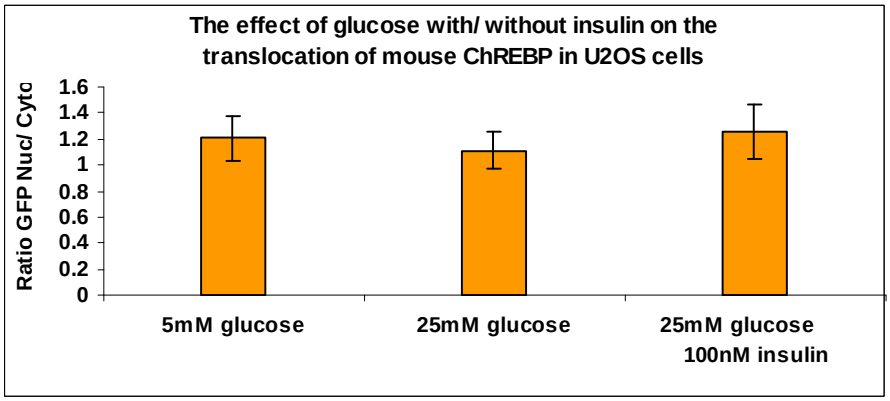

B

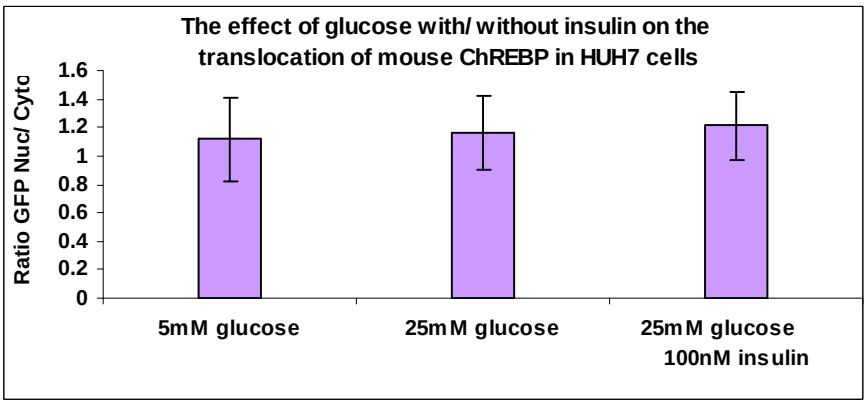

C

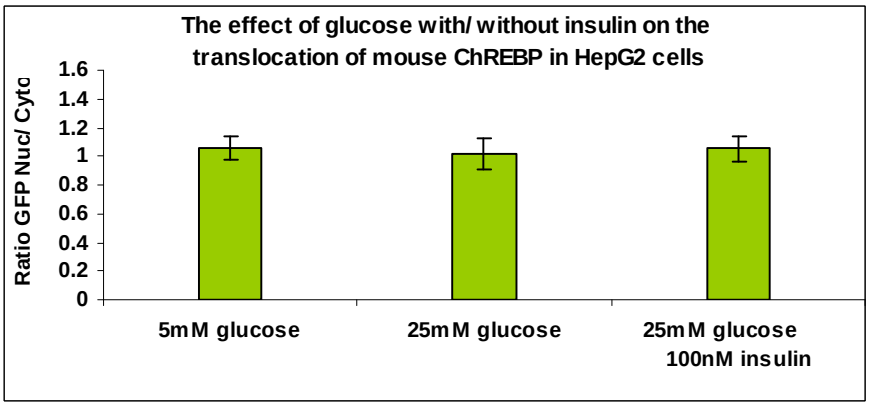

Figure 47. Glucose and insulin effect on the mouse ChREBP translocation in U2OS (A), HUH7 (B) and HepG2 (C) cells.

5 mM glucose without insulin or 25 mM of glucose with/without 100 nM insulin. The data, from three independent experiments were shown. It was clearly noticed that there were no significant effects on the translocation of the

transcription factor measured after 1 h glucose or insulin stimulation by the fluorescence microscope on the three cell types investigated.

4-2-4. Sequencing of the Mouse ChREBP

Due to my results which showed that there were no significant effects of glucose and insulin on translocation of mouse ChREBP in U2OS, HUH7 and HepG2 cells. I was suspicious that the mouse ChREBP sequence in the vector might have a mutation. Therefore the sequencing of mouse ChREBP gene was done in the DIfE, (German Institute of Human Nutrition) the department of clinical Nutrition.

In Figure 48 the results of the sequencing showed that, the first four amino acids of the ChREBP (shown in red) were not encoded in GFP-mouse ChREBP. These four missing amino acids could be responsible for a different conformation of the protein which would affect its regulation.

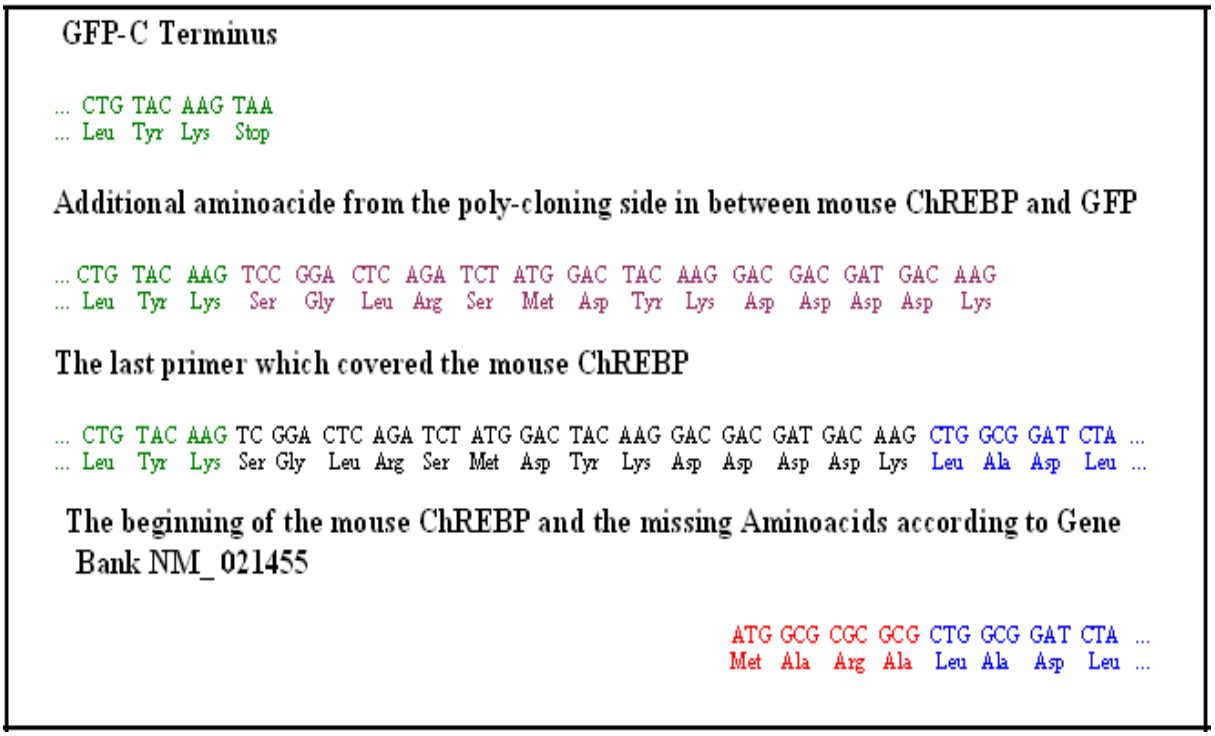

Figure 48. The sequencing of the mouse ChREBP

The sequencing of the mouse ChREBP shows a GFP encoding part (green), fourteen amino acids linking GFP and ChREBP (violet) and the ChREBP encoding part (red, blue). The upper line in each case shows the cDNA

sequence, and the lower line the amino acid code. The missing area of the ChREBP gene in ChREBP is marked red.

4-3. TrueORF cDNA clones and precision shuttle vector

Entry (human ChREBP) and destination (AC and AN) GFP vectors were purchased from Origene company. The TrueORF vector system was generated to express the open reading frame ORF of a ChREBP. (Figure 49). The plasmid contains the promoter and enhancers of the human cytomegalovirus (CMV) immediate-early gene to drive mammalian gene expression, and the T7 promoter for in vitro transcription/translation. A Kozak consensus sequence is included in the plasmid to enhance mammalian expression.

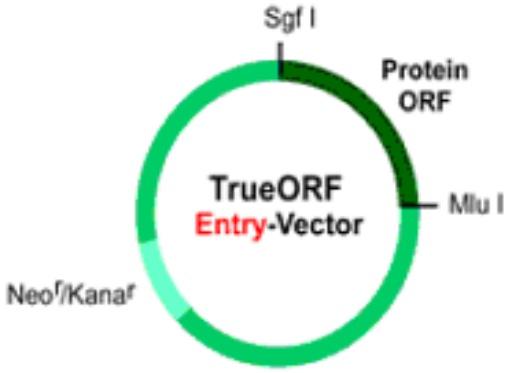

Figure 49. The True ORF cDNA clones in the pCMV6-Entry vector.

Two rare-cutting restriction enzymes are utilized in transferring an ORF between vectors. Most subcloning from the Entry to a destination vector involves Sgf l/Asis l (present in 0.37% of human ORF) and Mlu l (4%). The subcloning strategy maintains insert orientation and reading frame, eliminating the need to resequence the insert after each transfer. Because the Entry and destination vectors have different antibiotic resistance genes, selection after subcloning is a very simple process.

4-3-1. Digestion of TrueORF Entry (human ChREBP), and destination (AC and AN) GFP vectors.

It was necessary to confirm identities of each vector, Entry (human ChREBP), destination (AC and AN) GFP, which were bought from Origene company according to the gene bank and the vector map before use them in this study.

Entry (human ChREBP) and destination (AC and AN) GFP vectors arrived from the company as 10µg lyophilized plasmid DNA. Each plasmid was diluted with 200 µl water to 50 ng/µl. Entry-human ChREBP, and the GFP-AC and GFP-AN destination vectors were transformed in One shot competent E. coli (top 10), and seede on LB agar plates containing 25 µg/ml kanamycin for Entry-human ChREBP) and containing 100 µg/ml ampicillin for the GFP-AC and GFP-AN destination vectors. The Plasmids of the transformed E.coli was extracted by mini preparation, the ratio, absorbance and concentration (µg/ml) were measured (as shown in the following table).

Sample	Absorbance	Ratio	Concentration (µg/ml)
Entry (human ChREBP)	0.834	1.862	417
AC GFP vector	1.266	1.915	633
AN GFP vector	0.728	2.779	364

Restriction analysis of Entry (human ChREBP), and destination GFP-AC and GFP-AN vectors confirmed identities of the plasmids.

The recognition sites of enzymes in human ChREBP and GFP-AC and GFP-AN destination vectors were predicted with the program vector NTI by Invitrogen. Agarose gel electrophoresis with the isolated digested plasmids with Mlu l and Sgf l revealed one band for each 7436 bp. While, Sma l and EcoR l resulted two bands for each, 7239, 197 bp and 5701, 1735 bp respectively (Figure 50). For GFP-AC and GFP-AN destination vectors, Mlu 1, Sgf 1and Sma l were used. Mlu 1 and Sgf 1 produced one band for each 6598 and 6601 bp respectively. On the other hand, Sma l resulted two bands for each, 5609, 989 bp and 5612, 989 bp respectively. (Figures 51, 52)

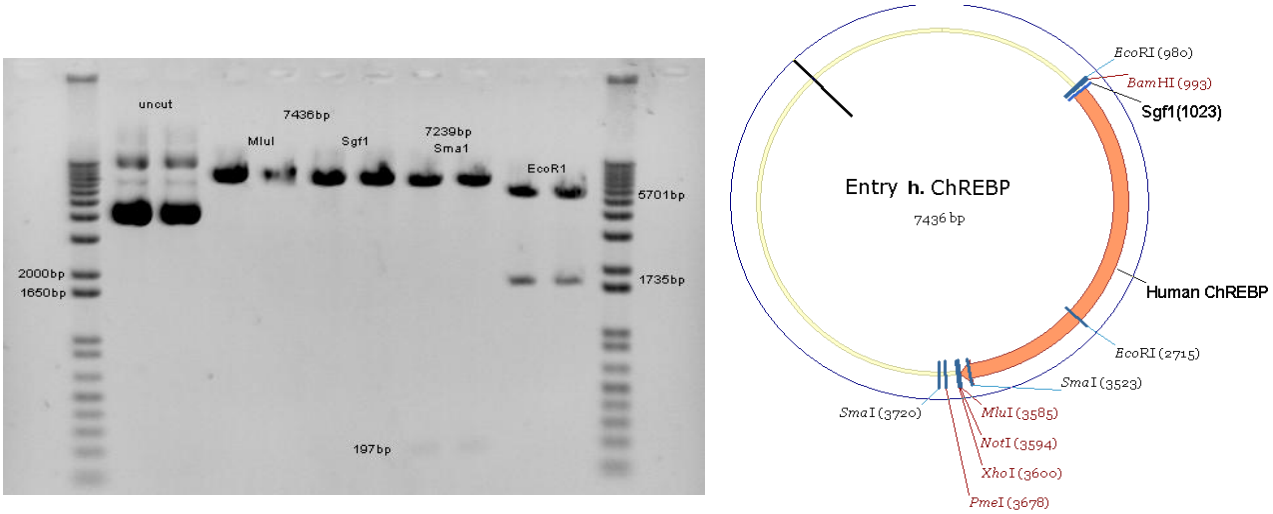

Figure 50. Restriction sites of Entry (human ChREBP) with Mlu1, Sgfl, Smal and EcoRl. DNA plasmid was digested and analysed in 1% agarose gel. Each lane contains 20 ng digested plasmid DNA. DNA bands are in accord with the fragment sizes calculated on the basis of the vector maps.

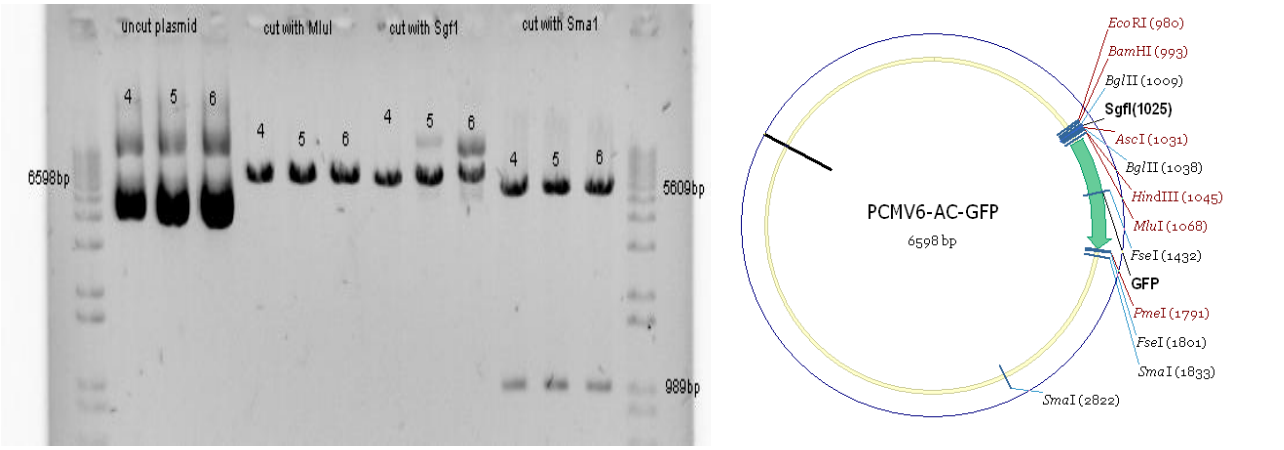

Figure 51. Restriction sites of destination AC-GFP vector with Mlu 1, Sgf l, and Sma l. DNA plasmid was digested and analysed in 1% agarose gel. Each lane contains 20 ng digested plasmid DNA. DNA bands are in accord with the fragment sizes calculated on the basis of the vector maps.

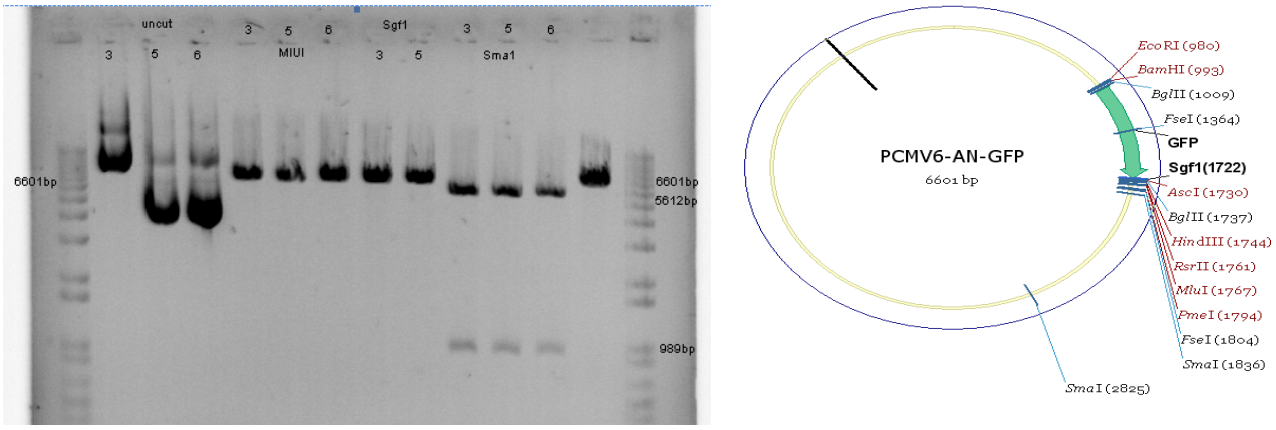

Figure 52. Restriction sites of destination AN-GFP vector with Mlu 1, Sgf l, and Sma l. DNA plasmid was digested and analysed in 1% agarose gel. Each lane contains 20 ng digested plasmid DNA. DNA bands are in accord with the fragment sizes calculated on the basis of the vector maps.

4-3-2. Ligation between human ChREBP and GFP-AC and GFP-AN destination vectors

Double cut for human ChREBP and GFP-AC and GFP-AN destination vectors with Mlu 1 and Sgf 1 was made. 2 µg of GFP-AC and GFP-AN destination vector (big fragment) after Mlu 1 and Sgf 1 (6555bp) as a vector and 1.5 µg of human ChREBP (small fragment) after Mlu 1 and Sgf 1 (2562 bp) as an insert (Figure 53). After ligation between human ChREBP and GFP-AC and GFP-AN destination vector, the size of the new vectors pGFP- human ChREBP and p human ChREBP-GFP was 9115 and 9118 bp respectively as calculated by the vector map. (Figure 54 A,B)

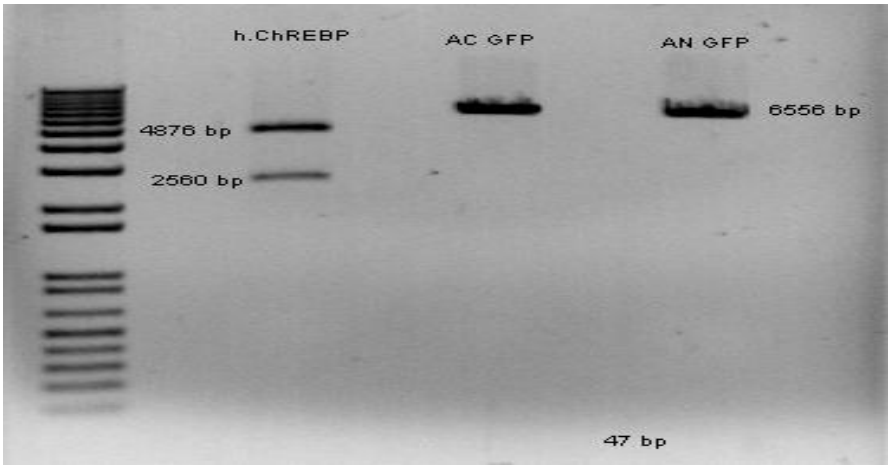

Figure 53. Double cut of Entry human ChREBP and destination (AC, AN) GFP vectors. Mlu 1 and Sgf 1 digest was expected to result in 2 fragments of 4876, 2560 and 6556, 47 bp for Entry human ChREBP and destination (AC, AN) GFP vectors respectively. 47 bp was not expected to be visible in the agarose gel due to its small size.

A

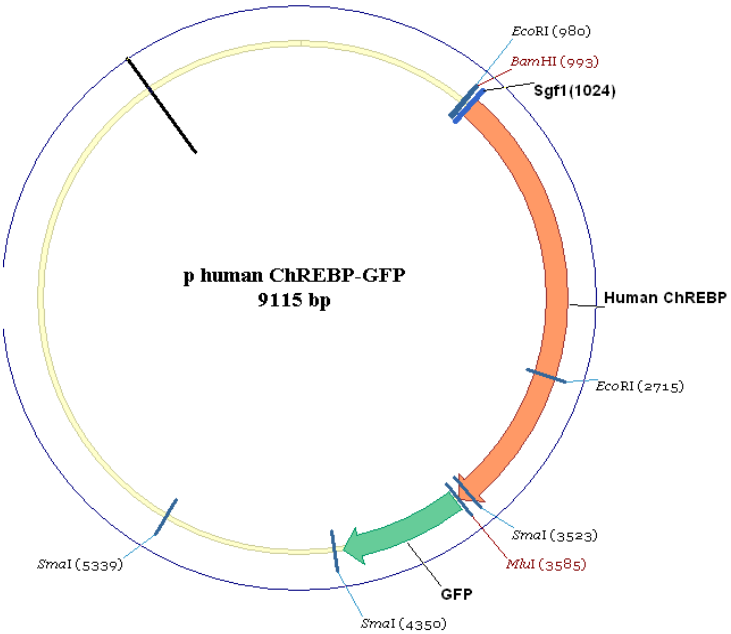

B

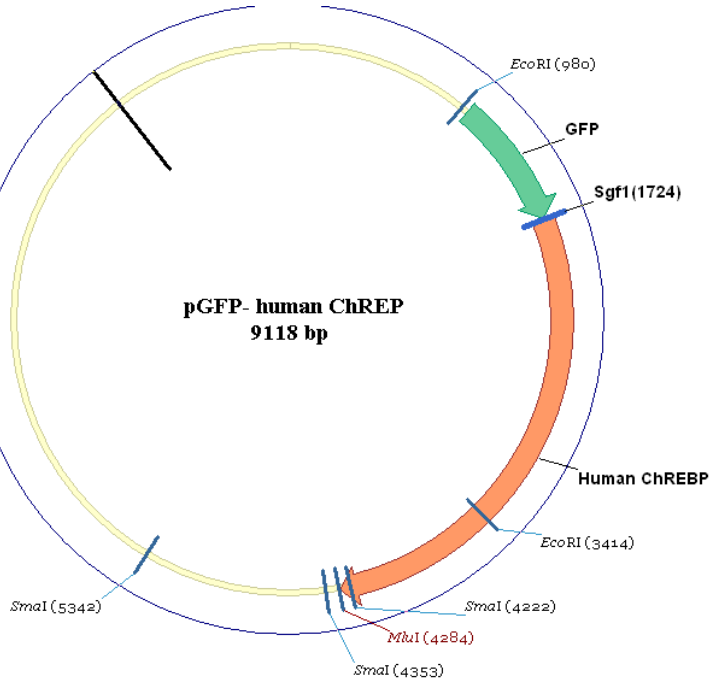

Figure 54. Entry human ChREBP inside AC- GFP vector (A) and AN- GFP vector (B) after ligation creating p human ChREBP-GFP and p GFP- human ChREBP.

4-3-3. Digestion of AC and AN human ChREBP GFP vectors

After transformation and extraction of p human ChREBP-GFP and pGFP- human ChREP vectors with mini preparation, the ratio, absorbance and the concentration (µg/ml) were measured. There were 1.847, 1.123 and 561.5; 1.835, 1.0, and 500 for AC and AN human ChREBP respectively. The restriction enzymes Mlu 1, Sgf l, EcoR 1 and Sma 1 were used to test the plasmids and the result was according to the expected.

The restriction digest of p human ChREBP-GFP and pGFP- human ChREP vectors with Mlu 1 and Sgf 1 produced one fragment for each 9115 and 9118 bp respectively (Figure 55). EcoR 1 revealed two bands at 7380, 1735 bp and 6684, 2434 bp for p human ChREBP-GFP and pGFP- human ChREP vectors respectively. While, Sma 1 was expected to result in three fragments 7299, 989 and 827; 7998, 989 and 131 bp for p human ChREBP-GFP and pGFP- human ChREP vectors respectively. 131 bp was not expected to be visible in the agarose gel due to its small size. (see Figure 56). This result was predicted with the program vector NTl by Invetrogene.

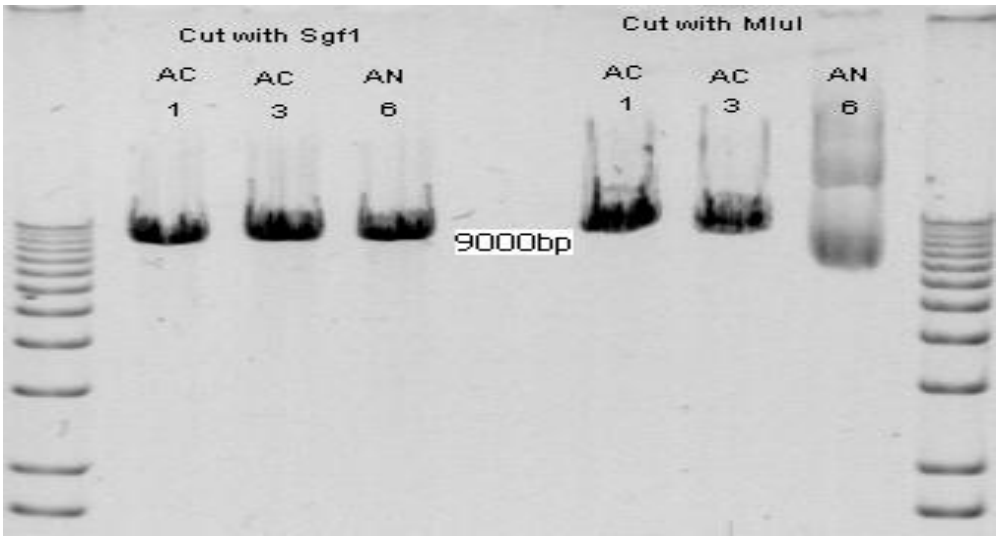

Figure 55. Restriction sites of p human ChREBP-GFP and pGFP- human ChREP vectors with Mlu 1 and Sgf l.

Plasmid DNA was digested and analysed in 1% agarose gel. Each lane contains 20 ng digested plasmid DNA. DNA bands are in accord with the fragment sizes calculated on the basis of the vector maps.

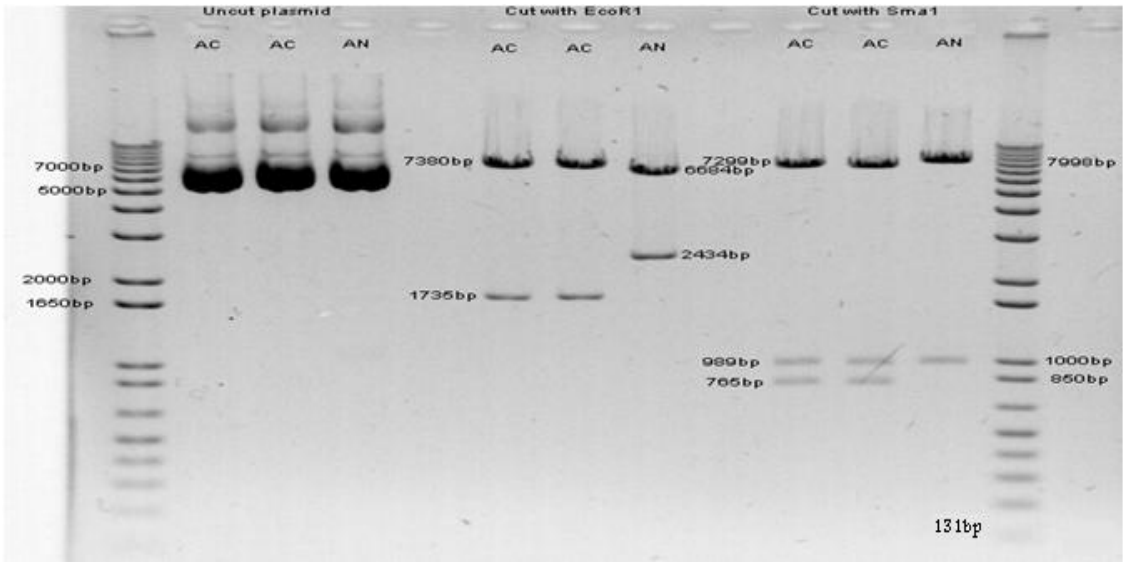

Figure 56. Restriction sites of p human ChREBP-GFP and pGFP- human ChREP vectors with EcoR 1 and Sma 1

Plasmid DNA was digested and analysed in 1% agarose gel. Each lane contains 20 ng digested plasmid DNA. DNA bands are in accord with the fragment sizes calculated on the basis of the vector maps.

4-3-4. Sequencing of the human ChREBP

To confirme identities of human ChREBP, sequencing of the human ChREBP was done in the DIfE (German Institute of Human Nutrition). Different sequencing primers (shown in 3.1.5 Sequencing Primers in Materials section) were used and the result was as expected as Figure 57(A,B), it showed that the structure of human ChREBP is correct and there are no missing amino acids and the result of sequencing showed also that the most regions of human ChREBP were covered by the sequencing primers. The first one (VP1.5 ggactttccaaaatgtcg) covered the first part of human ChREBP plus some base pair of the vector (shown in orange line), the second one (P1 tactacaagaagtggctccgtaa) covered the second part of human ChREBP (shown in black line), the third one (P9 ccggaggagggtgctggatacaa) covered the third part of human ChREBP (shown in green line) and the last sequencing primer (P5 ggcagtgaacggcggctgtcagg) which covered the last part of human ChREBP, extended about 96 bp in GFP (shown in red line) and this is a strong evidence that I cloned the correct structure of human ChREBP. (Figure 58).

A

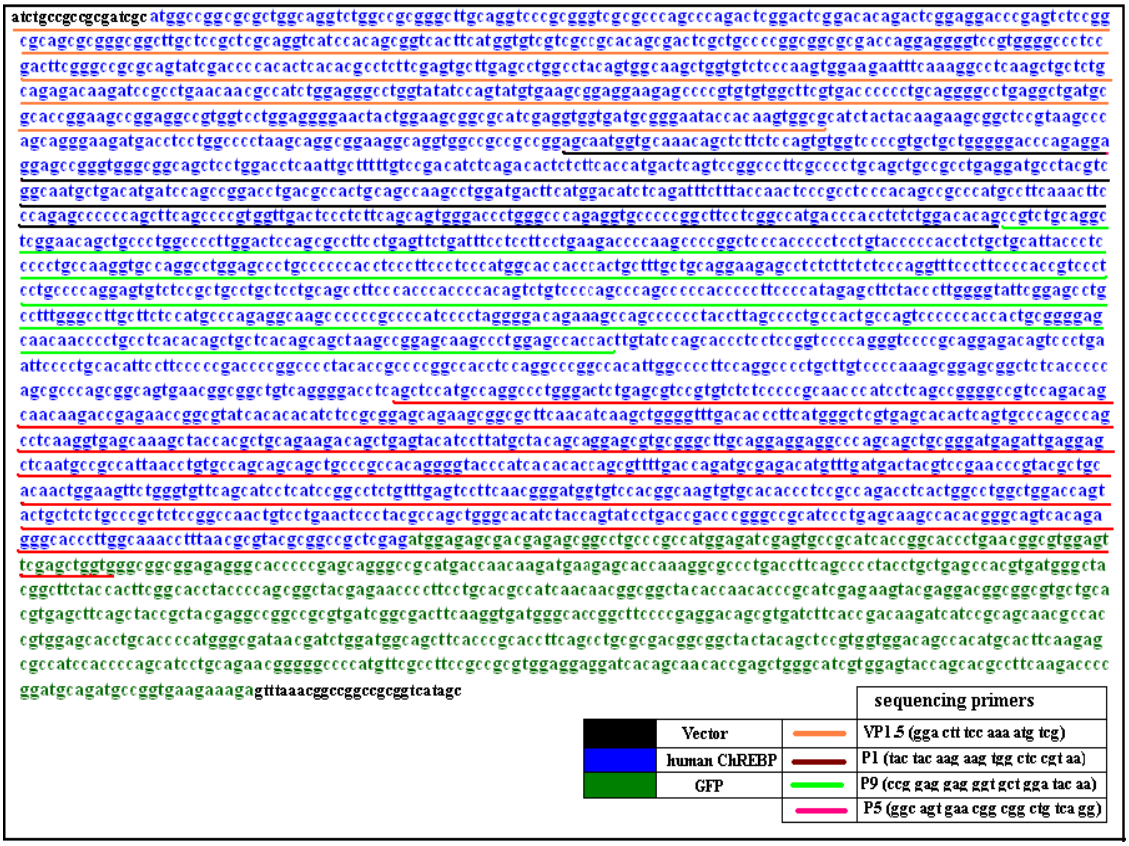

B

The beginning of the human ChREBP according to Gene Bank NM_032951

ATG GCC GGC GCG CTG GCA GGT CTG GCC GCG GGC TTG .....
Met Ala Gly Ala Leu Ala Gly Leu Ala Ala Gly Leu .....

The sequencing primer which cover the first part of human ChREBP

ATC TGC CGC CGC GAT CGC ATG GCC GGC GCG CTG GCA GGT CTG GGC GCG GGC TTG CAG GTC .....
Ile Cys Arg Arg Asp Arg Met Ala Gly Ala Leu Ala Gly Leu Ala Ala Gly Leu Gln Val .....

The sequencing primer which cover the sacond part of human ChREBP

AGC AAT GGT GCA AAC AG TCT TCT CCA GTG TGG TCC CCG TGC TGC TGG GGG ACC CAG AGG .....
Ser Asn Gly Ala Asn Ser Ser Ser Pro Val Trp Ser Pro Cys Cys Trp Gly Thr Gln Arg .....

The sequencing primer which cover the third part of human ChREBP

CCG TCT GCA GGC TCG GAA CAG CTG CCC TGG CCC CTT GGA CTC CAG CGC CTT CCT GAG TTC .....
Pro Ser Ala Gly Ser Glu Glu Leu Pro Trp Pro Leu Gly Leu Gln Arg Leu Pro Gly Phe .....

Additional aminoacids from the poly-cloning side in between human ChREBP and GFP

CCC TTG GCA AAC CCT TAA CGC GTA CGC GGC CGC TCG AGA TGG AGA GCG ACG AGA GCG .....
Pro Leu Ala Asn Val stop Arg Val Arg Gly Arg Ser Arg Trp Arg Ala Thr Arg Ala .....

Figure 57 . Sequencing of Part of phuman ChREBP-GFP vector(A). The whole Sequencing of human ChREBP (B).

The sequencing of Part of phuman ChREBP-GFP vector is shown: human ChREBP (black), GFP encoding part (green), the part of vector before the ChREBP (violet), the upper line puts in each case the cDNA sequence, and the lower line the matching amino acid code.

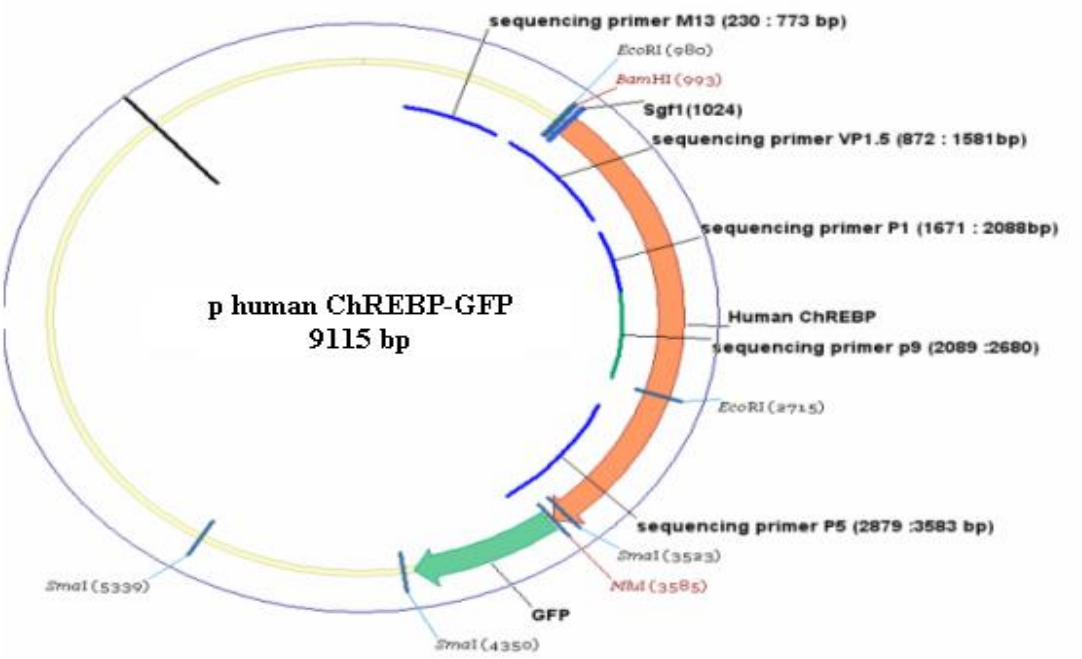

Figure 58. Sequencing of the p human ChREBP-GFP vector.

4-3-5. The effect of glucose concentration with or without insulin on the translocation of human ChREBP in HUH7, HepG2 and U2OS

Glucose activates ChREBP by stimulating its gene expression and by regulating its entry from the cytosol into the nucleus thereby promoting its binding to carbohydrate responsive element (ChoRE) present in the promoter regions of its target genes (Uyeda & Repa 2006). ChREBP is required for the induction of L-pyruvate kinase (L-PK), which is exclusively dependant on glucose. Induction of FAS and ACC genes is under the combined action of ChREBP and of SREBP-1c in response to glucose and insulin, respectively. (Denechaud *et al*. 2008b)

To determine the influence of different dietary elements on the activity of cloned human ChREBP in vitro (labeled by green fluorescence protein) and its translocation from cytoplasm to nucleus, ,monitored by fluorescence microscope, first the effect of glucose concentration (low and high) and insulin on the translocation of human ChREBP

in different kind of cells (HUH7, HepG2 and U2OS) was tested to select the suitable cells for this investigation and the best concentration of glucose and insulin activate ChREBP and promoting its translocation from the cytoplasm to the nucleus.

To visualize the subcellular localization of human ChREBP at low and high glucose concentrations, the different kind of cells (HUH7, HepG2 and U2OS) were transfected with p human ChREBP-GFP expression vector and incubated for 5 h at 5mM glucose and 10% FCS, then the medium was changed to 5mM glucose and 2% FCS over night before 1 hr starvation with 5mM glucose and 0% FCS. The cells were incubated with 5 or 25mM glucose in the presence or absence of 100 nM insulin for 2 h before fixation, then the cells were analysed by florescence microscope.

The results in Figures 59, 60 showed the effect of glucose concentration (low and high) with or without insulin on the translocation of human ChREBP in HUH7and HepG2 celllines. It was clearly noticed that there was no significant different observed between all samples in different cases. These result are not in accordance with (Dentin *et al.* 2005a) An important difference is, that they used primary cultures of murine hepatocytes. They indicated that the GFP-fused ChREBP was mainly detected in the cytosol of hepatocytes at low glucose concentrations with or without insulin and migrated into the nucleus when hepatocytes were cultured at high glucose and insulin concentrations.

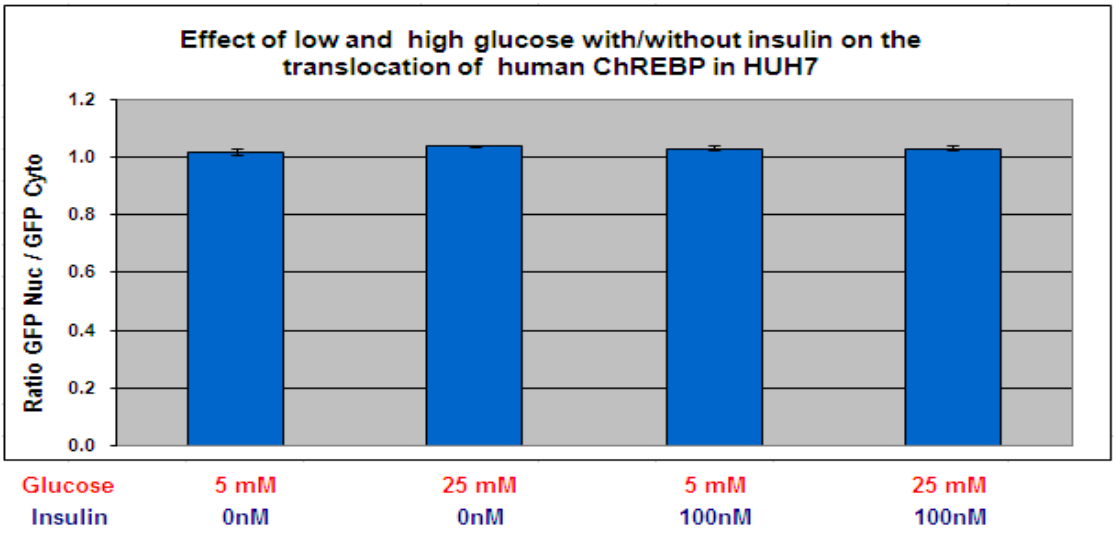

Figure 59. Effect of low and high glucose concentration in the presence or absence of 100 nM insulin on the subcellular localization of human ChREBP in HUH7.

The cells were transfected with human ChREBP expression vector and incubated for 5 h with 5mM glucose and 10% FCS, then the medium was changed to 5mM glucose and 2% FCS over night, after that 1 hr starvation with 5mM glucose and 0% FCS was done. The cells were incubated with 5 or 25mM glucose in the presence or absence of 100 nM insulin for 2 h before fixation, then the cells were analysed by florescence microscope.

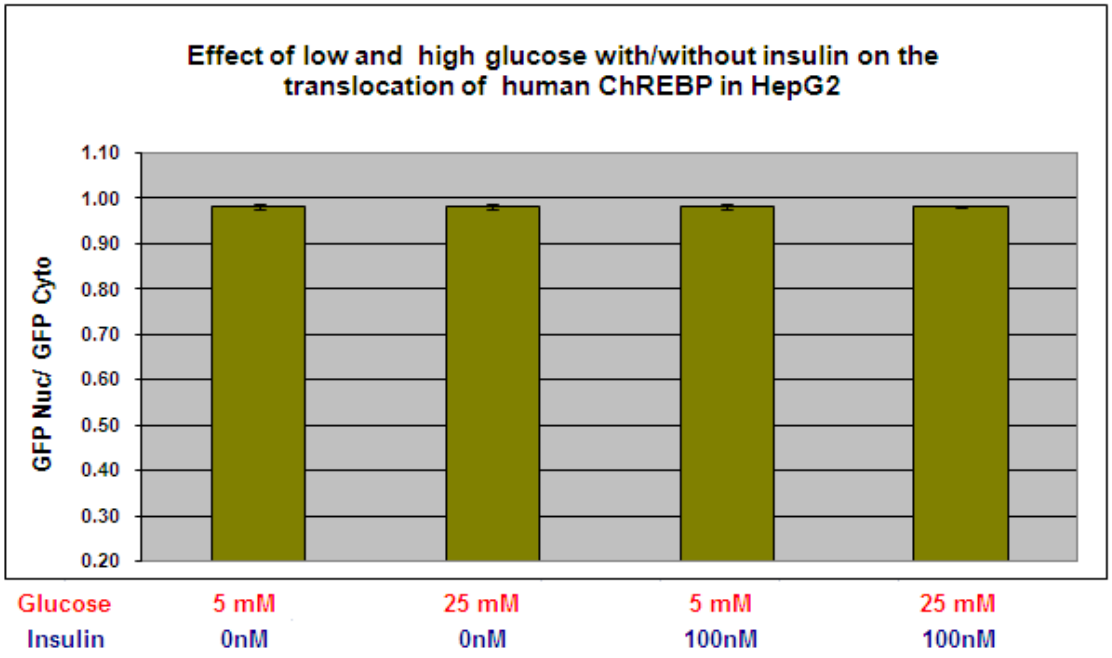

Figure 60. Effect of low and high glucose concentration in the presence or absence of 100 nM insulin on the subcellular localization of human ChREBP in HepG2. The cells were transfected with human ChREBP expression vector and incubated for 5 h with 5mM glucose and 10% FCS, then the medium was changed to 5mM glucose and 2% FCS over night, after that 1 hr starvation with 5mM glucose and 0% FCS was done. The cells were incubated with 5 or 25mM glucose in the presence or absence of 100 nM insulin for 2 h before fixation, then the cells were analysed by florescence microscope.

On the other hand, the represented results in Figure 61 indicated that in the presence of 25 mM glucose and 100 nM insulin, the human ChREBP was induced and translocated from the cytoplasm to the nucleus in U2OS cells. At low glucose concentration (5 mM) with or without insulin no significant amount of ChREBP was detected. The nuclear translocation of human ChREBP in U2OS cells was significantly

different (P=0, 00069) between 5 and 25 mM glucose without insulin; (P=0,00144) between 5mM glucose with and without 100nM insulin; (P=0,0037) between 25mM glucose with and without 100nm insulin; (P=0,00566) between 5 and 25 mM glucose with 100nm insulin and (P=0,000085) between 5mM glucose without insulin and 25 mM glucose with 100nm insulin. From the previous result, the highest significant difference was between high glucose (25 mM) with 100 nm insulin and low glucose without insulin, which due to the positive effect of glucose and insulin on ChREBP activation and its nuclear translocation.

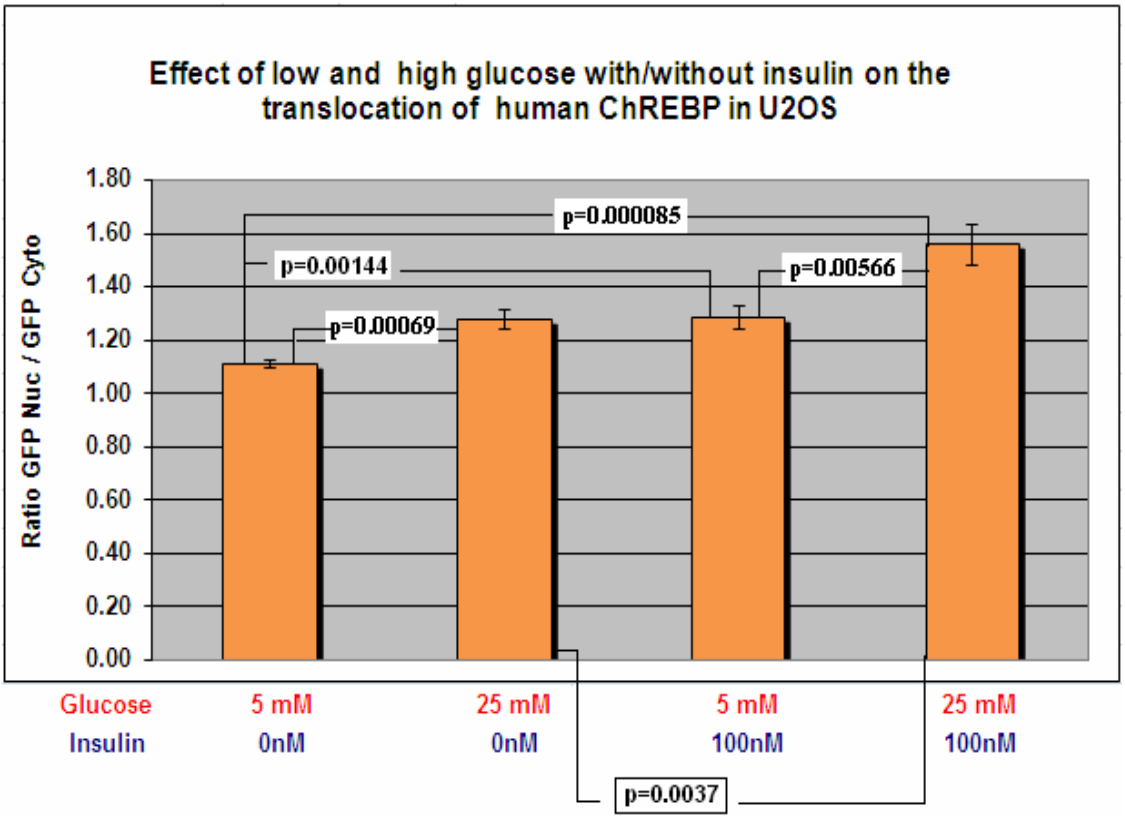

Figure 61. Effect of low and high glucose concentration in the presence or absence of 100 nM insulin on the subcellular localization of human ChREBP in U2OS. The cells were transfected with human ChREBP expression vector and incubated for 5 h at 5mM glucose and 10% FCS, then the medium was changed to 5mM glucose and 2% FCS over night, after that 1 hr starvation with 5mM glucose and 0% FCS was done.

The cells were stimulated with 5 or 25mM glucose in the presence or absence of 100 nM insulin for 2 h before fixation, then the cells were analysed by florescence

microscope. These results are coincide with (Dentin et al. 2005a), who reported that incubation of hepatocytes with glucose and insulin led to a 4.5-fold increase in ChREBP content in the cytosol, leading to its translocation to the nucleus (Dentin et al. 2005a). Compatible findings were observed by (Denechaud et al. 2008b) who mentioned that when overnight-fasted mice were refed a high-carbohydrate (HCHO) diet for 18 h, ChREBP phosphorylation on Ser196 was low and ChREBP protein was predominantly located in the nucleus (Denechaud et al. 2008a). He et al. (He et al. 2004) reported that in the presence of 25 mM glucose, the mRNA level of ChREBP was dramatically induced during adipogenesis in 3T3-L1 preadipocyte. At a lower glucose concentration (5 mM) no significant amount of ChREBP mRNA was detectable (He et al. 2004).

Several recent studies suggested that high ambient glucose, insulin, PPARγ agonist, liver X receptor and polyunsaturated fatty acids may affect ChREBP mRNA expression levels (Denechaud *et al.* 2008b). Interestingly, liver X receptors have been shown to directly stimulate ChREBP mRNA expression in addition to their known regulation of lipogenesis through SREBP-1c and FAS (Yahagi *et al.* 2002). Furthermore, in ob/ob mice, a well-characterized genetic model of obesity, insulin resistance, and hyperinsulinemia, ChREBP expression level is substantially higher, suggesting a potential role of insulin in stimulating ChREBP production (Dentin *et al.* 2006a); (Sirek *et al.* 2009).

4-3-6. The effect of fructose and some artificial sweeteners on the translocation of human ChREBP in U2OS cells

4-3-6-1. Fructose

A diet high in fructose induces metabolic syndrome including insulin resistance, hypertriglyceridemia and hypertension in animal models (Hwang *et al.* 1987), and shows similar effects in humans (Stanhope *et al.* 2009). Liver is the major site of fructose metabolism (McGuinness & Cherrington 2003). Because fructose enters the glycolytic/gluconeogenic pathway as trioses in liver, metabolizing fructose requires simultaneous activation of part of glycolysis, de novo lipogenesis, part of gluconeogenesis and glycogen synthesis. An increase in both insulin and glucose concentrations is required for most glycolytic/lipogenic genes to be fully expressed in the liver. Carbohydrate response element-binding protein (ChREBP) is activated in high

glucose and binds to carbohydrate response element (ChRE) (Yamashita *et al.* 2001). ChREBP upregulates lipogenic genes such as PK (Yamashita *et al.* 2001), FAS (Rufo *et al.* 2001), acetyl-CoA carboxylase (ACC) (O'Callaghan *et al.* 2001) and possibly stearoyl-CoA desaturase 1 (SCD1) (Wang *et al.* 2006) in response to high glucose. Paradoxically, G6Pase gene also has ChRE (Pedersen *et al.* 2007), and is up-regulated by high glucose in cultured hepatocytes (Massillon 2000); (Koo *et al.* 2009).

The results in Figure 62 showed the effect of fructose concentration (5 and 25mM) with or without 100 nM insulin on the translocation of human ChREBP in U2OS cells. It was clearly noticed that there was no significant difference observed between samples in absence of insulin. On the other hand, there was highly significant difference (p= 0.00026) observed between control and high fructose in presence of insulin.

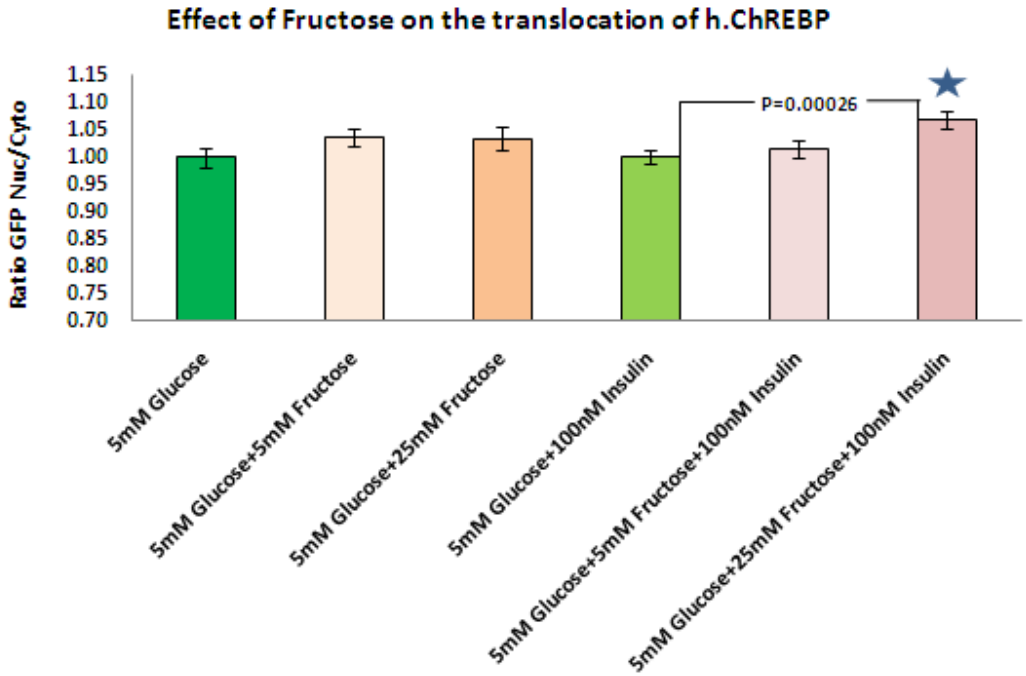

Figure 62. Effect of low and high (5 and 25 mM) fructose concentration in the presence or absence of 100 nM insulin on the subcellular localization of human ChREBP in U2OS.

The cells were transfected with human ChREBP expression vector and incubated for 5 h at 5mM glucose and 10% FCS, then the medium was

changed to 5mM glucose and 2% FCS over night, after that 1 hr starvation with 5mM glucose and 0% FCS was done. The cells were stimulated with 5 and 25 mM fructose in the presence or absence of 100 nm insulin for 2 h before fixation, then the cells were analysed by florescence microscope.

These results are compatible to *in vivo* investigations by Koo et al. (Koo *et al.* 2009) study, they indicated that ChREBP is regulated at multiple levels. High glucose and insulin concentration stimulates ChREBP gene expression both in vitro and in vivo (Dentin *et al.* 2004). In Koo et al (2009) study, dietary fructose modestly increased ChREBP gene expression compared to dietary glucose although the increase did not reach statistical difference. The data showed that, ChREBP increased its DNA binding activity by fructose feeding, Dietary fructose induced PK, FAS and G6Pase genes (Koo *et al.* 2008), all of which possess ChRE in their promoter region, suggesting ChREBP may mediate the fructose effects on these genes. Furthermore, mice with ChREBP gene deletion displayed severe sucrose/ fructose intolerance, suggesting a critical role of ChREBP in fructose metabolism. (Iizuka *et al.* 2004)

4-3-6-2. The artificial sweeteners (cyclamate, aspartame, saccharine and stevioside)

First discovered in the late 19th century in the United States, saccharin (and later cyclamate, aspartame, and sucralose) enabled individuals to experience sweet tastes in food with dramatic reductions in caloric consumption over nutritive sweeteners. Between 1890 and 1930, saccharin was the only artificial sweetener produced in the United States, and its consumption was limited to diabetics who eschewed sugar for medical reasons. Beginning in the 1950s with saccharin and cyclamates, extending to aspartame in the early 1980s, and now with sucralose, chemical sweeteners have found a primary market among consumers who could consume nutritive sweeteners, but choose not to, in order to lose weight or maintain weight. This shift in consumer practices can be linked to three marketplace shifts: (a) the development of second-generation sweeteners, such as cyclamates and aspartame and improved saccharin blends that improved the taste of artificially sweetened products; (b) the rise in popularity of dieting and diet programs among americans in the late 20th century; and (c) the improved marketing and branding

practices of sweetener manufacturers, food companies, and diet product lines that produce or use artificial sweeteners. (de la Pen~a 2010)

Therefore, the aim of this study was to assess the influence of some artificial sweeteners (cyclamate, aspartame, saccharine and stevioside) on the activity of cloned human ChREBP in vitro (labeled by green fluorescence protein) and its translocation from cytoplasm to nucleus which monitored by fluorescence microscope. In the absence of any sweeteners (cyclamate, aspartame, saccharine and stevioside), glucose and insulin, the activity of human ChREBP and its translocation from cytoplasm to nuclease was not significantly different (P>0.05).

Cyclamate

0.1 mM and 1 mM of cyclamate with or without insulin were tested. It was clearly noticed that there was no significant difference observed between all samples in absence of insulin and there was no effect of 0.1 mM of cyclamate in the presence of insulin. On the other hand, there was significant different (p= 0.007) observed between control and 1 mM cyclamate in the presence of insulin. (**Figure 63**)

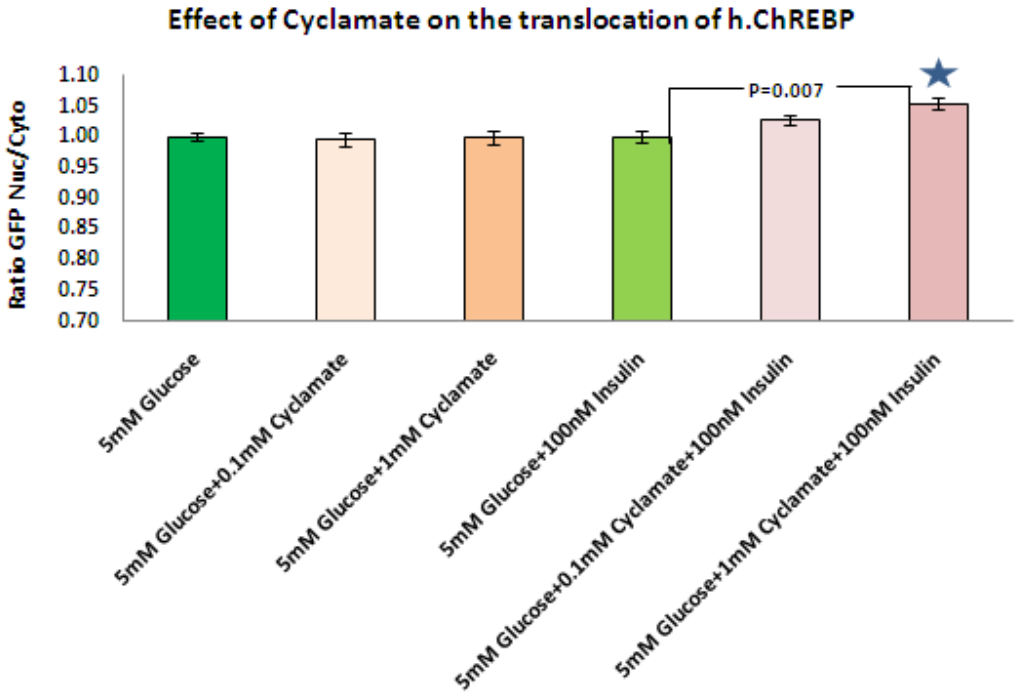

Figure 63. Effect of (0.1 and 1mM) cyclamate in the presence or absence of 100 nm insulin on the subcellular localization of human ChREBP in U2OS.

The cells were transfected with human ChREBP expression vector and incubated for 5 h at 5mM glucose and 10% FCS, then the medium was changed to 5mM glucose and 2% FCS over night, after that 1 hr starvation with 5mM glucose and 0% FCS was done. The cells were stimulated with 0.1 and 1mM cyclamate in the presence or absence of 100 nm insulin for 2 h before fixation, then the cells were analysed by florescence microscope.

Saccharine

0.1 mM and 1 mM of saccharine with or without insulin were tested. There was no significant different observed for 0.1 mM saccharine in presence or absence of insulin when compared with control. On the other hand, there was significant difference observed for 1 mM saccharine in absence or presence of insulin when compared with control (p= 0.006) and (p= 0.002) respectively. (Figure 64)

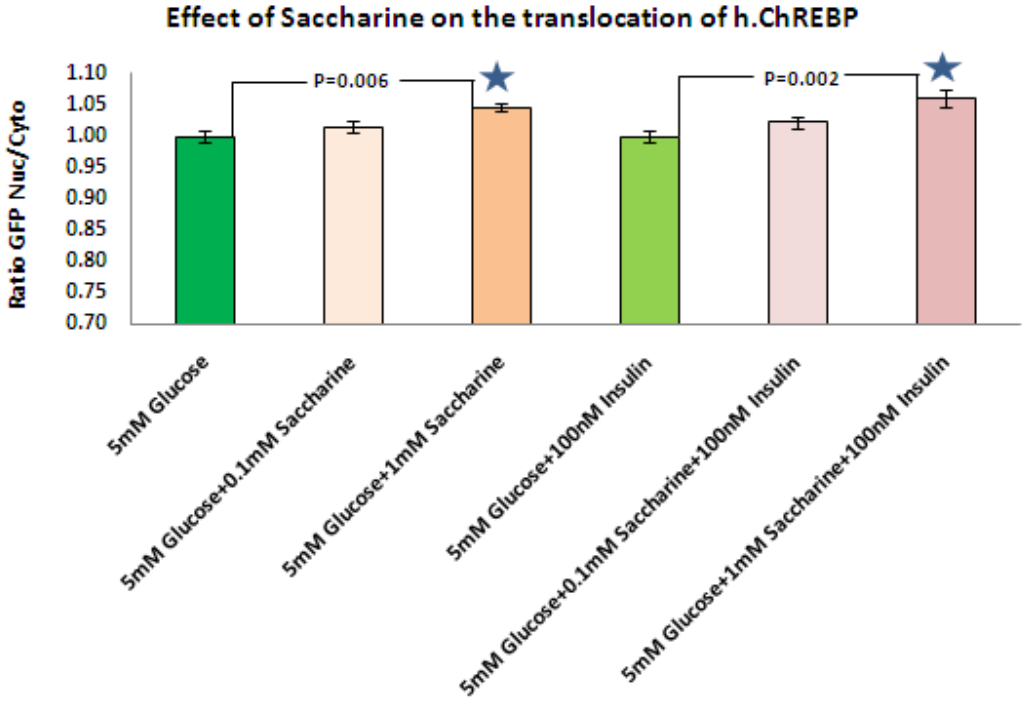

Figure 64. Effect of (0.1 and 1mM) saccharine in the presence or absence of 100 nm insulin on the subcellular localization of human ChREBP in U2OS.

The cells were transfected with human ChREBP expression vector and incubated for 5 h at 5mM glucose and 10% FCS, then the medium was changed to 5mM glucose and 2% FCS over night, after that 1 hr starvation with 5mM glucose and 0% FCS was done. The cells were stimulated with 0.1 and 1mM cyclamate in the presence or absence of 100 nm insulin for 2 h before fixation, then the cells were analysed by florescence microscope.

Aspartame

0.1 mM and 1 mM of aspartame with or without insulin were tested. There was no significant difference observed between all samples in absence or presence of insulin. (Figure 65)

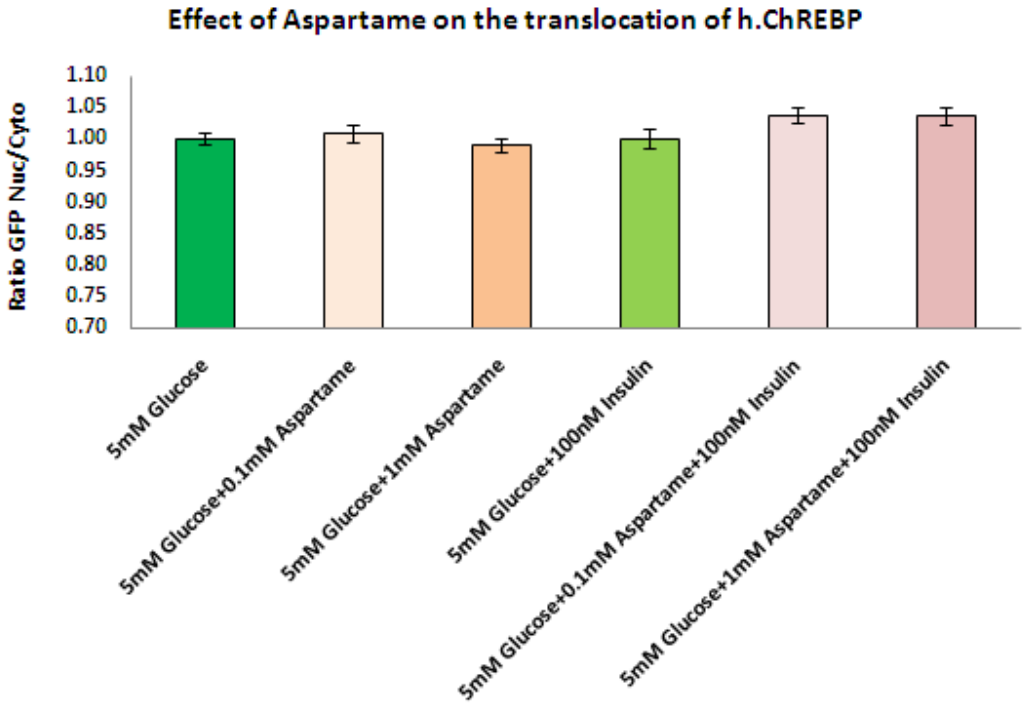

Figure 65. Effect of (0.1 and 1mM) aspartame in the presence or absence of 100 nm insulin on the subcellular localization of human ChREBP in U2OS.

The cells were transfected with human ChREBP expression vector and incubated for 5 h at 5mM glucose and 10% FCS, then the medium was changed to 5mM glucose and 2% FCS over night, after that 1 hr starvation with 5mM glucose and 0% FCS was done. The cells were stimulated with 0.1 and 1mM cyclamate in the presence or absence of 100 nm insulin for 2 h before fixation, then the cells were analysed by florescence microscope.

Stevioside

10 µM and 100 µM of stevioside with or without insulin were tested. There was no significant difference observed between all samples in absence or presence of insulin. (Figure 66)

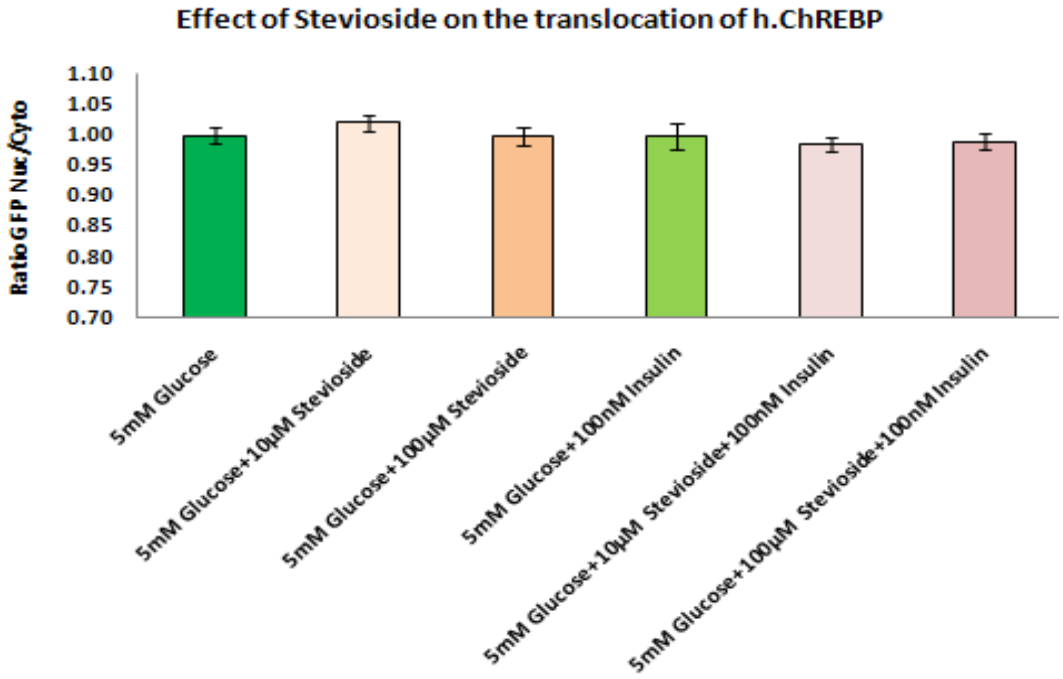

Figure 66. Effect of (10 and 100 µM) stevioside in the presence or absence of 100 nm insulin on the subcellular localization of human ChREBP in U2OS.

The cells were transfected with human ChREBP expression vector and incubated for 5 h at 5mM glucose and 10% FCS, then the medium was changed to 5mM glucose and 2% FCS over night, after that 1 hr starvation with 5mM glucose and 0% FCS was done. The cells were stimulated with 0.1 and 1mM cyclamate in the presence or absence of 100 nm insulin for 2 h before fixation, then the cells were analysed by florescence microscope.

The present results document that sodium cyclamate and sodium saccharine increased the translocation of ChREBP from cytoplasm to the nucleus, in opposite to aspartame and stevioside that show no effects. No information was so far available on the effect of artificial sweeteners on the activity and the translocation of ChREBP from cytoplasm to the nuclease in vitro.

4-3-7. The effect of polyunsaturated fatty acids (PUFAs) on the translocation of human ChREBP in U2OS cells

Polyunsaturated fatty acids (PUFAs) are potent inhibitors of hepatic glycolysis and de novo lipogenesis, through the inhibition of transactivation of genes involved in glucose utilization and lipid synthesis, including L-pyruvate kinase (L-PK), fatty acid synthase (FAS), and acetyl-CoA carboxylase (ACC). By regulating these pathways, PUFAs promote a shift from fatty acid synthesis and storage to oxidation (Jump & Clarke 1999). Carbohydrate-responsive element–binding protein 1 (ChREBP) was shown to play a pivotal role in the induction of glycolytic and lipogenic genes by glucose (Dentin *et al.* 2004) by its capacity to bind to the ChoRE present in promoters of these target genes (Ishii *et al*. 2004). ChREBP is expressed in liver and is responsive to the nutritional state.

In agreement with (Kawaguchi *et al.* 2001) study, the GFP-human ChREBP was mainly detected in the cytosol of U2OS at low glucose concentrations with or without insulin and migrated into the nucleus when U2OS were cultured at high glucose and insulin concentrations (Figure 67). The GFP-human ChREBP also showed appropriate nuclear translocation when U2OS were cultured at high glucose and insulin concentrations and in the presence of Docosahexaenoic acid (DHA) at all different concentrations. These results was not in accordance with (Dentin *et al*. 2005a) who reported that DHA suppressed ChREBP activity and its translocation, and this difference in results may be due to using U2OS cells in my study which caused lack of some essential hepatic enzymes.

In contrast, PUFAs (linoleic acid and eicosapentanoic acid (EPA)) markedly inhibited nuclear translocation of the GFP-human ChREBP at all concentrations but highly significantly ($p= 0.0183$) at 10 µM with EPA. It was noticed that the inhibition of nuclear translocation of the GFP-human ChREBP decreased with the increase of PUFAs

concentration up to 300µM, this response may be due to the increase of NaOH concentration (the solvent of PUFAs). Figures (68, 69) demonstrating that inhibition in ChREBP translocation into nucleus was specific to PUFAs. It was proposed that the PUFAs inhibition of glucose-induced L-PK gene transcription resulted from AMPK mediated phosphorylation of ChREBP at Ser568, which then inactivated its DNA-binding activity (Kawaguchi *et al.* 2002). The activation of AMPK would result from the increased AMP concentrations generated by PUFAs activation in acyl-coA (Kawaguchi *et al.* 2002).

Supplementing a HCHO diet with oils rich in (n-6) and (n-3) PUFAs results in an inhibition of a wide array of glycolytic and lipogenic enzymes including L-PK, FAS, or ACC (Jump 2004). The present study shows that PUFAs [essentially (n-3) and (n-6) fatty acids], may downregulate ChREBP gene expression by altering ChREBP translocation from the cytosol to the nucleus.

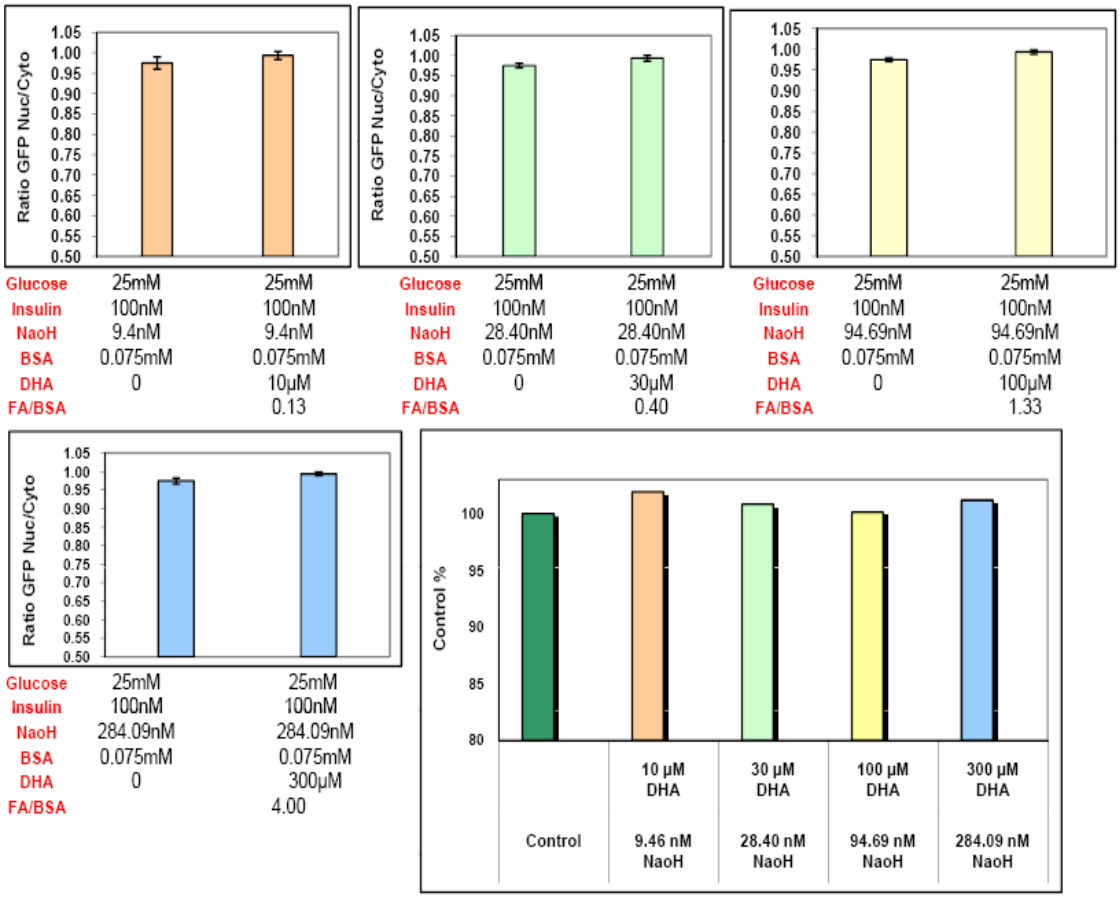

Figure 67. The effect of DHA on the translocation of human ChREBP**.**

A GFP-human ChREBP was transfected in cultured U2OS cells in the presence of 25 mM glucose plus 100 nM insulin and treated or not with different concentrations (10, 30, 100, and 300 µM) of DHA for 2 hours. Every concentration had its separate control (same amount of NaoH, BSA, and FA/BSA ratio) to avoids the conflict of other factors with the effect of DHA. The data, from three independent experiments were shown.

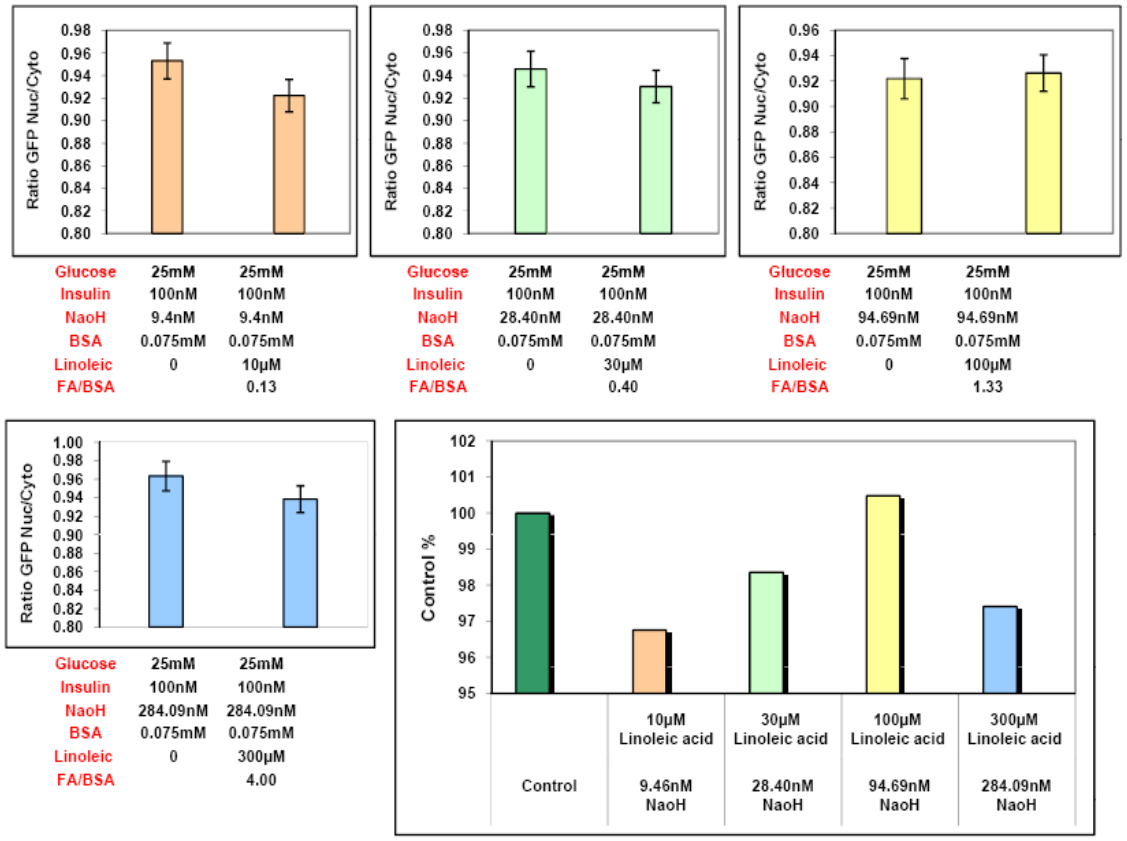

Figure 68. The effect of linoleic acid on the translocation of human ChREBP.

A GFP-human ChREBP was transfected in cultured U2OS cells in the presence of 25 mM glucose plus 100 nM insulin and treated or not with different concentrations (10, 30, 100, and 300 µM) of linoleic acid for 2 hours. Every concentration had its separate control (same amount of NaoH, BSA, and FA/BSA ratio) to avoids the conflict of other factors with the effect of linoleic acid. The data, from three independent experiments were shown.

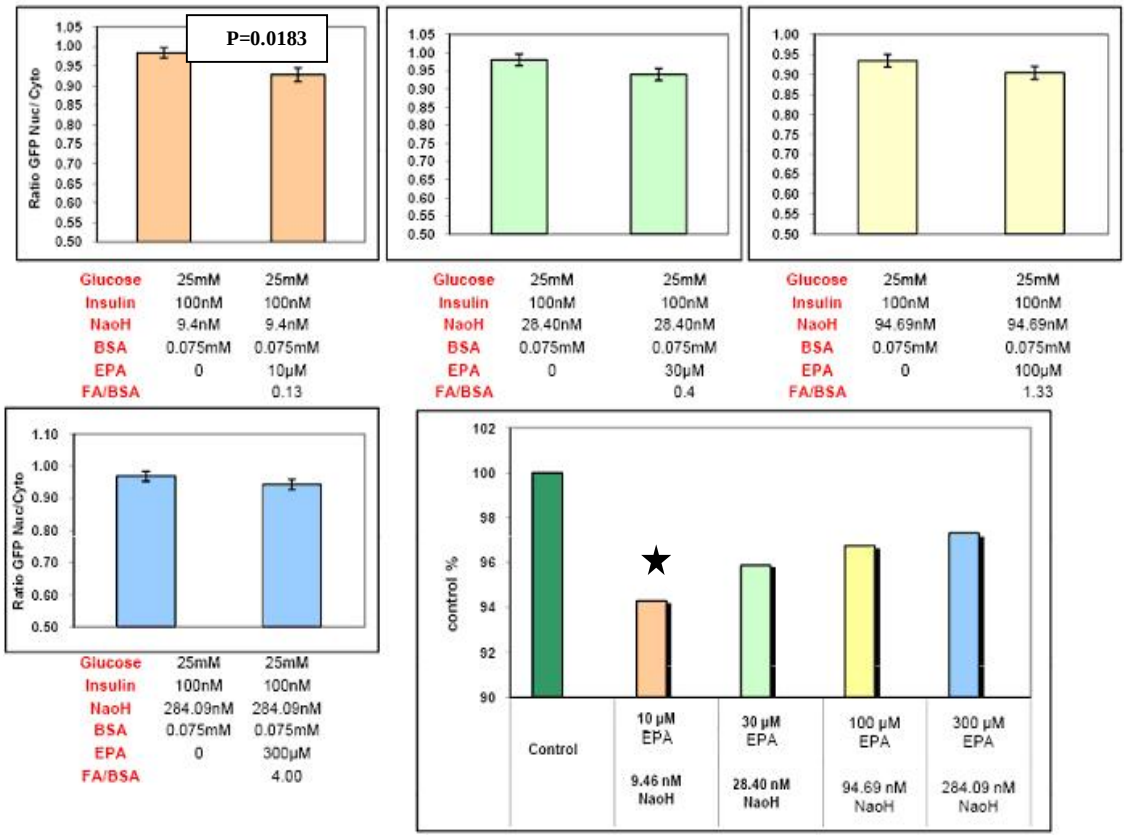

Figure 69. The effect of EPA on the translocation of human ChREBP.

A GFP-human ChREBP was transfected in cultured U2OS cells in the presence of 25 mM glucose plus 100 nM insulin and treated or not with different concentrations (10, 30, 100, and 300 µM) of EPA for 2 hours. Every concentration had its separate control (same amount of NaoH, BSA, and FA/BSA ratio) to avoids the conflict of other factors with the effect of EPA. The data, from three independent experiments were shown.

4-3-8. The effect of oleic acid and oleuropein (as main component of olive fruit) on the translocation of human ChREBP in U2OS cells

The olive fruit, its oil, and the leaves of the olive tree have a rich history of nutritional, medicinal, and ceremonial uses (Soni *et al.* 2006). In addition to cereals, the olive is an important crop in the mediterranean basin, which produces 98% of the world total (approximately 11 million tons), and lends important economic and dietetic benefits to the people of that region.(Japń-Lujȣn *et al.* 2006). (El & Karakaya 2009)

Oleic acid was most effective at depressing lipogenesis and cholesterologenesis; decreased label incorporation into cellular palmitic, stearic, and oleic acids was detected. ACC activity was strongly reduced (80%) by oleic acid. Oleic acid also reduced the activity of 3-hydroxy-3-methylglutaryl coenzyme A reductase (HMGCR). The inhibition of ACC and HMGCR activities is corroborated by the decreases in ACC and HMGCR mRNA abundance and protein levels. The downregulation of ACC and HMGCR activities and expression by oleic acid could contribute to the reduced lipogenesis and cholesterologenesis. (Natali *et al*. 2007)

Therefore, this investigation was undertaken to study the effect of oleic acid (C18:1) and oleuropein on the translocation of human ChREBP in U2OS cells. To determine whether the oleic acid and oleuropein mediated inhibition in ChREBP gene expression was correlated to its influence on ChREBP translocation. The GFP-human ChREBP vector was transfected in cultured U2OS cells and analyzed following incubations in the presence of 25 mM glucose plus 100 nM insulin and treated or not with different concentrations (10, 30, 100, 300, and 1000 µM) of oleic acid or oleuropein for 2 hours. I excluded the last concentration (1000 µM) results because it causes poisoning of the cells (data not shown). With taking into account that every concentration had its separate control (same amount of NaoH, BSA, and oleic acid or oleuropein /BSA ratio) to avoids the conflict of other factors with the effect of oleic acid or oleuropein.

As shown in Figure 70, oleic acid markedly inhibited nuclear translocation of the GFP-human ChREBP at all concentrations but highly significantly ($p= 0.0208$) at 10 µM. It was noticed that the inhibition of nuclear translocation of the GFP-human ChREBP decreased with the increase of PUFAs concentration up to 300µM, this response may be due to the increase of NaOH concentration (the solvent of PUFAs). The alteration in ChREBP translocation is compatible to a suppression of ACC by oleic acid in vitro. This result was in accordance with (Natali *et al*. 2007) who reported that ACC activity was reduced (50%) by C20:4 and (80%) by C18:0 and C18:1 cis addition to the C6 glioma cells. A general decrease of fatty acid synthesis by exogenous fatty acids was observed; the reduction was particularly pronounced when the C18:1 cis or C18:1 trans isomer was added to the culture medium. Overall, the reduction of cholesterogenesis by exogenous fatty acids was often less pronounced, compared with fatty acid synthesis, especially in the case of C18:1 trans. It might be argued that the observed reduction of label

incorporation into fatty acids and cholesterol after fatty acid addition could be attributable to the precursor-dilution effect by exogenous fatty acids. Betta-oxydation of fatty acids and consequently the generation of acetyl-CoA might dilute the [^{14}C] acetyl-CoA pool derived from [^{14}C] acetate and may lead to a lower apparent synthesis rate of ^{14}C-labeled fatty acids and [^{14}C] cholesterol. (Natali *et al.* 2007)

In contrast, the GFP-human ChREBP showed appropriate nuclear translocation when U2OS were cultured at high glucose and insulin concentrations and in the presence of Oleuropein at all different concentrations (Figure 71).

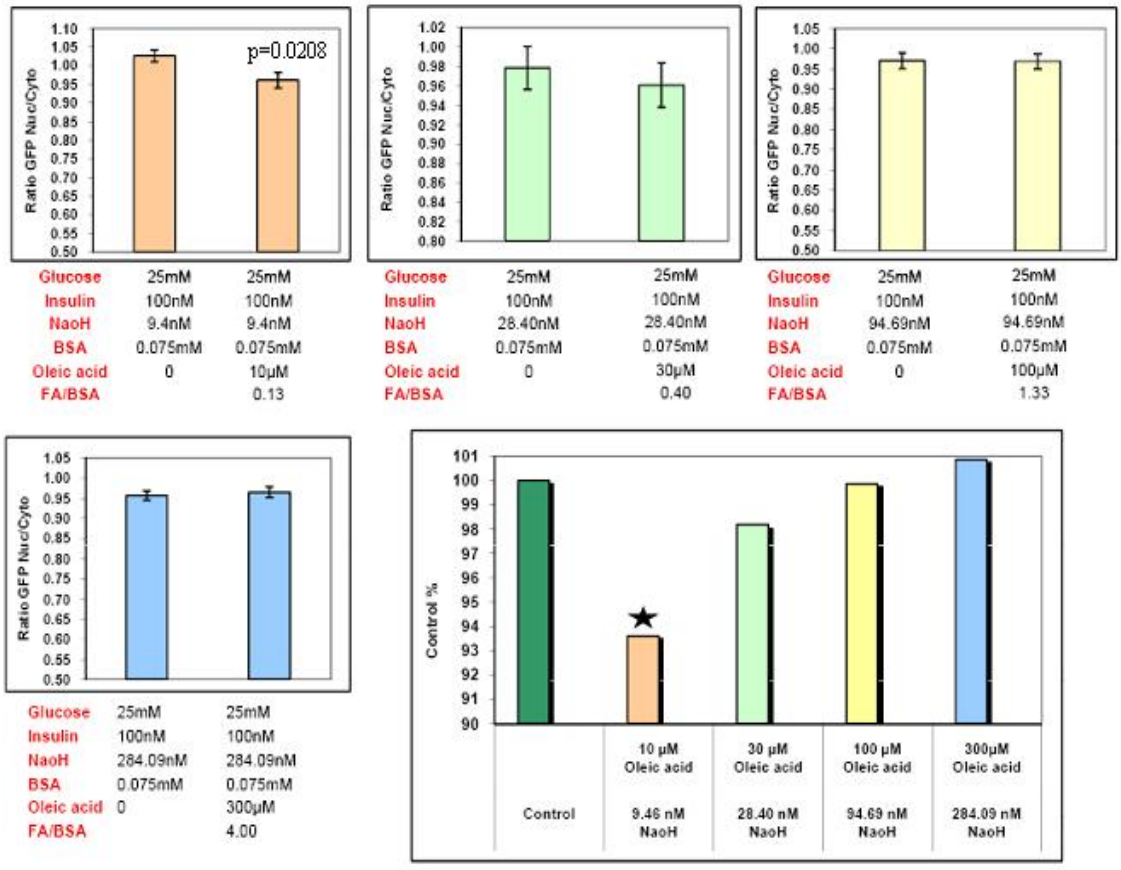

Figure 70. The effect of oleic acid on the translocation of human ChREBP.

A GFP-human ChREBP was transfected in cultured U2OS cells in the presence of 25 mM glucose plus 100 nM insulin and treated or not with different concentrations (10, 30, 100, and 300 µM) of oleic acid for 2 hours. Every concentration had its separate control (same amount of NaoH, BSA,

and FA/BSA ratio) to avoids the conflict of other factors with the effect of oleic acid. The data, from three independent experiments were shown.

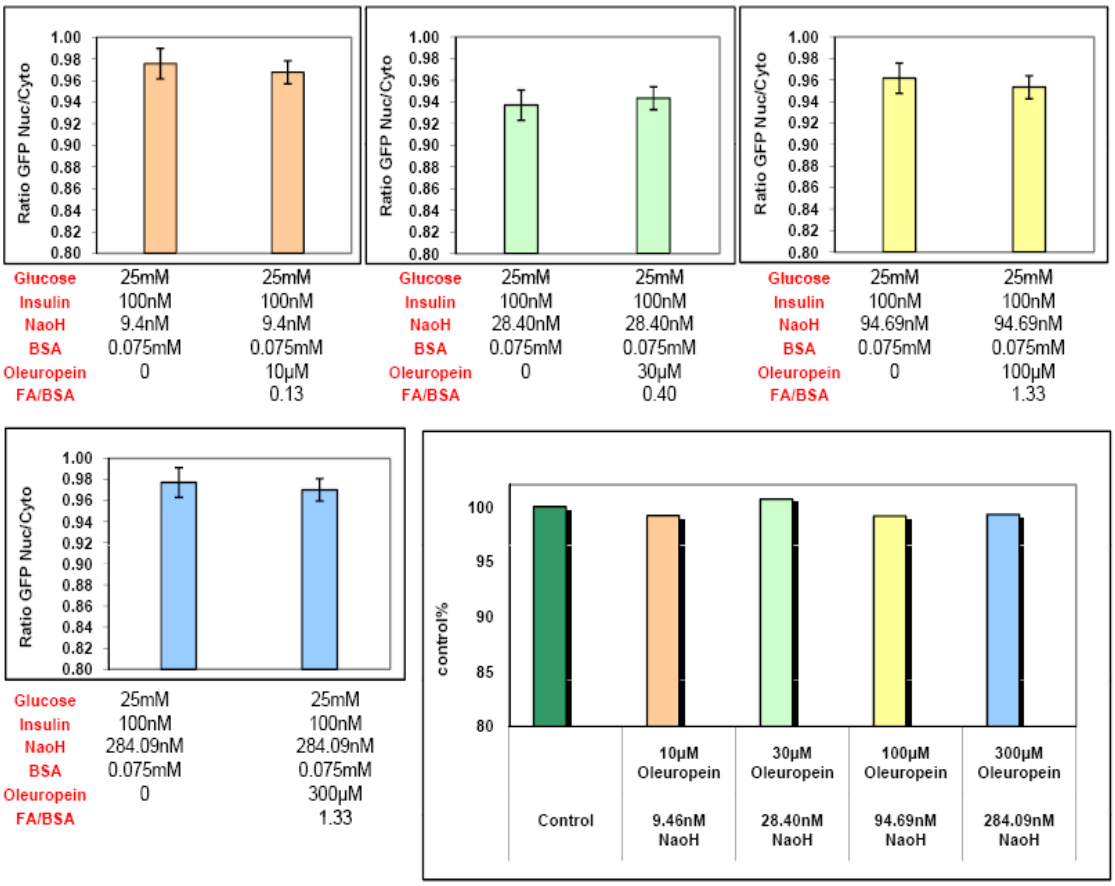

Figure 71. The effect of oleuropein on the translocation of human ChREBP.

A GFP-human ChREBP was transfected in cultured U2OS cells in the presence of 25 mM glucose plus 100 nM insulin and treated or not with different concentrations (10, 30, 100, and 300 μM) of oleuropein for 2 hours. Every concentration had its separate control (same amount of NaoH, BSA, and FA/BSA ratio) to avoids the conflict of other factors with the effect of oleuropein. The data, from three independent experiments were shown.

PUFAs suppress the nuclear translocation of ChREBP in cultured hepatocytes. Nuclear translocation of ChREBP is one of the important processes in the glucose activation of L-PK or FAS gene transcription (Kawaguchi *et al.* 2001). To determine

whether the PUFAs mediated inhibition in ChREBP gene expression was correlated to altered translocation of ChREBP, the effect of PUFAs [Linoleic acid (C18:2), DHA (Docosahexaenoic, acid (C22:6)) and EPA (Eicosapentanoic acid (C20:5))] on the subcellular localization of ChREBP was investigated. The GFP-human ChREBP vector was transfected in cultured U2OS cells which were than in the presence of 25 mM glucose plus 100 nM insulin and treated or not with different concentrations (10, 30, 100, 300, and 1000 µM) of PUFAs for 2 hours. I excluded the last concentration (1000 µM) because it cause poisoning for the cells (data not shown). With taking into account that every concentration had its separate control (same amount of NaoH, BSA, and FA/BSA ratio) to avoids the conflict of other factors with the effect of PUFAs. see Figure 72)

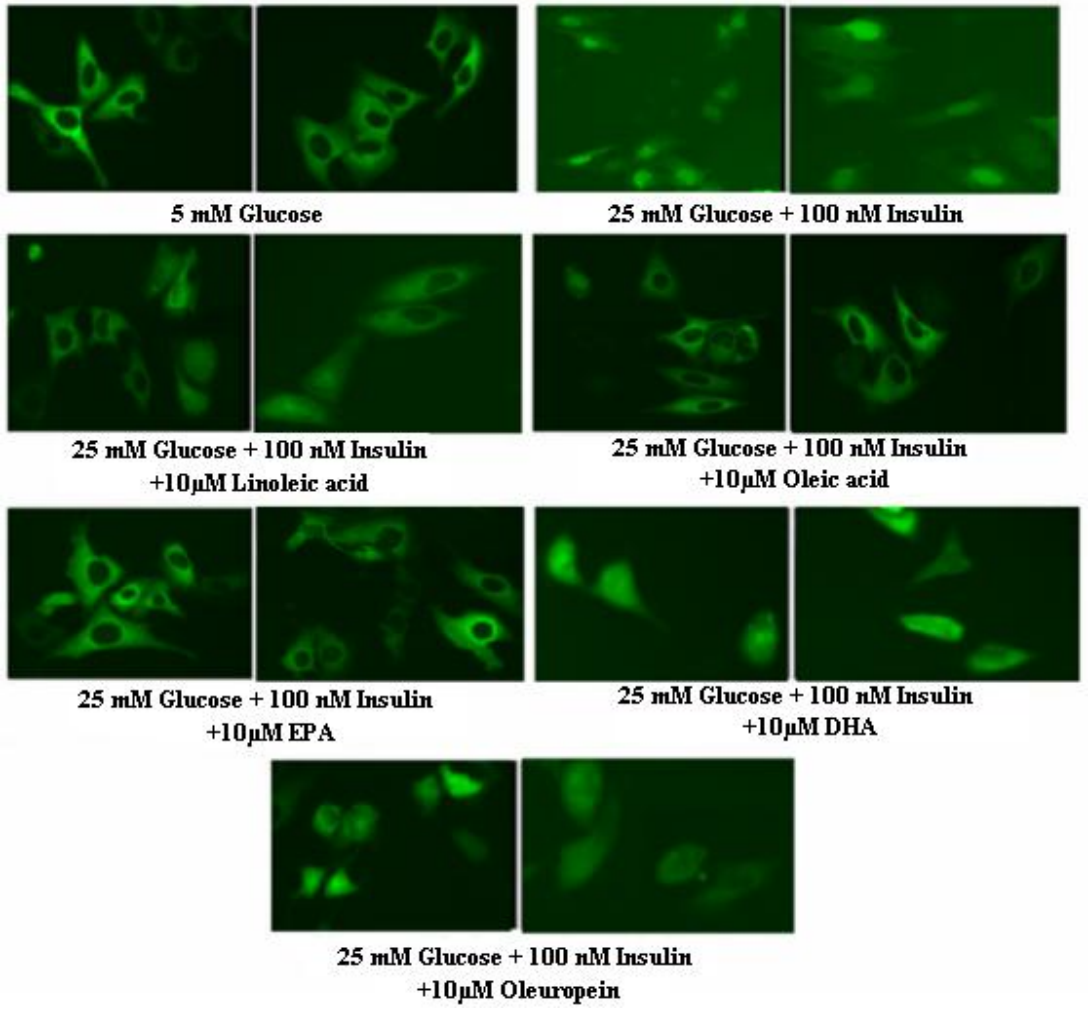

Figure 72. Representative images of subcellular localization of GFP-fused ChREBP.

Representative images of subcellular localization of GFP-fused ChREBP under 5 mM glucose without insulin; and 25 mM glucose plus 100 nM

insulin with or without 10 µM of albumin-bound of DHA [C22:6 (n-3)], linoleic acid [C18:2 (n-6)], EPA [C20:5]

4-3-9. U2OS stable transfection with h. ChREBP

Stable transfection is the type of transfection where genetic material that is introduced into a cell is retained beyond reproduction. Transfection is the process in which foreign DNA is introduced into eukaryotic cells through chemically-created "gates" in the cell membrane. Only stable transfections allow the new DNA to be reproduced when the cell divides to create daughter cells. Stable transfections that are experimentally useful are induced by co-transfecting another gene that can give the cell a selection advantage, typically resistance to a particular antibiotic. After mitosis, the cells produced are exposed to the antibiotic. The cells with tranfected with the corresponding antibiotic resistance gene will survive, while most of the normal cells will die. After many rounds of mitosis and antibiotic, only cells with the expressed resistance gene will survive. Stable transfections are at the core of gene therapy. Only through a stable transfection can a faulty gene be permanently replaced**.** The generation of stably-transfected cell lines is essential for a wide range of applications, such as gene function studies (Grimm 2004), drug discovery assays or the production of recombinant proteins. In contrast to transient expression, stable expression allows long term, as well as defined and reproducible, expression of the gene of interest. (Wurm 2004). I succeeded to generate stable transfection cell line by transfection of U2OS cells with the p human ChREBP-GFP vector that also encodes for neomycin phosphotransferase gene. Transfected cells that express neomycin phosphotransferase were selected by medium supplemented with G418 antibiotic. Cultures were propagated in which about 80% of the stable transfected cells showed GFP expression. Because GFP is 3`to ChREBP in the use p human ChREBP-GFP the expression of GFP predicts the espression of human ChREBP (Figure 73).

This stable cell line should have the virtues of better reproducible resuts. The use of these cells will enable to save the time and costs because no additional transfections are necessary.

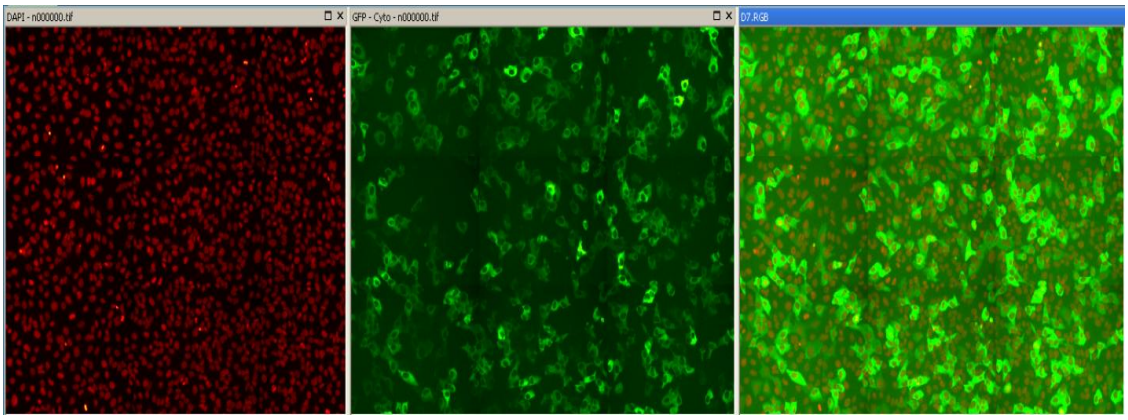

Figure 73. U2OS stable transfection cell line with p human ChREBP-GFP.

DAPI staining corresponded to the nucleus and was shown in red. GFP was shown green and showed the localization of the GFP marked transcription factor. If DAPI-and GFP pictures were merged, one could recognize by the yellow compound color if the GFP signal existed in the nucleus.

5- CONCLUSION

In the context of the regulation of lipid metabolism in liver, the role of the transcription factor carbohydrate responsive element binding protein (ChREBP) was investigated. ChREBP is important for the regulation of glycolysis, lipogenesis and inhibition of mitochondrial beta-oxidation. ChREBP has a pivotal role in the control of these pathways. This signal transduction is of utmost importance for concepts of nutrition. If hepatic lipogenesis is inhabitable by n3 and n6 fatty acids, their intake should influence the development of fatty liver.

First I tried to clone human ChREBP in a Green Fluorescent Protein (GFP) encoding vector but I did not succeed Figures (42, 43). So, I tried to test the influence of the different dietary elements on the translocation of mouse GFP-ChREBP which kindly provided by Ms. Catherine Postic, Insitut Cochin, Département d' Endocrinologie, Métabolisme et Cancer, Université Paris Descartes, Paris, France. I noticed that there were no significant effects of glucose and insulin on translocation of mouse ChREBP in U2OS, HUH7 and HepG2 cells. The results of the sequencing showed that, the first four amino acids of the mouse ChREBP were not encoded in the GFP-mouse ChREBP vector. These four missing amino acids could be the responsible for a different conformation of the protein which would affect its regulation Figure (48).

Finally, I succeeded to construct an expression vector coding for GFP tagged human ChREBP using a human ChREBP cDNA vector created by OriGene Technologies and an expression vector encoding GFP Figures (57, 58). With this construct I tested the influence of different dietary elements on this regulation that is scarcely investigated. The action of ChREBP and its translocation from cytoplasm to the nucleus was monitored by fluorescence microscope. The influence of different fatty acids (MUFA and PUFA n3/n6) on the translocation of the human ChREBP was tested. In addition the impact of polyphenols from olive oil and different kind of sweeteners on this translocation was examined.

My in vitro results demonstrate that in the presence of 25 mM glucose and 100 nM insulin, the human ChREBP translocated from the cytoplasm to the nucleus in U2OS cells (P=0.005). At low glucose concentration (5 mM) with or without insulin no significant amount of ChREBP in the nucleus was notable Figure (61). There was

no significant difference observed between low fructose (5mM) with or without 100 nM insulin and high fructose (25mM) without insulin. On the other hand, there was highly significant difference (p= 0.00026) observed between control and high fructose in presence of insulin Figure (62). 0.1 and 1 mM of cyclamate, saccharine and aspartame with or without insulin were tested. There was no significant difference observed between all samples in absence of insulin except with 1 mM saccharine (p= 0.006) and there was no effect of concentration 0.1 mM for all substances and 1 mM of aspartame in the presence of insulin. On the other hand, there was significant difference (p= 0.007) and (p= 0.002) observed between control and 1 mM cyclamate and saccharine respectively, in the presence of insulin (Figures 63, 64 and 65). Figure (66) showed that there was no significant effect of 10 µM and 100 µM of stevioside in absence or presence of insulin.

From the present study, it can be concluded that there was no significant effect of docosahexaenoic acid and oleuropein on nuclear translocation of the GFP-human ChREBP at all concentrations tested (10, 30, 100, and 300 µM) Figures (67, 71). In contrast, linoleic, eicosapentanoic and oleic acids markedly inhibited nuclear translocation of the p human ChREBP- GFP at all concentrations but significantly (p= 0.0183 and 0.0208) at 10 µM for eicosapentanoic and oleic acids respectively, Figures 68, 69, and 70).

From the previous results, the replacement of sugar by artificial sweeteners (aspartame and stevioside) in the diet may be of importance in liver disease. Dietary fish oil might be useful for preventing fatty liver disease because it contains n-3 fatty acids, such as eicosapentaenoic acid. A Mediterranean diet has been proposed for the prevention of metabolic syndrome. The major part of its beneficial effect is a high supply of energy coming from monounsaturated fatty acids (oleic acid), mainly from olive oil which prevent the translocation of human ChREBP into the nucleus which may prevent or improve fatty liver disease.

6- REFERENCES

Abdelmalek MF & Diehl AM 2007 Nonalcoholic fatty liver disease as a complication of insulin resistance. Med Clin North Am. 91 1125-49.

Abid A, Taha O, Nseir W, Farah R GM & Assy N 2009 Soft drink consumption is associated with fatty liver disease independent of metabolic syndrome. J Hepatol. 51 918-24.

Abu-Elheiga L, Oh W, Kordari P & Wakil SJ 2003 Acetyl-CoA carboxylase 2 mutant mice are protected against obesity and diabetes induced by high-fat/high-carbohydrate diets. Proc Natl Acad Sci U S A. 100 10207-12.

Adams LA & Lindor KD 2007 Nonalcoholic fatty liver disease. Ann Epidemiol. 17 863-9.

Adamson AW, Suchankova G, Rufo C, Nakamura MT & Teran-Garcia M 2006 Hepatocyte nuclear factor-4alpha contributes to carbohydrate-induced transcriptional activation of hepatic fatty acid synthase. Biochem J. 399 285-95.

Agius L, Peak M & Van Schaftingen E 1995 The regulatory protein of glucokinase binds to the hepatocyte matrix, but, unlike glucokinase, does not translocate during substrate stimulation. Biochem J. 309 711-3.

Ahmed FE & Thomas DB 1992 Assessment of the Carcinogenicity of the Nonnutritive Sweetener Cyclamate. Critical Reviews in Toxicology 22 81-118.

Ahmed MH & Byrne CD 2007 Modulation of sterol regulatory element binding proteins (SREBPs) as potential treatments for non-alcoholic fatty liver disease (NAFLD). Drug Discov Today. 12 740-7.

Angulo P 2002 Nonalcoholic fatty liver disease. N Engl J Med. 346 1221-31.

Assy N, Nasser G, Kamayse I, Nseir W, Beniashvili Z, Djibre A & Grosovski M 2008 Soft drink consumption linked with fatty liver in the absence of traditional risk factors. Can J Gastroenterol. 22 811-6.

Audreith LF & Sveda M 1944 Preparation and Properties of Some N-Substituted Sulfamic Acids. J.Org.Chem. 9 89-101.

Barclay WR, Meager KM & Abril JR 1994 Heterotrophic production of long-chain omega-3-fatty-acids utilizing algae and algae-like microorganisms. Journal of Applied Phycology 6 123-129.

Barlattani M 1970 Rassegne sintetiche di terapia. II problema dei ciclamati. CI Terap 52 565.

Billin AN, Eilers AL, Coulter KL, Logan JS & Ayer DE 2000 MondoA, a novel basic helix-loop-helix-leucine zipper transcriptional activator that constitutes a positive branch of a max-like network. Mol Cell Biol. 20 8845-54.

Bollen M, Keppens S & Stalmans W 1998 Specific features of glycogen metabolism in the liver. Biochem J. 336 19-31.

Botolin D, Wang Y, Christian B & Jump DB 2006 Docosahexaneoic acid (22:6,n-3) regulates rat hepatocyte SREBP-1 nuclear abundance by Erk- and 26S proteasome-dependent pathways. J Lipid Res. 47 181-92.

Brahmachari G, Mandal LC, Roy R, Mondal S & Brahmachari AK 2010 Stevioside and Related Compounds – Molecules of Pharmaceutical Promise A Critical Overview. Arch Pharm (Weinheim). 344 5-19.

Brown MS & Goldstein JL 1997 The SREBP pathway: regulation of cholesterol metabolism by proteolysis of a membrane-bound transcription factor. Cell. 89 331-40.

Brown RJ, Walter M & Rother KI 2009 Ingestion of diet soda before a glucose load augments glucagon-like peptide-1 secretion. Diabetes Care. 32 2184-6.

Browning JD & Horton JD 2004 Molecular mediators of hepatic steatosis and liver injury. J Clin Invest. 114 147-152.

Burke SJ, Collier JJ & Scott DK 2009 cAMP opposes the glucose-mediated induction of the L-PK gene by preventing the recruitment of a complex containing ChREBP, HNF4{alpha}, and CBP. FASEB J 23 2855-65.

Burnett L 2007 SWEETNESS LITE?: ARTIFICIAL SWEETENER CONTROVERSIES FROM SACCHARIN TO SUCRALOSE. In Satisfaction of the Winter 2007 Food and Drug Law Course Requirement, pp 1-25. Ed L Burnett. Harvard Law School.

Burr GO, Burr MM & Miller E 1930 On the nature and role of the fatty acids essential in nutrition. Journal of Biological Chemistry 86 587.

Cairo S, Merla G, Urbinati F, Ballabio A & Reymond A 2001 WBSCR14, a gene mapping to the Williams--Beuren syndrome deleted region, is a new member of the Mlx transcription factor network. Hum.Mol Genet 10 617-627.

Carmen GY & Victor SM 2006 Signalling mechanisms regulating lipolysis. Cell Signal. 18 401-8.

Ceriello A 2000 Oxidative stress and glycemic regulation. Metabolism. 49 27-9.

Cha JY & Repa JJ 2007 The liver X receptor (LXR) and hepatic lipogenesis. The carbohydrate-response element-binding protein is a target gene of LXR. J Biol.Chem. 282 743-751.

Charlton M. 2004 Nonalcoholic fatty liver disease: a review of current understanding and future impact. Clin Gastroenterol Hepatol. 2 1048-1058.

Chatsudthipong V & Muanprasat C 2009 Stevioside and related compounds: therapeutic benefits beyond sweetness. Pharmacol.Ther. 121 41-54.

Chaudhry J, Ghosh NN, Roy K & Chandra R 2007 Antihyperglycemic effect of a new thiazolidinedione analogue and its role in ameliorating oxidative stress in alloxan-induced diabetic rats. Life Sciences 80 1135-42.

Chen G, Liang G, Ou J, Goldstein JL & Brown MS 2004 Central role for liver X receptor in insulin-mediated activation of Srebp-1c transcription and stimulation of fatty acid synthesis in liver. Proc.Natl.Acad.Sci U S.A 101 11245-11250.

Cho E, Spiegelman D, Hunter DJ, Chen WY, Stampfer MJ, Colditz GA & Willett WC 2003 Premenopausal fat intake and risk of breast cancer. J Natl Cancer Inst. 95 1079-85.

Choi YH, Kim I, Yoon KD, Lee SJ, Kim CY, Yoo KP & et al. 2002 Supercritical fluid extraction and liquid chromatographic-electrospray mass spectrometric analysis of stevioside from Stevia rebaudiana leaves. Chromatographia 55 617-20.

Chu K, Miyazaki M, Man WC & Ntambi JM 2006 Stearoyl-coenzyme A desaturase 1 deficiency protects against hypertriglyceridemia and increases plasma high-density lipoprotein cholesterol induced by liver X receptor activation. Mol Cell Biol. 26 6786-98.

Clark JM & Diehl AM 2003 Nonalcoholic fatty liver disease: an underrecognized cause of cryptogenic cirrhosis. JAMA 289 3000-4.

Clarke SD 2004 The multi-dimensional regulation of gene expression by fatty acids: polyunsaturated fats as nutrient sensors. Curr Opin Lipidol. 15 13-8.

Coleman RA, Lewin TM, Van Horn CG & Gonzalez-Bar ́MR 2002 Do long-chain acyl-CoA synthetases regulate fatty acid entry into synthetic versus degradative pathways? J Nutr. 132 2123-6.

Colosia AD, Marker AJ, Lange AJ, el-Maghrabi MR, Granner DK, Tauler A, Pilkis J & Pilkis SJ 1988 Induction of rat liver 6-phosphofructo-2-kinase/fructose-2,6-bisphosphatase mRNA by refeeding and insulin. J Biol Chem. 263 18669-77.

Cournarie F, Azzout-Marniche D, Foretz M, Guichard C, Ferre P & Foufelle F 1999 The inhibitory effect of glucose on phosphoenolpyruvate carboxykinase gene expression in cultured hepatocytes is transcriptional and requires glucose metabolism. FEBS Letters 460 527-32.

da Silva Xavier G, Rutter GA, Diraison F, Andreolas C & Leclerc I 2006 ChREBP binding to fatty acid synthase and L-type pyruvate kinase genes is stimulated by glucose in pancreatic beta-cells. J Lipid Res. 47 2482-91.

Davail S, Rideau N, Bernadet MD, André JM, Guy G & Hoo-Paris R 2005 Effects of dietary fructose on liver steatosis in overfed mule ducks. Horm Metab Res. 37 32-5.

de la Pen~a C 2010 Artificial sweetener as a historical window to culturally situated health. Ann N Y Acad Sci. 1190 159-65.

de Luis O, Valero MC & Jurado LA 2000 WBSCR14, a putative transcription factor gene deleted in Williams-Beuren syndrome: complete characterisation of the human gene and the mouse ortholog. Eur.J Hum.Genet 8 215-222.

DE MATOS MA, MARTINS AT & AZOUBEL R 2006 Effects of Sodium Cyclamate on the Rat Placenta: A Morphometric Study. J.Morphol. 24 137-142.

Decaux JF, Antoine B & Kahn A 1989 Regulation of the expression of the L-type pyruvate kinase gene in adult rat hepatocytes in primary culture. J Biol Chem. 264 11584-90.

Denechaud PD, Bossard P, Lobaccaro JM, Millatt L, Staels B, Girard J & Postic C 2008a ChREBP, but not LXRs, is required for the induction of glucose-regulated genes in mouse liver. Journal of Clinical Investigation 118 956-964.

Denechaud PD, Dentin R, Girard J & Postic C 2008b Role of ChREBP in hepatic steatosis and insulin resistance. FEBS Letters 582 68-73.

Dentin R, Benhamed F, Hainault I, Fauveau V, Foufelle F, Dyck JR, Girard J & Postic C 2006a Liver-specific inhibition of ChREBP improves hepatic steatosis and insulin resistance in ob/ob mice. Diabetes 55 2159-2170.

Dentin R, Benhamed F, Pegorier JP, Foufelle F, Viollet B, Vaulont S, Girard J & Postic C 2005a Polyunsaturated fatty acids suppress glycolytic and lipogenic genes through the inhibition of ChREBP nuclear protein translocation. Journal of Clinical Investigation 115 2843-2854.

Dentin R, Denechaud PD, Benhamed F, Girard J & Postic C 2006b Hepatic gene regulation by glucose and polyunsaturated fatty acids: a role for ChREBP. J Nutr. 136 1145-1149.

Dentin R, Girard J & Postic C 2005b Carbohydrate responsive element binding protein (ChREBP) and sterol regulatory element binding protein-1c (SREBP-1c): two key regulators of glucose metabolism and lipid synthesis in liver. Biochimie 87 81-86.

Dentin R, Pegorier JP, Benhamed F, Foufelle F, Ferre P, Fauveau V, Magnuson MA, Girard J & Postic C 2004 Hepatic glucokinase is required for the synergistic action of ChREBP and SREBP-1c on glycolytic and lipogenic gene expression. J Biol.Chem. 279 20314-20326.

Dhe-Paganon S, Duda K, Iwamoto M, Chi YI & Shoelson SE 2002 Crystal structure of the HNF4 alpha ligand binding domain in complex with endogenous fatty acid ligand. J Biol Chem. 277 37973-6.

Dhingra R, Sullivan L, Jacques PF, Wang TJ, Fox CS, Meigs JB, D'Agostino RB, Gaziano JM & Vasan RS 2007 Soft drink consumption and risk of developing cardiometabolic risk factors and the metabolic syndrome in middle-aged adults in the community. Circulation. 116 480-8.

Diaz Guerra MJ, Bergot MO, Martinez A, Cuif MH, Kahn A & Raymondjean M 1993 Functional characterization of the L-type pyruvate kinase gene glucose response complex. Mol Cell Biol. 13 7725-33.

DiRusso CC, Li H, Darwis D, Watkins PA, Berger J & Black PN 2005 Comparative biochemical studies of the murine fatty acid transport proteins (FATP) expressed in yeast. J Biol Chem. 280 16829-37.

Doiron B, Cuif MH, Chen R & Kahn A 1996 Transcriptional glucose signaling through the glucose response element is mediated by the pentose phosphate pathway. J Biol Chem. 271 5321-4.

Donnelly KL, Smith CI, Schwarzenberg SJ, Jessurun J, Boldt MD & Parks EJ 2005 Sources of fatty acids stored in liver and secreted via lipoproteins in patients with nonalcoholic fatty liver disease. J Clin Invest. 115 1343-51.

Duplus E, Glorian M & Forest C 2000 Fatty acid regulation of gene transcription. J Biol Chem. 275 30749-52.

Edgecombe SC, Stretch GL & Hayball PJ 2000b Oleuropein, an antioxidant polyphenol from olive oil, is poorly absorbed from isolated perfused rat intestine. J Nutr. 130 2996-3002.

Edgecombe SC, Stretch GL & Hayball PJ 2000a Oleuropein, an antioxidant polyphenol from olive oil, is poorly absorbed from isolated perfused rat intestine. J Nutr. 130 2996-3002.

EHHP 2000 Artificial sweeteners – What's out there? Nutrition Notes Newsletter 1 3.

El SN & Karakaya S 2009 Olive tree (Olea europaea) leaves: potential beneficial effects on human health. Nutr Rev. 67 632-8.

Elkins R 1997 Stavia: Nature's sweetener. Orem: Woodland Publishing.

Elshourbagy NA, Near JC, Kmetz PJ, Sathe GM, Southan C & et al. 1990 Rat ATP Citrate-Lyase molecular cloning and sequence analysis of A full-length cDNA and mRNA abundance as a function of diet, organ, and age. The Journal Of Biological Chemistry 265 1430-1435.

Fahlberg C & Remsen I 1879 Ueber die Oxydation des Orthotoluolsulfamids. Berichte der deutschen chemischen Gesellschaft 12 469-473.

Ferland A, Brassard P & Poirier P 2007 Is aspartame really safer in reducing the risk of hypoglycemia during exercise in patients with type 2 diabetes? Diabetes Care. 30 e59.

Ferrannini E & Balkau B 2002 Insulin: in search of a syndrome. Diabet Med. 19 724-9.

Flowers MT, Miyazaki M, Liu X & Ntambi JM 2006 Probing the role of stearoyl-CoA desaturase-1 in hepatic insulin resistance. J Clin Invest. 116 1478-81.

Foretz M, Guichard C, Ferre P & Foufelle F 1999a Sterol regulatory element binding protein-1c is a major mediator of insulin action on the hepatic expression of

glucokinase and lipogenesis-related genes. Proc.Natl.Acad.Sci.U.S.A 96 12737-12742.

Foretz M, Pacot C, Dugail I, Lemarchand P, Guichard C, Le Liepvre X & et al. 1999b ADD1/SREBP-1c Is Required in the Activation of Hepatic Lipogenic Gene Expression by Glucose. Molecular and Cellular Biology 19 3760-8.

Foufelle F & Ferr´e P 2002 New perspectives in the regulation of hepatic glycolytic and lipogenic genes by insulin and glucose : a role for the transcription factor sterol regulatory element binding protein-1c. Biochem.J. 366 377-391.

Foufelle F, Girard J & Ferre P 1996 Regulation of lipogenic enzyme expression by glucose in liver and adipose tissue: a review of the potential cellular and molecular mechanisms. Adv Enzyme Regul. 36 199-226.

Geuns JM 2003 Stevioside. Phytochemistry 64 913-21.

Gregori C, Guillet-Deniau I, Girard J, Decaux JF & Pichard AL 2006 Insulin regulation of glucokinase gene expression: evidence against a role for sterol regulatory element binding protein 1 in primary hepatocytes. FEBS Letters 580 410-4.

Grimm S 2004 The art and design of genetic screens: mammalian culture cells. Nature Reviews Genetics 5 179-189.

Gumieniczek A 2005 Effects of pioglitazone on hyperglycemia-induced alterations in antioxidative system in tissues of alloxan-treated diabetic animals. Exp Toxicol Pathol. 56 321-6.

Hansmannel F, Mordier S & Iynedjian PB 2006 Insulin induction of glucokinase and fatty acid synthase in hepatocytes: analysis of the roles of sterol-regulatory-element-binding protein-1c and liver X receptor. Biochem J. 399 275-83.

Hardie DG 1992 Regulation of fatty acid and cholesterol metabolism by the AMP-activated protein kinase. Biochim Biophys Acta. 1123 231-8.

Hardie DG 2007 AMP-activated/SNF1 protein kinases: conserved guardians of cellular energy. Nature Reviews Molecular Cell Biology 8 774-785.

Hardie DG & Carling D 1997 The AMP-activated protein kinase--fuel gauge of the mammalian cell? Eur J Biochem. 246 259-73.

Hardie DG, Carling D & Carlson M 1998 The AMP-activated/SNF1 protein kinase subfamily: metabolic sensors of the eukaryotic cell? Annu Rev Biochem. 67 821-55.

Harris WS 2003 n-3 Long-chain polyunsaturated fatty acids reduce risk of coronary heart disease death: extending the evidence to the elderly. Am J Clin Nutr. 77 279-80.

Havel PJ 2005 Dietary fructose: implications for dysregulation of energy homeostasis and lipid/carbohydrate metabolism. Nutr Rev. 63 133-57.

He Z, Jiang T, Wang Z, Levi M & Li J 2004 Modulation of carbohydrate response element-binding protein gene expression in 3T3-L1 adipocytes and rat adipose tissue. AJP - Endocrinology and Metabolism 287 E424-E430.

Hertzel AV & Bernlohr DA 2000 The mammalian fatty acid-binding protein multigene family: molecular and genetic insights into function. Trends Endocrinol Metab. 11 175-80.

Horton JD, Bashmakov Y, Shimomura I & Shimano H 1998 Regulation of sterol regulatory element binding proteins in livers of fasted and refed mice. Proc Natl Acad Sci U S A. 95 5987-92.

Hue L 2001 Regulation of Gluconeogenesis in Liver. In The Endocrine System, edn 2, pp 649-657.

Hunt MC & Alexson SE 2002 The role Acyl-CoA thioesterases play in mediating intracellular lipid metabolism. Prog Lipid Res. 41 99-130.

Hutapae AM, Toskulakao C, Buddhasukh D, Wilairat P & Glinsukon T 1997 Digestion of Stevioside, a Natural Sweetener, by Various Digestive Enzymes. Journal of Clinical Biochemistry and Nutrition 23 177-186.

Hwang IS, Ho H, Hoffman BB & Reaven GM 1987 Fructose-induced insulin resistance and hypertension in rats. Hypertension. 10 512-6.

Iizuka K, Bruick RK, Liang G, Horton JD & Uyeda K 2004 Deficiency of carbohydrate response element-binding protein (ChREBP) reduces lipogenesis as well as glycolysis. Proceedings of the National Academy of Sciences 101 7281-7286.

Iizuka K & Horikawa Y 2008 ChREBP: a glucose-activated transcription factor involved in the development of metabolic syndrome. Endocr J 55 617-624.

Iizuka K, Miller B & Uyeda K 2006 Deficiency of carbohydrate-activated transcription factor ChREBP prevents obesity and improves plasma glucose control in leptin-deficient (ob/ob) mice. Am J Physiol Endocrinol Metab. 291 E358-64.

Innis SM 2007 Fatty acids and early human development. Early Hum Dev. 83 761-6.

Ishii S, Iizuka K, Miller BC & Uyeda K 2004 Carbohydrate response element binding protein directly promotes lipogenic enzyme gene transcription. Proceedings of the National Academy of Sciences 101 15597-15602.

Iynedjian PB, Jotterand D, Nouspikel T, Asfari M & Pilot PR 1989 Transcriptional induction of glucokinase gene by insulin in cultured liver cells and its repression by the glucagon-cAMP system. J Biol Chem. 264 21824-9.

Iynedjian PB, Ucla C & Mach B 1987 Molecular Cloning of Glucokinase cDNA DEVELOPMENTAL AND DIETARY REGULATION OF GLUCOKINASE mRNA IN RAT LIVER. THE JOURNAL OF BIOLOGICAL CHEMISTRY 262 6032-38.

Japٕn-Lujلn R, Luque-Rodrيguez JM & Luque de Castro MD 2006 Dynamic ultrasound-assisted extraction of oleuropein and related biophenols from olive leaves. J Chromatogr A. 1108 76-82.

JEMAI H, EL FEKI A & SAYADI S 2009 Antidiabetic and Antioxidant Effects of Hydroxytyrosol and Oleuropein from Olive Leaves in Alloxan-Diabetic Rats. J Agric Food Chem. 57 8798-804.

Joseph SB, Laffitte BA, Patel PH, Watson MA & Matsukuma KE 2002 Direct and indirect mechanisms for regulation of fatty acid synthase gene expression by liver X receptors. J Biol Chem. 277 11019-25.

Julien C, Berthiaume L, Hadj-Tahar A, Rujput AH, Bedard PJ, Di Paolo T, Julien P & Calon F 2006 Postmortem brain fatty acid profile of levodopa-treated Parkinson disease patients and parkinsonian monkeys. Neurochem Int. 48 404-414.

Jump DB 2004 Fatty acid regulation of gene transcription. Crit Rev Clin Lab Sci. 41 41-78.

Jump DB, Botolin D, Wang Y, Xu J, Christian B & Demeure O 2005 Fatty acid regulation of hepatic gene transcription. J Nutr. 135 2503-6.

Jump DB, Botolin D, Wang Y, Xu J, Demeure O & Christian B 2008 Docosahexaenoic acid (DHA) and hepatic gene transcription. Chem Phys Lipids. 153 3-13.

Jump DB & Clarke SD 1999 Regulation of gene expression by dietary fat. Annu Rev Nutr. 19 63-90.

Just T, Pau HW, Engel U & Hummel T 2008 Cephalic phase insulin release in healthy humans after taste stimulation? Appetite. 51 622-7.

Kabashima T, Kawaguchi T, Wadzinski BE & Uyeda K 2003 Xylulose 5-phosphate mediates glucose-induced lipogenesis by xylulose 5-phosphate-activated protein phosphatase in rat liver. Proc.Natl.Acad.Sci.U.S.A 100 5107-5112.

Kahn BB, Alquier T, Carling D & Hardie DG 2005a AMP-activated protein kinase: ancient energy gauge provides clues to modern understanding of metabolism. Cell Metab. 1 15-25.

Kahn R, Buse J, Ferrannini E & Stern M 2005b The metabolic syndrome: time for a critical appraisal: joint statement from the American Diabetes Association and the European Association for the Study of Diabetes. Diabetes Care. 28 2289-304.

Kamtchouing P, Kahpui SM, Djomeni Dzeufiet PD, T'edong L, Asongalem EA & Dimoa T 2004 Anti-diabetic activity of methanol/methylene chloride stem bark extracts of Terminalia superba and Canarium schweinfurthii on streptozotocin-induced diabetic rats. J Ethnopharmacol. 104 306-9.

Karaoz E, Gultekin F, Akdogan M, Oncu M & Gokcimen A 2002 Protective role of melatonin and a combination of vitamin C and vitamin E on lung toxicity induced by chlorpyrifos-ethyl in rats. Exp Toxicol Pathol. 54 97-108.

Katsurada A, Iritani N, Fukuda H, Matsumura Y, Nishimoto N & et al. 1990 Effects of nutrients and hormones on transcriptional and post-transcriptional regulation of acetyl-CoA carboxylase in rat liver. Eur.J.Biochem. 190 435-441.

Katsurada A, Iritani N, Fukuda H, Matsumura Y, Noguchi T & Tanaka T 1989 Effects of nutrients and insulin on transcriptional and post-transcriptional regulation of glucose-6-phosphate dehydrogenase synthesis in rat liver. Biochim Biophys Acta 1006 104-110.

Kawaguchi T, Osatomi K, Yamashita H, Kabashima T & Uyeda K 2002 Mechanism for fatty acid "sparing" effect on glucose-induced transcription: regulation of carbohydrate-responsive element-binding protein by AMP-activated protein kinase. J Biol.Chem. 277 3829-3835.

Kawaguchi T, Takenoshita M, Kabashima T & Uyeda K 2001 Glucose and cAMP regulate the L-type pyruvate kinase gene by phosphorylation/dephosphorylation of the carbohydrate response element binding protein. Proc.Natl.Acad.Sci.U.S.A 98 13710-13715.

Kelley DE, Goodpaster BH & Storlien L 2002 Muscle triglyceride and insulin resistance. Annu Rev Nutr 22 325-46.

Kelley GL, Allan G & Azhar S 2004 High dietary fructose induces a hepatic stress response resulting in cholesterol and lipid dysregulation. Endocrinology. 145 548-55.

Kersten S 2001 Mechanisms of nutritional and hormonal regulation of lipogenesis. EMBO Rep. 2 282-6.

Kim JB, Spotts GD, Halvorsen YD, Shih HM, Ellenberger T, Towle HC & Spiegelman BM 1995 Dual DNA binding specificity of ADD1/SREBP1 controlled by a single amino acid in the basic helix-loop-helix domain. Mol Cell Biol. 15 2582-8.

Kim SY, Kim HI, Kim TH, Im SS, Park SK, Lee IK, Kim KS & Ahn YH 2004 SREBP-1c mediates the insulin-dependent hepatic glucokinase expression. J Biol Chem. 279 30823-9.

Kinghorn AD & Soejarto DD 1985 Current status of stevioside as a sweetening agent for human use. In Economic and medical plant research, pp 1-52. Eds H Wagner, H Hikino & NR Farnsworth. London: Academic Press.

Kokatnur MG, Oalmann MC, Johnson WD, Malcom GT & Strong JP 1979 Fatty acid composition of human adipose tissue from two anatomical sites in a biracial community. Am J Clin Nutr. 32 2198-205.

Koo HY, Miyashita M, Cho BH & Nakamura MT 2009 Replacing dietary glucose with fructose increases ChREBP activity and SREBP-1 protein in rat liver nucleus. Biochem.Biophys.Res Commun.

Koo HY, Wallig MA, Chung BH, Nara TY, Cho BH & Nakamura MT 2008 Dietary fructose induces a wide range of genes with distinct shift in carbohydrate and lipid metabolism in fed and fasted rat liver. Biochimica et Biophysica Acta 1782 341-348.

Koo SH, Dutcher AK & Towle HC 2001 Glucose and insulin function through two distinct transcription factors to stimulate expression of lipogenic enzyme genes in liver. J Biol Chem. 276 9437-45.

Kopelman PG 2000 Obesity as a medical problem. Nature. 404 635-43.

Laffitte BA, Chao LC, Li J, Walczak R, Hummasti S & Joseph SB 2003 Activation of liver X receptor improves glucose tolerance through coordinate regulation of

glucose metabolism in liver and adipose tissue. Proc Natl Acad Sci U S A. 100 5419-24.

Lazar MA & Willson TM 2007 Sweet dreams for LXR. Cell Metab. 5 159-61.

Lee Y, Wang MY, Kakuma T, Wang ZW, Babcock E, McCorkle K, Higa M, Zhou YT & Unger RH 2001 Liporegulation in diet-induced obesity. The antisteatotic role of hyperleptinemia. J Biol Chem. 276 5629-5635.

Letexier D, Peroni O, Pinteur C & Beylot M 2005 In vivo expression of carbohydrate responsive element binding protein in lean and obese rats. Diabetes Metab 31 558-566.

Liang G, Yang J, Horton JD, Hammer RE, Goldstein JL & Brown MS 2002 Diminished hepatic response to fasting/refeeding and liver X receptor agonists in mice with selective deficiency of sterol regulatory element-binding protein-1c. J Biol Chem. 277 9520-8.

Liimatta M, Towle HC, Clarke S & Jump DB 1994 Dietary polyunsaturated fatty acids interfere with the insulin/glucose activation of L-type pyruvate kinase gene transcription. Mol Endocrinol. 8 1147-53.

Ma L, Robinson LN & Towle HC 2006 ChREBP*Mlx is the principal mediator of glucose-induced gene expression in the liver. J Biol.Chem. 281 28721-28730.

Ma L, Sham YY, Walters KJ & Towle HC 2007 A critical role for the loop region of the basic helix-loop-helix/leucine zipper protein Mlx in DNA binding and glucose-regulated transcription. Nucleic Acids Res. 35 35-44.

Ma L, Tsatsos NG & Towle HC 2005 Direct role of ChREBP.Mlx in regulating hepatic glucose-responsive genes. J Biol Chem. 280 12019-27.

Magaå MM & Osborne TF 1996 Two tandem binding sites for sterol regulatory element binding proteins are required for sterol regulation of fatty-acid synthase promoter. J Biol Chem. 271 32689-94.

Magnuson BA, Burdock GA, Doull J, Kroes RM, Marsh GM & et al. 2007 Aspartame: a safety evaluation based on current use levels, regulations, and toxicological and epidemiological studies. Crit Rev Toxicol. 37 629-727.

Mangelsdorf DJ, Thummel C, Beato M, Herrlich P, Schütz G & et al. 1995 The nuclear receptor superfamily: the second decade. Cell. 83 835-9.

Marchesini G, Brizi M, Bianchi G, Tomassetti S, Bugianesi E & et al. 2001 Nonalcoholic fatty liver disease: a feature of the metabolic syndrome. Diabetes. 50 1844-50.

Marchesini G, Brizi M, Morselli-Labate AM, Bianchi G, Bugianesi E, McCullough AJ, Forlani G & Melchionda N 1999 Association of nonalcoholic fatty liver disease with insulin resistance. Am J Med. 107 450-5.

Massillon D 2000 Regulation of the glucose-6-phosphatase gene by glucose occurs by transcriptional and post-transcriptional mechanisms. Differential effect of glucose and xylitol. J Biol Chem. 276 4055-62.

Mata de Urquiza A, Liu S, Sjoberg M, Zetterstrom RH, Criffith W, Sjovall J & Perlmann T 2000 Docosahexaenoic acid, a ligand for the retinoid X receptor in mouse brain. Science. 290 2140-4.

Matschinsky FM 1996 A lesson in metabolic regulation inspired by the glucokinase glucose sensor paradigm. Diabetes. 45 223-41.

Matsuzaki H, Daitoku H, Hatta M, Tanaka K & Fukamizu A 2003 Insulin-induced phosphorylation of FKHR (Foxo1) targets to proteasomal degradation. Proc.Natl.Acad.Sci.U.S.A 100 11285-11290.

McGuinness OP & Cherrington AD 2003 Effects of fructose on hepatic glucose metabolism. Curr Opin Clin Nutr Metab Care. 6 441-8.

Meroni G, Cairo S, Merla G, Messali S, Brent R, Ballabio A & Reymond A 2000 Mlx, a new Max-like bHLHZip family member: the center stage of a novel transcription factors regulatory pathway? Oncogene. 19 3266-77.

Mezey E 1998 Dietary fat and alcoholic liver disease. Hepatology. 28 901-5.

Miksicek RJ & Towle HC 1983 Use of a cloned cDNA sequence to measure changes in 6-phosphogluconate dehydrogenase mRNA levels caused by thyroid hormone and dietary carbohydrate. J Biol Chem. 258 9575-9.

Mirbagheri SA, Rashidi A, Abdi S, Saedi D & Abouzari M 2007 Liver: an alarm for the heart? Liver Int. 27 891-4.

Mitro N, Mak PA, Vargas L, Godio C, Hampton E, Molteni V, Kreusch A & Saez E 2007 The nuclear receptor LXR is a glucose sensor. Nature 445 219-223.

Moore F, Weekes J & Hardie DG 1991 Evidence that AMP triggers phosphorylation as well as direct allosteric activation of rat liver AMP-activated protein kinase. A

sensitive mechanism to protect the cell against ATP depletion. Eur J Biochem. 199 691-7.

Moore KM & Knauft DA 1989 The Inheritance of High Oleic Acid in Peanut. The Journal of Heredity 80 252-253.

Moriizumi S, Gourdon L, Lefrançois-Martinez AM, Kahn A & Raymondjean M 1998 Effect of different basic helix-loop-helix leucine zipper factors on the glucose response unit of the L-type pyruvate kinase gene. Gene Expr. 7 103-13.

Natali F, Siculella L, Salvati S & Gnoni GV 2007 Oleic acid is a potent inhibitor of fatty acid and cholesterol synthesis in C6 glioma cells. J Lipid Res. 48 1966-75.

New, M. B. and Wijkstroem, U. N. Use of fishmeal and fish oil in aquafeeds. Further thoughts on the fishmeal trap. 975, 61. 2002. FAO Fisheries Circular .

Ref Type: Report

Nielsen SJ & Popkin BM 2004 Changes in beverage intake between 1977 and 2001. Am J Prev Med. 27 205-10.

Nseir W, Nassar F & Assy N 2010 Soft drinks consumption and nonalcoholic fatty liver disease. World J Gastroenterol 16 2579-2588.

Ntambi JM 1992 Dietary Regulation of Stearoyl-CoA Desaturase 1 Gene Expression in Mouse Liver. THE JOURNAL OF BIOLOGICAL CHEMISTRY 267 10925-10930.

Nutter MK, Lockhart EE & Harris RS 1943 The chemical composition of depot fats in chickens and turkeys. Journal of the American Oil Chemists' Society 20 231-234.

O'Brien RM & Granner DK 1996 Regulation of gene expression by insulin. Physiol Rev. 76 1109-61.

O'Brien RM, Streeper RS, Ayala JE, Stadelmaier BT & Hornbuckle LA 2001 Insulin-regulated gene expression. Biochem Soc Trans. 29 552-8.

O'Callaghan BL, Koo SH, Wu Y, Freake HC & Towle HC 2001 Glucose regulation of the acetyl-CoA carboxylase promoter PI in rat hepatocytes. J Biol Chem. 276 16033-9.

Oi-Kano Y, Kawada T, Watanabe T, Koyama F, Watanabe K, Senbongi R & Iwai K 2008 Oleuropein, a phenolic compound in extra virgin olive oil, increases uncoupling protein 1 content in brown adipose tissue and enhances noradrenaline and adrenaline secretions in rats. J Nutr Sci Vitaminol 54 363-70.

Ou J, Tu H, Shan B, Luk A, DeBose-Boyd RA, Bashmakov Y, Goldstein JL & Brown MS 2001 Unsaturated fatty acids inhibit transcription of the sterol regulatory element-binding protein-1c (SREBP-1c) gene by antagonizing ligand-dependent activation of the LXR. Proc Natl Acad Sci U S A. 98 6027-32.

Pape ME, Lopez-Casillas F & Kim KH 1988 Physiological regulation of acetyl-CoA carboxylase gene expression: effects of diet, diabetes, and lactation on acetyl-CoA carboxylase mRNA. Arch Biochem Biophys. 267 104-9.

Patton GM, Fasulo JM & Robins SJ 1994 Hepatic phosphatidylcholines: evidence for synthesis in the rat by extensive reutilization of endogenous acylglycerides. J Lipid Res. 35 1211-21.

Pawar A, Xu J, Jerks E, Mangelsdorf DJ & Jump DB 2002 Fatty acid regulation of liver X receptors (LXR) and peroxisome proliferator-activated receptor alpha (PPARalpha) in HEK293 cells. J Biol Chem. 277 39243-50.

Pedersen KB, Zhang P, Doumen C, Charbonnet M, Lu D, Newgard CB, Haycock JW, Lange AJ & Scott DK 2007 The promoter for the gene encoding the catalytic subunit of rat glucose-6-phosphatase contains two distinct glucose-responsive regions. AJP - Endocrinology and Metabolism 292 E788-E801.

Petersen KF, Dufour S, Befroy D, Lehrke M, Hendler RE & Shulman GI 2005 Reversal of Nonalcoholic Hepatic Steatosis, Hepatic Insulin Resistance, and Hyperglycemia by Moderate Weight Reduction in Patients With Type 2 Diabetes. Diabetes. 54 603-608.

Petersen KF & Shulman GI 2002 Pathogenesis of skeletal muscle insulin resistance in type 2 diabetes mellitus. Am J Cardiol. 90 11G-18G.

Postic C, Dentin R, Denechaud PD & Girard J 2007 ChREBP, a Transcriptional Regulator of Glucose and Lipid Metabolism. Annu.Rev.Nutr. 27 179-192.

Postic C & Girard J 2008 Contribution of de novo fatty acid synthesis to hepatic steatosis and insulin resistance: lessons from genetically engineered mice. Journal of Clinical Investigation 118 829-838.

Postic C, Shiota M, Niswender KD, Jetton TL, Chen Y, Moates JM, Shelton KD, Lindner J, Cherrington AD & Magnuson MA 1999 Dual roles for glucokinase in glucose homeostasis as determined by liver and pancreatic beta cell-specific gene knock-outs using Cre recombinase. J Biol.Chem. 274 305-315.

Prodolliet J & Bruelhart M 1993 Determination of aspartame and its major decomposition products in foods. J AOAC Int. 76 275-82.

Proszkowiec-Weglarz M, Richards MP, Humphrey BD, Rosebrough RW & McMurtry JP 2009 AMP-activated protein kinase and carbohydrate response element binding protein: A study of two potential regulatory factors in the hepatic lipogenic program of broiler chickens. Comp Biochem.Physiol B Biochem.Mol Biol.

Puigserver P, Rhee J, Donovan J, Walkey CJ, Yoon JC, Oriente F, Kitamura Y, Altomonte J, Dong H, Accili D & Spiegelman BM 2002 Insulin-regulated hepatic gluconeogenesis through FOXO1-PGC-1alpha interaction. Nature. 423 550-5.

Pyle DJ, Garcia RA & Wen Z 2008 Producing Docosahexaenoic Acid (DHA)-Rich Algae from Biodiesel-Derived Crude Glycerol: Effects of Impurities on DHA Production and Algal Biomass Composition. J Agric Food Chem. 56 3933-9.

Rongnoparut P, Verdon CP, Gehnrich SC & Sul HS 1991 Isolation and characterization of the transcriptionally regulated mouse liver (B-type) phosphofructokinase gene and its promoter. J Biol Chem. 266 8086-91.

Rufo C, Teran-Garcia M, Nakamura MT, Koo SH, Towle HC & Clarke SD 2001 Involvement of a unique carbohydrate-responsive factor in the glucose regulation of rat liver fatty-acid synthase gene transcription. J Biol Chem. 276 21969-75.

Saggerson D 2008 Malonyl-CoA, a key signaling molecule in mammalian cells. Annu Rev Nutr. 28 253-72.

Sain OL & Berman JM 1984 Efectos adversos de edulcorantes en pediatria sacarina y ciclamato. / Side effects of artificial sweeteners in pediatrics. Sacharin and cyclamates. Arch.argent.pediatr 82 209-11.

Samuel VT, Liu ZX, Qu X, Elder BD, Bilz S, Befroy D, Romanelli AJ & Shulman GI. 2004 Mechanism of hepatic insulin resistance in non-alcoholic fatty liver disease. J Biol Chem 279 32345-32353.

Sanal MG 2008 The blind men 'see' the elephant-the many faces of fatty liver disease. World J Gastroenterol. 14 831-844.

Sasaki K, Cripe TP, Koch SR, Andreone TL, Petersen DD, Beale EG & Granner DK 1984 Multihormonal regulation of phosphoenolpyruvate carboxykinase gene transcription. The dominant role of insulin. Journal of Biological Chemistry 259 15242-15251.

Seppala-Lindroos A, Vehkavaara S, Hakkinen AM, Goto T, Westerbacka J, Sovijarvi A, Halavaara J & Yki-Jarvinen H 2002 Fat accumulation in the liver is associated with defects in insulin suppression of glucose production and serum free fatty acids independent of obesity in normal men. J Clin Endocrinol Metab. 87 3023-8.

Shih HM, Liu Z & Towle HC 1995 Two CACGTG motifs with proper spacing dictate the carbohydrate regulation of hepatic gene transcription. J Biol Chem. 270 21991-7.

Shimomura I, Bashmakov Y, Ikemeto S, Horton JD, Brown MS & Goldstein JL 1999 Insulin selectively increases SREBP-1c mRNA in the livers of rats with streptozotocin-induced diabetes. Proceedings of the National Academy of Sciences 96 13656-13661.

Shimomura I, Shimano H, Korn BS, Bashmakov Y & Horton JD 1998 Nuclear sterol regulatory element-binding proteins activate genes responsible for the entire program of unsaturated fatty acid biosynthesis in transgenic mouse liver. J Biol Chem. 273 25299-306.

Simopoulos AP 1999 Essential fatty acids in health and chronic disease. Am J Clin Nutr 70 560S-569S.

Simopoulos AP 2002 Omega-3 fatty acids in wild plants, nuts and seeds. Asia Pacific Journal of Clinical Nutrition 11 s163-s173.

Sirek AS, Liu L, Naples M, Adeli K, Ng DS & Jin T 2009 Insulin stimulates the expression of Carbohydrate Response Element Binding Protein (ChREBP) by attenuating the repressive effect of POU homeodomain protein Oct-1. Endocrinology.

Soni MG, Burdock GA, Christian MS, Bitler CM & Crea R 2006 Safety assessment of aqueous olive pulp extract as an antioxidant or antimicrobial agent in foods. Food Chem Toxicol. 44 903-15.

Stanhope KL, Schwarz JM, Keim NL, Griffen SC & et al. 2009 Consuming fructose-sweetened, not glucose-sweetened, beverages increases visceral adiposity and lipids and decreases insulin sensitivity in overweight/obese humans. J Clin Invest. 119 1322-34.

Stegink LD 1987 The aspartame story: a model for the clinical testing of a food additive. Am J Clin Nutr. 46 204-15.

Stein SC, Woods A, Jones NA, Davison MD & Carling D 2000 The regulation of AMP-activated protein kinase by phosphorylation. Biochem J. 345 437-43.

Stoeckman AK, Ma L & Towle HC 2004 Mlx is the functional heteromeric partner of the carbohydrate response element-binding protein in glucose regulation of lipogenic enzyme genes. J Biol.Chem. 279 15662-15669.

Stoeckman AK & Towle HC 2002 The role of SREBP-1c in nutritional regulation of lipogenic enzyme gene expression. J Biol Chem. 277 27029-35.

Sudjana AN, D'Orazio C, Ryan V, Rasool N, Ng J, Islam N, Riley TV & Hammer KA 2009 Antimicrobial activity of commercial Olea europaea (olive) leaf extract. Int J Antimicrob Agents. 33 461-3.

Suenaga A, Wada T & Ichibagase H 1983 Studies on synthetic sweetening agents. XVIII. Metabolism of sodium cyclamate. (7). Dicyclohexylamine, a metabolite of sodium cyclamate in rabbits and rats. Chem Pharm Bull (Tokyo) 31 2079-84.

Tassabehji M 2003 Williams-Beuren syndrome: a challenge for genotype-phenotype correlations. Hum Mol Genet. 12 R229-37.

Thomas EL, Hamilton G, Patel N, O'Dwyer R, Doré CJ, Goldin RD, Bell JD & Taylor-Robinson SD 2005 Hepatic triglyceride content and its relation to body adiposity: a magnetic resonance imaging and proton magnetic resonance spectroscopy study. Gut. 54 122-127.

Thorens B 1996 Glucose transporters in the regulation of intestinal, renal, and liver glucose fluxes. Am J Physiol. 270 G541-G553.

Towle HC 2005 Glucose as a regulator of eukaryotic gene transcription. Trends Endocrinol Metab. 16 489-94.

Tsatsos NG & Towle HC 2006 Glucose activation of ChREBP in hepatocytes occurs via a two-step mechanism. Biochem.Biophys.Res.Commun. 340 449-456.

Ulven SM, Dalen KT, Gustafsson JA & Nebb HI 2005 LXR is crucial in lipid metabolism. Prostaglandins Leukot Essent Fatty Acids. 73 59-63.

Unger RH & Orci L 2002 Lipoapoptosis: its mechanism and its diseases. Biochim Biophys Acta. 1585 202-12.

Untoro J, Schultink W, West CE, Gross R & Hautvast JG 2006 Efficacy of oral iodized peanut oil is greater than that of iodized poppy seed oil among Indonesian schoolchildren. Am J Clin Nutr. 84 1208-14.

Uyeda K & Repa JJ 2006 Carbohydrate response element binding protein, ChREBP, a transcription factor coupling hepatic glucose utilization and lipid synthesis. Cell Metab. 4 107-10.

Van Schaftingen E, Detheux M & Veiga da Cunha M 1994 Short-term control of glucokinase activity: role of a regulatory protein. The FASEB Journal 8 414-9.

Vandercammen A & Van Schaftingen E 1990 The mechanism by which rat liver glucokinase is inhibited by the regulatory protein. Eur J Biochem. 191 483-489.

Vaulont S, Munnich A, Decaux JF & Kahn A 1986 Transcriptional and post-transcriptional regulation of L-type pyruvate kinase gene expression in rat liver. J Biol Chem. 261 7621-5.

Vaulont S, Vasseur-Cognet M & Kahn A 2000 Glucose regulation of gene transcription. J Biol Chem. 275 31555-8.

Villarreal JE, Lombardini L & Cisneros-Zevallos L 2007 Phytochemical constituents and antioxidant capacity of different pecan [Carya illinoinensis (Wangenh.) K. Koch] cultivars. Food Chemistry 102 1241-1249.

Viollet B, Foretz M, Guigas B, Horman S, Dentin R, Bertrand L, Hue L & Andreelli F 2006 Activation of AMP-activated protein kinase in the liver: a new strategy for the management of metabolic hepatic disorders. The Journal of Physiology 574 41-53.

Viollet B, Guigas B, Leclerc J, Hebrard S, Lantier L, Mounier R, Andreelli F & Foretz M 2009 AMP-activated protein kinase in the regulation of hepatic energy metabolism: from physiology to therapeutic perspectives. Acta Physiol (Oxf) 196 81-98.

Wang Y, Botolin D, Christian B, Busik C, Xu J & Jump DB 2005 Tissue-specific, nutritional, and developmental regulation of rat fatty acid elongases. J Lipid Res. 46 706-15.

Wang Y, Botolin D, Xu J, Christian B, Mitchell E, Jayaprakasam B, Nair M, Peters JM, Busik J, Olson LK & Jump DB 2006 Regulation of hepatic fatty acid elongase and desaturase expression in diabetes and obesity. Journal of Lipid Research 47 2028-2041.

Weber A, Marie J, Cottreau D, Simon MP, Besmond C, Dreyfus JC & Kahn A 1984 Dietary control of aldolase B and L-type pyruvate kinase mRNAs in rat. Study of

translational activity and hybridization with cloned cDNA probes. J Biol Chem. 259 1798-802.

Williamson JR & Krebs HA 1961 Acetoacetate as fuel of respiration in the perfused rat heart. Biochem J. 80 540-7.

Wolfrum C, Borrmann CM, Borchers T & Spener F 2001 Fatty acids and hypolipidemic drugs regulate peroxisome proliferator-activated receptors alpha - and gamma-mediated gene expression via liver fatty acid binding protein: a signaling path to the nucleus. Proc Natl Acad Sci U S A. 98 2323-8.

Wu C, Kang JE, Peng LJ, Li H, Khan SA, Hillard CJ, Okar DA & Lange AJ 2005 Enhancing hepatic glycolysis reduces obesity: differential effects on lipogenesis depend on site of glycolytic modulation. Cell Metab 2 131-140.

Wurm FM 2004 Production of recombinant protein therapeutics in cultivated mammalian cells. Nature Biotechnol, 22 1393-1398.

Xu HE, Lambert MH, Montana VG, Parks DJ & Blanchard SG 1999a Molecular recognition of fatty acids by peroxisome proliferator-activated receptors. Mol Cell. 3 397-403.

Xu J, Christian B & Jump DB 2003 Regulation of rat hepatic L-pyruvate kinase promoter composition and activity by glucose, n-3 polyunsaturated fatty acids, and peroxisome proliferator-activated receptor-alpha agonist. J Biol Chem. 281 18351-62.

Xu J, Nakamura MT, Cho HP & Clarke SD 1999b Sterol regulatory element binding protein-1 expression is suppressed by dietary polyunsaturated fatty acids. A mechanism for the coordinate suppression of lipogenic genes by polyunsaturated fats. J Biol Chem. 274 23577-83.

Yahagi NSH, Hasty AH, Matsuzaka T & Ide T 2002 Absence of sterol regulatory element-binding protein-1 (SREBP-1) ameliorates fatty livers but not obesity or insulin resistance in Lep(ob)/Lep(ob) mice. J Biol Chem. 277 19353-7.

Yamamura HI, Lee IP & Dixon RL 1968 Study of the sympathomimetic action of cyclohexylamine, a possible metabolite of cyclamate. J Pharm Sci. 57 1132-4.

Yamashita H, Takenoshita M, Sakurai M, Bruick RK, Henzel WJ, Shillinglaw W, Arnot D & Uyeda K 2001 A glucose-responsive transcription factor that regulates carbohydrate metabolism in the liver. Proc.Natl.Acad.Sci.U.S.A 98 9116-9121.

Zelcer N & Tontonoz P 2006 Liver X receptors as integrators of metabolic and inflammatory signaling. J Clin Invest. 116 607-14.

Zhang Y, Yin L & Hillgartner FB 2003 SREBP-1 integrates the actions of thyroid hormone, insulin, cAMP, and medium-chain fatty acids on ACCalpha transcription in hepatocytes. J Lipid Res. 44 356-68.